DISSERTATION

Submitted to
The combined faculties for Natural Sciences and Mathematics of the Ruperto-Carola University of Heidelberg, Germany for the degree of Doctor of Natural Sciences

Presented by
Harshal Patil
born in Savda Tal Raver, India

Date of oral examination: _____

Studies on zygote morphogenesis in rodent malaria parasite, *Plasmodium berghei*

Referees: Prof. Andrew P. Waters
Prof. Dr. Freidrich Frischknecht
Prof. Dr. Michael Lanzer

Eidesstattliche Erklärung

Hiermit erkläre ich, dass alle Ergebnisse in dieser Doktorarbeit auf meiner eigenen Arbeit beruhen, mit Ausnahme der folgenden Daten, Datenanalysen und Plasmid-Konstruktion: die Umwandlung der primären Datensets in Excel Datensets der RNA Sequenzierungs Daten wurde von Dr Nicholas Dickinson, Genome and Data Analyst and Glasgow Polyomics Team, University of Glasgow, durchgeführt; elektonmikroskopische Bilder und deren Analyse wurde mit Hilfe von Frau Margaret Mullin, EM technische Angestellte, University of Glasgow, durchgeführt; die Bedienung des FACS Gerätes sowie die FACS Datenanalyse wurde mit Hilfe von Dr Katie Hughes, Postdoctoral Researcher, Professor Andrew Waters Laboratory, durchgeführt; die Ookineten Mobilität wurde mit Hilfe von Dr Nishia Philip, Research Associate, Professor Andrew Waters Laboratory, berechnet; das ISP::mCherry Plasmid wurde von Ms Christina Manakanata, einer ERASMUS Studentin, die unter meiner Anleitung gearbeitet hat, generiert. Alle Beiträge anderer sind an den entsprechenden Stellen der Doktorarbeit erwähnt und anerkannt.

Diese Doktorarbeit ist nicht für einen akademischen Grad (Dr. rer. nat.) an einer anderen Institution eingereicht worden.

Die hier präsentierte Doktorarbeit wurde von dem Autoren der Arbeit in der Zeit von Oktober 2011 bis May 2015 im Rahmen des EU FP7 Progamms „EVIMalaR“ unter der gemeinsamen Anleitung von Professor Andrew Paul Waters, Wellcome Trust Centre for Molecular Parasitology, University of Glasgow und Professor Dr. Friedrich Frischknecht, Zentrum für Infektiologie - Parasitologie, Ruprecht Karls Universität, Heidelberg, durchgeführt.

…… ……

Datum Harshal Patil

Acknowledgements

This PhD project is funded by the European Union's Seventh Framework Programme for Research (EU FP7) under European Virtual Institute for Malaria Research (EVIMalaR).

This project has immensely benefited from the wisdom and experience of Prof. A. P. Waters, University of Glasgow. I thank him for his patience, trust and open-mindness throughout the period of PhD and giving me an opportunity to work under for EVIMalaR PhD programme and critically reviewing my project time to time and for guidance and inspiration. I also thank Prof. Dr. Friedrich Frischknecht and Prof. Dr. Michael Lanzer, University of Heidelberg for acting as my supervisors their comments, suggestions and guidance.

I am grateful to Dr. Katie Hughes, University of Glasgow who has been very kind to supervise me and to teach me the fundamentals at the bench. I also thank following people at the University of Glasgow, University of Heidelberg and European Molecular Biology Laboratory including group members of Prof. Waters, Prof.Dr. Frischknecht and Prof. Dr. Lanzer lab for their kind co-operation during my PhD.

Mrs. Rachael Cameron for parasite transfections

Mrs. Angela Mcbridge for mosquito maintenance

Mrs. Margaret Mullin and Dr. Sonya Taylor for their introduction to and help during electron microscopy

Dr. Mhairi Stewart during RNA extraction

Dr. Nisha Philip for motility assays and discussion

Dr. Anubhav Srivastava for statistical analysis and IT help

Dr. Abhinav Sinha for regular discussions and suggestions

Ms. Anne Graham for Lab support

Dr. Volodymyr Nechyporuk-Zloy for imaging

Glasgow Polyomics Facility for sequencing RNA

Dr Nickolas Dickens for processing raw RNA-Sequencig data

Dr. Scott Johnston & Dr. Ian Salt for introducing and allowing me to use their Odyssey® Sa Infrared Imaging System

Ms. Sandra Niebel, Ms. Alessia Valdarno, Ms. Elisa Kless, Ms. Yvonne Maier for EVIMalaR related administrative support in Heidelberg

Ms. Miriam Griesheimer, Secretory to Prof. Dr. Michael Lanzer for admistration related support Mr. Kartik Bane, Ms. Sonia Moliner Cubel and Ms. Priyanka Fernandes for helping with regular discussions

Ms. Maria Mayorga, Ms. Pauline Conlon for coordinating stipend

Ms. Diah Yulianti and Mr. Tim Nuernberger during EVIMalaR|BioMalPar conferences

Ms. Jill Moore and Ms. Lisa Milne for all the visa applications

All EVMalaR mates for making my PhD a wonderful time

Ms. Gillian Murray, Ms. Amanda Baird, Ms. Hansa Pertab for EVIMalaR related administrative support in Glasgow

Ms. Martina Galvan and The Hartmut Hoffmann-Berling International Graduate School, University of Heidelberg for administrative support

The College of Medical, Veterinary and Life Sciences-Graduate School, University of Glasgow for administrative support

I am also thankful to my students- Ms. Christina Manakanata, EARASMUS student and Mr. Tim Hannay, Medical Student for providing me an opportunity to supervise them which helped enhance my leadership abilities.

Further, I am grateful to Prof. Sylke Muller for translating the summary and declaration of this thesis in German, Prof. Markus Meissner, Dr. Lisa Ranford Cartwright – University of Glasgow for assessing my work every year and providing various ideas and research directions.

I am also thankful to our collaborators Dr. Oliver Bilker, Wellcome Trust Sanger Institute, UK; Dr. Marc-Jan Gubbels, Boston College, USA; Prof. Judith Green, London School of Hygiene & Tropical Medicine, UK; Dr. Jacquin C. Niles, Massachusetts Institute of Technology, USA and Dr. Inga Siden-Kiamos, Institute of Molecular Biology and Biotechnology, Greece for providing project related materials and protocols.

Finally, I would like to appreciate the efforts of my entire family, especially my parents- Mrs. Prabhavati Patil and Mr. Prakash Patil, my wife- Rucha and my sister- Mrs. Priti Gavade without whom I would not have reached this far.

Abbreviations

> haploid	more than haploid
µm	micrometer
2DG	2-Deoxy-D-glucose
2N	diploid
4N	tetraploid
5FC	5-fluorocytosine
8N	octaploid or octoploid
ACT	Artemisinin Based Combination Therapy
AMA-1	apical merozoite antigen 1
aPKC	atypical Protein Kinase C
AUFG	Activated- unfertilized female gamete
bp	base pairs
cdc24	cell division cycle 24
cdc42	cell division cycle 42
CDPK1	calcium-dependent protein kinase
CelTOS	cell traversal protein of Plasmodium ookinetes and sporozoites
CITH	homolog of worm CAR-I and fly Trailer Hitch)
CO2	carbon di-oxide
CRISPER/Cas9	clustered regularly interspaced short palindromic repeats and Cas9 endonuclease-mediated genome editing
CRMPs	cysteine repeat modular proteins
CSP	circumsporozoite protein
CTRP	circumsporozoite- and thrombospondin-related adhesive protein
DAPI	4', 6-diamidino-2-phenylindole
DDT	Dichlorodiphenyltrichloroethane
DG	dense granules
DOZI	development of zygote inhibited
EBA	erythrocyte binding antigen
ECP-1	egress cysteine protease 1
EGF	epidermal growth factor
ELISA	Enzyme-Linked Immunosorbent Assay
ER	endoplasmic reticulum
FIP	family of interacting proteins
FPKM	fragments per Kilobase of open reading frame per million reads
G6PD	Glucose-6-phosphate dehydrogenase
GAK	cyclin G-associated kinase
GAP	GTPase-activating protein
GAP40	glideosome associated protein 40
GAP45	glideosome associated protein 45
GAP50	glideosome associated protein 50
GAP70	glideosome associated protein 70
GAPM3	glideosome associated protein with multiple membrane spans 3

GDI	Guanine nucleotide dissociation inhibitor
gDNA	genomic DNA
GEF	GDP/GTP exchange factor OR Guanine nucleotide exchange factor
GFP	Green Fluorescent Protein
GPI	glycosylphosphatidylinositol
GRA	granule protein
h	hour
hpa	hours post-activation
hpi	hours post-infection
i.p.	intraperitoneal
i.v.	intravenously
IMC	Inner Membrane Complex
IPTP	intermittent preventive treatment of pregnant women
IPTP-SP	intermittent preventive treatment of pregnant women using sulfadoxine-pyrimethamine
iRBC	infected red blood cell
IRS	Indoor Residual Spraying
ISP1	IMC sub-compartment protein 1
ISP3	IMC sub-compartment protein 3
ITN	Insecticide-treated nets
kd	Kilobase pairs
LCCL	Limulus clotting factor C, Coch-5b2, Lgl1
LLIN	Long-Lasting Insecticidal Nets
MACPF	membrane-attack complex/perforin
MAEBL	membrane antigen/erythrocyte binding-like
MAEBL	membrane antigen/erythrocyte binding-like
MAOP	membrane-attack ookinete protein
MAP Kinase	Mitogen-activated Protein Kinase
MDCK	Madin-Darby Canine Kidney
MDV/PEG3	male development-1/protein of early gametocyte 3
min	minutes
mRNP	messenger ribonucleoprotein particles
MSP1	Merozoite Surface Protein 1
MTOC	microtubule-organizing center
N	haploid
NEK 2/4	NIMA (never in mitosis/Aspergillus) related Kinases
NIMA	never in mitosis/Aspergillus
nm	nano meter
NSF	N-ethylmaleimide-sensitive factor
O2	oxygen
ODS	oocyst derived sporozoites
Pb	Plasmodium berghei
PbG2	Plasmodium berghei glycine at position 2

PbRab11A	Plasmodium berghei Rab11A
PC12 cells	cell line derived from a Pheochromocytoma of the rat adrenal medulla.
PCR	Polymerase Chain Reaction
PDEδ	Phosphodiesterases δ
Pf	Plasmodium falciparum
PfEMP1	P. falciparum-infected erythrocyte membrane protein 1
PI4K	phosphatidylinositol-4 kinases
PK7	protein kinase 7
PPLP3/4/5	perforin-like proteins
PPLPs	perforin-like proteins
PPM	metallo-dependent protein phosphatases 2 and 5
PV	parasitophorous vacuole
Pv	Plasmodium vivax
PVM	parasitophorous vacuole membrane
RAMA	rhoptry associated membrane antigen)
RBCs	red blood cells
RESA	Ring-infected Erythrocyte Surface Antigen
RH5	reticulocyte binding protein-like homologue 5
RIMA	Ring membrane antigen
RON	Rhoptry bulb neck proteins
ROP	Rhoptry proteins
SGS	salivary gland derived sporozoites
SHLP1	Shewanella-like protein phosphatase
SIT	sterile insect technique
SNAP	SNARE-associated proteins
SNARE	soluble N-ethylmaleimide-sensitive factor attachment protein receptors
SOAP	secreted ookinete adhesive protein
SP	Sulphadoxine-pyrimethamine
SPECT2	sporozoite microneme protein is essential for cell traversal 2
SPK	Spitzenkórper
SPN	subpellicular network
SRPK	serine/arginine-rich protein kinase
SUB1/2	Subtilisin-like protease 1/2
TAR	transcriptinally arrested WT-GFP retorts
TBV	Transmission blocking vaccines
TgCAM 1/2	Toxoplasma gondii calcium-binding protein 1/2
TgDLC	Toxoplasma gondii dynein light chain
TgMORN1	Toxoplasma gondii Membrane Occupation and Recognition Nexus 1
TGN	trans golgi network
TJ	Tight Junction
TM	transmembrane
TRAP	thrombospondin-related anonymous protein
UOS3	upregulated in oocyst sporozoites 3
WARP	von Willebrand factor A-domain-related protein
WT	wild type

x	times
ZFN	zinc-finger nucleases

Contents

Contents

Summary

Development of polarity is well studied in cell systems such as mammalian neurons, epithelial cells and *Caenorhabditis elegans* zygotes. In *Plasmodium* the spherical and presumed apolar female gamete morphs during the 24 hours after fertilisation in the mosquito midgut into a polarised ookinete, however, little is known about how *Plasmodium* zygotes develop polarity. It is known that endocytosis-mediated protein transport is generally necessary for the establishment and maintenance of polarity in epithelial cells and neurons, and Rab11A GTPase is an important regulator of protein transport via recycling endosomes. Rab11A has been predicted to be involved in cytokinesis in *Plasmodium falciparum* and is essential in *Plasmodium berghei*. Here I show the expression profile of *P. berghei* Rab11A (PbRab11A) across the life cycle and use a promoter swap strategy to investigate the role of PbRab11A in ookinete development. By expressing PbRab11A under the *clag* promoter or *ama-1* promoter, its expression in sexual stages is greatly reduced while its essential expression in asexual blood stages is maintained. Whilst gamete production and fertility rates remained unaffected, the ookinete conversion rates of CLAG and AMA-1 promoter swap mutants are reduced by up to 99% and 98% respectively and transmission through the mosquito is prevented. TEM analysis and immunofluorescence microscopy of developmental and structural markers show that Rab11A-CLAG promoter swap mutant zygotes lay down the Inner Membrane Complex (IMC) and are apically oriented but appear stop morphological progression and remain spherical. Western blot and transcriptome analysis of Rab11A - CLAG promoter swap mutant suggest marginal expression delay as well as deregulation of some of the transcripts of ookinete development and structural markers, and the majority of deregulated transcripts are independent of previously shown translationally stored transcripts. We predict that Rab11A is not involved in the establishment of *P. berghei* zygote polarity, mitosis, activation of stored mRNAs nor extensive reactivation of post-meiotic transcription but conceivably in the delivery of plasma membrane to the growing apical outgrowth which is expected to be a coordinated process of Rab11A mediated membrane trafficking and cytoskeletal dynamics.

As a second line of enquiry, the establishment of polarity in *P. berghei* zygote with respect to the point of male and female gamete fusion is ongoing. Establishment of polarity in embryos and zygotes is dependent on the development of the axis of polarity and fertilization signals mediated by the male gamete in *C. elegans* and some plants. Establishment of the axis of polarity and therefore the emergence of apical complex with respect to the point of gamete

fusion has not been previously studied in *Plasmodium*. To visualise the process of fertilization, membrane localized green fluorescence protein (GFP) expressing *P. berghei* male gamete producer parasites were generated. Female specific protein phosphatase with kelch-like domain (PPKL), IMC sub-compartment protein 1 (ISP1) and Glideosome-associated protein 50 (GAP50) are known to be associated with the apical complex, and are essential for *P. berghei* zygote to ookinete transition. Further, female specific MTOC (Microtubule Organising Center) markers - spindle pole body protein (SPBP) is also predicted to be associated with apical complex development during zygote to ookinete transition. Therefore, to investigate the emergence of the apical bud with respect to the point of gamete fusion during fertilization and through the zygote to ookinete transition, female gamete specific membrane localized mCherry expressing or PPKL/ ISP1/ GAP50/ SPBP labelled with mCherry expressing *P. berghei* parasite cell lines were generated in male gamete specific GFP producing *P. berghei* parasites. Initial fluorescent microscopy confirms the stage specific red-green fluorescence in respective transgenic *P. berghei* parasite lines. Further studies to confirm the hypothesis that the point of male gamete fusion cues for the point of emergence of apical bud in the zygote are ongoing.

Zusammenfassung

Die Entwicklung von Polarität ist in Zellsystemen, wie menschlichen Neuronen und Epithelzellen sowie der Zygote des Nematoden *Caenorhabditis elegans*, gut untersucht. Die direkt nach der Befruchtung spärische Zygote von *Plasmodium*, verändert ihre Gestalt innerhalb der ersten 24 Stunden nach der Befruchtung im Moskitomitteldarm in den polarisierten Ookineten. Es ist jedoch wenig darüber bekannt wie die Zygote von *Plasmodium* diese Polarität entwickelt.

Es ist bekannt, dass Endozytose-vermittelter Proteintransport für die Etablierung und Beibehaltung der Polarität in Epithelzellen und Neuronen notwenig ist; die GTPase Rab11A ist ein wichtiger Regulator von Proteintransport; das Protein ist an dem Recycling von Endosomen massgeblich beteiligt. Rab11A ist vermutlich an der Zytokinese in *P. falciparum* beteiligt und das Protein ist essentiell für *P. berghei.*

Hier zeige ich das Expressionsprofil von Rab11A in verschiedenen Stadien des Lebenszyklus von *P. berghei* und ich untersuche die Rolle der Rab11A GTPase für die Ookinetenentwicklung dieser Parasiten mit Hilfe der Promotor-Swap Strategie. *P. berghei rab11a* wurde unter der Kontrolle des CLAG- oder des AMA1-Promotors in *P. berghei* exprimiert, was zur Reduzierung des Expressionslevel des Proteins in den sexuellen Stadien der Parasiten führte, während die Expression in den asexuellen Stadien nicht beeinflusst wurde. Die Ergebnisse zeigen, dass weder Gametenproduktion noch Fertilität durch den Promotor-Swap beinträchtig waren, während die Ookineten-Bildung der CLAG-und AMA-1 Promotor-Swap Mutanten um 99% beziehungsweise 98% reduziert war; die Entwicklung des sexuellen Transmissionszyklus der Mutanten war komplett unterbrochen. Transmissionselektronmikroskopie und Immunfluoreszenzmikroskopie der Ookineten Entwicklung sowie von Struktur-Markern zeigten, dass die Rab11A-CLAG Promotor-Swap Mutanten den „Inner Membrane Complex“ (inneren Membrankomplex; IMC) bilden und dass sie apikal orientiert sind, aber sie scheinen sich morphologisch nicht zu entwickeln und verbleiben abgerundet. Western Blot Analysen und Transkriptom Analysen der *P. berghei* Rab11A – CLAG Promotor-Swap Mutanten zeigten, dass Expression einiger Transkripte leicht verspät war, und dass ausserdem einige Transkripte der Ookineten-Entwicklung und Struktur-Marker misreguliert waren. Ausserdem konnte gezeigt werden, dass die Mehrzahl der misregulierten Transkripte unabhängig von früher beschriebenen, translationell gespeicherten Transkripten sind. Wir nehmen an, dass Rab11A nicht an der Etablierung der *P.*

berghei Zygotenpolarität, Mitose, der Aktivierung der gespeicherten mRNAs oder an der extensiven Reaktivierung der post-meitotischen Transkription beteiligt ist. Vielmehr vermuten wir, dass das Protein an der Bereitstellung und Lieferung von Bestandteilen der Plasmamembran beteiligt ist, die notwenig ist, um die morphologischen Veränderungen zu erlauben, die mit apikalem Wachstum verbunden sind. Unsere Daten deuten darauf hin, dass Rab11A die Prozesse des Membrantransports und die Dynamik des Zytoskelets, beides notwendig für das Auswachsen des Apikalpols, koordiniert.

Eine zweite Fragestellung im Zusammenhang mit der Polaritäts-Entwicklung in der *P. berghei* Zygote ist die Fusion von männlichen und weiblichen Gameten. Die Polarität in Embryos und Zygoten ist in der Regel von der Polaritätsachse abhängig und wird von Fertilisationsmarkern des männlichen Gameten vermittelt.

Die Etablierung der Polaritätsachse und damit die Entstehung des Apikalkomplexes in Zusammenhang mit der Gametenfusion ist bisher in *Plasmodium* nicht untersucht worden. Um den Prozess der Fertilisation zu analysieren, wurden Parasiten genetisch so manipuliert, dass sie männliche Gameten generieren, die membranlokalisiertes grün fluoreszierndes Protein (GFP) exprimieren. Es ist bekannt, dass Proteine, wie das weibliche Gameten-spezifische Protein Phosphatase mit kelch-ähnlicher Domaine (PPKL), das „inner membrane complex“ (IMC) sub-Kompartiment Protein 1 (ISP1) und das Glideosome-assoziierte Protein 50 (GAP50), mit dem Apiklalkomplex assoziert sind. Desweiteren wissen wir, dass diese Proteine essentiell für den Übergang von Zygote zum Ookineten sind. Ausserdem ist der Mikrotubuli-Organisations Zentrum (MTOC) Marker, das Spindelpolkörper Protein SPBP, vermutlich mit der Entwicklung des Apikalkomplexes während der Entwicklung des Ookineten assoziiert. Aus diesen Gründen wurden all diese weiblichen Gamtenmarker mit mCherry getagged und die Plasmide wurden in die Parasiten transfiziert, die bereits den männlichen GFP-Marker exprimierten. Diese Mutanten exprimierten beide Fluoreszenzmarker und ihre Expression wurde fluoreszenzmikroskopisch von Fertilisation der Gameten bis zur Entstehung des Apikalkomplexes in Ookineten, untersucht, um den Prozess der Entstehung des Apikalkomplexes detaliert zu studieren. In den ersten Studien konnten grün und rot fluoreszierende Parasiten gezeigt werden. Die transgenen Parasitenlinien stehen jetzt für weitere Analysen zur Verfügung, um die Hyopthese zu testen, dass der Fusionspunkt des männlichen Gameten mit dem weiblichen Gameten der Entstehungspunkt des Apikalkomplexes ist.

Chapter 1: Introduction

1.0 Introduction to Malaria

Malaria has been a major disease of human since past and it continues to be a major public health concern. It is estimated that around 3.2 billion people are under threat of getting infected and acquiring malaria, and around 1.2 billion people are at great risk. In 2013, 198 million cases of malaria were estimated globally and 584,000 malaria deaths were recorded of which 90% of deaths were in Africa. This indicates a decrease of 30% and 47% in malaria cases incidence and mortality rates since 2000 respectively. 78% of total death victims were children under the age of 5 years (World_Malaria_Report 2014). Regardless of remarkable malaria control it still remains a major public health issue in low and lower-middle income countries (Figure 1.0), primarily affecting poor communities having least access to preventive, diagnosis and treatment services. Therefore, malaria control and eradication are intricately associated with the health system and infrastructure development and poverty reduction (World_Malaria_Report 2014).

1.1 Causative agents of human malaria

Malaria in humans is caused by obligate intracellular protozoa parasites from phylum Apicomplexan and genus *Plasmodium*, which are intra-erythrocytic protozoan parasites. The major cause of human mortality is *P. falciparum*, predominantly located in Africa. The second most common species is *P. vivax*, mainly located in Southeast Asia. *P. vivax* may remain dormant for months or even years in liver and the dormant stage is known as the hypnozoite (Krotoski 1989, Hulden 2011, Markus 2011, Markus 2011, Dembélé, Franetich et al. 2014). African individuals lacking the Duffy antigen on the surface of red blood cells (RBCs) were considered to be resistant to *P. vivax* blood stage infection. Interestingly, recent evidence suggests that *P. vivax* can infect individuals having Duffy negative erythrocytes (Herrera, Gómez et al. 2005, Ryan, Stoute et al. 2006, Maestre, Muskus et al. 2010, Ménard, Barnadas et al. 2010, Mendes, Dias et al. 2011, Carvalho, Queiroz et al. 2012, Woldearegai, Kremsner et al. 2013, Zimmerman, Ferreira et al. 2013, Ngassa Mbenda and Das 2014). The other species that infect humans are *P. malariae, P. ovale* and *P knowlesi* (Putaporntip, Hongsrimuang et al. 2009, Antinori, Galimberti et al. 2013, Calderaro, Piccolo et al. 2013). Recently, a natural infection of simian *Plasmodium* species - *P. cynomolgi* to human was reported in Malaysia (Ta, Hisam et al. 2014).

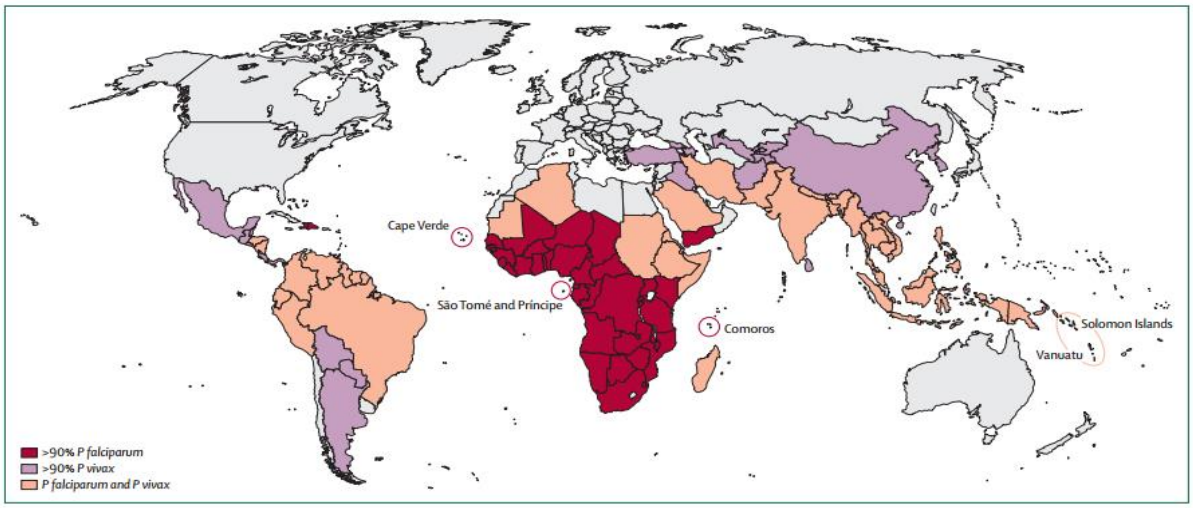

Figure 1.0 Global malaria map showing the proportion of human malaria caused by *P. falciparum* and *P. vivax*.

A global malaria map showing more than 90% infections caused by either *P. falciparum* in countries highlighted in dark red or *P. vivax* in countries highlighted by faint purple. Faint orange is the area of mixed infections by both *P. falciparum* as well as *P. vivax*. Source: (Feachem, Phillips et al. 2010) – reproduced with permission.

1.2 Strategies for malaria control and elimination

1.2.1 Vector management

Anopheles mosquitoes are the vectors principally responsible for transmission of *Plasmodium*, the major species being *An. gambiae* and *An. funestus*. Vector management has been the most effective of all the measures taken to control malaria. Insecticide-treated nets (ITN) and/or Long-Lasting Insecticidal Nets (LLINs), Indoor Residual Spraying (IRS) and environmental management have been shown to reduce malaria transmission significantly. In the 1950s, DDT (dichlorodiphenyltrichloroethane) was heavily used in indoor spraying for the control of vectors of malaria and other vector borne diseases, e.g. leishmaniasis, however, after that use of DDT moved towards pyrethroids which are less toxic to humans and other non-target organisms. Resistance to pyrethroids has now emerged, putting challenges to malaria control programme (N'Guessan, Corbel et al. 2007, Yadouleton, Padonou et al. 2010, Asale, Getachew et al. 2014). The emergence of resistance was due to extreme use of insecticides in households and pesticides in agriculture (Akogbeto, Djouaka et al. 2005, Yadouleton, Asidi et al. 2009, Nkya, Poupardin et al. 2014). Therefore, alternative strategies for vector control should be put in place to minimize the contact of vector and human. Another strategy to control the vector borne diseases is the use of the sterile insect technique (SIT) to impede mating habits. SIT relies on interfering with the genetic system of vectors in order to make the males sterile by the use of radiation, chemicals, *Wolbachia*-mediated cytoplasmic incompatibility or genetic modification and mass release of sterile males, which compete with wildtype (WT) males to fertilize with WT females producing no offspring or offspring which are not viable after part of their life cycle. One of the most successful examples of SIT is the eradication of Screwworm, a pathogen of cattle and mammals and occasionally infects humans, from North America (Krafsur, Whitten et al. 1987). Early studies on the utilization of SIT for malaria control have shown promising results, although these technologies are still in their initial stages [reviewed by (Oliva, Vreysen et al. 2014, Gentile, Rund et al. 2015)]. Use of current vector control strategies, its management and monitoring of insecticide resistance along with the development of new technologies such as SIT is imperative if malaria control is to be achieved.

1.2.2 Treatment and diagnosis of malaria

To treat malaria infection and illness, to eliminate the dormant stages and to prevent transmission of *Plasmodium* parasites, antimalarial drugs are used. Hopes of malaria eradication started with the use of chloroquine. Along with DDT and ITNs, chloroquine proved substantially successful to reduce the burden of malaria in 1950s, however, malaria eradication efforts were affected due to increased resistance to chloroquine (Harinasuta, Suntharasamai et al. 1965, Sandhinand, Pinswasdi et al. 1965) as well as to the insecticides. And in the 1970s, the use of mefloquine and other quinine derivative along with sulfadoxine-pyrimethamine (SP) resulted in the emergence of multi-drug resistance. The resistance against SP was previously found in Asia and have been developed in Africa (Wongsrichanalai, Pickard et al. 2002). New artemisinin based combination therapy (ACT) is proving beneficial in treating previous drug resistant malaria parasites, including immature gametocytes (lifecycle stage of malaria parasite responsible for infection of mosquitoes when they bite humans, see section 1.3 of the life cycle of *Plasmodium*) and have been widely used (Eastman and Fidock 2009, Grueninger and Hamed 2013). With the use of ACT and vector management, reduction in malaria morbidity and mortality has been achieved to the greatest extent to date, however, elimination of malaria still requires the strategic use of malaria treatments with preventive measures (malERA_Consultative_Group_on_Drugs 2011). These approaches include mass drug administration (von Seidlein and Greenwood 2003), mass screening and targeted treatment (Aregawi, Ali et al. 2011), and focal screening and targeted treatment of malaria hotspots (Lawpoolsri, Klein et al. 2009). To achieve a radical cure, it is necessary to use ACT treatment with the combination of gametocidal agent (a drug that destroys gametocytes as a result preventing communal transmission of malaria) such as primaquine, however, primaquine are oxidative anti-malarials and can cause haemolytic anaemia on individuals with glucose-6-phosphate dehydrogenase (G6PD) deficiency and there is difficulty detecting this deficiency (Kuwahata, Wijesinghe et al. 2010, Smithuis, Kyaw et al. 2010, Hoyer, Nguon et al. 2012, Grueninger and Hamed 2013, Ashley, Recht et al. 2014). Research is needed to develop screening tests for G6PD deficiency as well as the detection of malaria diagnosis.

The conventional clinical diagnosis of malaria was based on signs and symptoms of malaria such as headache, fever, diarrhoea, chills, tiredness, nausea, vomiting and muscle ache. Laboratory methods using microscopy have been a gold standard in malaria diagnosis,

however, new rapid diagnostic test/ molecular tests based on PCR and ELISA provide more accuracy, specificity and have the ability to differentiate between various *Plasmodium* species (Tangpukdee, Duangdee et al. 2009, Port, Nguetse et al. 2014, Thongdee, Chaijaroenkul et al. 2014).

Malaria in pregnancy is a threat to mother and baby having the risk of maternal anaemia and low birth weight (Brabin 1983, Guyatt and Snow 2001, Fitri, Jahja et al. 2014). Multiple approaches are employed to reduce the risk of malaria in pregnancy, such as intermittent preventive treatment of pregnant women using sulfadoxine-pyrimethamine (IPTp-SP) and use of ITNs. At least two doses of SP are administered in IPTp despite of absence of parasites (Mubyazi, Bloch et al. 2005, Hill and Kazembe 2006, Menéndez, Bardají et al. 2010, Harrington, Mutabingwa et al. 2011, Gutman, Mwandama et al. 2013, Mbu, Takang et al. 2014). However, some studies show increased resistance to the IPTp-SP particularly in East and Southern Africa and therefore increasing the need for development of new drugs and strategies (Feng, Simpson et al. 2010, Harrington, Mutabingwa et al. 2011).

1.2.3 Malaria vaccines

People living in malaria endemic regions develop protective immunity against malaria symptoms throughout childhood (Marsh and Howard 1986, Bull, Lowe et al. 1999, Nielsen, Staalsoe et al. 2002) and this developed immunity is responsible for some protection against malaria (Marsh and Kinyanjui 2006, Doolan, Dobaño et al. 2009). Protection against infection by passive transfer of antibodies from immunized individuals to non-immunized individuals had been shown (COHEN, McGREGOR et al. 1961, MCGREGOR 1964) and this is supported by studies in rodents (Martínez, Yandar et al. 2009, Sack, Miller et al. 2014). This principle led to the development of human malaria vaccine. Despite of active attempts of vaccine development over the past 50 years, developing an effective vaccine remains a challenge. Even with multiple attempts, several vaccine candidates have been studies from 'whole parasite' approach and to 'subunit approach' have had highly variable efficacy. Attenuated sporozoites, the mosquito stage of malaria parasite responsible for infection of humans (see section 1.3 life cycle of *Plasmodium*), with chemical and genetic modification are being studied as possible malaria vaccine candidates (Hoffman, Goh et al. 2002, Roestenberg, McCall et al. 2009, Teirlinck, McCall et al. 2011), however, there are some difficulties associated with this of having high cost, scaling up and dose requirement (Hill

2011) including the possibility of a threat of reversibility (Richards and Beeson 2009). Therefore, alternative approaches of subunit vaccine development are evaluated (Stanisic, Barry et al. 2013). Currently, only one candidate appears to show promising results known as RTS,S and is likely to unveil in 2015 (Barry and Arnott 2014), although RTS,S is partially protective and diminishes over time (Stoute, Kester et al. 1998, Doherty, Pinder et al. 1999, Bojang 2006, Cohen, Benns et al. 2010, Swysen, Vekemans et al. 2011, Stanisic, Barry et al. 2013, Barry and Arnott 2014, Umeh, Oguche et al. 2014). Therefore, the second generation of vaccine needs to have higher efficacy than RTS,S for malaria eradication. Recently, several vaccine candidates are being studied, with function at every stage of parasite life cycle and categorized as follows.

(1) Pre-erythrocytic vaccines: Pre-erythrocytic vaccines intend to prevent infection at sporozoite (a human infective form of *Plasmodium*) stage such as RTS,S or at the liver stages of the parasite to counteract the emergence of parasites into the bloodstream. However, this vaccine might not be ideal, as only few sporozoites are injected by a vector and this may not be sufficient to produce an immune response as only one sporozoite is sufficient to establish an infection in hepatocytes (Hill 2011, Barry and Arnott 2014).

(2) Blood stage vaccines: The majority of vaccines are developed to target the blood stages of *Plasmodium* as all of the symptoms of malaria occur at the blood stages. These vaccines are designed to protect against the blood stages of parasite, i.e. merozoite stages, therefore, targeting exposed merozoite surface antigens or antigens contained in the apical organelles (organelles containing secretory proteins involved in the invasion of host cells, e.g. RH5, AMA-1, MSP1-19 etc, see results 1.3.2 for details about blood stages of *Plasmodium*) is one approach (Richards and Beeson 2009). Another example of a blood stage vaccine candidate is targeting the exported surface protein of *P. falciparum*-infected RBCs (erythrocytes) known as erythrocyte membrane protein 1 (PfEMP1), which facilitates adhesion of iRBCs (infected red blood cells) to different host receptors and is related to pregnancy associated malaria (Doritchamou, Bertin et al. 2012, Hviid and Jensen 2015). Blood stage vaccines are also meant to prevent transmission stages i.e. gametocytes (Richards and Beeson 2009, Hill 2011, Barry and Arnott 2014). Examples of antigens present on the surface of gametocytes are Pfs48/45 and Pfs230 (Jones, Grignard et al. 2015).

(3) Transmission blocking vaccines (TBV): These vaccines are targeted against the antigens expressed during mosquito stages of parasite life cycle such as antigens expressed in gametocytes or ookinetes. Despite the fact these vaccines would not prevent the disease or an infection of an individual; they would significantly assist in preventing transmission (Hill 2011, Barry and Arnott 2014) and therefore are an important strategy when considering the elimination of malaria. TBV are categorised as antigens present either on the surface of gametocytes (pre-fertilization) e.g. Pfs48/45 and Pfs230 or on the surface of zygotes and ookinetes (post-fertilization) e.g. Pfs25 and Pvs25 (Wu, Ellis et al. 2008, Miyata, Harakuni et al. 2011).

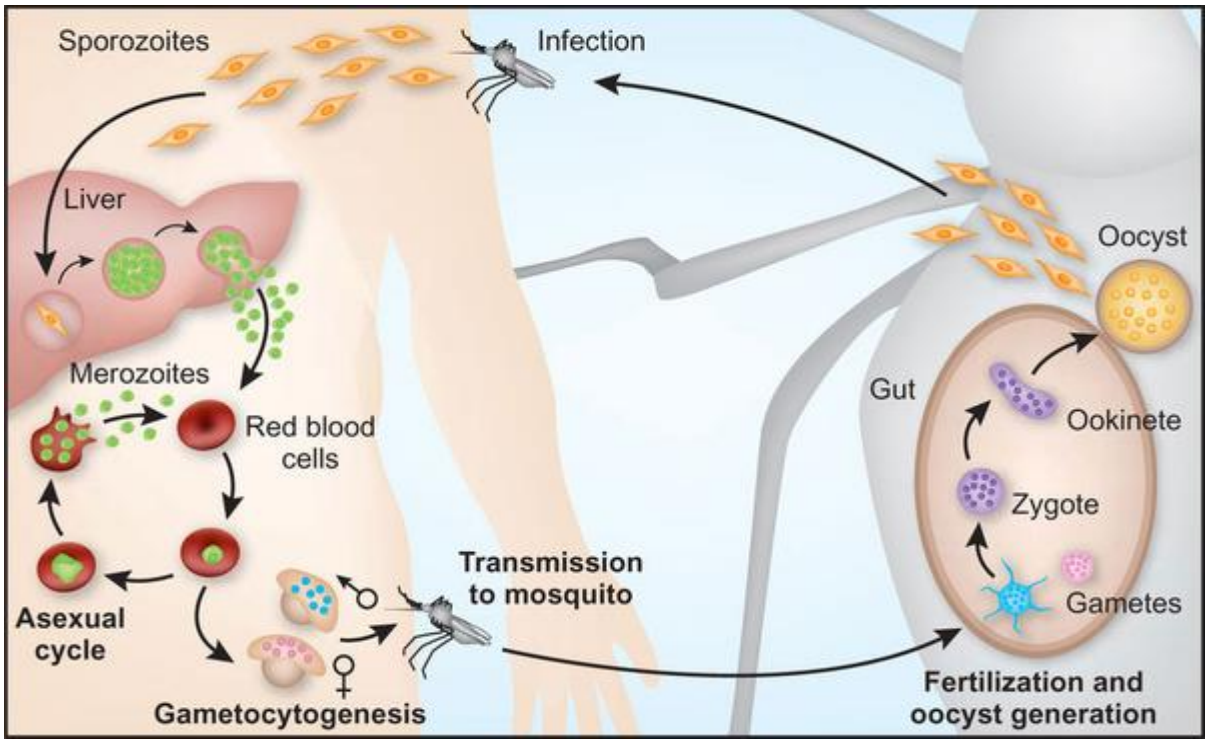

Figure 1.3.1 Life Cycle of Malaria parasite.

Image taken from (Pasvol 2010).

Sporozoites are injected through mosquito during blood meal and travel to liver to infect hepatocytes. Within hepatocytes, sporozoites grow and form liver stage merozoites (Pre-erythrocytic stage) which are released into the blood stream to start erythrocytes/blood stages. Merozoites keep infecting RBCs through continuous asexual lifecycle stages of ring to trophozoites to schizonts. Very few asexual blood stage parasites undergo sexual development to form male and female gametocytes (erythrocytic stages). During a blood meal, gametocytes are taken up into the mosquito midgut. Within 10 minutes (min) gametocytes activate and rapture RBCs and male gametocytes exflagellate to form up to 8 male gametes (microgametes) and single male gamete fertilize with a female gamete (macrogamete) to form a zygote. Within 20-24 h zygote undergoes morphological changes to form a banana shape invasive form called an ookinete, which crosses the mosquito midgut epithelium to form the oocyst under basal lamina. After maturation, oocyst releases thousands of sporozoites into hemoceol. Sporozoites then travel to mosquito salivary gland and ready to transmit into to new host during a blood meal (mosquito stages).

1.3 Life cycle of *Plasmodium*

Malaria is a disease of mankind since antiquity caused by *Plasmodium* species. These apicomplexan parasites are part of the alveolate group (Cavalier-Smith 1993) and are obligate intracellular parasites of medical importance. Alveolates include *Plasmodium* species causative agents of malaria and *Toxoplasma*, which causes toxoplasmosis, *Cryptosporidia* is an opportunistic pathogen of human and animals, *Eimeria sp*. are poultry and cattle pathogens, while *Babesia* and *Theileria* are cattle parasites. The alveolate group also consists of free living protozoa such as *Paramecium* and *Tetrahymena* and also the dinoflagellates (Baker 2010). These parasites require a vertebrate and an arthropod host to complete the life cycle (figure 1.3.1). Many advances in our understanding of the biology of *Plasmodium* come from the use of rodent models e.g. *P. berghei*, *P. chabaudi* and *in-vitro* culture of human parasite *P. falciparum.* The molecular mechanism of development of malaria parasites in their host is not completely clear. To tackle malaria, it is necessary to understand the missing links of parasites.

1.3.1 Pre-erythrocytic stage

The mammalian life cycle of *Plasmodium* starts with the injection of parasite form known as sporozoite in the skin during the mosquito blood meal. Although, mosquitoes carry vast number of sporozoites, only few sporozoites get deposited into the skin during a blood meal (Beier, Davis et al. 1991). This infection by sporozoites is clinically silent and does not induce immunological factors. After deposition into the skin, sporozoites enter the blood stream and in few minutes rapidly travel to the liver (Vaughan, Aly et al. 2008, Ménard, Tavares et al. 2013). Sporozoites leave the blood circulation through the liver sinusoidal endothelium and pass through Kupffer cells - resident macrophages of the liver (Vaughan, Aly et al. 2008, Ménard, Tavares et al. 2013). A family of five putative secreted proteins termed as perforin-like proteins (PPLPs) is conserved across the *Plasmodium species.* All of the PPLPs consist of a MACPF-like (membrane-attack complex/perforin) domain involved in pore formation. PPLP1/SPECT2 (sporozoite microneme protein is essential for cell traversal) is expressed in sporozoites and has a critical function in crossing the liver sinusoidal cells(Ishino, Chinzei et al. 2005). Sporozoites continue to pass through several hepatocytes to infect a final hepatocyte and establish infection with the formation of the parasitophorous vacuole (PV) (Hollingdale, Leef et al. 1981, Mazier, Beaudoin et al. 1985, Spielmann, Montagna et al.

2012). The pre-erythrocytic stages i.e. sporozoites are present in small numbers and therefore represent a transmission bottleneck and are suitable for vaccine development, offering a chance of prevention of malaria (Ménard, Tavares et al. 2013). After invading hepatocytes, sporozoites differentiate from a slender form to a large spherical liver stage form (also called a liver trophozoite) (Mikolajczak and Kappe 2006), which then undergoes schizogony to form thousands of merozoites (Coppens, Sullivan et al. 2010). Another aspect of liver stages is about modification of hepatocytes and controlling hepatocyte survival which is beyond the scope of this report (Mikolajczak and Kappe 2006, Vaughan, Aly et al. 2008, Ménard, Tavares et al. 2013). The parasitophorous vacuole membrane (PVM) (Spielmann, Montagna et al. 2012) is lysed and merozoites are exposed to hepatocyte cytoplasm, ready to pack into vesicles, called merosomes, and bud out from hepatocyte membrane. Merosomes travel to the heart and arrive in the lungs where they liberate merozoites which are ready to invade RBCs (Mikolajczak and Kappe 2006, Baer, Klotz et al. 2007, Vaughan, Aly et al. 2008, Ménard, Tavares et al. 2013).

1.3.2 Blood stages

1.3.2.1 Asexual stages of malaria parasite

Merozoite invasion of RBCs is essential for asexual blood stage replication and establishment of malaria pathology. After invasion by *P. falciparum*, the intra-erythrocyte merozoite grows within a parasitophorous vacuole (PV) and develops into ring stage (0-22 hours post-infection, hpi) to trophozoite (22-36 hpi) and apparently to schizont (36-48 hpi) containing 16 or more merozoites in approximately 48 hpi. Subsequently, these merozoites are released by rupturing of red blood cell and invade nearby RBCs. Merozoite invasion of RBC is a rapid process and can occur within 1 min in *P. falciparum* (Gilson and Crabb 2009). Many proteins required for invasion are essential and unique to parasite species and the fact that merozoites are extracellular and therefore exposed to host immune system means that merozoites surface antigens are viewed as potential targets for blood stage vaccine development as well as targets for the design of novel drug compounds (Cowman and Crabb 2006, Boyle, Wilson et al. 2013). The invasion step consists of contact of the merozoite and RBC, reorientation of merozoite apical end to attach to the RBC and formation of a tight junction (TJ) followed by invasion (Gilson and Crabb 2009, Riglar, Richard et al. 2011). Merozoite invasion of RBC is a series of coordinated process of cell signalling events and consists of number of receptor

ligand events (Boyle, Wilson et al. 2013). Numerous merozoite antigens having roles in RBC invasion have been identified and are located at the apical end of the merozoite e.g. MSP1, EBA and PfRh, PfRh5 and basigin interaction, AMA1 –RON2 and etc. (Weiss, Gilson et al. 2015).

RBCs are devoid of a nucleus and other cell organelles and are highly specialized cells designed to transport O_2 and CO_2. They have great ability of deformity enabling their movement through the microvasculature (An and Mohandas 2008). RBC modification is essential for parasite survival as RBCs lack the support systems that parasite might hijack and therefore must be made by parasite to survive (Moxon, Grau et al. 2011). Inside erythrocyte, merozoites hide from the host immune system as it grows; it induces modification of the host cell to facilitate import of nutrients, dispose of waste, and export of proteins across parasite-plasma membrane, PVM and erythrocyte cytosol. RBCs are full of haemoglobin and the intracellular parasite uses the amino acids obtained from haemoglobin digestion (Goldberg 2005) for protein synthesis and haematin - a by-product of haemoglobin digestion is stored in a crystalline form called haemazoin (Pagola, Stephens et al. 2000). Other changes in RBCs are formation of PV, PVM and formation of new membranous structures, Maurer's clefts (Lanzer, Wickert et al. 2006, Wickert and Krohne 2007) which are involved in protein export. Many alterations are made to the RBC membrane including formation of novel channels in PVM (de Koning-Ward, Gilson et al. 2009) and RBC membrane (Staines, Powell et al. 2004), small protrusions on the surface of the iRBC called knobs where erythrocyte membrane protein such as PfEMP1 and other virulent proteins are transported (Cooke, Mohandas et al. 2004, Haldar, Hiller et al. 2005, Moxon, Grau et al. 2011, Prajapati and Singh 2013). These modifications to the iRBC membrane allow the parasite to adhere to vasculature endothelial cells causing rosetting and cytoadherence thus avoiding splenic clearance. Cytoadherence and rosetting cause severe malaria and organ complications.

1.3.2.2 Sexual differentiation and gametogenesis

Very few asexual blood stage parasites, after ring stage, are differentiated into sexual stages to become male and female gametocytes (micro or macro gametocytes respectively) - intraethyrthocytic precursors of the parasite sexual stage. Differentiation of asexual to sexual stages is crucial for transmission of parasite to complete the life cycle. Sex through gamete mating, which occurs in the mosquito midgut, gives an opportunity of genetic recombination

with other genotypes. The ratio of gametocytes to asexual stages can be very low, in one of the *P. falciparum* study it is calculated as 1:156 (Eichner, Diebner et al. 2001) however, it is known to be varying (Boyle, Wilson et al. 2013, Wampfler, Mwingira et al. 2013). The half-life of gametocytes is variable from 2.4 days to 6.4 days (Talman, Domarle et al. 2004). The ratio of male to female gametocytes is generally 1:3 as observed in *P. falciparum*, however, the ratio may be variable and vary between clones as discussed (Talman, Domarle et al. 2004, Baker 2010). Additionally, environmental factors might influence the gametogenesis in malaria parasite such as density of parasites, RBC lysis and cyclic AMP metabolism, the presence of anti-malarial drugs, growth inhibitors and immunological factors discussed by (Alano and Carter 1990, Baker 2010). The master regulator of sexual commitment was completely unknown, however recently Sinha et al and Kafsack et al have shown that AP2-G, a conserved member of the parasite specific ApiAP2 family of DNA-binding proteins, is essential for the commitment to sexual stages in *P. berghei* and *P. falciparum* respectively (Kafsack, Rovira-Graells et al. 2014, Sinha, Hughes et al. 2014). Further, recent studies show that expression of *ap2-g* itself is epigenetically regulated by class II histone deacetylases protein - histone deacetylase 2 (Coleman, Skillman et al. 2014) and heterochromatin protein 1 (Brancucci, Bertschi et al. 2014) in *P. falciparum*. A proteomic study of *P. falciparum* detected 1289 proteins, of which 315 are solely present in gametocytes, 103 are shared in between schizonts and trophozoite, 163 shared with gametes and 350 are shared with trophozoites, schizonts, gametes and gametocytes (Lasonder, Ishihama et al. 2002). Gender specific distribution of gene expression has also been shown in the rodent malaria parasite, *P. berghei* gametocytes (Khan, Franke-Fayard et al. 2005). Transcriptional data shows that almost 250-300 genes are specifically up-regulated in *Plasmodium* gametocytes (Khan, Franke-Fayard et al. 2005, Silvestrini, Bozdech et al. 2005, Young, Fivelman et al. 2005). This indicates the expression of a large number of different sets of genes in gametocytes. Considering the importance of gametocytes, sexual stages are regarded to have potential for vaccine and drug development to stop the transmission of malaria (Baker 2010). A wide range of potential surface antigens which can reduce the transmission have been investigated. Current potential TBV candidates are the surface antigens expressed of sexual stages such as P48/45 (Roeffen, Mulder et al. 1996, Bousema, Drakeley et al. 2007), P230 (Eksi, Czesny et al. 2006, van Dijk, van Schaijk et al. 2010) and HAP2 (Blagborough and Sinden 2009, Miura, Takashima et al. 2013) which are essential for fertility of male gametes.

In *P. falciparum*, gametocytogenesis is a long process (8-12 days) and consists of stage I to V which are defined by morphology (Hawking, Wilson et al. 1971, Sinden 2009). A sexually committed merozoite grows and become enlarged and elongated occupying most of the RBC. A stage I gametocyte is difficult to discriminate from trophozoite in Giemsa stain, still typical pigmentation pattern and roundness may be noticeable (Baker 2010). In *P. berghei*, gametogenesis is short (~30h) as compared to *P. falciparum* and therefore different developmental stages I to V are difficult to distinguish and *P. berghei* gametocytes remain spherical. After commitment to the sexual development protein synthesis and haemoglobin digestion decrease while DNA synthesis ceases (Raabe, Billker et al. 2009, Baker 2010, Guttery, Holder et al. 2012). Nucleic acid synthesis is restricted to RNA synthesis which are transcriptionally repressed in female gametocytes in the form of quiescent messenger ribonucleoprotein particles (mRNPs) that include a DDX6 class RNA helicase called DOZI (development of zygote inhibited) (Mair, Braks et al. 2006). Although asexual stages are haploid (N), the DNA content of *P. berghei* gametocytes is more than haploid and less than diploid (~1.2N) most likely due to selective gene amplification (Janse, van der Klooster et al. 1986). Apparently, gametocytes are arrested at G_0 phase of cell cycle (Guttery, Holder et al. 2012).

1.3.3 Mosquito stages

Within the vector, the parasite undergoes multiple transition stages which can potentially be effectively blocked for malaria control which are a) gamete formation and fertilization to zygote; b) zygote to ookinete; c) Ookinete to oocyst and finally d) oocyst to sporozoite development (Beier 1998). As a consequence of the bottleneck in parasite numbers during the early stages of this process (Sinden and Billingsley 2001), the first 24h between gametes and ookinete are likely to be the best potential targets for a transmission blocking strategy. Understanding parasite-vector biology could reveal the mechanisms of parasite development and therefore help design the anti-malaria-transmission strategies.

1.3.3.1 Fertilization and zygote to ookinete transition

The *Plasmodium* parasite enters the vector midgut through the blood meal and gametocytes are activated. Within 10 minutes, gametes (both male and female) start to emerge from

erythrocytes stimulated by a change of environmental conditions, which includes a temperature drop of around 5°C, pH shift to about 8 from 7.3, presence of xanthurenic acid (Nijhout and Carter 1978, Billker, Shaw et al. 1997, Billker, Lindo et al. 1998, Garcia, Wirtz et al. 1998), cGMP dependent activation of Protein Kinase G (PKG) which controls mobilization of Ca^{2+} through regulation of phosphoinositide metabolism (Brochet, Collins et al. 2014).

Unlike the egress of merozoites, egress of gametes is a less well-understood process and has been shown to be blocked with gene deletion or inhibition with the treatment of protease inhibitors such as Pfg377 deletion in *P. falciparum* female gametocytes (de Koning-Ward, Olivieri et al. 2008) or protease inhibitors and PPLP2 deletion in both gametocytes (Sologub, Kuehn et al. 2011, Wirth, Glushakova et al. 2014) and actin-II and PPLP2 in *P. berghei* male gametocytes (Deligianni, Morgan et al. 2011, Deligianni, Morgan et al. 2013) or PbGEST in both (Ponzi, Sidén-Kiamos et al. 2009, Talman, Lacroix et al. 2011). MDV-1/PEG3 (male development-1/protein of early gametocyte 3) has an important role in the mosquito transmission as MDV-1/PEG3 defective male and female gametocytes are largely unable to disrupt PVM and erythrocyte membrane (Lal, Delves et al. 2009, Ponzi, Sidén-Kiamos et al. 2009). Changes in the shape and fusion of osmophilic bodies with the plasma membrane releasing the content in the surrounding PV just before the emergence of gametes cause gametogenesis (Sinden, Canning et al. 1976).

Male gametocytes undergo three successive genome replications from >haploid to octaploid (>N to 8N) and segregation and assembly of each nucleus with the MTOC (Microtubule Organizing Centre), axoneme and tubulin (Sinden, Canning et al. 1976) leading to the release of 8 microgametes, in a process known as exflagellation, while macrogamete DNA content remains >haploid (~1.2N) (Janse, van der Klooster et al. 1986, Janse, Ponnudurai et al. 1988). A Ca^{2+}-dependent protein kinase (CDPK4) is responsible for DNA replication in male gametocytes (Billker, Dechamps et al. 2004) and phosphorylates MAP2 Kinase (mitogen activated protein) which is predicted to regulate cytokinesis in the male gametocyte during exflagellation (Tewari, Dorin et al. 2005).
PPLP2 is dispensable in asexual blood stage, however, is important for male exflagellation highlighting differences in the mechanisms of egress of merozoites and the egress of gametocytes from RBC (Deligianni, Morgan et al. 2013, Wirth, Glushakova et al. 2014). A *Plasmodium* homologue of serine/arginine-rich protein kinase (SRPK) is also essential for

male gamete exflagellation as deletion of *srpk* completely blocks the male gamete exflagellation (Tewari, Straschil et al. 2010). Recently, a copper-transporting P-type ATPase has been shown to be critical for the fertility of both male and female gametes (Kenthirapalan, Waters et al. 2014) and egress from the host cell and the formation of beating flagella is dependent on the functional actin-II (Deligianni, Morgan et al. 2011).

A free microgamete swiftly swims to find a macrogamete and fuses to fertilise. The process of male and female gametes fusion largely remains unknown, yet studied with ultrastructural analysis (Aikawa, Carter et al. 1984, Sinden 1984, Sinden, Hartley et al. 1985) and as explained in section 1.5. In *Plasmodium*, P48/45 is required for gamete adhesion (van Dijk, Janse et al. 2001) and HAP2 is required for fusion (Liu, Tewari et al. 2008), therefore, depicting P48/45 and HAP2 as potential transmission-blocking candidates. After fusion, male nucleus (~1.2N) enters the macrogamete then gives rise to a diploid (2N) zygote which undergoes meiosis (Sinden, Hartley et al. 1985) and becomes tetraploid (4N) (Janse, van der Klooster et al. 1986), however, karyokinesis does not take place. NIMA (never in mitosis/Aspergillus) related Kinases - Nek4 and Nek2 are essential for the DNA replication after fertilization where male and female nuclei remain separate or fuse to form a diploid zygote, however, further development is aborted in Nek4 and Nek2 gene deletion mutants (Reininger, Billker et al. 2005, Reininger, Tewari et al. 2009). Atypical protein kinase 7 (PK7) associated with the melatonin signalling in asexual blood stages of *P. falciparum* (Koyama, Ribeiro et al. 2012) and Cyclin G-associated kinase (GAK) involved in the clathrin-mediated membrane trafficking (Shimizu, Nagamori et al. 2009) play a major role in *Plasmodium* zygote morphogenesis, however, their exact function remains to be elicited (Tewari, Straschil et al. 2010). The zygote is spherical presumably without obvious polarity and undergoes complex changes. The success of fertilization depends on the stored mRNAs in mRNPs as deletion of either DOZI (Mair, Braks et al. 2006) or the Sm-like factor CITH (homolog of worm CAR-I and fly Trailer Hitch) (Mair, Lasonder et al. 2010) inhibit the zygote to ookinete transformation in *P. berghei*. DOZI negative zygotes remains diploid unlike CITH negative zygotes, which undergo meiosis and become a tetraploid but further zygote to ookinete development remains aborted in both gene deletions (Mair, Lasonder et al. 2010). This implies further activation of transcription only after the completion of DNA replication, and development of the zygote as far as meiosis depends on stored mRNAs which include mRNAs of *ap2-o* transcription factor responsible for initiation of ookinete specific gene transcription (Yuda, Iwanaga et al. 2009). It is thought that *de novo* transcription within

a developing ookinete does not initiate until retort outgrowth (approximately until 7-8h post-fertilization) and development of the parasite until retort stage can proceed reliant solely on stored mRNAs (Guerreiro, Deligianni et al. 2014) (A. Srivastava- Waters group, Unpublished). Activation of set of stored mRNAs in developing zygote has been shown to be reliant on a CDPK1 (Sebastian, Brochet et al. 2012).

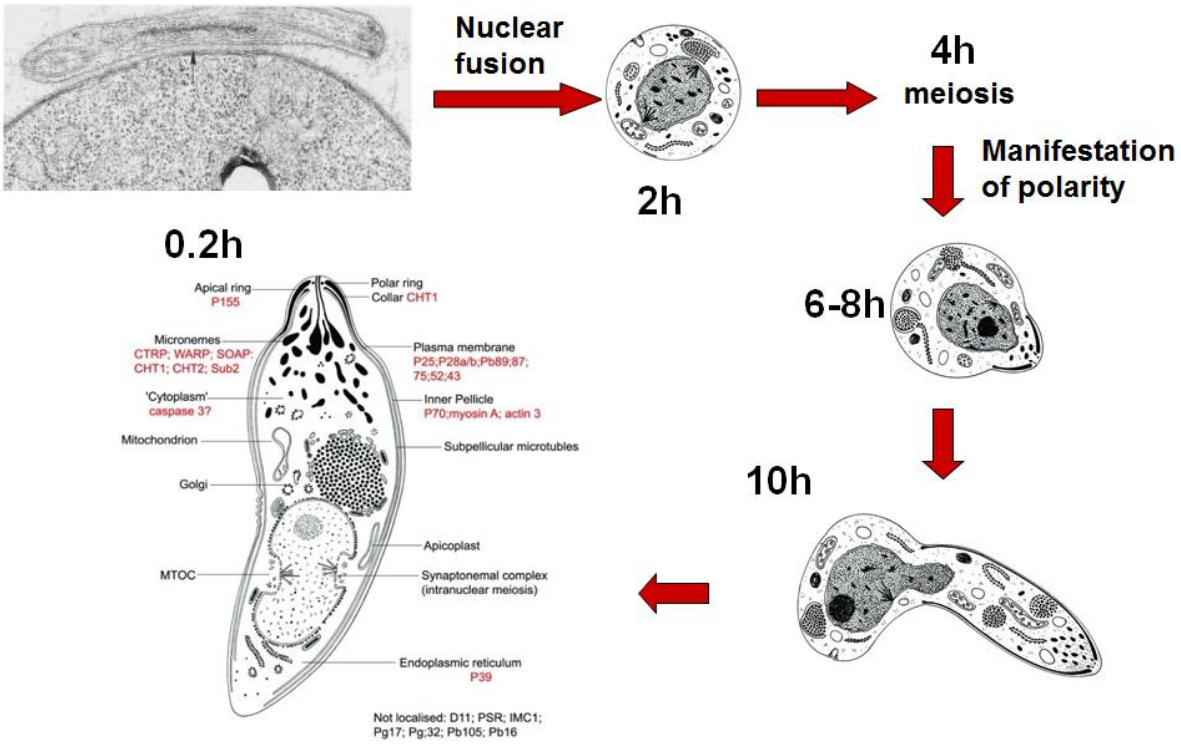

Figure 1.3.2 Development of ookinete from zygote.

Fusion of male and female gametes leads to a spherical zygote which is assumed to be a non-polar cell. After about 2-3h nuclear DNA underdoes meiosis without karyokinesis and cytokinesis and zygote becomes tetraploid. After about 6h apical complex starts emerging from spherical zygote and zygote transforms itself into a banana shaped specialized cell called ookinete, which is invasive, polar and motile.

Source: Prof. A. P. Waters adapted from Sinden (2004) and kindly donated for this thesis.

Microtubules start elongating and after about 6-8h the apical complex starts emerging from zygote (Aikawa, Carter et al. 1984, Sinden, Hartley et al. 1985). In *P. berghei*, the integrity of microtubules is dependent on a Protein Phosphatase with Kelch-Like Domains (PPKL) (Guttery, Poulin et al. 2012, Philip, Vaikkinen et al. 2012) and two unique IMC [reviewed in (Morrissette and Sibley 2002, Santos, Lebrun et al. 2009, Harding and Meissner 2014)] (Inner Membrane Complex is a layer of flattened membranous vesicles present beneath the plasma membrane) sub-compartment proteins (ISP1 and ISP3) are required for apical polarity from gametocytes to ookinete and ISP1 being essential (Poulin, Patzewitz et al. 2013). Within 24h the zygote completely transforms itself into a specialized banana shaped cell called an ookinete which has defined polarity with micronemes, polar ring and collar at its apical end (figure 1.3.2) (Aikawa, Carter et al. 1984, Sinden, Hartley et al. 1985, Morrissette and Sibley 2002). Microneme maturation and differentiation depends on SHLP1 (Shewanella-like protein phosphatase) (Patzewitz, Guttery et al. 2013), paternally donated Formin-like protein MISFIT (Bushell, Ecker et al. 2009) and partially on PPM2 and PPM5 (metallo-dependent protein phosphatases 2 and 5) (Guttery, Poulin et al. 2014). MISFIT is also involved in ookinete DNA replication along with phosphatase PPM2 (Bushell, Ecker et al. 2009, Guttery, Poulin et al. 2014).

The polar ring acts as a MTOC from where subpellicular microtubules extend into the body of the cell. The cell structure is supported with a sac of IMC having an aperture at either of the ends and the space between the plasma membrane and IMC is known as supra-alveolar space (Raibaud, Lupetti et al. 2001). Underneath IMC, subpellicular microtubules extend from the apical end spanning at least ¾ of an ookinete towards the posterior end, the subpellicular network (SPN), and a framework of a family of related IMC proteins recently grouped as alveolins (Gould, Tham et al. 2008) exist. Microtubules appear to be connected to the cytoplasmic side of the IMC via 9nm intra-membranous particles and the IMC shows pores which are predicted to be involved in trafficking of components between parasite endoplasm and supra-alveolar space (Raibaud, Lupetti et al. 2001). Recently, it was identified that a family of six-pass transmembrane proteins, termed the GAPM (Glideosome associated protein with multiple-membrane spans) may have a role in tethering IMC or actin-myosin motor (necessary for parasite motility and invasion) to the cytoskeleton (Bullen, Tonkin et al. 2009). Another vital yet poorly studied organelle of the ookinete is the crystalloid which is also present in young oocysts. The crystalloid contains proteins of LCCL family which are

essential for oocyst to sporozoite progression (Carter, Shimizu et al. 2008, Saeed, Carter et al. 2010, Guerreiro, Deligianni et al. 2014).

Compared with sporozoites and merozoites, ookinetes are the largest motile form of the malaria parasite and develop in an extracellular environment. *P berghei* ookinetes are 7-8 μm long and ~1.5 μm wide and other *Plasmodium* species show some variability. All zoites (merozoites, sporozoites and ookinete) have an apical complex involved in host cell invasion containing various secretory organelles: Rhoptries (required for host cell adhesion and PV formation), micronemes (host cell adhesion and rupture) and dense granules (DG, involved in post-invasion host cell modification) (Kats, Cooke et al. 2008). The apical organelles found in three invasive forms are similar. Most of our understanding of host cell invasion has come from studies on the merozoite as less is known about the apical proteins found in the ookinete and sporozoite. During invasion process, parasite pushes itself into RBC by creating PV with the help of actin-myosin motor (Opitz and Soldati 2002) (Ookinete motility is explained in detail at section 1.4.2), and discharges the content of micronemes, rhoptries and dense granules which are vital for the host cell invasion and intracellular survival of the parasite (Gilson and Crabb 2009, Riglar, Richard et al. 2011). However, microscopic observations denote that ookinete has micronemes and does not have dense granules and rhoptries (Lal, Prieto et al. 2009). This assumption was later validated by the absence of rhoptry proteins in ookinetes (Tufet-Bayona, Janse et al. 2009). Recent findings suggest that microneme proteins have roles in motility and invasion, whereas dense granule and rhoptry components participate in PV formation.

An ookinete microneme proteome analysis has identified 345 proteins including many proteins associated with ookinete infectivity e.g. chitinase, CTRP, SOAP, P28, WARP, CelTOS (See below for more detail about these proteins) and some putative novel proteins such as M1 aminopeptidase and the chaperone, protein disulphide isomerase (Lal, Prieto et al. 2009). Numerous other proteins of known vesicle trafficking (Rab11a, Rab1, Rab6, Rab7, SNARE and many more), motility (MyosinA, MTIP, actin) and signalling (CDPK1 and CDPK4) have also been reported to be part of the microneme, except subtilisin 2 and MAOP (see table 1.3 and description below for more details about these proteins) were not identified (Lal, Prieto et al. 2009). *P. berghei* proteomic and transcriptomic data show up-regulation of tri-carboxylic acid cycle, oxidative phosphorylation and many mitochondrial proteins in gametocytes and abundant in ookinetes, along with up-regulated yet poorly understood BIR

proteins in the mosquito stages indicating pre-adaptation to life in mosquito (Hall, Karras et al. 2005).

P25 and P28 are the predominant surface proteins of ookinete membrane and are similar in human-, rodent- and bird-infectious species of *Plasmodium* (Tomas, Margos et al. 2001). These are synthesized just after the formation of female gamete and expression is enormously increased after 6-12h post-gametogenesis (Kumar and Carter 1985, Fries, Lamers et al. 1990, Paton, Barker et al. 1993, Vlachou, Lycett et al. 2001). Both proteins consist of N-terminal signal sequence followed by three to four epidermal growth factor (EGF) domains and a glycosylphosphatidylinositol (GPI) anchor (Tomas, Margos et al. 2001, Saxena, Singh et al. 2006) and are detected in ookinete surface proteome along with CTRP (circumsporozoite- and thrombospondin-related adhesive protein) (Wass, Stanway et al. 2012)(Wass, Stanway et al. 2012)(Wass, Stanway et al. 2012). P25 and P28 are effective candidates for transmission-blocking vaccine as the antibodies against the P25 and P28 can significantly inhibit ookinete to oocyst development, and functions of P25 and P28 are overlapping to some extent (Tomas, Margos et al. 2001). Possibly, P25 and P28 have a role in the ookinete surface interaction with midgut environment such as protection of the ookinete with midgut lethal factors or recognition, attachment and penetration of midgut epithelial cells where laminin of basal lamina acts as ligand for ookinete attachment (Vlachou, Lycett et al. 2001, Wass, Stanway et al. 2012). P25 structure has been studied in *P. vivax* which shows that PvP25 (*P. vivax* P25) consists of a triangular prism structure made up of four EGF like domains bound to the parasite surface by GPI anchor, and the residues forming triangular structures are conserved in P25 and P28 of all *Plasmodium* species (Saxena, Singh et al. 2006). Homology modelling suggest that PvP28 (*P. vivax* P28) also consist of triangular structure made up of four EGF like domains except the presence of C loop in EGF domain IV (Sharma, Ambedkar et al. 2009). Recently, PvP25 has been to shown to interact with *An. albimanus* midgut microvilli protein calreticulin suggesting its role in midgut recognition (Rodríguez, Martínez-Barnetche et al. 2007).

CTRP is an adhesive protein belonging to *Plasmodium* sporozoite surface protein family called thrombospondin-related anonymous protein (TRAP), and somewhat similar with the circumsporozoite protein (Trottein, Triglia et al. 1995). TRAP family proteins have combination of two adhesive elements - the von Willebrand factor A-domain (A domain) and the thrombospondin type I repeat, a transmembrane domain (TM) and a cytoplasmic tail

domain (Heiss, Nie et al. 2008). CTRP is secreted through micronemes (Lal, Prieto et al. 2009) and essential for ookinete motility (Dessens, Beetsma et al. 1999, Yuda, Sakaida et al. 1999). In *P. berghei*, CTRP is expressed about 10h post-activation (hpa) of gametocytes (Dessens, Beetsma et al. 1999, Yuda, Sakaida et al. 1999) and is required for binding of basal lamina components - collagen and laminin (Arrighi and Hurd 2002, Mahairaki, Voyatzi et al. 2005) but not for *in vitro* oocyst development (Nacer, Underhill et al. 2008).

Chitinase is another important enzyme secreted by ookinete microneme which hydrolyses chitin in peritrophic matrix, the chitin and protein rich thick barrier which is formed after a blood meal and disintegrates following digestion of blood meal (Shahabuddin and Kaslow 1994, Langer and Vinetz 2001) along with other proteases, however, is not absolutely required to overcome the peritrophic matrix (Dessens, Mendoza et al. 2001).

Recent research efforts have elucidated a number of unknown ookinete molecules that may perform vital functions in the mechanism of epithelium recognition, assist in the ookinete adhesion and transverse through epithelial cells such as SOAP (secreted ookinete adhesive protein) is involved in the interactions with mosquito laminin (Dessens, Sidén-Kiamos et al. 2003). Although the oocyst development is reduced in *soap*$^{-}$ *P. berghei* ookinetes, it is not absolutely required for the ookinete to oocyst transformation (Dessens, Sidén-Kiamos et al. 2003, Nacer, Underhill et al. 2008).

PPLP3 also known as MAOP (membrane attack ookinete protein) (Kadota, Ishino et al. 2004) and PPLP5 (Ecker, Pinto et al. 2007) are expressed in the ookinetes and involved in host epithelium membrane rupture and invasion while function of PPLP4 (Raibaud, Brahimi et al. 2006) is still to be verified. Large aggregates of Subtilisin-like protease 2 (SUB2), usually implicated in the invasion process of blood stage merozoites by processing of MSP1 (Merozoite Surface Protein 1) and modifying RBC surface along with other proteases, were found in ookinete invaded mosquito midgut cells while exhibiting a granular localisation pattern in the ookinete cytoplasm. Therefore, SUB2 appears to be secreted into invaded mosquito midgut cells and is probably engaged in disruption of cytoskeleton there (Han, Thompson et al. 2000). Surprisingly, SUB2 and MAOP were not detected in ookinete microneme proteome (Lal, Prieto et al. 2009) or whole cell ookinete proteome (Hall, Karras et al. 2005). Additional proteins implicated in molecular interaction of the ookinete with midgut epithelial cells, invasion and traversal are: enolase interacting with the midgut epithelium and

conversion of plasminogen to plasmin therefore helping invasion process (Ghosh, Coppens et al. 2011), WARP (von Willebrand factor A-domain-related protein) possibly have a role in motility and attachment of ookinetes to epithelium (Yuda, Yano et al. 2001) and CelTOS (cell traversal protein of *Plasmodium* ookinetes and sporozoites) is required for ookinete migration through the epithelial cell cytoplasm to basal lamina i.e. transversal (Kariu, Ishino et al. 2006) [reviewed in (Angrisano, Tan et al. 2012)] (See Table 1.3 for details of proteins involved in ookinete attachment, motility and invasion through the midgut epithelium including some proteins involved in ookinete development).

Ookinetes exhibit three distinct motility patterns: stationary rotation, translocational spiralling, and straight-segment during the invasion of the mosquito midgut epithelium (Vlachou, Zimmermann et al. 2004). The motility of ookinete is achieved through the actin-myosin motor (Opitz and Soldati 2002) embedded in the plasma membrane and IMC (Ookinete motility is explained in detail at section 1.4.2). The motile ookinete leaves the tightly packed blood bolus and invades peritrophic matrix and midgut epithelium tissue and enters haemolymph to develop into the oocyst. Whether ookinete invades a specific cell type of midgut epithelium or not and if the infected epithelium dies or is there any *Plasmodium*/Anopheles species specific variation between invading epithelium remains controversial (Shahabuddin and Pimenta 1998, Han, Thompson et al. 2000, Zieler and Dvorak 2000, Shahabuddin 2002).

Name	Function	Reference
P25	Probably involved in ookinete entry into mosquito midgut and protection of ookinete from midgut enzymes	(Tomas, Margos et al. 2001)
P28	Probably involved in ookinete entry into mosquito midgut and protection of ookinete from midgut enzymes	(Tomas, Margos et al. 2001)
CTRP	Ookinete motility and interaction with basal lamina	(Dessens, Beetsma et al. 1999, Yuda, Sakaida et al. 1999, Templeton, Kaslow et al. 2000, Nacer, Underhill et al. 2008)
Chitinase	Penetration of peritophic membrane	(Dessens, Mendoza et al. 2001, Tsai, Hayward et al. 2001)
SOAP	Ookinete interactions with mosquito laminin	(Dessens, Sidén-Kiamos et al. 2003, Nacer, Underhill et al. 2008)
MOAP/PPLP3	host epithelium membrane rupture and invasion	(Kadota, Ishino et al. 2004)
PPLP5	host epithelium membrane rupture and invasion	, (Ecker, Pinto et al. 2007)
SUB2	Possibly disrupting the actin cytoskeleton on midgut epithelium	(Han, Thompson et al. 2000)
enolase	Interaction with midgut epithelium and plasminogen	(Ghosh, Coppens et al. 2011)
WARP	Motility and attachment of ookinetes to epithelium	(Yuda, Yano et al. 2001)
CelTOS	Oonkine migration through midgut epithelium	(Kariu, Ishino et al. 2006)
M1 aminopeptidase	Possibly protein breakdown in ookinete stages (haemoglobin breakdown in asexual stages)	(Florent, Derhy et al. 1998, Allary, Schrevel et al. 2002, Lal, Prieto et al. 2009, Sahi, Rai et al. 2014, Drinkwater, Bamert et al. 2015)
Putative secreted ookinete protein 2 (PSOP2)	Possible midgut recognition and transversal	(Ecker, Bushell et al. 2008)
Putative secreted ookinete protein 7 (PSOP7)	Possible midgut recognistion and transversal	(Ecker, Bushell et al. 2008)

protein disulfide isomerase	Catalyses the oxidation, reduction and isomerisation of disulfide bonds	(Florent, Mouray et al. 2000, Mahajan, Noiva et al. 2006, Lal, Prieto et al. 2009)
Guanylate cyclase-β	Ookinete motility	(Hirai, Arai et al. 2006, Moon, Taylor et al. 2009)
Protein Kinase G (PKG)	Ookinete motility (studied through inhibitor interactions)	(Moon, Taylor et al. 2009, Brochet, Collins et al. 2014)
Phosphodiesterases δ (PDEδ)	Gametogenesis and ookinete morphology	(Taylor, McRobert et al. 2008, Moon, Taylor et al. 2009)
CDPK3	Ookinete motility	(Ishino, Orito et al. 2006, Siden-Kiamos, Ecker et al. 2006)
SHLP1	Microneme maturation	(Patzewitz, Guttery et al. 2013)
MISFIT	Microneme maturation, ookinete DNA replication, oocyst formation	(Bushell, Ecker et al. 2009)
PPM2	Zygote/Ookinete DNA replication, possibly micromeme development	(Guttery, Poulin et al. 2014)
PPM5	Microneme development	(Guttery, Poulin et al. 2014)
MDV-1/PEG3	Egress of gametes from host cell and reduced ookinete transformation	(Lal, Delves et al. 2009, Ponzi, Sidén-Kiamos et al. 2009)

Table 1.3 *Plasmodium* ookinete proteins associated with midgut transversal.

1.3.3.2 Oocysts and sporozoites development in mosquito

An oocyst is another mosquito stage of parasite which undergoes multiple mitoses to generate up to 13000 haploid sporozoites in an extracellular environment. Little is known about oocyst development. *P. berghei* oocyst size grows in 10-12 days up to 30-40μm in diameter (Thathy, Fujioka et al. 2002), making it one of the largest stages of the whole parasite life cycle. It is surrounded by plasma membrane and a thick capsule containing dividing nuclei and cytoplasmic membranes with a network of flattened cisternae and vesicles at the periphery (Thathy, Fujioka et al. 2002). Oocysts further develop to form a multi-nuclei pool of lobes called sporoblast. Following the assembly of MTOC-subpellicular microtubules, apical complex, nuclei and IMC; sporozoites bud-off from sporoblast. Another GPI anchored protein called circumsporozoite protein (CSP) plays a key role in the oocyst development as *csp*$^{-}$ oocysts are incapable of sporozoite formation (Ménard, Sultan et al. 1997, Thathy, Fujioka et al. 2002). CSP is present and its labelling increases from the surface of lobes in sporoblast till mature sporozoites formation (Thathy, Fujioka et al. 2002). This whole process takes up to 21 days from blood meal to infective salivary gland sporozoites (Sinden and Billingsley 2001, Baton and Ranford-Cartwright 2005). Release of sporozoites from the oocyst is dependent on egress cysteine protease 1 (ECP1) and it also has a vital role after oocyst egress of sporozoites which remains unidentified (Aly and Matuschewski 2005). Once the sporozoites pass the basal lamina and enter into the hemocoel, they are carried away to all the organs via hemolymph circulation and pass through only salivary gland epithelial cells which is mediated by TRAP (thrombospondin-related anonymous protein) (Sultan, Thathy et al. 2001) and several other proteins for example TRAP-like molecule UOS3 (up-regulated in oocyst sporozoites 3) (Mikolajczak, Silva-Rivera et al. 2008), cysteine repeat modular proteins (CRMPs) CRMP-1 and CRMP-2 (Thompson, Fernandez-Reyes et al. 2007), MAEBL (membrane antigen/erythrocyte binding-like) protein (Kappe, Kaiser et al. 2003) reviewed elsewhere (Aly, Vaughan et al. 2009). Gliding motility of sporozoites is mediated by an actin-myosin motor (Opitz and Soldati 2002) which is similar to that employed by ookinetes and merozoites. After crossing the epithelial lining of salivary gland, sporozoites enter secretary cavity where they remain viable for the life of a mosquito and are ready to transmit again into vertebrate hosts. These salivary gland sporozoites, then injected into the new host skin during blood meal of female Anopheles mosquito and travel to liver (Yuda, Sakaida et al. 1999, Ghosh, Edwards et al. 2000, Vanderberg and Frevert 2004, Amino, Thiberge et al. 2006). Although oocyst derived sporozoites (ODS) and salivary gland derived sporozoites (SGS)

show identical morphology under light microscope, *P. berghei* ODS are less infective to mammalian cells than SGS (Matuschewski, Nunes et al. 2002). In agreement to this, the microarray (Mikolajczak, Silva-Rivera et al. 2008) and proteomic profile (Lasonder, Janse et al. 2008) of SGS is different from the proteome of ODS. In *P. gallinaceum*, SGS cannot re-invade the salivary gland if injected into haemocoel, however, can infect chickens. On the other hand, ODS can invade salivary gland but shows reduced infectivity to chickens suggesting the irreparable pattern of programming (Touray, Warburg et al. 1992). This exhibits the differential pattern of regulation of the malaria parasite to acclimatize in mosquito and vertebrate host.

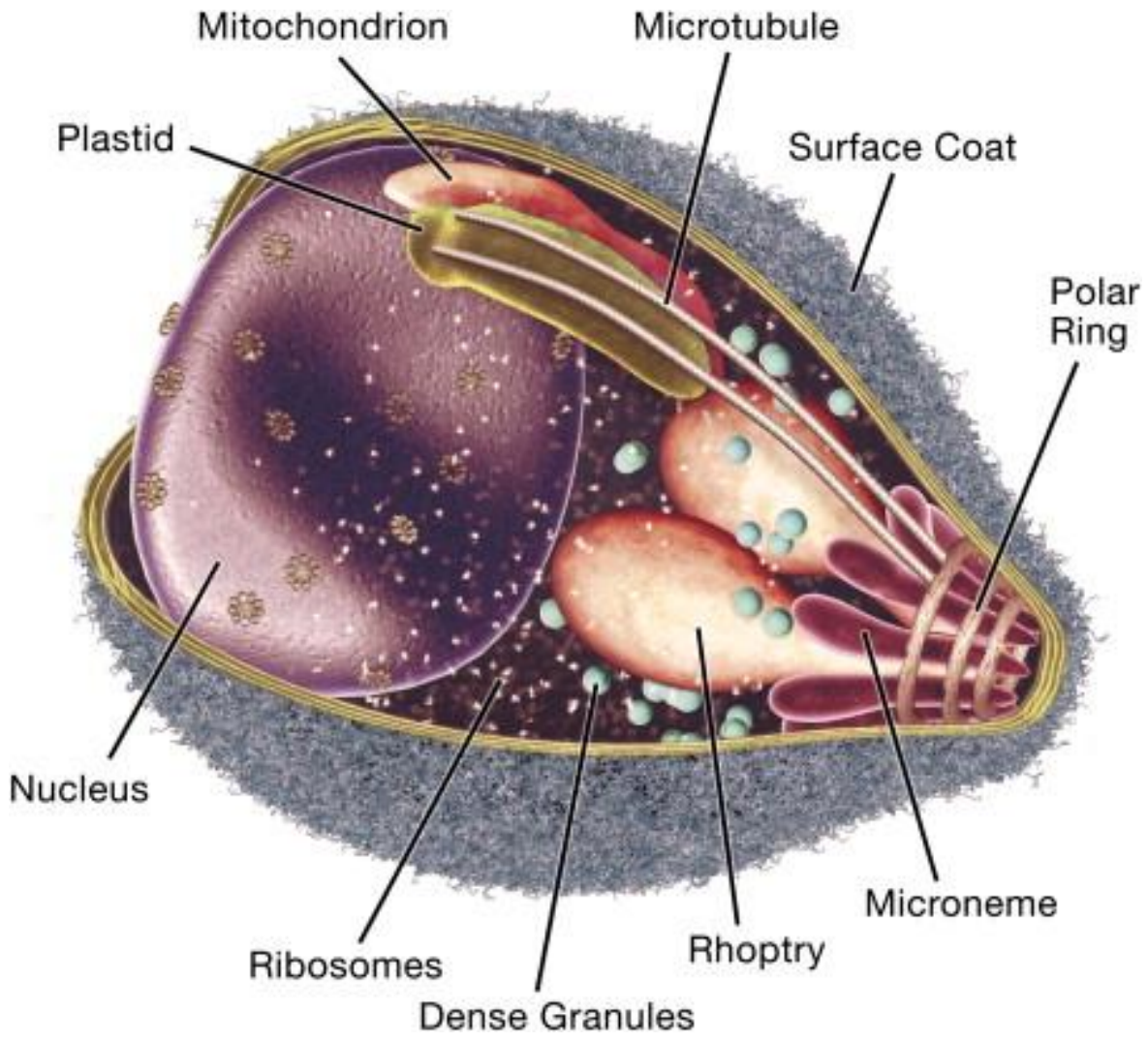

Figure 1.4.1 Structure of apical complex in merozoite.

A merozoite showing apical complex: polar ring, micronemes, rhoptries, dense granules and subpellicular microtubules and internal organelles.

Source: (Cowman and Crabb 2006)

1.4 Cytoskeleton and Inner membrane complex of Apicomplexan parasites

All apicomplexan parasites are obligate intracellular parasites having a very complex cell cycle, involving differentiation into diverse host tissue. All apicomplexan share morphological and replicative similarities and have a collection of unique cell components such as the apical complex and pellicle. The pellicle consists of plasma membrane, IMC and SPN (figure 1.4.2) while apical complex (figure 1.4.1) consists of three specialised secretory organelles: micronemes, rhoptries and dense granules. The apical complex also consists of polar rings, which acts as MTOC, and the conoid.

1.4.1 Apical complex

At the apical end of motile parasite stages subpellicular microtubules gather in a ring like structure called apical polar ring which acts as MTOC (Russell and Burns 1984). The conoid is a cone shaped structure made up of spiral filaments and in *T. gondii*, these filaments are called conoid filaments which are made up of tubulin and share structural features with microtubules but are not microtubules (Hu, Roos et al. 2002). The conoid remains covered under the shell of subpellicular microtubules and is thought to project out with upper polar ring upon calcium signal when parasites are motile in the extracellular environment (Mondragon and Frixione 1996, Hu, Roos et al. 2002). In *T. gondii*, the conoid consists of TgDLC, TgCAM1, and TgCAM2 along with a further predicted 59 proteins (Hu, Johnson et al. 2006). The conoid is supposed to play the mechanical role during invasion and is not present in all Apicomplexans (Morrissette and Sibley 2002) including *Plasmodium* (Morrissette and Sibley 2002). Nevertheless, *Plasmodium* has a cone like electron dense structure with a central aperture surrounding the polar ring in connection with IMC called collar (Moon, Taylor et al. 2009, Philip, Vaikkinen et al. 2012, Sebastian, Brochet et al. 2012).

Micronemes are small oval shaped secretory organelles, through calcium signalling microneme release its content mostly adhesion proteins required for invasion and entry into host cells, also contribute for gliding motility of parasite and egress from the host cell.

Content of *P. berghei* ookinete micronemes (CTRP, SOAP, WARP, chitinase, etc.) and their functions are described above in section 1.3.2.2.

Rhoptries are rather large club-shaped organelles having a bulbous body and narrow neck which pass through the conoid and has opening at apical tip and rhoptries are formed *de novo* in daughter cells (Bannister, Hopkins et al. 2000). *P. berghei* rhoptry proteome suggests that about 36 proteins are localized in rhoptries. Among these potential rhoptry proteins are homologues of known rhoptry proteins, some are proteases and lipid metabolism enzymes, 11 of them are secreted during the host cell invasion and are associated either with RBC membrane or with PVM (Sam-Yellowe, Florens et al. 2004). Rhoptry neck components in *T. gondii* are designated as RON proteins and some of them are conserved in *Plasmodium* (Alexander, Mital et al. 2005). Following microneme secretion, the content of rhoptries is secreted after the attachment of host cell at the beginning of invasion process and involved in PV formation. However, some of the neck proteins studied in *Plasmodium* are reticulocyte-binding homologous (Rh) Rh1/2a/2b/4/5 involved in merozoite invasion [reviewed in (Proellocks, Coppel et al. 2010, Counihan, Kalanon et al. 2013)], and RON 2/4/5 are involved in TJ formation along with microneme protein AMA1 (apical membrane antigen 1). Rhoptry bulb proteins (ROP) are generally distinct (Boothroyd and Dubremetz 2008) and in *T. gondii* ROP proteins have kinase activity. On the contrary, rhoptry bulb proteins studied in *P. falciparum* predicted to have kinase activity and they have been implicated in a variety of roles from rhoptry biogenesis, host cell invasion, PV formation, and host-cell modification, however, the study done about this is limited and is reviewed by (Counihan, Kalanon et al. 2013). Some of the well characterised examples of *P. falciparum* rhoptry bulb proteins are: RAMA (rhoptry associated membrane antigen) is an essential protein thought to be involved in the rhoptry biogenesis and interacts with RAP/LMW (Rhoptry-associated protein/ low molecular weight) complex (Richard, Kats et al. 2009), Rhoptry-associated protein 1 (RAP1) is transferred to PV after the invasion (Richard, Kats et al. 2009) and rhoptry high molecular weight (RhopH) protein complexes have several functions after invasion such as cytoadherance, RBC membranes permeabilization assist in nutrient acquisition and possibly associated with Maurer's Clefts [reviewed by (Proellocks, Coppel et al. 2010, Counihan, Kalanon et al. 2013)].

Dense granules (DG) are microspheres surrounded by unique membrane present in the invasive forms of Apicomplexa (Mercier, Adjogble et al. 2005). Most of our understanding

about DG comes from studies done in *T. gondii* and *Sarcocystis tenella* (Mercier, Adjogble et al. 2005). Unlike micronemes and rhoptries, DG exocytosis is mediated by Rabs and the NSF/SNAP/SNARE machinery and not dependent on intracellular calcium rise (Chaturvedi, Qi et al. 1999). DG membrane fuses with parasite membrane at sup-apical region to release the content and DG secretion appear to take place during the first hour of invasion along with PV formation (Mercier, Adjogble et al. 2005. In *T. gondii*, DG contains a group of small proteins (GRA 1 to 9 proteins) (Mercier, Adjogble et al. 2005). The first identified *Plasmodium* DG proteins are Pf155/RESA (Ring-infected Erythrocyte Surface Antigen) thought to cross PVM and interacts with RBC cytoskeleton, a ring membrane antigen RIMA (Blackman and Bannister 2001) and possibly two subtilisin-like serine proteases PfSUB1 (Blackman, Fujioka et al. 1998) and PfSUB2 accountable for chopping of MSP1 complex and thus allows parasite entry into PV (Barale, Blisnick et al. 1999). However, PfSUB2 was also claimed to be localized to micronemes (Harris, Yeoh et al. 2005) and this is supported by detection of PbSUB2 in midgut epithelium infected with ookinete given the fact *P. berghei* ookinetes lack dense granules.

1.4.2 Pellicle

Although the rhoptry and dense granule structure described above are not thought to be present in ookinete stages of the parasites (Lal, Prieto et al. 2009, Tufet-Bayona, Janse et al. 2009), the Pellicle and underlying IMC structures are present in both the merozoite and ookinete stages. All invasive form (sporozoites, merozoites, ookinetes) cell structures are supported by a pellicle consist of a plasma membrane and underneath plasma membrane a double layer structure of flattened membranous sacs is termed as Inner membrane complex (IMC) (Morrissette and Sibley 2002, Santos, Lebrun et al. 2009, Harding and Meissner 2014). These flattened vesicles are interconnected with the cytoskeleton and provide structural rigidity and shape to the cell, scaffold for daughter cell generation and location for actin-myosin based motor complex called glideosome (Opitz and Soldati 2002) necessary for parasite motility, also helps in host cell invasion (Hu, Mann et al. 2002, Khater, Sinden et al. 2004, Baum, Richard et al. 2006, Jones, Kitson et al. 2006, Agop-Nersesian, Naissant et al. 2009, Bullen, Tonkin et al. 2009, Frénal, Polonais et al. 2010).

The IMC is multi-functional and composed of multiple proteins which can be grouped according to their structure and functions as transmembrane proteins, alveolins (Gould, Tham

et al. 2008) and non-alveolins (Kono, Herrmann et al. 2012). Actin-myosin motor is, situated in between the outer layer of IMC and plasma membrane, composed of a class XIV unconventional myosin - myosin A (MyoA) (Herm-Götz, Weiss et al. 2002), Myosin tail interacting protein (MTIP) (Bergman, Kaiser et al. 2003) and glideosome associated proteins GAP45, GAP50 (Gaskins, Gilk et al. 2004). Recently, additional glideosome associated proteins GAP40 and GAP70 have been identified (Frénal, Polonais et al. 2010). GAP45 acts as a molecular glue connecting IMC in close contact with plasma membrane (Sebastian, Brochet et al. 2012) and GAP50 is a transmembrane protein resides in alveoli (Gaskins, Gilk et al. 2004, Bosch, Paige et al. 2012) and functions anchoring acto-myosin motor complex and possibly GAP40 could also have the role in anchoring motor complex. MyoA is firmly associated with IMC through glideosome complex and MyoA-actin interaction is necessary for parasite motility (Dobrowolski and Sibley 1996, Meissner, Schlüter et al. 2002). During an invasion of host cells, transmembrane proteins of TRAP family released from microneme are thought to make intracellular connection with actin via aldolase (Trottein, Triglia et al. 1995, Dessens, Beetsma et al. 1999, Jewett and Sibley 2003, Baum, Richard et al. 2006, Ramakrishnan, Dessens et al. 2011) and MyoA glides over actin filament pushing parasite in forward direction. IMC is connected to subpellicular microtubules via GAPM proteins which interact with actin-myosin motor as well as SPN (Raibaud, Lupetti et al. 2001, Bullen, Tonkin et al. 2009) as explained in section 1.3.2.2. Further details of the IMC are extensively reviewed by (Harding and Meissner 2014).

A network of intermediate filaments known as subpellicular network (SPN) is located on the cytoplasmic side of IMC which provides mechanical strength to the pellicular membranes (Mann and Beckers 2001, Gould, Tham et al. 2008). Subpellicular microtubules originating from the apical polar ring also provide support to the pellicular membrane and runs almost ¾ towards the posterior end. SPN is composed of family of IMC1 proteins of structurally related to ciliates and dinoflagellate algae protein family called ‘alveolins’ (Gould, Tham et al. 2008). In *Plasmodium*, there are 13 alveolins have been described (IMC1a to IMC1h and IMC1i to IMC1m) (Al-Khattaf, Tremp et al. 2014). Alveolins are expressed at different stages and possess intermittent tandem repeats of 12 amino acids (Al-Khattaf, Tremp et al. 2014). In *P. berghei*, deletion studies have shown that IMC1a is expressed in sporozoites (Khater, Sinden et al. 2004) and immunofluorescence studies detected IMC1a in ookinetes (Philip, Vaikkinen et al. 2012), IMCb is expressed in ookinetes (Tremp, Khater et al. 2008) and IMC1h is expressed in sporozoites as well as ookinetes (Tremp and Dessens 2011, Volkmann, Pfander

et al. 2012) are associated with morphological abnormalities while IMC1c (expressed almost throughout the life cycle) and IMC1e (expressed in mosquito stages, weak expression in blood stages) are essential in asexual blood stages (Tremp, Al-Khattaf et al. 2014). Another novel protein expressed in *P. berghei* ookinetes to sporozoites stages and co-localizes to SPN is G2 (glycine at position 2). PbG2 does not show structural similarity with known alveolins and gene disruption study indicates its role in subpellicular microtubule assembly and parasite transmission is abolished (Tremp, Carter et al. 2013).

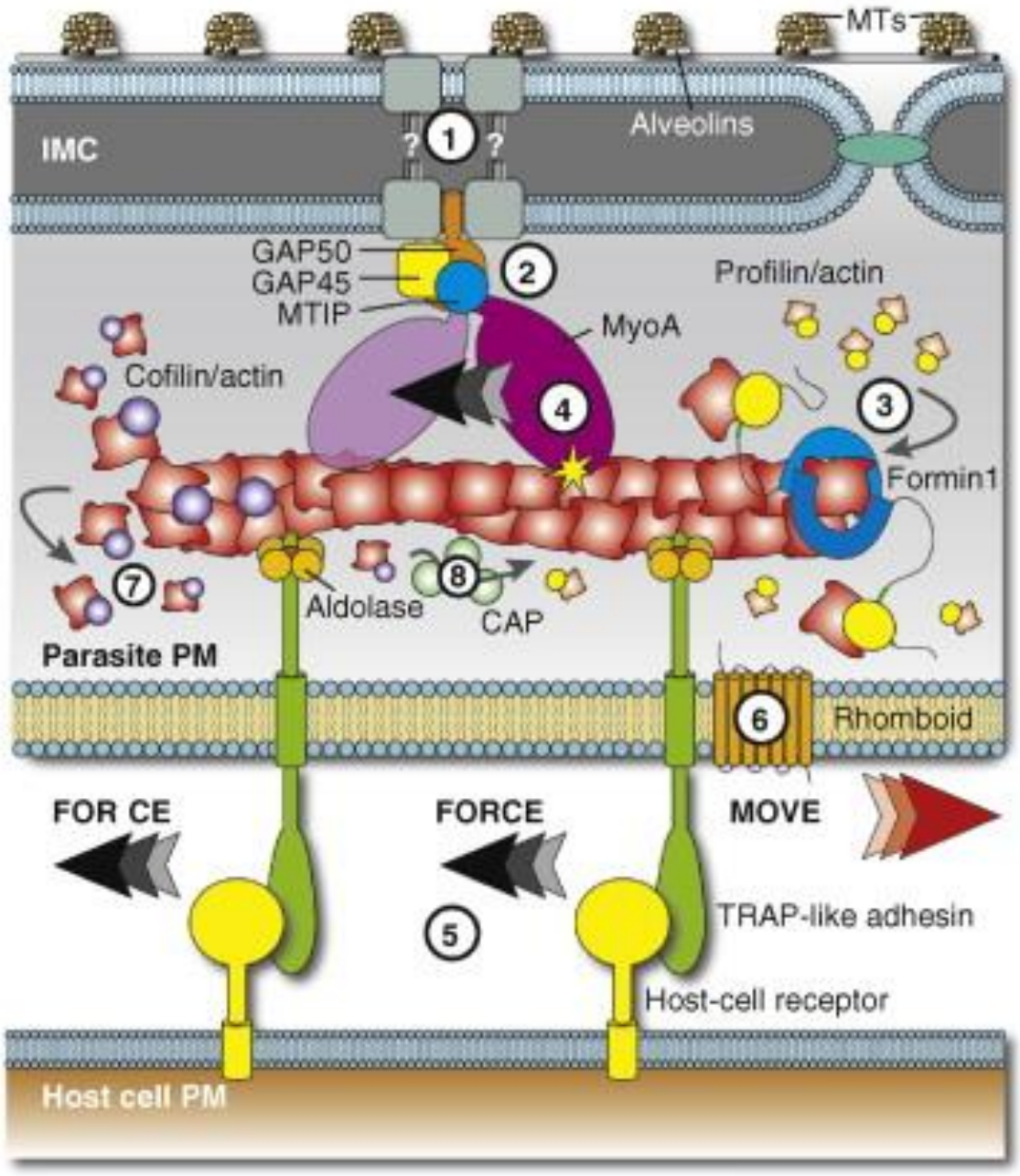

Figure 1.4.2 Model of glideosome and associated IMC proteins.

Schematic of glideosome complex and related IMC proteins of *Plasmodium* and *Toxoplasma* showing invasion of host cell. MyoA is attached to MTIP and connected to IMC by glideosome proteins GAP50 and GAP45. After intracellular signals, actin is polymerised, secreted TRAP like adhesin proteins are moved outward through the parasite plasma membrane and MyoA glides over the F-actin to move parasite. Microtubules are shown connected to IMC and not all the proteins are shown.

Figure adapted from (Baum, Gilberger et al. 2008)

1.5 Comparison of cell biology of replication and daughter cell formation in asexual cells and zygote

The mechanism of apicomplexan cell division is relatively different from the mammalian cell division. The generic eukaryotic cell cycle employs checkpoints e.g. CDK (cyclin dependent kinases) to ensure the regulation of cell development. In G1 phase, cells grow in size and cell cycle checkpoints ensure accurate functions of DNA synthesis machinery while in S phase actual DNA synthesis takes place. During G2 phase, the cell grows and checkpoints ensure preparation for mitosis, a machinery which is divided into four sub-phases: prophase, metaphase, anaphase and telophase. At the beginning of prophase, chromosomes may condense and nuclear envelope partially or completely disappears after division of centrosome (consisting of a pair of centrioles) which acts as MTOC. During metaphase, centromeres (part of chromosomes) are connected to spindle microtubules of MTOC via kinetochores (a DNA binding protein). At anaphase, sister chromatids are pulled in opposite directions towards the spindle poles followed by telophase where nuclear membrane reappears and chromosomes decondense and the cell starts to divide into daughter cells via cytokinesis. G_0 phase may exist after cytokinesis depending on the cell type and its function where cells cease growth and goes into quiescence [reviewed in (Gerald, Mahajan et al. 2011, Francia and Striepen 2014)].

In contrast, in *Plasmodium* parasites the nuclear envelope does not disappear (also known as cryptomitosis or closed mitosis) and this caused difficulties in analysing interactions of chromosomes with spindle microtubules (Read, Sherwin et al. 1993). During asexual blood stages, the apicomplexan parasite undergoes multiple rounds of DNA replication yielding a polyploid cell (syncytium) and nuclear division is initially non-synchronous (Read, Sherwin et al. 1993) though the last round of replication is synchronous (Vaishnava, Morrison et al. 2005) and daughter cells are formed by budding out each haploid nucleus from the plasma membrane, this mechanism is known as schizogony. According to the mechanism to produce progeny cells and the number of progeny cells, the kind of nuclear division and cytokinesis in apicomplexan, cell division can be differentiated into three mechanisms: (1) Schizogony used by *Plasmodium sp.* and *Eimeria tenella* (as described above). (2) endodyogeny - In *T. gondii*, single round of DNA replication and nuclear mitosis occurs followed by assembly of two daughter cells inside the mother cell, which is similar to generic cell division, however, cell division takes place via budding of daughter cells unlike in mammalian cells where cell

fission occurs (3) endopolygony is used by *Sarcocystis neurona* where multiple DNA replications take place without nuclear division with a cell having only a polyploid nucleus and daughter cells are formed at the surface of the mother cell coinciding with last round of mitosis and karyokinesis then the polyploid nucleus packs individual haploid nucleus into each daughter cell [reviewed in (Francia and Striepen 2014)].

Cytokinesis in mammalian cells is a true cell division where a mother cell divides into the daughter cells. Whilst in apicomplexa, cytokinesis occurs via budding and mother cell may split into two or more daughter cells. Assembly of daughter cells has been widely studied in *T. gondii* (endodyogeny) where duplication of centrosome provides cue for development of daughter cytoskeleton scaffold formation which comprise of IMC and subpellicular microtubules. This scaffold grows and after cytokinesis two daughter cells are formed (Hu, Mann et al. 2002, Anderson-White, Beck et al. 2012, Francia and Striepen 2014). The mechanism of *Plasmodium* daughter cell assembly during schizogony largely remains unknown. TgMORN1 a marker of endodyogeny is conserved across apicomplexa (Gubbels, Vaishnava et al. 2006) and is localized to form a ring like structure near each nucleus in late schizonts, however this needs further confirmation (Ferguson, Sahoo et al. 2008). In early schizonts (showing up to 8 nuclei) PfGAP50, GAPM1 and GAPM2 are expressed in daughter cells and localized to developing IMCs of daughter cells (Bullen, Tonkin et al. 2009, Yeoman, Hanssen et al. 2011). GAP45 with MyoA and MTIP are translated in the cytoplasm and form a complex and successively interact with GAP50, likely at IMC (Ridzuan, Moon et al. 2012). Recently, an Aurora-related kinase, *Pfark-1* has been shown to be engaged with SPB (spindle pole body) of a subset of nuclei within individual schizonts (Reininger, Wilkes et al. 2011).

The zygote to ookinete transformation has been studied in *P. yoelii nigeriensis, P. berghei* and *P. gallinaceum* about 30 years ago through ultrastructural analysis (Sinden, Canning et al. 1976, Aikawa, Carter et al. 1984, Sinden, Hartley et al. 1985). During fertilization a male gamete nuclei and axoneme are visible in the zygote (fertilized female gamete) cytoplasm where a male nucleus seems moving towards the female nucleus via ER (endoplasmic reticulum) (Aikawa, Carter et al. 1984). Before fusion the axoneme separates from the microgamete nucleus and chromosomes decondense (Sinden, Canning et al. 1976). In the course of zygote to ookinete development only one round of DNA replication takes place generating a 4N zygote (Janse, van der Klooster et al. 1986) through meiosis (Sinden, Hartley et al. 1985) and unlike schizogony the zygote does not undergo karyokinesis and cytokinesis

rather develops into an invasive ookinete. Successive fertilization with multiple male gametes appeared to be prevented and nucleus of zygote becomes elongated in *P. gallinaceum* (Aikawa, Carter et al. 1984) however, elongated nucleus is not observed in *P. berghei* zygotes (Sinden, Hartley et al. 1985). Within 2h to 2.5h an electron dense structure, possibly the collar (and surrounding pre-IMC) appears just beneath the plasma membrane and near the nuclear membrane/ nuclear tip which grows surrounding the cell. Two centrioles were observed in *P. gallinaceum* zygotes (Aikawa, Carter et al. 1984) but not in *P. berghei* zygotes (Sinden, Hartley et al. 1985) At about 6h post-fertilization of gametocytes, a small tip protrudes out of spherical zygote showing collar, polar ring flanked by the inner membrane complex and subpellicular microtubules and the whole complex grows and defined retort outgrowth is visible with collar and microtubules running towards the posterior end along with the IMC. During this development, the cytoplasm becomes more electron dense with an increase in mitochondrial number, endoplasmic reticulum and Golgi like structures (micronemes) and crystalloids (Aikawa, Carter et al. 1984, Sinden, Hartley et al. 1985). Within 20-24h the zygote completely transforms itself into banana shape (ookinete).

Despite these ultrastructural studies, molecular markers involved in zygote to ookinete development have only just begun to be understood. IMC sub-compartment proteins - PbISP1 and PbISP3 are polarized to the membrane of late female gametocytes and follow the development of zygote retort shape. Ultrastructural analysis shows PbISP1 is majorly localized to IMC near the apical region and marginally with apical collar and polar rings during zygote to ookinete development and both the ISPs are partially co-localise with IMC marker GAP45 and cytoskeletal marker α-tubulin (Poulin, Patzewitz et al. 2013). Alveolar proteins required for normal morphology of *P. berghei* ookinetes, IMC1b localizes to the periphery of protrusion of developing zygote (Tremp, Khater et al. 2008) while IMC1h localises to the periphery of ookinetes and is absent from apical and posterior ends (Tremp and Dessens 2011, Volkmann, Pfander et al. 2012). Another alveolar protein required for sporozoite morphology, PbIMC1a was not detected in ookinetes using anti-GST-tagged peptide (456-632) antibody raised against PbIMC1a (Khater, Sinden et al. 2004), however, it was shown to localise at the periphery and the apical tip of ookinetes excluding only in the apical region (Philip, Vaikkinen et al. 2012). At about 6h post fertilization, PPKL majorly concentrates at the pellicle of the growing zygote. Motility motor proteins - MyoA and MTIP are localised to the periphery with more concentration at apical collar region. Although, secreted microneme proteins - chitinase and CTRP are present throughout the cell cytoplasm,

they are concentrated at the apical tip of the *P. berghei* ookinete as shown by immunofluorescence studies (Philip, Vaikkinen et al. 2012). Additionally PbG2 was identified as a late marker of ookinete, localized to the periphery of ookinete as well as to the apical cap like structure with central aperture (Tremp, Carter et al. 2013). PbMDV-1 localization is found to be dynamic during zygote to ookinete transition, being cytoplasmic in early zygotes to polarized at the apical complex during retort outgrowth and apparently at posterior end of the ookinete (Lal, Delves et al. 2009).

In general, some of the above markers are associated from pre-fertilization of female gamete (e.g ISP1) to mature ookinetes (e.g.G2) and some of them have a critical role in oocysts to sporozoite development. During the zygote to ookinete development, a number of processes are known to happen such as activation of stored mRNAs, translation and delivery of zygote to ookinete developmental and structural markers to their respective location, reactivation of further transcription, secretion of microneme content and apparently assembly of IMC and SPN including microtubule extension remains poorly understood. Further questions such as whether or not the extra plasma membrane is needed for zygote transformation and how plasma membrane delivery is regulated with respect all the above changes remains stimulating. Complex DNA replication mechanisms of *Plasmodium* and all other apicomplexa indicate the molecular machinery engaged in DNA replication is complicated. Despite the unique characteristics of *Plasmodium* cell cycle, homologues of eukaryotic cell cycle regulators - CDK and cyclins are described in *Plasmodium* (Doerig, Endicott et al. 2002, Merckx, Le Roch et al. 2003, Anamika, Srinivasan et al. 2005, Francia and Striepen 2014).

1.6 Generation of cell polarity

All zooites formed by the Apicomplexa are polarized cells exhibiting an asymmetric distribution of content with defined apical and posterior ends. One of the key events during mosquito transmission of the parasite is the initial development from (what is assumed to be) a non-polar zygote to a motile and polarized ookinete. This is essential for the parasite to be able to escape the hostile environment of the mosquito midgut and unique in *Plasmodium* as it occurs out-with a host cell. Although little is known about the generation of polarity in *Plasmodium* species, it has been studied in other organisms. All eukaryotes achieve cell polarity through a conserved set of proteins which includes signalling molecules of the *rho* family of GTPases, cytoskeleton assembly and recruitment, mobilization of proteins from the intracellular pool to the tip of growth via vesicle delivery (Nelson 2003). Although, the *rho* family GTPases such as Cdc42 and its homologues seem to be conserved in majority of organisms studied, there are species specific varieties of polarity determining proteins with little discernible general conservation (Chant 1994).

1.6.1 Apical organelles and generation of polarity in fungi

In fungal systems, the proteins involved in hyphal tip growth and polarity all together constitute a polarisome or sometime referred Spitzenkórper (SPK) which drives the growth of cell in a defined direction. Currently, the development of polarity is a popular topic in filamentous fungus and yeast. SPK is mainly associated with fungal cell morphogenesis, present at actively growing tips/ hyphae and vanishes when growth terminates and consists of microfilaments, microtubules, micro and macrovesicles and ribosomes (Grove and Bracker 1970, Howard 1981, Riquelme and Sánchez-León 2014). Recycling of SPK vesicles is very rapid and occurs in minutes (Dijksterhuis and Molenaar 2013), however, very little is known about the content of these vesicles. Nevertheless, it can be expected to contain components of the cell membrane, proteins needed for membrane extension, fusion and signalling molecules since it is present at the growing end.

The few components identified in such vesicles are Rab GTPase sec4 homologue in Aspergillus Niger (Billker, Lindo et al. 1998), plenty of chitin synthase containing vesicles (chitosomes) near the hyphal tip in Ustilago maydis (Weber, Assmann et al. 2006), in

Aspergillus nidulans (Takeshita, Ohta et al. 2005) and in Neurospora crassa (Sietsma, Beth Din et al. 1996). N. crassa also shows the presence of GS-1 - a protein required for synthesis β-1,3-glucan (component of cell wall) in SPK (Verdín, Bartnicki-Garcia et al. 2009) indicating cell wall synthesis and secretion are polar processes. In Aspergillus nidulans, FlbB a protein involved in sexual morphogenesis is localised to SPK suggesting SPK might serve as a signalling hub for coordinating developmental transitions (Etxebeste, Herrero-García et al. 2009). Cytoplasmic calcium plays a significant role in eukaryotic signal transduction and it seems to be present at the tip growth of polarised cell; likewise a high calcium gradient is seen at the hyphae tip growth of N. crassa (Silverman-Gavrila and Lew 2001, Torralba, Heath et al. 2001). Cell secretary and endocytic pathways are heavily reliant on the cytoskeleton for their proper functioning where myosin, kinesin and dyneins have been shown to be involved in membrane trafficking (Goodson, Valetti et al. 1997). Some consequences of kinesin and dynein deficiency are the loss of establishment of SPK and reduced numbers of vesicles in SPK respectively (Seiler, Nargang et al. 1997, Riquelme, Roberson et al. 2002). In Aspergillus nidulans, actin associated motor proteins- MyoA and MyoE (Myosin E) are enriched at the hyphal tip growth. MyoA is essential for viability and necessary for polarised growth, secretion and plays role in endocytosis (McGoldrick, Gruver et al. 1995, Yamashita and May 1998, Yamashita, Osherov et al. 2000). MyoE is responsible for moving vesicles to SPK while MyoB (Myosin B) is required for septation and branching and not present in SPK (Taheri-Talesh, Xiong et al. 2012). Together with vesicles, microfilament and microtubule; the presence of ribosomes is also reported in the SPK indicating the active translation at the hyphal tip (Grove and Bracker 1970, Howard 1981). The exocyst, a multi-protein complex required for the final step of the exocytosis, helps tethering vesicles to plasma membrane and is necessary for the formation of SPK in N. crassa (Riquelme, Bredeweg et al. 2014). Proteins involved in the polarisome could be transported to the apical complex by one of two mechanisms: (1) proteins synthesized in cytoplasm and moved to vesicles through the signal sequence to transport to apical complex (2) mRNAs are moved to the apical complex and then translated (localized translation). It is not clear whether the polarisome is same as the SPK or part of it, but both of them share many components. A key unanswered question is what determines the position of tip outgrowth. Observations of filamentous branching of an Aspergillus niger ‘ramosa’ mutant suggest that SPK vanishes before new branches are formed (Reynaga-Pena and Bartnicki-Garcia 1997). This indicates the site selection of polarity might be spontaneous by ‘symmetry breaking’ or involves other mechanisms such as external cues (cell-cell contact, chemo-attractants or morphogen gradients) implicating signalling proteins

(e.g. Cdc42 and Cdc24 mechanism) in which case the SPK is only required for maintenance of polarity (Virag and Harris 2006).

During mating, pheromones secreted by opposite partners are sensed through G protein signalling pathway which further directs the formation of polarity in yeast (Johnson 1999). Chant (Chant 1994) reported that the cell builds an axis of polarity first which is controlled by conserved Rho family GTPase- Cdc42 in yeast, *Saccharomyces cerevisiae*. The cytoskeleton is established corresponding to the axis of polarity marking front and back and other organelles orient accordingly. Most of the bud selection markers are transmembrane proteins (TM) which can interact with GTP and GDP bound state governed by GEF (GDP/GTP exchange factor or Guanine nucleotide exchange factor) and GTPases and apparently interacts with Cdc42 (Park and Bi 2007). In support of this, Bud1 (also known as Rsr1), a ras-like GTPase mediates polarity in yeast through activation of Cdc42. Rsr1, a marker of bud selection site, is evenly scattered on the plasma membrane and interacts with itself to form a homodimer and its GDP-GTP exchange factor Bud5 along with Cdc42 and Cdc24 (GEF of Cdc42) (Park, Kang et al. 2002, Kozminski, Beven et al. 2003, Kang, Béven et al. 2010). According to recent study, *S. cerevisiae* shows multiple polarity (bud) selection sites where only one final polarity site wins and the polarity complex is possibly stabilized by actin (Wu, Savage et al. 2013). Activation of Cdc42 leads to its localization at the selected bud site (Howell and Lew 2012) and is governed by GEF and GAP (GTPase-activating protein) regulators. Cdc42 and Cdc24 are the central proteins to cell polarity development and deletion of *cdc42* and *cdc24* is not possible in yeast showing its essentiality. Temperature sensitive *cdc42* and *cdc24* mutants of yeast show all the internal growth patterns except bud formation is ceased (Sloat, Adams et al. 1981, Johnson and Pringle 1990). Cdc42 recruits and utilises variety of effector proteins such as Bem1 to form polarity complex whereby activating formins (e.g.Bni1p and Bnr1p). Actin filaments nucleation mediated by formins is essential to establish the delivery of secretory vesicles towards the bud site (Evangelista, Zigmond et al. 2003, Chen, Kuo et al. 2012). Furthermore, Cdc42 diffuses from the bud site and regulates the vesicle trafficking towards the bud site in order to maintain the polarity of the cell. The role of vesicle trafficking in polarity establishment in higher eukaryotes is explained in section 1.6.2.

1.6.2 Generation of polarity across various cell systems

Cell polarity is vital to carry out specific functions such as cell growth, migration, protein transport and invasion (Nelson 2003). Proteins involved in the regulation of mammalian epithelial cell polarity can be grouped as 1) Par proteins (localized to the sub-apical region) 2) Crumbs complexes (also localised to the sub-apical region) 3) Scribble complex (localised at the baso-lateral region) 4) Planer polarising Vang and Frizzled complex (Muthuswamy and Xue 2012). These proteins interact with each other during polarity development and are often found altered in cancer (Muthuswamy and Xue 2012). Polarity establishment and development is regulated by internal as well as external factors. Internal factors such as protein trafficking, microtubules and actin dynamics while external factors are cell-cell and cell-matrix interactions regulate the cell polarity in epithelium [reviewed in (Muthuswamy and Xue 2012)]. Here we discuss the protein trafficking and its regulation via Rab GTPase across various cell systems.

Protein trafficking is important for the establishment and maintenance of cell polarity, and epithelial cells use both exocytic and endocytic pathway for polarity development (Nelson and Yeaman 2001). Membrane targeted proteins transported from ER to Golgi and apparently to the membrane with the help of coat proteins such as COPII, COPI and adapter protein complex (e.g. AP-1, AP-2, AP4 and AP-1B). Apparently, SNAREs (soluble N-ethylmaleimide-sensitive factor attachment protein receptors) proteins (e.g. Syntaxins - STX1A, STX1B, STX2, STX3 and STX4) assist in docking and fusion of protein containing vesicles at the membrane (Muthuswamy and Xue 2012, Keder and Carmena 2013). Other major regulators of protein trafficking are Rab GTPases, among them Rab8 (Esseltine, Ribeiro et al. 2012) and Rab11 [reviewed in (Jing and Prekeris 2009)] have direct link in the establishment of polarity.

1.6.3 Introduction to Rab GTPases

The members of Ras GTPase subfamily (Ras, Ral, Rap, Rho and Rab) are majorly involved in cell growth, differentiation and survival [reviewed in (Reuther and Der 2000, D'Adamo, Masetti et al. 2014)]. Rab proteins belong to a small Ras GTPase family and regulate vesicle transport in eukaryotes. To date, about 70 *rabs* have been found in humans demonstrating the

potential complexity of vesicle transport [reviewed in (D'Adamo, Masetti et al. 2014)]. Small GTPases are active when bound to GTP and remain inactive in GDP bound form. Complexity of GTPase function is achieved by the huge number of interacting proteins, among those most common are: Guanine nucleotide exchange factors (GEFs), helping to bind GTP to small GTPases (activating GTPases), associated with membranes; GTPase activating proteins (GAPs) which help GTPases to dissociate from GDP (inactivating GTPases). Guanine nucleotide dissociation inhibitors (GDIs) help small GTPase having a farnesyl or the geranylgeranyl group in their C-terminus in cytosol/ membrane alterations [reviewed in (Behnia and Munro 2005, Cherfils and Zeghouf 2013)]. Conservation of Rab GTPases in eukaryotes from yeast to mammals indicates the importance of Rab GTPase during cell development. Small GTPases and their regulators including GEFs, GAPs and GDIs operate critical pathways for cell development and therefore are linked to many human diseases such as cancer, cardiovascular, infectious and developmental diseases [reviewed in (Finlay 2005, Newey, Velamoor et al. 2005, Tidyman and Rauen 2009, Loirand and Pacaud 2010, Vigil, Cherfils et al. 2010) respectively]. Generally, Rab GTPases are involved in protein trafficking and endocytic recycling and some of them are predicted to be involved in plasma membrane delivery [reviewed in (D'Adamo, Masetti et al. 2014)], and Rab GTPases are also known to interact with cytoskeletal components.

1.6.4 Role of Rab GTPases in protein trafficking

Rab11 and its effector Rip11 have been found to regulate apical membrane trafficking in epithelial cells (Prekeris, Klumperman et al. 2000). Polarised cells such as Madin-Darby Canine Kidney (MDCK) cells exhibits domain specific early endosomes such as apical (distributed in the apical plasma membrane to the nucleus) and basolateral early endosomes (distributed down in basolateral plasma membrane) to carry out protein transport in respective region (Apodaca, Katz et al. 1994, Matter and Mellman 1994). E-cadherin, required for cell polarity and cell-cell contact, is localized to the Rab11 positive intermediate compartment in HeLa and MDCK cells. A rab11 mutant (constitutively active Rab11Q70L-GFP) disrupts the localization of E-cadherin in polarised MDCK cells suggesting a significant role of Rab11 in targeting proteins involved in polarity development (Lock and Stow 2005). In intestinal epithelial cells, the localization of atypical Protein Kinase C (aPKC) and Ste20 family kinase Mst4 (responsible for phosphorylation of ezrin - a protein important for the apical plasma membrane and microvilli development in a variety of epithelial cells) to the apical region is

dependent on Rab11A and Myosin Vb (Dhekne, Hsiao et al. 2014). In mammalian cells, Rab11 endosomes have been shown to carry microtubule nucleating materials at spindle pole (Hehnly and Doxsey 2014) (figure 1.7B).

Neurons are highly polarised and differentiated cells with distinct dendritic and axonal domains, internally carry differential compartments to carry biochemical signals and therefore the range of Rabs regulate the vesicle trafficking involved in a variety of functions [reviewed at (Villarroel-Campos, Gastaldi et al. 2014)] for example Rab10 binds kinesin1 through the adaptor protein JIP1 and regulates the transport of vesicles towards the axonal outgrowth of hippocampal neurons (Deng, Lei et al. 2014), Rab8 (involved in the regulation of trafficking, docking and fusion of intracellular membrane compartments) regulates endocytosis of mGluR1a (metabotropic glutamate receptor1a), a neurotransmitter receptor (Esseltine, Ribeiro et al. 2012). Plus, it has been shown that Rab35 activates other Rabs (Rab8, Rab13 and Rab36) through a common interacting protein MICAL-L1 during neurite outgrowth of PC12 cells indicating a novel mechanism by which master Rab can recruit multiple Rabs during cell growth (Kobayashi, Etoh et al. 2014). Additional forms of Rabs are present and some of them belong to TGN while other resides in endosome network and their role might vary depending on the cell system. A detailed description of Rab proteins involved in neurite development is given in Table 1.6. Furthermore, Cdc42 and other members of Rho and Rac family seem to be associated in the animal neuronal biology where they recruit downstream signalling components such as Par proteins and aPKC (Horton and Ehlers 2003).

Other models studied for polarity establishment are Drosophila and *Caenorhabditis elegans*. The regulators of Drosophila apical polarity also include Cdc42, aPKC, Crumbs and adaptor or scaffolding proteins (Tepass 2012). In *Drosophila*, Rab11 is shown to regulate oocyst polarization: OSK protein is localized to the oocyst posterior end and is required for the formation of pole cells and abdominal segment. The localization of *osk* mRNA at the posterior pole is Rab11 dependent whereas OSK itself is also required for partial localization of Rab11 at the oocyst posterior pole (Dollar, Struckhoff et al. 2002), therefore Rab11 plays a key role in determining the sub-cellular localization of both mRNA and protein. Moreover, Rab6 is shown to be involved in secretion, organisation of microtubule plus end at the posterior end of the oocyst and transportation and localization of *osk* mRNA (Januschke, Nicolas et al. 2007). In *F. distichus,* Rho family member Rac1 has been shown to localise zygote undergoing rhizoid tip growth (Fowler, Vejlupkova et al. 2004). This suggests that

Ras/ Rho family GTPases and their effectors are versatile proteins involved in the variety of cellular processes.

Protein	Localization	Effect on neurite elongation	Experimental models	References
Rab6	TGN	Promotes elongation through exocytotic trafficking	Primary neurons	Schlager et al. (2010)
Rab8	TGN, RE	Promotes outgrowth through polarized transport and actin relocalization	Primary neurons, fibroblasts	Huber et al. (1995) and Hattula et al. (2006)
Rab10	TGN	Positive regulator of secretory vesicles transport and neurite growth	Primary neurons	Wang et al. (2011b)
Rab13	TGN	Enhances outgrowth via exocytotic transport and actinin-4 relocalization	DRG, PC12 cells	Sakane et al. (2010) and Di Giovanni et al. (2005)
Rab5	EE	Inhibition and promotion have been described	Primary neurons, PC12 cells	Liu et al. (2007) and Mori et al. (2013)
Rab7	LE	Reduces TrkA signaling in endosomes, inhibiting neurite outgrowth	PC12 cells	Saxena et al. (2005)
Rab21	EE	Both positive and negative effects have been reported	Primary neurons, PC12 cells	Wang et al. (2011a) and Burgo et al. (2009)
Rab22	EE	Increases elongation through its effector Rabex5	PC12 cells	Wang et al. (2011a)
Rab11	RE	Promotes elongation through membrane trafficking and integrin recycling	Primary neurons, DRG, PC12 cells	Takano et al. (2012) and Eva et al. (2010)
Rab17	RE, EE	Enhances dendritic growth and branching	Primary neurons	Mori et al. (2012)
Rab35	RE	Promotes elongation through Arf6 inactivation and EHD1 recruitment to RE	PC12 and N1E-115 cells	Chevallier et al. (2009) and Kobayashi and Fukuda (2013)
Arf6	RE	Inhibits dendritic growth and branching, the axonal effect is not clear, although it seems to be also a negative regulator	Primary and retinal neurons, PC12 and N1E-115 cells	Hernandez-Deviez et al. (2002, 2004)

Tables 1.6 of Rab GTPase with subcellular localization and their functions in immortalised cell lines.

Reviewed by (Villarroel-Campos, Gastaldi et al. 2014) (Published with permission)

(A)

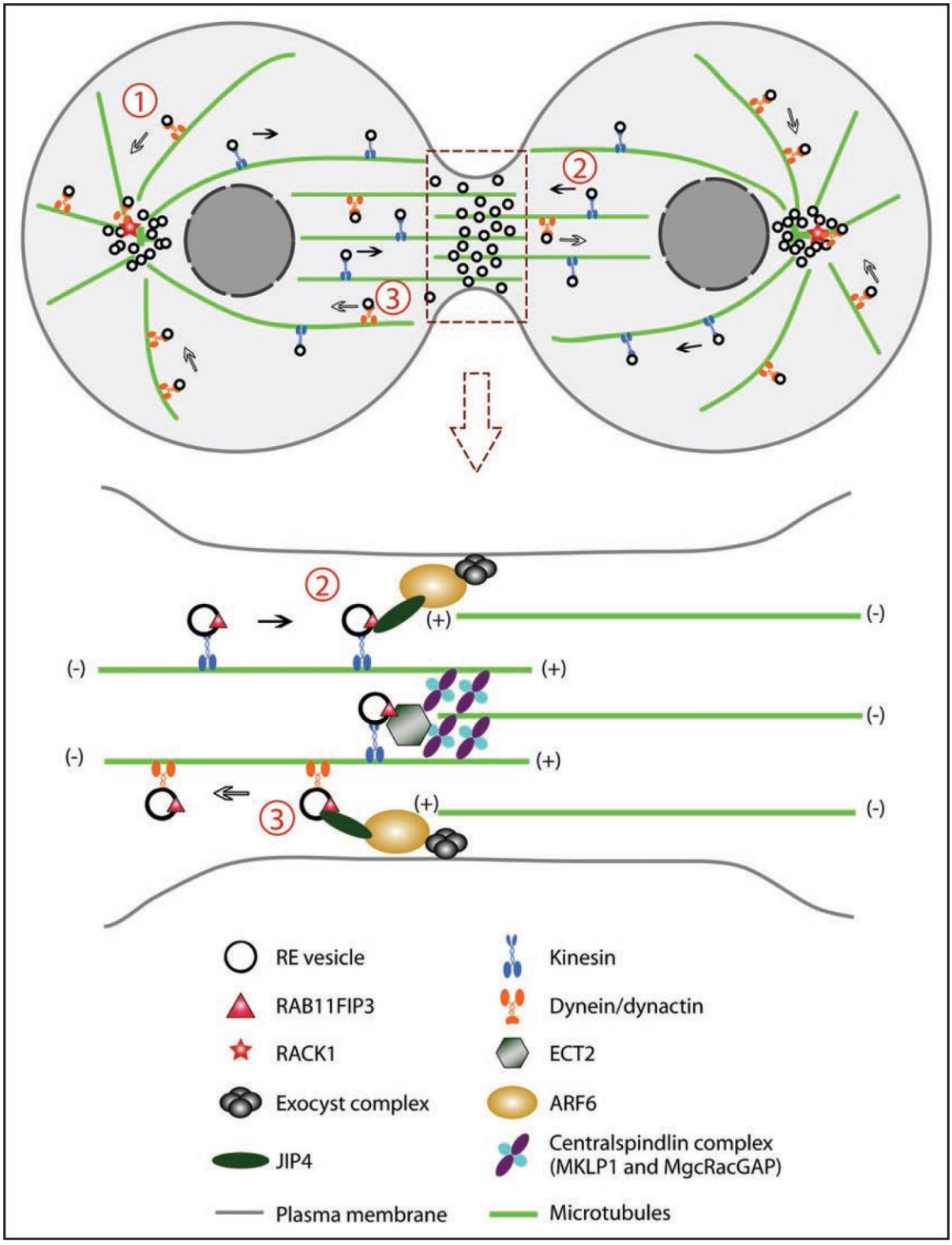
1
2
3
(+)
(-)
RE vesicle
RAB11FIP3
RACK1
Exocyst complex
JIP4
Plasma membrane
Kinesin
Dynein/dynactin
ECT2
ARF6
Centralspindlin complex
(MKLP1 and MgcRacGAP)
Microtubules

(B)

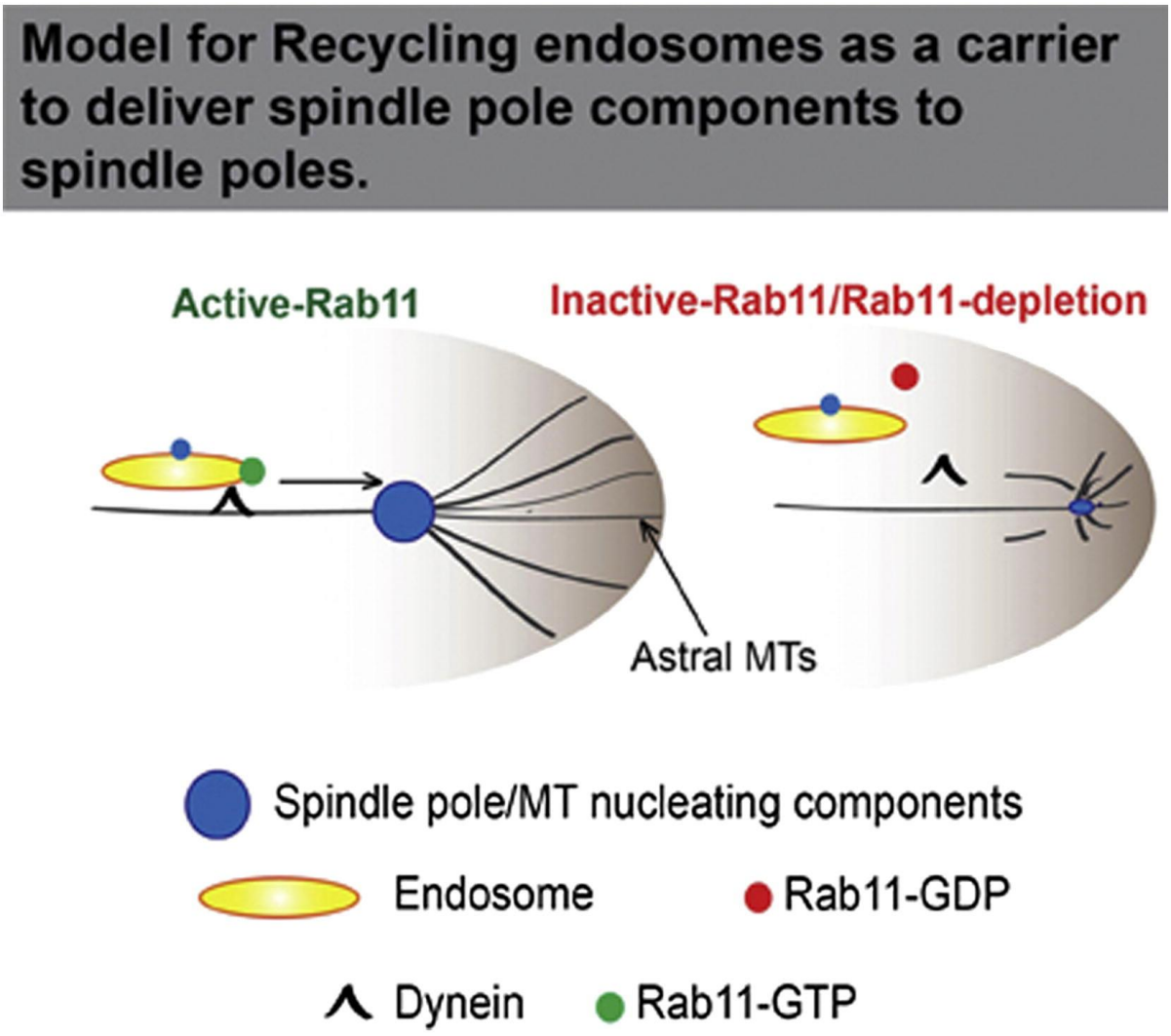

Figure 1.7 Models show role of Rab11 in microtubule nucleation and cytokinetes.

(A) Recycling endosomes travel through kinesin towards the cleavage site and donate the plasma membrane and are directed back to MTOC via dynein/ dynactin motors in animal models. Taken from (Ai and Skop 2009) (B) Model depicting Rab11 mediated endosomes carry microtubule nucleation components in human osteosarcoma cell line (U20S, HeLa) Taken from (Hehnly and Doxsey 2014).

1.7 Hypotheses

The aim of our study is to define the establishment and development of polarity in the malaria parasite, specifically the developing zygote. Since the active presence of Rab GTPases, regulators of protein tracking, in *Plasmodium* we asked if Rab GTPases might be responsible for either establishment, maintenance or in both the processes of polarity in *Plasmodium*. We particularly focused towards the Rab11A considering its previously described role in polarity development, microtubule nucleation and cytokinesis in higher eukaryotes. Rab11A is predicted to be associated with apicomplexan cytokinesis. Further, Rab11A transcript is abundant and is translationally repressed in *P. berghei* gametocytes. Therefore, we asked whether or not Rab11A has role in the establishment and development of *P. berghei* ookinete polarity.

Moreover, fertilization is important for the establishment of polarity in single cell embryo in *C. elegans* and fertilization process or a marker (e.g. centrins donated by male gametes in *C. elegans*) are critical for further development of embryos/ zygote in many organisms. Fertilization is not well studied in *Plasmodium* and it is unknown whether or not fertilization is important for establishment of polarity and/or further development in *Plasmodium*. Therefore, we also asked if the male gamete fusion site (point of male gamete fusion on the female gametes surface) cues for the polarity development in *Plasmodium* zygotes.

Thus, in *Plasmodium*, our research questions are:

1) Is Rab11A involved in the establishment and development of zygote polarity?

2) Is the point of microgamete fusion on the macrogamete the determinant for polarity in the ookinete?

1.8 *Plasmodium berghei*: model for malaria research

The focus of this research project is transmission stages, particularly gamete fertilization and ookinete development in the rodent malaria parasite, *P. berghei* as the cultivation of sexual stages of human malaria parasite, particularly *P. falciparum* is difficult. Furthermore, use of *P. falciparum* infected mosquitoes brings important safety considerations. On the other hand, *P. berghei* is extensively studied as a model for human malaria because much of the basic biology of human and rodent malaria is similar, also the genome organization and genetics is generally conserved (Matz and Kooij 2015). *P. berghei* offers a variety of techniques for genetic modification, *in vitro* cultivation of sexual stages on a large scale and to analyse various stages of the life cycle. The whole life cycle of *P. berghei* can be studied *in vivo* routinely and safely as it is not infectious to humans. The molecular basis of drug sensitivity and resistance is also similar in human and rodent malaria parasites. Moreover, the structure and function of potential candidates for vaccine development are analogous (Leiden_Malaria_Research_Group). Three participants in rodent malaria: *P. berghei*, rodent (mouse) and mosquito can be genetically modified and their genomes are known. Therefore, the rodent malaria parasite *P. berghei* can be employed for *in vivo* host parasite interactions. For these reasons studying *P. berghei* can shed light on the essential biology of *P. falciparum*.

1.9 Review of available techniques used for genetic modification of *Plasmodium*

Classical reverse genetic approaches cannot be employed for many blood stage haploid genes in *Plasmodium* since their deletion is lethal, e.g. Rab11A precluding their analysis by this approach in *P. berghei* asexual stages (Agop-Nersesian, Naissant et al. 2009). Therefore, conditional *Plasmodium* gene knockouts/knockdowns systems are required. In one approach called promoter exchange or promoter swap, the promoter of an essential blood stage gene is replaced by that of a blood stage active gene that is silent at the later stage of interest. For example, MyoA of *P. berghei* (PbMyoA) was expressed under *ama-1* promoter maintaining PbMyoA expression in blood stage development but turning off PbMyoA during gametocyte/zygote/ookinete development (Siden-Kiamos, Ganter et al. 2011). Similar approaches have been described elsewhere validating the approach (Laurentino, Taylor et al. 2011). However, protein can be carried over from the previous stage and leakiness may be observed depending upon the promoter used to make the approach potentially problematic.

Another approach called protein destabilization domain (DD) system uses the fusion of the destabilization domain of FKBP (ddFKBP) to protein under study which is targeted for degradation and stabilized when the ligand is present (Armstrong and Goldberg 2007, Striepen 2007). DD system is shown to work well in *P. falciparum*. However, the DD system is not always perfect and shows leakiness so that the amount of protein degradation is not enough to produce the phenotype. Furthermore, loss of protein function or mis-targeting of fusion proteins might occur and the system cannot be adapted for use with *P. berghei* since it requires the continuous binding of the small ligand Shield to stabilise the protein which is both very expensive and of unknown pharmacodynamic behaviour in the mouse bloodstream. Tight regulation is shown to work in a tetracycline regulatable system in *T. gondii* and less well in *P. falciparum* (Meissner, Krejany et al. 2005) and *P. berghei*, however has difficulties to apply at mosquito stages (Pino, Sebastian et al. 2012). Transcript knock down by antisense RNA has been reported in *Plasmodium* (Gardiner, Holt et al. 2000), however, there remain doubts about its specificity and efficacy.

In case of knockdown of proteins one cannot assay the phenotype immediately because of either the presence of a little amount of proteins or activation of supplementary pathways. And therefore re-routing of the protein of interest from its pocket of activity to somewhere

else is called Knock Sideways (Robinson, Sahlender et al. 2010, Hirst, Borner et al. 2012) has been applied to *P. berghei* (K. Hughes -Waters group, Unpublished data). RNA interference (RNAi) is not applicable in *Plasmodium* as some of the key enzymes required for RNA interference are absent (Baum, Papenfuss et al. 2009). However, the site specific recombinases (integrase family of recombinase) such as Cre recombinase/ loxP system have been shown to work in *T. gondii* (Brecht, Erdhart et al. 1999, Andenmatten, Egarter et al. 2013) and Flp/frt function in *P. berghei* (Lacroix, Giovannini et al. 2011). A plant derived auxin-inducible degron system (Nishimura, Fukagawa et al. 2009) has been shown to work in *P. falciparum* (Kreidenweiss, Hopkins et al. 2013) and is under application in *P. berghei* (N. Philip- Waters Group, Unpublished) along with Cre recombinase/ loxP system (R. Cameron, A Graham, R. Kent - Waters and Meissner group, Unpublished data).

Recently, a glucosamine dependent gene regulation of target genes bearing a glmS ribozyme in the 3′ untranslated region (UTR) has been described in *P. falciparum* (Prommana, Uthaipibull et al. 2013) along with highly efficient genome editing with customized zinc-finger nucleases (ZNF) (Straimer, Lee et al. 2012). Although, ZFN is highly efficient, it is not popular being time consuming, costly and laborious. Another powerful genome editing technique adapted from many organisms, CRISPER/Cas9 (clustered regularly interspaced short palindromic repeats and Cas9 endonuclease-mediated genome editing) has been applied to *P. falciparum* (Ghorbal, Gorman et al. 2014, Wagner, Platt et al. 2014), *P. yoelii* (Zhang, Xiao et al. 2014) and *T. gondii* (Shen, Brown et al. 2014) and is under application in *P. berghei* (O. Billker Group, Wellcome Trust Sanger Institute, Cambridge, unpublished data). Additionally, tetracycline dependent TetracylineRepressor-aptamer based system has been shown to reversibly regulate the gene expression in *P. falciparum* (Goldfless, Wagner et al. 2014) and is under development in *P. berghei* (H. Patil, C. Manakanata, T. Hannay - Waters group, Billker group, unpublished data).

Chapter 2: Materials and Methods

2.0 Materials

2.0.1 Molecular Biology products, kits and equipments

All the restriction enzymes were obtained from New England Biolabs. Plasmid ligations were performed using Roche rapid DNA ligation kit, plasmid DNA extractions were performed using QIAprep spin mini prep kit (Qiagen) and Highspeed plasmid midi kit (Qiagen) and plasmid gel extraction were performed by QIAquick Gel Extration Kit (Qiagen). PCR Clean ups were performed using QIAquick PCR purification Kit (Qiagen). TRIzol (Life Technolgoies), RNAeasy Universal mini kit (Qiagen) with RNase free DNase set (Qiagen) and SuperScript® III Reverse Transcriptase (Life Technologies) were used for isolation of total RNA.

Most of the primary antibodies were obtained from Proteintech raised against unique peptides predicted from the gene sequence (Table 2.0.1.1). Anti-enolase antibody is a peptide based (C-KTYDLDFKTPNNDK) antibody raised in rabbit from Biogenes. Rabbit anti-PPKL antibody (Ab) was obtained from Proteintech raised against recombinant PPKL and kindly offered by Dr. N. Philip, Waters group. Mouse anti-MTIP and mouse anti-GAP45, mouse anti α-tubulin antibodies were kind gifts from Prof. Judith Green, NIMR, London and Helen Banks respectively (Table 2.0.1.2). Anti-TgCentrinI antibody was kindly provided by Dr. Marc-Jan Gubbels, Boston College, USA.

Mouse anti-GFP monoclonal antibody (mAb), anti ϒ-tubulin mAb, rabbit anti-cMyc, mouse anti-human CentrinI 20H5 mAb and erythoid cell marker/ anti-mouse TER-119 PE-Cyanine5 (Cy5) are commercially available from Roche, Sigma, Abcam, Millipore and eBioscience respectively (Table 2.0.1.2). FITC and Cyanine3 (Cy3) tagged anti-P25 mAbs were received from Prof. Takafumi Tsuboi, Ehime University, Japan and grown and purified by AbD Serotec (Table 2.0.1.2).

Secondary antibodies used for immunofluorescence studies or FACS analysis such as: Alexa Fluor-594 Goat anti rabbit-IgG, Alexa Fluor-594 goat anti mouse-IgG, Alexa Fluor-488 goat anti-rabbit-IgG, Alexa Fluor-488 goat anti mouse-IgG, Alexa Fluor-633 goat anti mouse-IgG were obtained from Life Technologies. Secondary antibodies for conventional ECL (ThermoFisher^{TM} Pierce^{TM} ECL western blotting substrate) and films (Kodak Carestream Medical X-ray films) based western Polyclonal goat anti-rabbit or goat anti-mouse Ig/HRP

were obtained from Dako. For infrared imaging based western, secondary antibodies IRDye® 680LT Goat anti-mouse IgG and IRDye® 800CW Goat anti-rabbit IgG antibodies were obtained from LI-COR Biosciences. All the secondary antibodies were diluted to 1000 times for immunofluorescence and 10,000 times for western blotting with respective solutions (for more details see methods). All the primers used for PCR amplification and sequencing were ordered from Eurofins MWG Biotech (see Appendix A -Table 1 for primer details).

Equipment for gel electrophoresis and SDS PAGE were purchased from Biorad. Agarose for electrophoresis and ladders: 1kb Plus DNA ladder, PageRuler Plus Prestained Protein ladder (10 to 250kDa) were obtained from Roche and Life Technologies respectively.

Protein	Peptide used to raise antibody	Raised In	Ab dilution for immunofluorescence assays	Ab dilution for western blotting
Anti-MyoA	MAVTNEELKTAHKIVRRVS	Rabbit	1000	1000
Anti-DOZI	MAGKNILARAKNGTGKTAA	Rabbit	250	2500
Anti-CITH	ESTVALQNVRSYGTEGRRQPD	Rabbit	250	2500
Anti-GAP45	HKYENDSDKLETGSQLTL	Rabbit	1000	5000
Anti-GAP50	HKLGLKKRKTLDKVNSL	Rabbit	1000	1000
Anti-IMC1a	CEYKNLSEGKYMNDKEVEKE	Rabbit	1000	-
Anti-IMC1b	HDNEMPNMEKLYDQLSFQKC	Rabbit	1000	-
Anti-IMC1h	FEKIKKLLKVNKLVPSVSEV	Rabbit	1000	-
Anti-actinI	GNVKAGVAGDDAPRS	Rabbit	1000	1000
Anti-Rab11A	CRGKK INVDNDNDEDEKKTK	Rabbit	1000	1000
Anti-Rab11B	CKVDLAEEDETKRKVTYE	Rabbit	1000	1000
Anti-P28	CVSKPQAPGTGSETP	Rabbit	-	1000
Anti-CTRP	CLNGGETPHNSNMEFENVENN DGIIEEENEDFEVIDANDPMW	Rabbit	5000	5000
Anti-chitinase	HTEKQYKSLSHVDALC	Rabbit	4000	4000
Anti-Spindle Pole Body Protein	KKPNKKHKYTKKRNGH	Rabbit	1000	1000
Anti-iLov	RNARFLQGPETDQATVQK	Rabbit	-	1000

Table 2.0.1.1 Peptide raised primary antibodies from Proteintech used for immunofluorescence or western blotting.

Source	Protein	Raised In	Ab dilution for immune-fluorescence assays	Ab dilution for western blotting	Ab dilution for FACS analysis
Prof. Takafumi Tsuboi, Japan. Grown and purified by Serotec	FITC and Cy3 tagged anti-P25	Rabbit	2000	-	-
Roche	anti-GFP mAb	Rabbit	-	2000	-
Proteintech	anti-P25 mAb	Mouse	-	-	1000
eBioscience	Anti-mouse TER-119 PE-Cyanine5	Mouse	-	-	500
Dr. N Philip, Waters group	anti-PPKL	Rabbit	1000	1000	-
DR Judith Green NIMR, London	anti-enolase	Rabbit	-	4000	-
Helen Banks	anti α-tubulin	Mouse	2000	5000	-
Sigma	anti ϒ-tubulin mAb	Mouse	2000	-	-
Prof. Judith Green, NIMR, London	anti-MTIP	Rabbit	1000	1000	-
Dr. Marc-Jan Gubbels, Boston College, USA	Anti-TgCentrinI	Rabbit	1000	-	-
Abcam	anti-cMyc	Rabbit	-	1000	-
Millipore	anti-human CentrinI 20H5 mAb	Mouse	1000	-	-

Table 2.0.1.2 Primary antibodies obtained from external sources, their dilutions used for immunofluorescence, western blotting or FACS analysis.

2.0.2 Buffers, Media and Solutions

2.0.2 a) Ookinete culture medium: RPMI1640 (Sigma) containing 25 mM HEPES and 2 mM L-glutamine, 10 mM Na2CO3, 5 Uml-1 Penicillin, 5 µgµl-1 streptomycin, 50 µg ml-1 hypoxanthine, 50 mM xanthurenic acid, pH 8, 10 % (v/v) heat inactivated foetal bovine serum.

2.0.2 b) Schizont culture media: RPMI1640 (Sigma) containing 25 mM HEPES and 2 mM L-glutamine, 10 mM Na2CO3, 5 Uml-1 Penicillin, 5 µgµl-1 streptomycin, pH 8.0 with 25 % (v/v) foetal bovine serum

2.0.2 c) Luria Bertani (LB) Broth: Available commercially as LB broth powder (Tryptone 1%, Yeast extract 0.5%, NaCl 0.5%) from Sigma plus ampicillin 100µg/ml (if needed).

2.0.2 d) Luria Bertani (LB) Agar: Available commercially as LB broth powder (Tryptone 1%, Yeast extract 0.5%, NaCl 0.5%, 15% Agar) from Sigma plus ampicillin 100µg/ml.

2.0.2 e) Phosphate Buffered Saline (PBS): 10 times concentrated PBS (0.01M KH2 PO4, 1.37M NaCl, and 0.027M KCl, pH 7.0) commercially available from Roche. Working stock: diluted 10 times with d/w.

2.0.2 f) RichPBS: PBS supplemented with 2mM HEPES, 2mM Glucose, 0.4mM NaHCO3, 0.01% BSA

2.0.2 g) TNE buffer: 10 mM Tris pH 8.0, 5 mM EDTA pH 8.0, 100 mM NaCl

2.0.2 h) TBE buffer: 89mM Tris base, 89mM Boric acid, 2mM EDTA

2.0.2 i) Erythrocyte lysis buffer: 1.5M NH_4Cl, 0.1M $KHCO_3$, 0.01 EDTA

2.0.2 j) Heparin: 200 I.U./ml PBS (pH 7.2)

2.0.2 k) Phenylhydrazine: Phenylhydrazine- HCl stock solution (Merck): 12.5mg/ml (250mg phenylhydrazine dissolved in 10 ml 0.9% NaCl and store at -20°C).

2.0.2 l) Giemsa staining buffer: Giemsa solution (Merck) diluted in Sörensen staining buffer (KH2 PO4 - 2,541g per 5 liter, Na2 HPO4 .2 H2O - 0,5507g per 5 liter, adjust the pH to 7.2 with NaOH). A 12.5 % Giemsa staining buffer was used to stain slides for 15 minutes.

2.0.2 m) FACS buffer: 2% (v/v) Fetal Bovine Serum (defined), 0.05% (w/v) sodium azide (NaN3) and 2 mM EDTA in PBS.

2.0.2 n) Nycodenz solution: 138g Nycodenz powder (Axis Shield) dissolved in buffered medium (5mmol/l Tris/HCl, 3mmol/l KCl, 0.3 mmol/l Ca Na 2EDTA) (density 1.15g/ml at 20ºC). Autoclave for 20min at 120ºC and store at 4ºC

2.0.2 o) 5 X TBE electrophoresis buffer: 445 mM Tris, 445 mM Boric acid, 10 mM EDTA (pH 8.0)

2.0.2 p) 5X Agarose loading buffer: 50mM, 20% (w/v) Ficoll, 0.1% (w/v) Bromophenol blue in TE buffer (10 mM Tris-Cl, pH 8.0, 1 mM EDTA - pH 8.0 autoclaved at 121^0C/20min)

2.0.2 q) Net2+ buffer: 140 mM NaCl, 50 mM Tris- pH 7.4, 4mM Dithiothreitol, 0.01% Nonidet P-40 supplemented with complete EDTA free Protease Inhibitor Cocktail Tablets (Roche) (1 tablet/10ml)

2.0.2 r) SDS running buffer: 25 mM Tris, 190 mM Glycine, 0.1 % (w/v) SDS

2.0.2 s) Transfer buffer: 25 mM Tris, 190 mM Glycine, 0.1% (w/v) SDS, 20% Methanol

2.0.2 t) 2x Laemmli buffer: 4% SDS, 10% β-mercaptoethanol, 20 glycerol, 0.004% bromophenol blue, 0.125M Tris HCL, pH 6.8

2.1 Methods

2.1.1 Generation of constructs

2.1.1 a) Polymerase Chain Reactions: All the protein coding genes, 5'UTRs and 3'UTRs PCR amplifications were performed using either Expand high fidelity PCR system (Roche) or KAPA HiFi PCR system (KAPA Biosciences). PCR conditions were followed as per manufacturer's instructions. Diagnostic PCRs were performed using Taq DNA polymerase (5U/µl)(Invitrogen), 10x PCR buffer (200 mM Tris-HCL pH 8.4, 500 mM KCL) (Invitrogen), 50 mM $MgCl_2$ (Invitrogen), 10 pM/µl primers (Eurofins MWG Biotech) and PCR conditions were adjusted to 94^0C/ 30 seconds, 52^0 to 57^0C for 30 seconds, 68^0C for amplification for 30 cycles or as per manufacturer's instructions. All the gDNA were extracted by phenol-chloroform extraction method (see below).

2.1.1 b) Isolation of DNA by phenol-chloroform method: Parasite pellet (approximately 100µl) (see section 2.1.2 for parasite pellet) were re-suspended in 700µl of TNE buffer with 1% (v/v) SDS (100 µl of 10% SDS solution) and demineralised water to make up the total volume to 1ml and incubated at 37^0C for 10 minutes. 200 µg of Proteinase K (20 µl of a 10 mg/ml solution) was added and further incubated at 37^0C for 1h (divided all the volumes by two for smaller parasite pellets). Then added buffered phenol (Life Technologies) to make up the total volume up to 1.5 ml and mixed by inverting the tube several times, spun at maximum speed for 5 minutes, and upper aqueous phase was collected in a new tube. Similar steps were performed with buffered phenol:chroroform:isoamylalcohol (25:24:1) (Life Technologies) and chloroform:isoamylalcohol (obtained from Fisher Scientific as separate chemicals) (24:1). Final upper aqueous phase was collected in a new tube and 0.1 volume of 2M Sodium acetate (pH 5.2) and 2 volumes of 96% ethanol were added, mixed by inverting tube several time and DNA was precipitated overnight at -20^0C (ethanol precipitation method). Precipitated DNA was pelleted by 15-20 minutes spin at maximum speed/ 4^0C and washed with 500 µl of 70% ethanol, air dried and mixed with 50-500 µl of distilled water (depending on the size of parasite pellet initially started with).

2.1.1 c) Molecular cloning: Standard molecular methods were used for generation of plasmids via restriction enzymes and buffers (New England Biolabs). Ligations were performed using Rapid DNA ligation kit (Roche) as per manufacturer's instructions.

Amplification of plasmid copies were performed via transformation using heat shock method into competent *E. coli* fusion blue strain as follows: Competent *E. coli* fusion blue cells were thawed on ice. Mixed with ligation mixture (80 µl of cells with 20 µl of ligation mixture) gently pipetting up and down and incubated for 10 minute on ice. Heat shocked at 42^0C water bath for 45 seconds, and immediately kept on ice for 2 minutes and incubated with pre-warmed (37^0C) LB broth for 30-45 minutes at 37^0C wish shaking (250 rpm/min). Transformed *E. coli* cells were selected on LB agar plate containing 100 µg/ml ampicillin. Plasmid DNA extractions were performed using QIAprep spin miniprep kit or Hispeed plasmid midi kit (Qiagen). Diagnostic digestions and PCR reactions were analysed by electrophoresis on 0.8% agarose gel in TBE buffer and stained with Syber safe (Life Technologies).

2.1.1 d) Generation of *rab11a* promoter swap plasmids: A plasmid containing *3'UTR of snare, putative:*$_{promoter}$*clag:2cmyc::rab11a* called as pG72 (see Appendix A) was generated by Dr. L. Starnes-Waters Group. 3'UTR of *snare, putative* is a *rab11a* upstream gene and this region, required for recombination, needed updating and was amplified from gDNA of WT *P berghei* strain HPTBB by using forward primer GU1620 and reverse primer GU1621, and amplified 3'UTR of *snare, putative* was re-cloned into pG72 to obtain updated *3'UTR of snare, putative* in pG72 (henceforth referred as $_p$*clag:2cmyc::rab11a*).

Another plasmid $_p$*ama-1:2cmyc::rab11a* ('$_p$' stands for promoter) was obtained by replacing *clag* 5'UTR in Plasmid $_p$*clag:2cmyc::rab11a* with PCR amplified 1.7 Kb 5'UTR of *ama-1* (PBANKA_091500) ORF from gDNA of WT *P. berghei* strain HPTBB using forward primer GU1622 and reverse primer GU1623. Order of genes in Plasmid $_p$*clag:2cmyc::rab11a* and $_p$*ama-1:2cmyc::rab11a* was first determined by restriction digestion and these plasmids were sequenced (Eurofins MWG biotech) to check mutations and opened with *HindIII* and *NotI* and transfected in order to express endogenous Rab11A under the control of either *clag* or *ama-1* promoter by double homologous recombination (see Appendix A- Table 1 for primer details).

(**Note:** Plasmid $_p$*clag:2cmyc::rab11a* and $_p$*ama-1:2cmyc::rab11a* were referred as $_p$*clag::rab11a* and $_p$*ama-1::rab11a* throughout the report respectively.)

2.1.1 e) Generation of cMyc and iLOV tagged Rab11A plasmid: The 0.9kb 5'UTR of *rab11a* ORF was PCR amplified using forward primer GU2366 and reverse primer GU2367

and replaced by *clag* promoter in plasmid $_{p}$*clag:2cmyc::rab11a* (5' 600bp of rab11a) to generate plasmid $_{p}$*rab11a:2c-myc::rab11a*$_{0.6kb}$ (5' 600bp of *rab11a*). To tag Rab11A, small green fluorescent protein iLOV was PCR amplified with forward primer GU2491 and reverse primer GU2492 from p77_yhao_LOV (internal plasmid, see Appendix A) and ligated in between Rab11A endogenous promoter ($_{p}$*rab11a*) and *2c-myc* of $_{p}$*rab11a:2c-myc::rab11a*$_{0.6kb}$ to generate plasmid $_{p}$*rab11a:ilov:2c-myc::rab11a*$_{0.6kb}$ (5' 600bp of *rab11a*).

Another plasmid $_{p}$*rab11a:ilov:2c-myc::rab11a*$_{1.55kb}$ (complete *rab11a* ORF- 1559bp) was generated by PCR amplification of complete *rab11a* ORF (1559bp) using forward primer GU2857 and GU2858 and replacing *rab11a*$_{0.6kb}$ (5' 600bp of *rab11a*) from plasmid $_{p}$*rab11a:ilov:2c-myc::rab11a*$_{0.6kb}$. Gene order was confirmed by restriction digestion followed by sequencing (Eurofins MWG Biotech). Plasmids were opened by *HindIII* and *NotI* to tag *rab11a* by double homologous recombination (see Appendix A- Table 1 for primer details).

2.1.1 f) Generation of green male gametocyte plasmid: 1.5kb 5'UTR of *dynein heavy chain* (*DHCP*, PBANKA_041610) previously validated in the 820 line (Ponzi, Sidén-Kiamos et al. 2009) was amplified from gDNA of WT *P. berghei* strain HPTBB using forward primer GU1504 and reverse primer GU1505, and *gfp* was amplified using *gfp*-forward primer GU2042 and *gfp*-reverse primer GU1515 from pG78 (internal plasmid, see Appendix A). Then *dynein heavy chain* and *gfp* fragments were inserted into vector pG89 (K. Hughes, Waters Group, see Appendix A), in front of a transmembrane protein (TM), Triose Hexose Transporter (PBANKA_110790) (K. Hughes- Waters group unpublished) (*male specific promoter:gfp::TM*). After initial restriction digests to confirm correct inserts the plasmid was sequenced (Eurofins MWG Biotech) over the newly inserted and default protein coding gene regions and deemed to be correct and opened by *SacII* for double homologous recombination to occur. These parasites were referred as green male gametocyte producers (see Appendix A- Table 1 for primer details).

2.1.1 g) Generation of red female gametocyte plasmid: 2kb 5'UTR of LCCL domain containing protein (PBANKA_130070, *LDCP*) previously validated in the 820 line (Ponzi, Sidén-Kiamos et al. 2009) was amplified from gDNA of WT *P berghei* strain HPTBB using *LDCP* forward primer GU1587 and *LDCP* reverse primer GU1509, and *mcherry* was amplified using *mcherry*-forward primer GU2139 and *mcherry*-reverse primer GU2140 from pG89 (K. Hughes, Waters group). Then *LDCP* and *mcherry* fragments were inserted into vector green male plasmid (*male specific promoter:gfp::TM*), in front of a transmembrane

protein (TM), triose hexose transporter (PBANKA_110790). P230p (PBANKA_030600) homology arms were obtained from pL15 (internal plasmid, Appendix A) which are different than those used in green male plasmid. Confirming after restriction digests plasmid was sequenced (Eurofins MWG Biotech) and deemed to be correct, opened by *SacII* for double homologous recombination (see Appendix A- Table 1 for primer details).

2.1.1 h) Generation of plasmids for polarity development markers: The *mcherry* was amplified using *mcherry*-forward primer GU2139 and *mcherry*-reverse primer GU2140 from pG89 (K. Hughes, Waters group) and replaced with *gfp* in *ppkl::gfp* plasmid (Philip, Vaikkinen et al. 2012)(Appendix A) and *mcherry* amplified using *mcherry*-forward primer GU1934 and *mcherry*-reverse primer GU1935 was replaced with *gfp* in pL31-*gfp* (K. Hughes, Waters Group- unpublished) (Appendix A) to generate *ppkl::mcherry* and pL31-*mcherry* plasmids respectively.

To tag Spindle Pole Body protein (PBANKA_040210), 1.2kb 3'ORF was PCR amplified with forward primer GU2373 and reverse primer GU2374 from gDNA of WT *P. berghei* strain HPTBB and replaced with *ppkl* in *ppkl::mcherry* plasmid to generate *spindlepolebodyprotein::mcherry* construct.

The *gap50* (PBANKA_081900) was PCR amplified through gDNA of WT *P. berghei* strain HPTBB using oppositely facing and overlapping primers GU2003 (facing towards 3' end) and GU2004 (facing towards 5' end) containing *EcoRV* restriction site and the generated PCR products with overhangs (and *EcoRV* restriction site) was used for further PCR implication of *gap50* using forward primer GU2005 and reverse primer GU2002. Apparently generated *gap50* fragment containing *EcoRV* restriction site was placed upstream of *mcherry* in pL31-mcherry plasmid to generate *gap50::mcherry* construct.

The *isp1* (PBANKA_120940) was PCR amplified through gDNA of WT *P. berghei* strain HPTBB using oppositely facing and overlapping primers GU2866 (facing towards 3' end) and GU2867 (facing towards 5' end) containing *EcoRV* restriction site (similar strategy to generate *gap50:mcherry* plasmid)and the generated PCR products with overhangs and *EcoRV* restriction site was used for further PCR implication of *isp1* using forward primer GU2864 and reverse primer GU2865. Subsequently, generated *isp1* fragment containing *EcoRV* restriction site was replaced with *ppkl* in *ppkl:mcherry* to generate *isp1:mcherry* construct. Introduced *EcoRV* restriction site enables to open *isp1::mcherry* and *gap50::mcherry*

plasmids with *EcoRV* restriction enzyme without interfering with endogenous *isp1* and *gap50*, respectively, after transfection (see Appendix A- Table 1 for primer details).

All the gene ligations were confirmed by restriction digest followed by sequencing (Eurofins MWG Biotech) and deemed to be correct. Plasmid *ppkl:mcherry*, *gap50::mcherry*, *spindlepolebodyprotein::mcherry* and *isp1::mcherry* were opened by *BglII*, *EcoRV*, *BsaBI*, and *EcoRV* respectively for tagging respective genes by single cross over

2.1.2 *Plasmodium berghei* methods

2.1.2 a) Parasite maintenance: Parasites were maintained in Theiler's original (TO) or NIH Swiss outbred female mice (approximate weight 25 g and not less than 6 weeks old) mice according to UK home office licence.

2.1.2 b) Stabilate creation: Stabilates of transgenic and WT *P. berghei* HPTBB parasites were made by mixing equal amounts of infected blood (parasitemia between 1 to 10%) with PBS containing 30% (v/v) glycerol and 0.05 ml of heparin stock solution. Transferred suspension to cryovials (400 µl/cryovial) and stored gently at -80^{0}C in cardboard box for few hours and transferred to liquid nitrogen.

2.1.2 c) Infection of mice: Infection of mice was done by *intraperitoneal (i.p.)* injection either by fresh infected blood with PBS or by approximately 200µl of blood suspension (parasitemia 3-5% or volume adjusted according to parasitemia) from thawed cryovials. After infection mice develop parasitemia approximately in between 0.5-3% on day 3. For some experiments mice were given a dose of 100 µl phenylhydrazine (stock solution 12.5 mg/ml) (mice bodyweight ratio 125mg/kg) *i.p.* to enhance numbers of reticulocytes usually 2 days before infection.

2.1.2 d) Analysis of asexual stages: Parasitemia was monitored daily by making thin smears of mouse tail blood on glass slide, fixed with methanol for 1 second, air dried and stained with Giemsa staining buffer (12.5% v/v) for 15 minutes. Giemsa stained slides were rinsed in water and air dried to count the parasitemia under oil immersion (Immersion oil from Invitrogen) 100x lense of light microscope (Primo Star- Zeiss). Images were captured through PAXcam5 camera using PAXcam software and processed using Fiji/ImageJ software (National Institute of Health http://rsbweb.nih.gov/ij/ OR http://fiji.sc/Fiji). Blood was collected by cardiac puncture under terminal anaesthesia for various experiments.

2.1.2 e) In vitro culture of schizonts: Schizonts were generated by placing heart blood into schizont culture media (1ml blood into 30ml medium) followed by gasification (5% CO_2, 5% O_2, 90% N_2) and incubated at 37^{0}C for 16-18h. Examination of development of schizonts were done by taking small amount (0.2 to 0.5 ml) of schizont culture (spun for 30 seconds, maximum speed and discard supernatant) and preparing Giemsa stained slide.

2.1.2 f) Analysis of gametocytes: For enrichment of gametocytes mice were treated with sulfadiazine (30 mg/litre) in drinking water (tap water) for 48h to kill asexual parasite stages. Gametocytes were analysed by Giemsa staining of thin layer of tail blood. To analyse activation centres heart blood was placed immediately into ookinete culture medium (1x blood: 30 ookinete medium) and 10 µl of ookinete media with blood placed on a haemocytometer. After 15 minutes at 21^0C activation centres defined as actively moving clumps of cells were counted using 10X objective on the light microscope (Primo Star-Zeiss).

2.1.2g) In vitro culture of ookinete: For ookinete cultures, heart blood (1 ml) containing gametocytes was placed into ookinete culture medium (30ml) and incubated at 21^0C for 24h. Ookinete development was observed by Giemsa staining of thin smears (as done for schizont cultures). Ookinete conversion rate were calculated either from Giemsa staining or immunofluorescence microscopy using Cyanine3 tagged anti-P25 antibody (see immunofluorescence assay methods) of ookinete culture. Ookinete conversion rates were calculated according to following formula:

$$\%\ ookinete\ conversion = \left(\frac{number\ of\ ookinetes\ analysed\ through\ morphology\ i.e.\ banana\ shape\ x\ 100}{number\ of\ ookinetes\ (banana\ shape) + number\ of\ female\ or\ zygotes\ (round\ shape)}\right)$$

2.1.2 h) Purification by Nycodenz density gradient: Parasite cultures (30ml) [schizont culture, ookinete culture or blood containing gametocytes in richPBS (37^0C)] were transferred into 50ml falcon tubes. Using 10ml pipette and S1 pipette filler at zero speed (ThermoFisher), 10ml Nycodenz solution (53% Nycodenz stock solution/PBS for ookinetes and gametocytes and 55% Nycodenz stock solution/PBS for schizonts) was gently added at the bottom of parasite culture in order to get clear division between parasite culture and nycodenz solution, spun for 20 minutes in a swing out rotor with no brake at room temperature. A brown layer visible in between the interface of culture and Nycodenz solution was collected using Pasteur pipette and washed with respective culture solutions at 1800 rpm/ 6-8 minutes/ room temperature. Parasite purity was checked by Giemsa staining.

2.1.2 i)Transfection, parasite cloning and negative selection: Purified and linearized plasmid DNA was obtained by gel extraction (QIAquick Gel Extration Kit) of 50-100 µg digested plasmid DNA and subsequent ethanol precipitated similar to gDNA precipitation (see 2.1.1 b). >5µg of linearized plasmid DNA was mixed with schizonts of WT *P. berghei* strain HPTBB or WT-GFP *P. berghei* strain HPTBB (also called as 507tbb where constitutive expression of GFP under *ef1α* promoter)(Franke-Fayard, Trueman et al. 2004) or negatively selected green male gametocyte producer *P. berghei* line (for negative selection see below) and 100 µl of human T cell nucleofector solution (Lonza) in a cuvette, and electroporation was performed using an Amaxa nucleofector device (Lonza) (programme U33) according to manufacturer's instructions. Transfected parasite (transfectants) culture was injected *intravenously (i.v.)* into a TO female mouse obtained from Harlan labs. Transfectants were selected on pyrimethamine (7 mg/ml, pH 4.0) provided in drinking water (tap water) which was provided to the mouse from 24h post-transfection. Clones were obtained by diluting transfectants (showing integration of respective plasmid by diagnostic PCR) with richPBS in 10 mice such that 0.4 parasite per mouse was injected *i.v.* into each mouse. In most (all) cloning experiments 4 out of 10 (or fewer) mice became infected.

A mouse injected with transgenic *P. berghei* parasites having negative selection cassette integrated into the genome, was placed on 5-fluorocytosine (5FC) once the parasites were visible. Parasites were collected at approximately 3% parasitemia after decline of initial parasitemia (For more details see Chapter 4 Results – section 4.1 and figure 4.1.3 B) (Braks, Franke-Fayard et al. 2006, Maier, Braks et al. 2006, Orr, Philip et al. 2012).

2.1.2 j) Transmission: 200 or 300 mosquitoes (*Anophelese Stephensi*) were allowed to feed for 10 min on an infected mice (no phenylhydrazine treatment) having 2-8% parasitemia. Mosquito midguts were analysed at day 11 or 14 and either day 17/18 or 22/27. Midguts were examined with Leica M205 FA Fluorescence Stereomicroscope and images were capture using Leica DFC340FX camera and through LAS AF Lite 2.2.0 build 4758 (Leica Microsystems Ltd.) and processed through ImageJ/Fiji software (National Institute of Health http://rsbweb.nih.gov/ij/ OR http://fiji.sc/Fiji). Oocyst numbers were counted by live images.

2.1.2 k) Motility assay: MACS purified ookinetes were embedded in Matrigel and incubated for 1h at 210C before imaging. Time-lapse movies were acquired every 10 seconds for 10 min on a Leica M205 FA fluorescence stereomicroscope employing the GFP and mCherry filter sets (0.5 second exposure for each). Ookinete speeds were calculated on Fiji software

(National Institute of Health http://rsbweb.nih.gov/ij/ OR http://fiji.sc/Fiji) using the MtrackJ plugin (Meijering, Dzyubachyk et al. 2012).

2.1.2 l) Immunofluorescence assay: A thin smear of *P. berghei* ookinete or schizont culture or sporozoites or oocysts obtained from crushed midgut of *P. berghei* infected *Anophelese Stephensi* in PBS was air dried and fixed with 4% paraformaldehyde (Electron Microscopy Science- EM grade) for 10 minutes. Cells (slides) were rinsed with PBS and permeabilized with 0.1% Triton in PBS for 5minutes. PBS Rinsed and blocked with 1% BSA/PBS for 45 minutes followed by incubation with primary antibodies (Table 2.0.1.1 and Table 2.0.1.2) diluted with 1% bovine serum albumin (Sigma) in PBS (1% BSA/PBS) for an hour. Slides were washed 3 times 5 mins each with PBS and blocked with secondary antibodies (1:1000 in 1% BSA/PBS). PBS rinsed 3 times 5 min each followed by rinsed with 70% ethanol and absolute ethanol 1 min each, air-dried and mounted in VectaShield (Vectorlabs) containing DAPI (4', 6-diamidino-2-phenylindole) in glycerol for nuclear staining. Access VectaShield was blotted with medical wipes by gently pressing the cover slip which were fixed with nail vanish and parasites were examined either under Delta Vision Epifluorescence microscope (Applied Precision)/ 100x objective, images were captured with CoolSNAP HQ camera (Photometrics) and deconvoluted using SoftWoRx software (Applied Precision) or under Axioplane2 (Zeiss) 100x objective, images were taken through HAMAMATSU ORCA_ER camera (HAMAMATSU) and Velocity software 4.1.0 (PerkinElmer). Images were processed using ImageJ/Fiji (National Institute of Health http://rsbweb.nih.gov/ij/ OR http://fiji.sc/Fiji) as well as SoftWoRx explorer 1.3. Super-resolution images were captured through Elyra PS.1 super-resolution microscope (Zeiss) with sCMOS PCO camera and images were visualized with ZEN Black software (Zeiss) and processed with ZEN LITE software (Zeiss).

2.1.2 m) Live microscopy of *P. berghei* parasites: Small amount of (0.5ml) parasite cultures: iRBCs containing gametocytes (in ookinete medium or in richPBS kept at 37^0C) or after activation of gametocytes (1 to 24hpa, zygotes, retorts and ookinetes) were spun at maximum speed for 30 seconds and resuspended in PBS/richPBS with or without 10 μM Hoechst 33342 (Life Technologies) for 10 seconds and washed with PBS once (spun at maximum speed for 30 seconds) and re-suspended in small amount of PBS. Alternatively, parasite suspensions were probed with Cy3 tagged anti-P25 mAb (1:2000) in richPBS with or without 10 μM Hoechst 33342 on rotating mixer for 30 minutes, washed three times with PBS (spun at maximum speed, 30 seconds each) and re-suspended in small amount of PBS. A drop

of parasite suspension was placed on slide. A coverslip was placed on top of the drop, excess liquid was blotted with medical wipes and coverslip was sealed with nail vanish. After air-drying of nail vanish, images were captured by Deltavision or Axioplan microscopes as mentioned in above (method 2.1.2 l) with little variation in settings**.**

2.1.2 n) Western Blotting: For analysis of Rab11A and ookinete development markers parasites were collected at different growth stages. Mixed asexual blood stage parasites were collected from an infected mouse by cardiac puncture, filtered through CF11 cellulose columns (Whatman-GE Healthcare Life Sciences) to exclude mice white blood cells and immediately lysed with ice cold erythrocyte lysis buffer for 15 min on ice. Parasite pellets were then obtained by spinning at 1800 rpm for 10 minutes, washed with ice cold erythrocyte lysis buffer (spin for 30 seconds at maximum speed) and stored at -20^0C or proceeded immediately to sample lysis (see below). Schizonts, gametocytes and ookinete were obtained and purified by nycodenz density gradient as described above.

Equal amount of parasite material from mixed asexual stage, schizonts, gametocytes and ookinetes were lysed in Net2+ buffer, mixed with equal amount of 2X Laemmli sample buffer containing 15% (v/v) β-mercaptoethanol and separated on 10 or 12 % SDS polyacrylamide gels (SDS and Tris by Flowgen Biosciences). Subsequently proteins were transferred onto nitrocellulose membrane (Amersham- GE Healthcare Life Sciences), using electrophoretic transfer in transfer buffer. Membranes were then blocked with 5% milk/PBS-tween and probed with appropriate primary antibodies (see Table 2.0.1.1 and 2.0.1.2) in 5% milk/PBS-Tween (PBST) overnight at 4^0C. Blots were washed three times with PBST for 10 min each and re-probed with HRP coupled secondary antibody (Polyclonal Goat anti-Rabbit or anti-mouse Ig/HRP-Dako) 10,000 time diluted in 5% milk/PBST, for 1h at room temperature. Blots were visualised by treating with ECL solution (ThermoFisher™ Pierce™ ECL western blotting substrate) and exposed to X-ray film (Kodak Carestream Medical X-ray films) and developed. For infrared based western appropriate secondary antibodies were used (IRDye® 680LT Goat anti-mouse IgG and IRDye® 800CW Goat anti-rabbit IgG antibodies) and nitrocellulose blots were scanned on Odyssey® Sa Infrared Imaging System (LI-COR Biosciences). Blots were stripped two times 5 min each with 0.2M NaOH solution and intermittent washing with distilled water and re-blocked in PBST plus milk before re-probing with further antibodies typically GFP, actinI or enolase as loading controls (see Table 2.0.1.1 and Table 2.0.1.2 for concentrations of antibodies).

2.1.2 o) RNA isolation and Reverse transcriptase PCR: To prevent the post-meiotic transcription in WT-GFP zygotes, WT-GFP gametocytes immediately filtered through Plasmodipur filters (EuroProxima) were cultured in the ookinete culture medium supplemented with 5 μ/ml actinomycinD (Sigma) and collected after 24 hpa giving retorts (A. Srivastava-Waters group, Unpublished data).

To prevent fertilization of female gametes, unactivated gametocytes were cultured in richPBS containing 100 mM 2-Deoxy-D-glucose (Sigma) for 45min and filtered through Plasmodipur filters (EuroProxima), washed with 5ml ookinete medium and re-cultured in ookinete medium without 2-Deoxy-D-glucose (2DG) for 24h. Female gametocytes get activated and fertilization is prevented due to blockage in male gamete exflagellation (K. Hughes-Waters Group, Unpublished data) (see Chapter 3- Results section 3.6 for details).

Unactivated gametocyte (immediately filtered through Plasmodipur filter at 37^0C) and ookinetes (unactivated gametocytes were immediately filtered through Plasmodipur filters at 37^0C before setting up ookinete cultures at 21^0C) of WT-GFP and $_p$*clag::rab11a* parasites along with drug treated gametocytes obtained 24h after culturing (2-Deoxy-D-glucose and actinomycinD treated) were enriched with 53% nycodenz gradient and mixed vigorously with 1ml of TRIzol (ambion-Life Technologies) and stored either at -80^0C or immediately kept on ice for RNA isolation.

Total RNA were isolated using RNAeasy Universal Mini kit (Qiagen) with on-column DNase digestion by RNase free DNase set (Qiagen) according to manufacturer's instruction. Reverse transcriptase PCRs were performed using SuperScript® III Reverse Transcriptase kit (Life Technologies) according to manufacturer's instructions. RNA samples were sequenced through Glasgow Polyomics, UK (www.polyomics.gla.ac.uk).

2.1.2 p) RNA Sequencing: RNA Sequencing (RNA-Seq) reads were prepared (see Table 2.1.2.1 and Table 2.1.2.2 for parameters of RNA-Seq) using Life Technologies stranded mRNA library kit and sequencing was carried out on Life Technologies Ion Proton platform. Fastq files were quality controlled using FastQC (http://www.bioinformatics.babraham.ac.uk/projects/fastqc/, version 0.10.1) and trimmed for adapters and with a quality threshold >2=20 using cutadapt [(Martin 2011), version 1.6 version, "-m 16 -b GGCCAAGGCG -q 20"]. Reads were then aligned to the *Plasmodium berghei* ANKA genome [(Aurrecoechea, Brestelli et al. 2009) PlasmoDB version 11.1] using

Tophat [(Kim, Pertea et al. 2013). version 2.0.12 , "--keep-fasta-order -b2-D 20 --b2-R 3 --b2-N 1 --b2-L 20 --b2-i S,1,0.50 -g 10 -I 5000 --library-type fr-firststrand"]. In order to have maximum sensitivity to low abundance or divergent transcripts reads that failed to align with Tophat2 were extracted using bed tools (http://bedtools.readthedocs.org/en/latest/, version 2.19.1, "bamtofastq") and aligned to the same reference using bowtie2 local alignments [(Langmead and Salzberg 2012), version 2.2.1 , "--local -D 20 -R 3 -N 1 -L 20 -i S,1,0.50 --mm"]. The Tophat accepted hits and bow tie2 aligned reads were then merged to form the alignment for that sample using Picard tools (http://broadinstitute.github.io/picard/, version 1.112). Gene-level expression analysis was carried out using the cufflinks2 package [(Trapnell, Hendrickson et al. 2013) version 2.2.1] using annotated genes only (PlasmoDB VERSION 11.1 GFF file). Differential expression was carried out using cuffdiff (version 2.2.1). Subsequent analyses were carried out using the CummeRbund package (http://compbio.mit.edu/cummeRbund/, version 2.0).

Samples	Set1		Set2		Set3	
	Trimmed	**Raw**	**Trimmed**	**Raw**	**Trimmed**	**Raw**
WT-GFP gametocytes	9999709	10631567	10333258	10910347	9424540	10202613
$_{p}$*clag::rab11a* gametocyte	7380562	7724709	7658106	8236185	7493549	8107180
WT-GFP Ookinetes	8330977	8781630	6913529	7396991	8082056	8607430
$_{p}$*clag::rab11a* ookinetes	7386774	7956256	9882800	10630975	8867802	9418792
AUFG	8617514	9084250	8615066	9150651	7819104	8309714
TAR	7864661	8364489	8210194	8788797	7522889	8026224

Table 2.1.2.1 RNASeq reads trimmed and raw for three sets of parasite samples

AUFG – Activated-Unfertilized WT-GFP female gametocytes (2-Deoxy-D-glucose treated WT-GFP female gametes), TAR – Transcriptionally arrested WT-GFP retorts (actinomycinD treated WT-GFP gametocytes) See 2.1.2 o and 2.1.2 p for more details.

Set1

WT-GFP gametocytes1.merge.bam	
Stats for BAM file(s):	
Total reads: 8609950	
Mapped reads: 8609950	-100%
Forward strand: 4133611	-48.01%
Reverse strand: 4476339	-51.99%
Failed QC: 0	0%
Duplicates: 0	0%
Paired-end reads: 0	0%

$_{p}$*clag::rab11a* gametocytes1.merge.bam	
Stats for BAM file(s):	
Total reads: 3264448	
Mapped reads: 3264448	-100%
Forward strand: 2315093	-70.92%
Reverse strand: 949355	-29.08%
Failed QC: 0	0%
Duplicates: 0	0%
Paired-end reads: 0	0%

WT-GFP ookinetes1.merge.bam	
Stats for BAM file(s):	
Total reads: 5290409	
Mapped reads: 5290409	-100%
Forward strand: 2897080	-54.76%
Reverse strand: 2393329	-45.24%
Failed QC: 0	0%
Duplicates: 0	0%
Paired-end reads: 0	0%

AUFG1.merge.bam	
Stats for BAM file(s):	
Total reads: 2757519	
Mapped reads: 2757519	-100%
Forward strand: 1676352	-60.79%
Reverse strand: 1081167	-39.21%
Failed QC: 0	0%
Duplicates: 0	0%
Paired-end reads: 0	0%

$_{p}$*clag::rab11a* ookinetes1.merge.bam	
Stats for BAM file(s):	
Total reads: 6317982	
Mapped reads: 6317982	-100%
Forward strand: 3486291	-55.18%
Reverse strand: 2831691	-44.82%
Failed QC: 0	0%
Duplicates: 0	0%
Paired-end reads: 0	0%

TAR1.merge.bam	
Stats for BAM file(s):	
Total reads: 4920463	
Mapped reads: 4920463	-100%
Forward strand: 2628076	-53.41%
Reverse strand: 2292387	-46.59%
Failed QC: 0	0%
Duplicates: 0	0%
Paired-end reads: 0	0%

Set2

WT-GFP gametocytes2.merge.bam	
Stats for BAM file(s):	
Total reads: 8943276	
Mapped reads: 8943276	-100%
Forward strand: 4095083	-45.79%
Reverse strand: 4848193	-54.21%
Failed QC: 0	0%
Duplicates: 0	0%
Paired-end reads: 0	0%

$_p$*clag::rab11a* gametocytes2.merge.bam	
Stats for BAM file(s):	
Total reads: 5569828	
Mapped reads: 5569828	-100%
Forward strand: 2492556	-44.75%
Reverse strand: 3077272	-55.25%
Failed QC: 0	0%
Duplicates: 0	0%
Paired-end reads: 0	0%

WT-GFP ookinetes2.merge.bam	
Stats for BAM file(s):	
Total reads: 3555698	
Mapped reads: 3555698	-100%
Forward strand: 1958254	-55.07%
Reverse strand: 1597444	-44.93%
Failed QC: 0	0%
Duplicates: 0	0%
Paired-end reads: 0	0%

AUFG2.merge.bam	
Stats for BAM file(s):	
Total reads: 2221042	
Mapped reads: 2221042	-100%
Forward strand: 1378494	-62.07%
Reverse strand: 842548	-37.93%
Failed QC: 0	0%
Duplicates: 0	0%
Paired-end reads: 0	0%

$_p$*clag::rab11a* ookinetes2.merge.bam	
Stats for BAM file(s):	
Total reads: 7054508	
Mapped reads: 7054508	-100%
Forward strand: 3728459	-52.85%
Reverse strand: 3326049	-47.15%
Failed QC: 0	0%
Duplicates: 0	0%
Paired-end reads: 0	0%

TAR2.merge.bam	
Stats for BAM file(s):	
Total reads: 3703151	
Mapped reads: 3703151	-100%
Forward strand: 2022857	-54.63%
Reverse strand: 1680294	-45.37%
Failed QC: 0	0%
Duplicates: 0	0%
Paired-end reads: 0	0%

Set3			
WT-GFP gametocyte3.merge.bam		**$_p$*clag::rab11a* gametocytes*3*.merge.bam**	
Stats for BAM file(s):		**Stats for BAM file(s):**	
Total reads: 7128574		Total reads: 6836368	
Mapped reads: 7128574	-100%	Mapped reads: 6836368	-100%
Forward strand: 3587661	-50.33%	Forward strand: 3348360	-48.98%
Reverse strand: 3540913	-49.67%	Reverse strand: 3488008	-51.02%
Failed QC: 0	0%	Failed QC: 0	0%
Duplicates: 0	0%	Duplicates: 0	0%
Paired-end reads: 0	0%	Paired-end reads: 0	0%
WT-GFP ookinetes3.merge.bam		**AUFG3.merge.bam**	
Stats for BAM file(s):		**Stats for BAM file(s):**	
Total reads: 5834001		Total reads: 2158042	
Mapped reads: 5834001	-100%	Mapped reads: 2158042	-100%
Forward strand: 3390716	-58.12%	Forward strand: 1943669	-90.07%
Reverse strand: 2443285	-41.88%	Reverse strand: 214373	-9.93%
Failed QC: 0	0%	Failed QC: 0	0%
Duplicates: 0	0%	Duplicates: 0	0%
Paired-end reads: 0	0%	Paired-end reads: 0	0%
$_p$*clag::rab11a* ookinetes3.merge.bam		**TAR3.merge.bam**	
Stats for BAM file(s):		**Stats for BAM file(s):**	
Total reads: 4044348		Total reads: 3186032	
Mapped reads: 4044348	-100%	Mapped reads: 3186032	-100%
Forward strand: 2591261	-64.07%	Forward strand: 2147336	-67.40%
Reverse strand: 1453087	-35.93%	Reverse strand: 1038696	-32.60%
Failed QC: 0	0%	Failed QC: 0	0%
Duplicates: 0	0%	Duplicates: 0	0%
Paired-end reads: 0	0%	Paired-end reads: 0	0%

Tables 2.1.2.2 Number of reads aligned to the genome of *P. berghei* ANKA for comparison with the original read counts.

AUFG – Activated-Unfertilized WT-GFP female gametocytes (2-Deoxy-D-glucose treated WT-GFP female gametes), TAR – Transcriptionally arrested WT-GFP retorts (actinomycinD treated WT-GFP gametocytes) See 2.1.2 o and 2.1.2 p for more details.

2.1.2 q) GO term analysis: Generic GO slim terms were obtained using Princeton University's GOTERMMAPPER (http://go.princeton.edu/cgi-bin/GOTermMapper) for *P. falciparum* as GOTERMMAPPER is not available for *P. berghei*. Obtained GO parent terms were further grouped manually to less than 30 groups for convenience of representation in pie charts. For simplicity only Biological Process terms were shown.

2.1.2 r) Scanning and transmission electron microscopy: -For scanning electron microscopy *P. berghei* gametocytes 8hpa (in ookinete medium) were initially fixed with 0.1M Sodium Cacodylate buffer containing 2% Glutaraldehyde and 2% Paraformaldehyde. Additionally, parasites were fixed with chlorides (0.2% MgCl, 0.1% CaCl) for 1h and rinsed three times (5 min each) with 0.1M Sodium Cacodylate buffer (0.2% Mgcl, 0.1% Cacl) to remove Glutaraldehyde. Parasite sample drops were placed onto Poly-l-Lysine coated 10mm diameter glass coverslips and left to settle for 30 min to allow specimens to stick to glass surface, further fixed with 1% Osmium Tetroxide in Sodium Cacodylate buffer and rinsed 1h, following three changes of distilled water 10 minutes each to remove Osmium fixative. Successively, stained with 0.5% Uranyl Acetate aqueous solution for 1h in dark to avoid stain precipitation by light and dehydrated through ethanol series 30%, 50%, 70%, 90% for 10 min each then with 100% ethanol four times 5 min each, followed by four 5 min changes of dried 100% ethanol (dried 100% ethanol is 100% ethanol containing 3A molecular sieve). Parasite specimens attached to coverslips were critically point dried using a Polaron E3000 and Liquid CO2. Dried parasite specimens on coverslips were mounted onto aluminium pin stubs and gold Palladium coated using a Polaron SC515 sputter coater and examined on a JEOL6400 SEM running at 10kV and tiff images captured using Olympus Scandium software.

For transmission electron microscopy, after fixation of parasite samples with following fixatives: 2% Glutaraldehyde and 2% Paraformaldehyde containing 0.1M Sodium Cacodylate and chlorides (0.2% MgCl, 0.1% CaCl), parasites specimen suspensions were spun down to a pellet and cut into 1-2mm^{3} pieces and left in fixative for 1h. Rinsed three times - 5 minutes each with 0.1M Sodium Cacodylate buffer (0.2% MgCl, 0.1% CaCl) and subsequently rinsed with Sodium Cacodylate buffer containing Osmium Tetroxide for 1h, washed with three times distilled water 10 minutes each. *En bloc* stain with 0.5% Uranyl Acetate aqueous solution for 1h in dark and dehydrated through series of ethanol similar to SEM samples until dried ethanol step. Three 5 minute changes in Propylene Oxide (this solvent mixes better with resin and evaporates quickly) and mixing overnight with 1:1 Propylene Oxide: Araldite/ Epon

(TAAB 812) on rotator (Pure resin changes next day). Embed specimens in fresh resin transferred into moulds and polymerised in oven at 60^0C for at least 24h. Ultrathin sections 60-70nm thickness cut using a LEICA ULTRACUT UTC and a DRUKKER diamond Ultramicrotome knife angled at 6˚. Parasite specimen sections attached to 100 mesh formvar coated copper grids were contrast stained in 2% Methanolic Uranyl Acetate/5 mins and Reynolds Lead Citrate/ 5 mins and viewed on either a Tecnai T20 (FEI) running at 200kV or Leo 912AB TEM running 120kV and images captured using Gatan Digital Micrograph Software (Gatan, Japan). Images were processed using ImageJ (National Institute of Health http://rsbweb.nih.gov/ij/).

2.1.2 s) Flow Cytometry analysis: 1) Fertilization and analysis of meiosis by DNA content in WT-GFP and *$_p$clag::rab11a* zygotes were verified by flow cytometry. WT-GFP and *$_p$clag::rab11a* gametocytes were collected 4hpa and 24hpa in ookinete media and purified using 53% nycodenz density gradient centrifugation, washed with richPBS two times and vigorously vortexed three times 10 seconds each to break the zygote/ookinete clumps. Parasites were incubated with anti-P25 mAb (1:1000) in richPBS for 30 min on rotating mixer and washed with richPBS three times (spun at maximum speed, 30 seconds each) and re-probed with secondary antibodies Goat anti-mouse Alexa Flour 633 (1:1000) and erythroid cell marker anti-Ter119 PE/Cy5 antibody (eBioscience) (1:500) in richPBS containing 5 μM Hoechst 33342 for 30 min and washed two times with richPBS and with FACS buffer once (spun at maximum speed, 30 seconds each) and vortexed for 10 seconds. Parasites were re-suspended in 1ml FACS buffer and filtered through nylon filtration fabric NITEX 40 μm pore size (Cadisch Precision Meshes) to remove parasite aggregates. Samples were run on a FACS CyAn (BeckmanCoulter) equipped with a 405 nm, 488 nm and 633 nm laser and 5000 to 10000 events (infected RBCs) were acquired. Post-acquisition analysis was performed using Kaluza software (BeckmanCoulter). Due to unavailability of two colour background in the mutant (*$_p$clag::rab11a*) parasites, it was not possible to differentiate between male and female gametes using red/green colours as previously shown (Mair, Lasonder et al. 2010). A gating strategy was implemented to identify parasites (based on GFP and Hoechst positive). Activated gametocytes/ gametes were negative for RBC membrane detected by erythroid cell marker anti-Ter119 PE/Cy5 antibody, and female gametes/ zygotes become positive for P25 staining. Negative controls of uninfected RBCs, infected RBCs with asexual stages of parasites and unstained samples were used to validate the gating strategy. The DNA content

was then analysed by comparing the Hoechst 33342 stain levels of these parasites. All the experiments were performed on three independent occasions with similar results

2) For iLOV::2CMYC::Rab11A cell sorting (FACS cloning), schizont cultures of WT *P. berghei* HPTBB and *ilov::2cmyc::rab11a*$_{1.55kb}$ parasites were washed twice with richPBS and re-suspended in 1ml FACS buffer, filtered through NITEX 40 μm pore membrane to exclude of cell clumps. Parasites were sorted on FACSAria III (BD Biosciences) and analysed on BD FACSDIVA V8.0.1 .Cells were collected in numbers 50, 500 and 5000 for each parasite line and injected *i.p.* into TO female animals. Ookinete cultures of the resulting FACS cloned *ilov::2cmyc::rab11a*$_{1.55kb}$ were analysed by live fluorescence microscopy (methods 2.1.2 m).

Chapter 3: Results, Discussion and conclusion

Rab11A approach

3.0 Introduction: Rabs in *Plasmodium*

Evidence of the presence of Rab GTPase in *Plasmodium* came in early 1990s. Whilst studying the compartment and the mechanism of chloroquine effects in *P. falciparum*, Jambau et al discovered the presence of Rab proteins in *P. falciparum* (Jambou, Zahraoui et al. 1996). The first characterised *Plasmodium* Rabs were Rab4 and Rab6. PfRab4 (*Plasmodium falciparum* Rab4) localizes near plasma membrane, on the membranes of early endosome like structure and on small vesicles (Jambou, Zahraoui et al. 1996). Rab6 is the most widely studied *P. falciparum* Rab and has been described in the rodent malaria model *P. berghei* (Ming, VanWye et al. 1999), and its crystal structure has been solved (Chattopadhyay, Langsley et al. 2000, Chattopadhyay, Smith et al. 2000). Immunoelectron microscopy shows PfRab6 localization in the vicinity of trans-Golgi network (Golgi and vesicular structure) (Van Wye, Ghori et al. 1996) while immunofluorescence microscopy confirms dynamic localization of PfRab6 and it is expressed during asexual blood stages with highest presence at trophozoite stage (de Castro, Ward et al. 1996). PCR analysis allowed detection of further *P. falciparum* Rabs which are Rab1A, Rab1B, Rab5, Rab7, Rab11 (Langsley and Chakrabarti 1996) and ARA4 (de Castro, Ward et al. 1996). Rabs are associated with membranes via its C-terminal prenylation a process that is mediated by prenyl transferases whilst recycling of Rabs from donor to acceptor membrane is mediated by RabGDI. The presence of protein geranylgeranyl transferase-I along with protein farnesyl transferase (Chakrabarti, Azam et al. 1998) and RabGDIs (Attal and Langsley 1996) were demonstrated in *P. falciparum.*

Complete *Plasmodium* genome sequence (Bowman, Lawson et al. 1999, Gardner, Hall et al. 2002, Hall, Pain et al. 2002) analysis shows that *Plasmodium* spp encode 11 Rab GTPases (Quevillon, Spielmann et al. 2003) (similar to the number of *rabs* in yeast *S. cerevisiae* where Ypts/Rabs are well characterised, see figure 3.0 A) and also putative homologues of protein trafficking machinery such as GAP, GDI and SNARE proteins (www.plasmodb.org) suggestive of the existence of active trafficking. Potential functions of PfRabs were predicted by comparing with *S. cerevisiae* Rabs. It has been shown by RT-PCR that ten members of *P. falciparum* Rab family are expressed in erythrocytic stages of parasite except PfRab11B (*P falciparum* Rab11B) as no transcripts of it were detected (Quevillon, Spielmann et al. 2003). However, recent transcriptomic studies shows the presence of Rab11B in erythocytic stages (Langsley, van Noort et al. 2008, Otto, Böhme et al. 2014)(RNA-Seq by A Religa – Waters Group, unpublished). Rab GTPases are also present in other closely related Apicomplexan

parasites such as *T. gondii* which encode 12 Rabs (Kremer, Kamin et al. 2013), *Theileria* and *Babesia* parasites have 9 Rabs while *Cryptosporidia* have 8 Rabs (Langsley, van Noort et al. 2008). The complete family of 11 Rabs of *Plasmodium* has been characterized (Quevillon, Spielmann et al. 2003). Depending on the expression profile at erythrocytic stages, Rab proteins can be divided into three groups. The *rab1a, rab1b, rab5a* and *rab5c* transcripts fall in one cluster and appear to peak in trophozoite stage; *rab2*, *rab5b*, *rab6* and *rab11b* transcripts fall into another cluster and peak in late schizont stage whereas *rab7*, *rab11a* and *rab18* transcripts do not share any expression profile and therefore do not form any cluster (Langsley, van Noort et al. 2008).

Sequence analysis of PfRab5 proteins show that unlike all other PfRabs, PfRab5b might have a different function as it lacks C-terminal prenylation motif (geranylgeranylation motif) necessary for membrane attachment, however, it has a myristoylation site at N-terminus (Quevillon, Spielmann et al. 2003, Howe, Kelly et al. 2013, Ezougou, Ben-Rached et al. 2014). PfRab5b has been shown be associated with the plasma membrane as well as the food vacuole and PbRab5b is refractory to deletion in haploid blood stages. (Ezougou, Ben-Rached et al. 2014). During blood stages, PfRab5a localised to the haemoglobin-containing vacuoles and therefore predicted to be involved in haemoglobin uptake via haemoglobin-containing vacuoles transport to food vacuole (Elliott, McIntosh et al. 2008). Both PfRab5a and PfRab5b are mislocalized from parasite to erythrocyte upon inhibition of isoprenoid synthesis by MEP (methylerythritol 4-phosphate) pathway by small molecule fosmidomycin (Howe, Kelly et al. 2013). Rab5a shows presence of an unusual 30 amino acids insertion (compared with other Rabs of *P. falciparum*) indicating interactions with novel effectors (Quevillon, Spielmann et al. 2003). Additionally, Rab interactome studies have revealed the casein kinase 1 as an effector of Rab5b and cAMP-dependent protein kinase A as an effector of Rab5a and Rab7 in *P. falciparum* (Rached, Ndjembo-Ezougou et al. 2012). Also, PfRab7 was shown to localize at the putative endosome along with the retromer cargo-complex and putative Golgi-to-endosome protein sorting pathway was depicted in asexual blood stages (Krai, Dalal et al. 2014).

(A)

	LECA	Choanoflagellatea	Basal Metazoa	Vertebrata	Basal fungi	Basidiomycota	Saccharomycotina	Chlorophyta	Bryophyta	Angiospermae	Heterokontophyta	Apicomplexa	Kinetoplastida
Group I	Rab1	Rab1	Rab1	Rab1a	Ypt1	Ypt1	Ypt1	Rab1	Rab1	Rab1A	Rab1A	Rab1A	Rab1A
				Rab1b						Rab1B	Rab1B	Rab1B	
			Rab35	Rab35						Rab1C			
			Rab33	Rab33a									
				Rab33b									
			Rab19	Rab19									
				Rab43									
			Rab30	Rab30									
			RabX6										
	Rab8	Rab8	Rab8	Rab8a	Sec4	Sec4	Sec4	Rab8	Rab8	Rab8A	Rab8A	Rab8	
				Rab8b						Rab8B	Rab8B		
				Rab13							Rab8C		
				Rab12									
			Rab15	Rab15									
			Rab10	Rab10									
			Rab3	Rab3a									
				Rab3b									
				Rab3c									
				Rab3d									
			Rab26	Rab26									
				Rab37									
			Rab27	Rab27a									
				Rab27b									
			Rab34	Rab34									
				Rab36									
			RabX4										
			Rab45	Rab45									
			Rab44	Rab44a									
				Rab44b									
	Rab18	Rab18	Rab18	Rab18	Rab18	Rab18		Rab18	Rab18	Rab18A	Rab18	Rab18	Rab18
			Rab40	Rab40a						Rab18B			
				Rab40aL									
				Rab40c									
				Rab40d									
Group II	Rab5	Rab5	Rab5	Rab5a	Ypt51	Ypt51	Ypt51	Rab5	Rab5	Rab5A	Rab5	Rab5A	Rab5A
				Rab5b			Ypt10			Rab5B		Rab5B	Rab5B
				Rab5c									
				Rab17	Ypt52	Ypt52	Ypt52						
	Rab21	Rab21	Rab21	Rab21				Rab21	Rab21	Rab21	Rab21		Rab21
	Rab22	Rab22	Rab22	Rab22a				Rab22	Rab22	Rab22	Rab22	Rab22	
				Rab22b									
	Rab24		Rab24	Rab24				Rab24					
			Rab20	Rab20									
	RabX1	RabX1	RabX1		RabX1	RabX1	RabX1				RabX1		
Group III	Rab7	Rab7	Rab7	Rab7a	Ypt7	Ypt7	Ypt7	Rab7	Rab7	Rab7A1	Rab7	Rab7	Rab7
				Rab7b						Rab7A2			
		Rab9	Rab9	Rab9a	Ypt9	Ypt9	Ypt9			Rab7B1			
				Rab9b						Rab7B2			
	Rab23	Rab23	Rab23	Rab23	Rab23			Rab23	Rab23		Rab23	Rab23	Rab23
	Rab29	Rab29	Rab29										
	Rab32	Rab32	Rab32	Rab32	Rab32						Rab32		Rab32
				Rab38									
	Rab7L1	Rab7L1	Rab7L1	Rab7L1							Rab7L1		
Group IV	Rab2	Rab2	Rab2	Rab2a	Ypt2	Ypt2	Ypt2	Rab2	Rab2	Rab2A	Rab2A	Rab2	Rab2
				Rab2b						Rab2B	Rab2B		
			Rab39	Rab39a									
				Rab39b									
				Rab42									
	Rab4	Rab4	Rab4	Rab4a	Ypt4	Ypt4	Ypt4					Rab4	Rab4
				Rab4b									
	Rab11	Rab11	Rab11	Rab11a	Ypt3	Ypt3	Ypt31	Rab11	Rab11A	Rab11A1	Rab11A	Rab11A	Rab11
				Rab11b			Ypt32			Rab11A2	Rab11B	Rab11B	
				Rab25						Rab11B1	Rab11C		
										Rab11B2			
										Rab11B3			
									Rab11C	Rab11C1			
										Rab11C2			
									Rab11D	Rab11D1			
										Rab11D2			
										Rab11D3			
	Rab14	Rab14	Rab14	Rab14									Rab14
Group V	Rab6	Rab6	Rab6	Rab6a	Ypt6	Ypt6	Ypt6	Rab6	Rab6	Rab6A	Rab6	Rab6	Rab6
				Rab6b						Rab6B			
				Rab6c									
				Rab41									
Group VI	Rab28	Rab28	Rab28	Rab28				Rab28			Rab28A		Rab28
											Rab28B		
	RabL4	RabL4	RabL4	RabL4	RabL4			RabL4			RabL4		RabL4

(B)

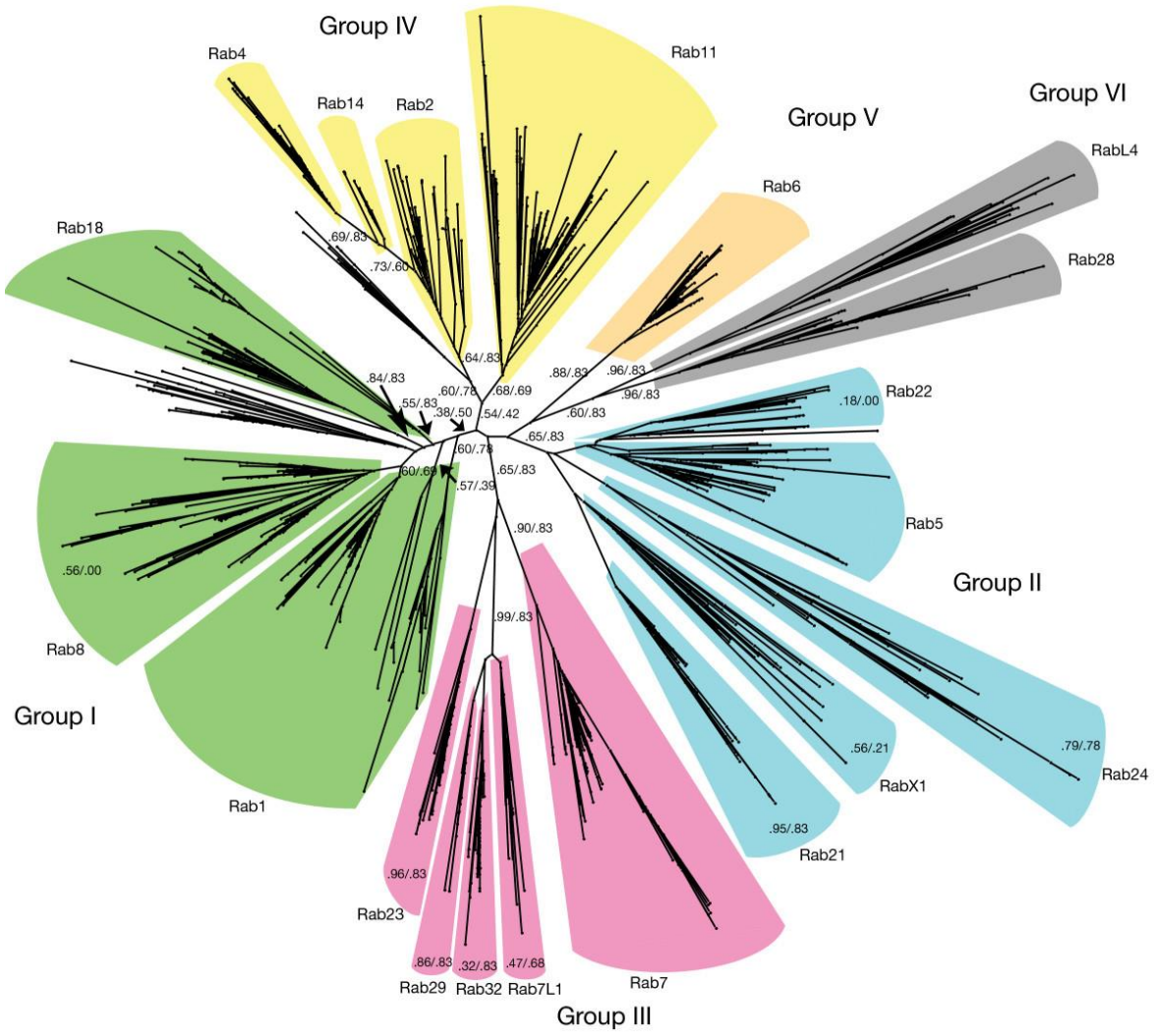
Group IV
Rab4
Rab14
Rab2
Rab11
Group V
Group VI
RabL4
Rab6
Rab28
Rab18
.69/.83
.73/.60
.64/.83
.84/.83
.60/.78
.68/.69
.55/.83
.38/.50
.54/.42
.88/.83
.96/.83
.96/.83
.60/.83
.18/.00
Rab22
.65/.83
.60/.78
.60/.69
.65/.83
.57/.39
Rab5
.90/.83
Group II
.56/.00
.99/.83
Rab8
Group I
.56/.21
.79/.78
Rab24
RabX1
Rab1
.95/.83
Rab21
.96/.83
Rab23
.86/.83
.32/.83
.47/.68
Rab7
Rab29
Rab32
Rab7L1
Group III

(C)

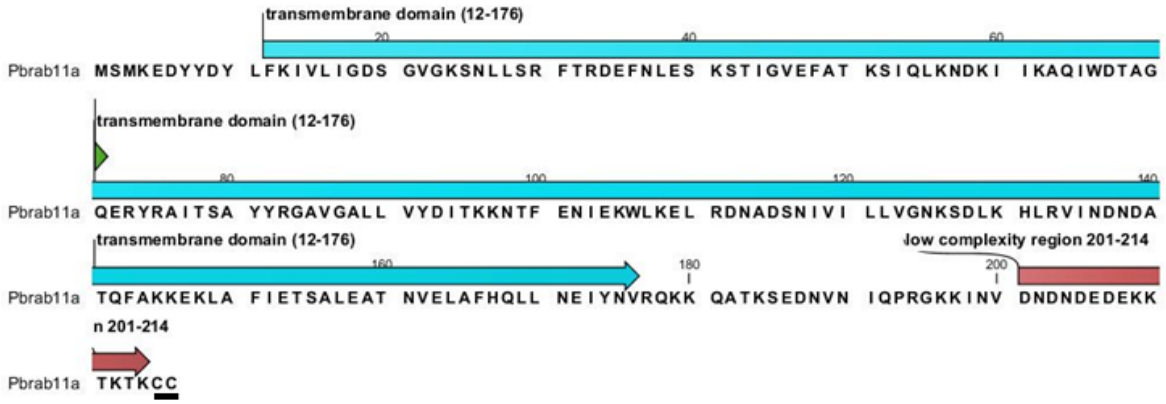

Figure 3.0 Phylogenic analysis of various eukaryotic Rabs and structure of *P. berghei* Rab11A.

(A) Table showing evolution of various Rabs in different phyla and (B) their phylogenic tree. (LECA: Last eukaryotic common ancestor). Chart and tree taken from (Klöpper, Kienle et al. 2012) (C) Domains of *Pbrab11a*: transmembrane domain 12-176 amino acids (aa) (blue), low complexity region 201-214 aa (brown) and C-terminal CC where is C is cysteine (underlined). Analysed from http://smart.embl-heidelberg.de

Rab proteins are probably involved in vesicle trafficking in *P. berghei*, and we will focus on the role of *Pbrab11a* (*P. berghei rab11a*) particularly in the regulation of protein trafficking during the development of ookinete (polarity).

Plasmodium Rab11 was first described in *P. falciparum* (*Pfrab11*). PfRab11 has a C-terminal extension of 20 amino acids when compared to human RAB11, and has two isoforms (Langsley and Chakrabarti 1996): *Pfrab11a* and *Pfrab11b* encoded by distinct genes. Rabs from different organisms have conserved domains particularly in GTP binding domain (Grosshans, Ortiz et al. 2006). Typically, all RAB proteins have a C-terminal CC, CXC motifs (where C stands for cysteine) which are isoprenylated (Khosravi-Far, Lutz et al. 1991, Howe, Kelly et al. 2013). Consistent with this a C-terminal CC domain has been found in PbRab11A (figure 3.0 C). Proteins embedded in vesicles are transported to their target via the microtubule and/or actin filament system. Rab11A is involved in regulating vesicular traffic during recycling endosomes (Ullrich, Reinsch et al. 1996) and assist in cytokinesis (Agop-Nersesian, Naissant et al. 2009) and interacts with PI4Ks (phosphatidylinositol-4 kinases) (McNamara, Lee et al. 2013, Burke, Inglis et al. 2014) and its effectors such as FIPs (Rab11A – family of interacting proteins)(Kelly, Horgan et al. 2012). PfRab11A is expressed in asexual blood stages and shows punctate localization in schizonts (Quevillon, Spielmann et al. 2003, McNamara, Lee et al. 2013). This is further supported by microarray analysis available on www.plasmodb.org (PF13_0119) and RNA-Sequencing data across lifecycle stages of *P. berghei* (A. Religa, Waters Group, unpublished)(Otto, Böhme et al. 2014)(figure 3.1.1).

T. gondii expressing ddFKBP-Rab11A dominant negative form (ddFKBP-Rab11A$_{DN}$) shows reduced invasion of host cells by~ 85%. Furthermore, Shld-1 treated parasites show significantly less parasites in PV(Herm-Gotz, Agop-Nersesian et al. 2007). This indicates that Rab11A is essential for extracellular and intracellular stages of this parasite. Additionally, no parasites were obtained upon deletion of *rab11a* in haploid blood stage of in *P. berghei* (*Pbrab11a* is PBANKA_141890) although parasites where the nuclear copy is deleted could be rescued by providing an episomal copy of GFP-Rab11A. Therefore, Rab11A is appears to be an essential gene for *P. berghei* (Agop-Nersesian, Naissant et al. 2009).

PfRab11A is shown to be associated with vesicular like structures in schizonts (Quevillon, Spielmann et al. 2003) and only Rab11A seems to be associated with rhoptries in *T. gondii* (*Tgrab11a*) (Bradley, Ward et al. 2005) suggesting a role of Rab11A in the rhoptry protein transport and release of rhoptry content during the invasion of host cells. PfRab11A also

localizes with rhoptries when they form (Agop-Nersesian, Naissant et al. 2009). However, Rab11A might carry out other functions during development of the parasite. Rab11A seems to co-localize with MSP1 in young schizonts and yet is largely separate (from MSP1) in merozoites (Agop-Nersesian, Naissant et al. 2009). Co-localization studies of GAP45 and Rab11A supports the notion that Rab11A mediates the delivery of GAP45 to IMC (Agop-Nersesian, Naissant et al. 2009). Pull-down experiments suggest that only Rab11A interacts with MTIP when compared with Rab5C and Rab7, suggesting that Rab11A guided transport is driven by MTIP/MLC motor (Agop-Nersesian, Naissant et al. 2009). During replication, *T. gondii* expressing $Rab11A_{DN}$ (i.e. $Rab11A_{N126I}$) showed no defects in the generation of various cell organelles such as Golgi, apicoplast, nucleus and mitochondrion including IMC formation and localization of sub-pellicular microtubules (Agop-Nersesian, Naissant et al. 2009). In *T. gondii*, the delivery of major surface antigen SAG-1 to cell membrane needs functional Rab11A as $Rab11A_{DN}$ shows patchy (abnormal) instead of smooth (normal) localization of SAG1 (Agop-Nersesian, Naissant et al. 2009). Over-expression of Rab11A is not deleterious. However, over-expression of MyoA tail generates defect in IMC assembly, daughter cell IMCs are completely collapsed within the mother cell (Agop-Nersesian, Naissant et al. 2009). Rab11A controls the necessary step after biogenesis of secretary organelles but before assembly of the motor complex during cell division. These data suggest that Rab11A along with unconventional myosin controls the IMC assembly and budding of daughter cells.

A *P. berghei* ookinete microneme proteome performed using a highly sensitive MudPIT method shows presence of Rab11A along with Rab1, Rab6, Rab7 and other proteins involved in secretory pathways indicating Rab11A could be involved in microneme trafficking (Lal, Prieto et al. 2009). Furthermore, the transcript encoding *rab11a* is one of 370 transcripts which are stabilized and translationally repressed by the DOZI translational repression complex in *P. berghei* (Mair, Braks et al. 2006), indicating its potential role in ookinete development. Taken together, the data indicates that Rab11A is encoded by an mRNA that is translationally repressed in gametocytes and might be associated with ookinete development at the level of determining the subcellular localization of mRNA and/or protein and thus influence the generation of zygote/ookinete polarity. Therefore, further investigation of Rab11A function in the fertilised female gamete (zygote) may reveal insights into the development of polarity in ookinetes, in *P. berghei*.

In addition, another isoform of Rab11A, Rab11B is exclusively required for IMC formation through vesicle transport from the Golgi in *T. gondii*. Disruption of IMC formation shows the random distribution of organelles several times indicating that loss of cell polarity due to loss of IMC. Disruption of IMC also blocks the development and relocation of posterior polar ring and the generation of multinucleated cells (nuclear division takes place but no cytokinesis). However, these studies suggest that these multinucleated cells may or may not undergo daughter cells formation. This shows that formation of polar ring is dependent on IMC formation. However, other phenomena such as segregation of the centrocone and Golgi, polymerisation of sub-pellicular microtubules are independent of Golgi to IMC vesicular transport. Blocking microtubule polymerization by plant herbicide oryzalin also blocks IMC formation. This indicates that IMC formation is dependent on sub-pellicular microtubule formation but not vice-versa (Agop-Nersesian, Egarter et al. 2010). Therefore, presumably after completion of IMC formation, Rab11A mediated vesicle transport is needed for the completion of cytokinesis (Agop-Nersesian, Naissant et al. 2009), similar to other eukaryotes (Chapter 1- figure 1.7 A).

3.1 PbRab11A is expressed throughout *P. berghei* lifecycle and localizes to the periphery and apical tip of the ookinete

To analyse the expression of PbRab11A (PBANKA_141890), we examined Rab11A transcript profile (RNASeq data by A. Religa- Waters Group, Unpublished)(Otto, Böhme et al. 2014) which demonstrated the presence of Rab11A mRNA at ring, trophozoite, schizont and ookinetes while gametocytes the greatest abundance of Rab11A mRNA (figure 3.1.1 A). A polyclonal antibody raised against C-terminal end of Rab11A (Cysteine tagged peptide C-RGKK INVDN DNDED EKKTK, Proteintech) (figure 3.1.1 B) was used to detect the protein. Western analysis of WT parasites which constitutively expresses GFP (WT-GFP$_{CON}$, henceforth referred as WT-GFP for simplicity) (Franke-Fayard, Trueman et al. 2004) showed the expression of PbRab11A across mixed asexual stages, schizonts, gametocytes and ookinetes (figure 3.1.1 C). Post-activation of gametocytes, expression of PbRab11A gradually increases with maximum expression in fully developed ookinetes (figure 3.1.1 D). In schizonts and mature ookinetes, an extra band is detected indicating possible differential regulation of Rab11A (dotted arrows in figure 3.1.1 C and D). The reason for the expression and the nature of the additional smaller band detected with the anti-Rab11A sera is not yet known.

Immunofluorescence microscopy showed expression of PbRab11A in WT-GFP parasites (Franke-Fayard, Trueman et al. 2004) at mature schizonts (individual merozoites), 6h zygotes, ookinetes, oocysts as well as midgut sporozoites (figure 3.1.2). In merozoites, oocyst (day10) and midgut sporozoites (day10), the localization of Rab11A is cytoplasmic. In the 6h zygote, Rab11A localization is cytoplasmic and appears punctate while in the ookinete Rab11A is more peripheral and focused at apical tip suggesting a role of Rab11A at the apical complex (figure 3.1.2).

(A)

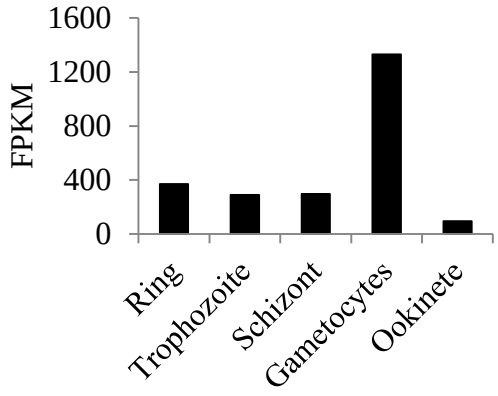

(B)

MSMKEDYYDY LFKIVLIGDS GVGKSNLLSR FTRDEFNLES KSTIGVEFAT KSIQLKNDKI[60]
IKAQIWDTAG QERYRAITSA YYRGAVGALL VYDITKKNTF ENIEKWLKEL RDNADSNIVI[120]
LLVGNKSDLK HLRVINDNDA TQFAKKEKLA FIETSALEAT NVELAFHQLL NEIYNVRQKK[180]
QATKSEDNVN IQPRGKKINV DNDNDEDEKK TKTKCC[216]

C-RGKKINV DNDNDEDEKK TK

(C)

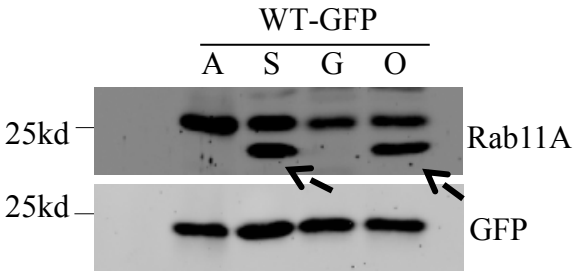

(D)

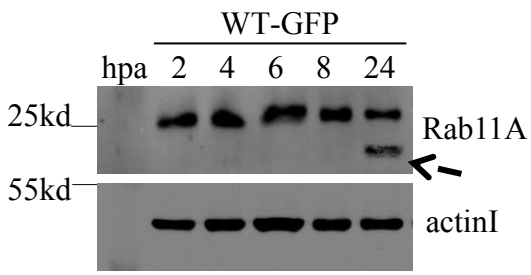

Figure 3.1.1 Rab11A expression during *P. berghei* lifecycle stages.

(A) PbRab11A transcription profile in FPKM (fragments per Kb of open reading frame per million reads) at ring, trophozoite, schizont, gametocytes and ookinete stage (Source: RNA-Seq data by A. Religa - Waters Group, unpublished) (Otto, Böhme et al. 2014). (B) Sequence of PbRab11A with the cysteine tagged peptide used to raise polyclonal rabbit anti-PbRab11A antibody shown in bold. (C) Expression of Rab11A in: A, mixed asexual stages; S, schizonts; G, unactivated gametocytes and O, ookinete and (D) after post-activation of gametocytes i.e. zygote to ookinete development using rabbit anti-PbRab11A antibody. Blots were scanned on Odyssey® Sa Infrared Imaging System (LI-COR Biosciences). Arrows indicate the additional small PbRab11A band in schizont and ookinete. hpa= hours post-activation (of gametocytes).

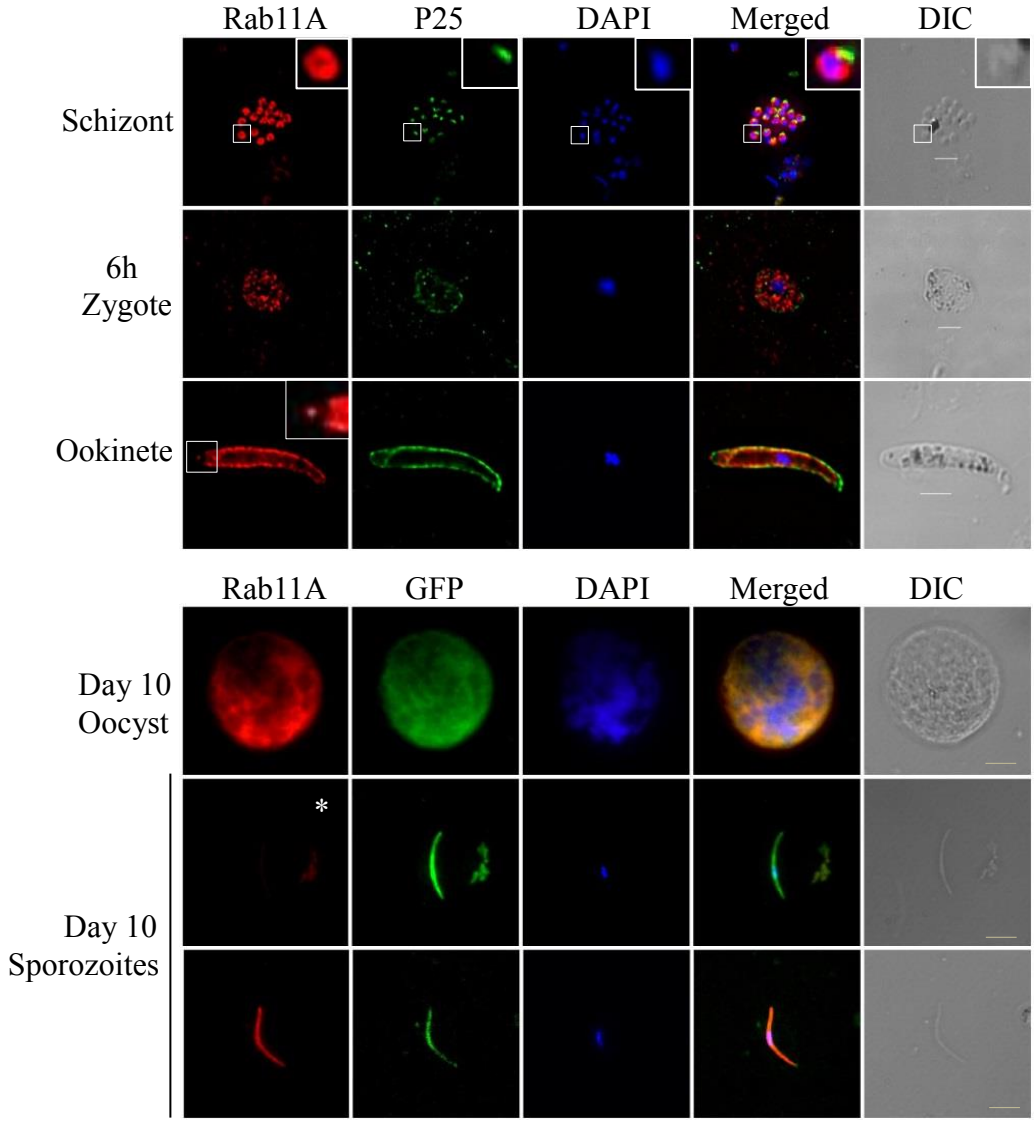

Figure 3.1.2 Rab11A localization during *P. berghei* lifecycle.

Localization of Rab11A in WT-GFP parasites determined through anti-PbRab11A antibody during blood stage: schizont (separated merozoites), mosquito stages: zygote, ookinete, day 10 oocyst and midgut sporozoites. Rab11A localization is predominantly cytoplasmic in merozoites, oocyst and sporozoites while cytoplasmic and punctate in 6h zygote. In ookinetes, Rab11A localization is peripheral as well as focused at the apical tip. Inset shows a magnified image of separated merozoite and ookinete tip in respective images. Scale 3 μm. (Schizonts, zygote and ookinete images are Deltavision deconvoluted single slices. Oocysts and sporozoites images are taken through Axioplan)

*Negative control- no anti-PbRab11A antibody in WT-GFP sporozoite.

3.2 N-terminal fluorescent tagging of PbRab11A using endogenous 5'UTR is not possible.

To study the localization in live parasites, C-terminal tagging is the standard approach in *Plasmodium*. However, to avoid interfering with conserved C-terminal geranylgeranylation and to study PbRab11A localization in live parasites, a double cross-over strategy was used for N-terminal tagging of PbRab11A with a small green fluorescent protein – iLOV (342bp) (Chapman, Faulkner et al. 2008, Christie, Hitomi et al. 2012) and two copies of C-MYC expressed under PbRab11A endogenous 5'UTR (877bp upstream of *rab11a* ORF) [Plasmid *ilov::2c-myc::rab11a*$_{0.6kb}$ with the selectable marker (SM) human *dhfr/ts*] (figure 3.2.1 A, D upper). The plasmid *ilov::2c-myc::rab11a*$_{0.6kb}$ with human *dhfr/ts* was generated and transfected to WT *P. berghei* HPTBB parasites (no constitutive green fluorescence) and transgenic clones were selected and analysed by diagnostic PCRs (figure 3.2.1 B). The selectable marker (human *dhfr/ts*) from plasmid *ilov::2c-myc::rab11a*$_{0.6kb}$ underwent genomic integration excluding *ilov* and possibly 2*c-myc* during homologous recombination. The possibility of exclusion of *ilov* and 2*c-myc* is assumed to be due to the presence of the endogenous *rab11a* 5'UTR which might have undergone recombination (figure 3.2.1 C).

A second version of the double crossover tagging plasmid (*ilov::2c-myc::rab11a*$_{1.55kb}$) with complete *rab11a* ORF of 1559bp included for recombination was generated (figure 3.2.1 D lower), transfected in WT *P. berghei* HPTBB and cloned by flow cytometry (Kenthirapalan, Waters et al. 2012) and referred as FACS Clones. Diagnostic PCR of FACS clones showed correct integration of SM (5'-end), however multiple attempts failed to confirm the integration of *ilov* and *2cmyc* at the 3'-end (figure 3.2.2 A). Therefore, to check the size and localization of iLOV::2CMYC::Rab11A, western blotting was performed using the rabbit anti-PbRab11A antibody which demonstrated that the size of "transgenic" Rab11A was similar to WT (figure 3.2.2 B). Live images of *ilov::2c-myc::rab11a* ookinetes appeared similar to WT ookinetes (show background green fluorescence) and were not fluorescent (figure 3.2.2 C). Therefore, the genotype of FACS cloned *ilov::2c-myc::rab11a* parasites seem to be without *ilov* and *2cmyc* (like in figure 3.2.1 C) confirming N-terminal tagging of *Pbrab11a* with *ilov* and *2cmyc* using *Pbrab11a* endogenous 5'UTR was not successful.

(A)

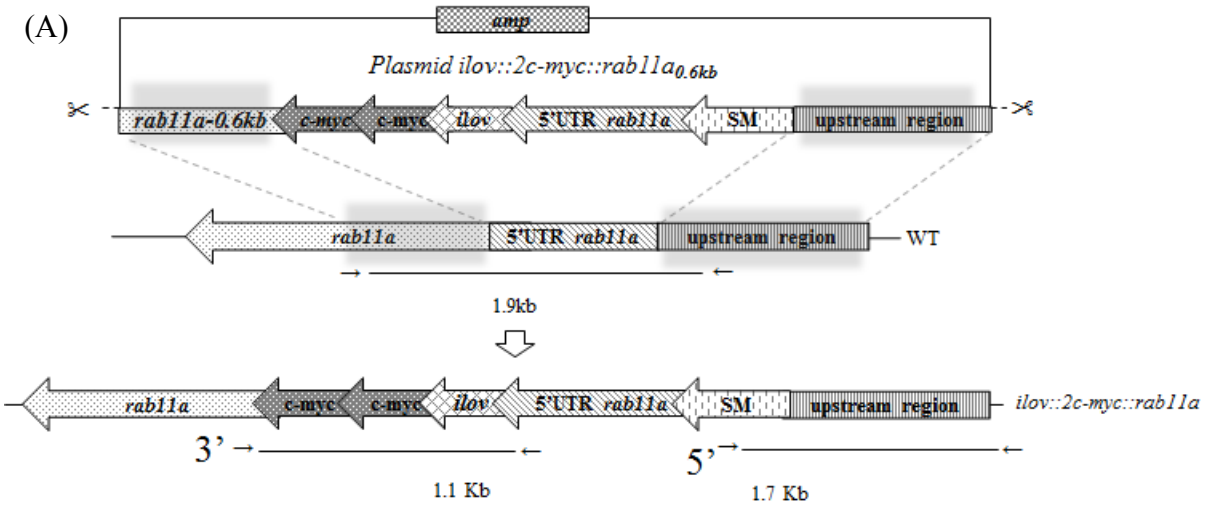

(B)

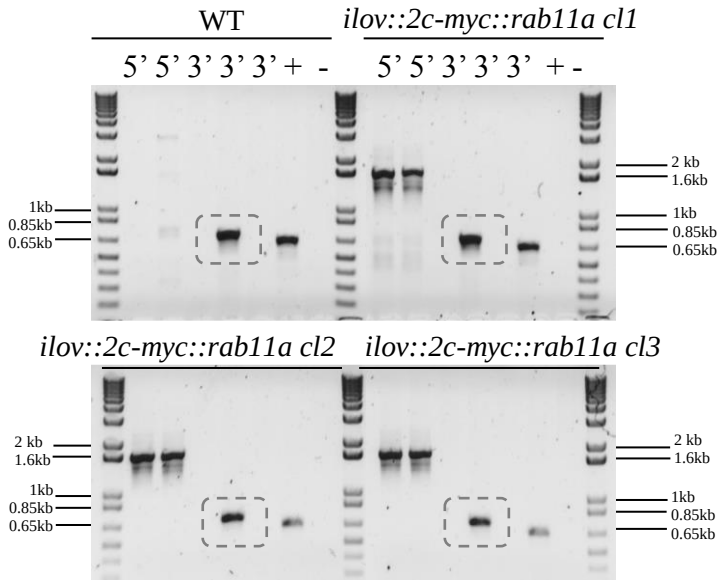

ilov size is 300 bp

1.1kb-0.34kb= 0.7bp

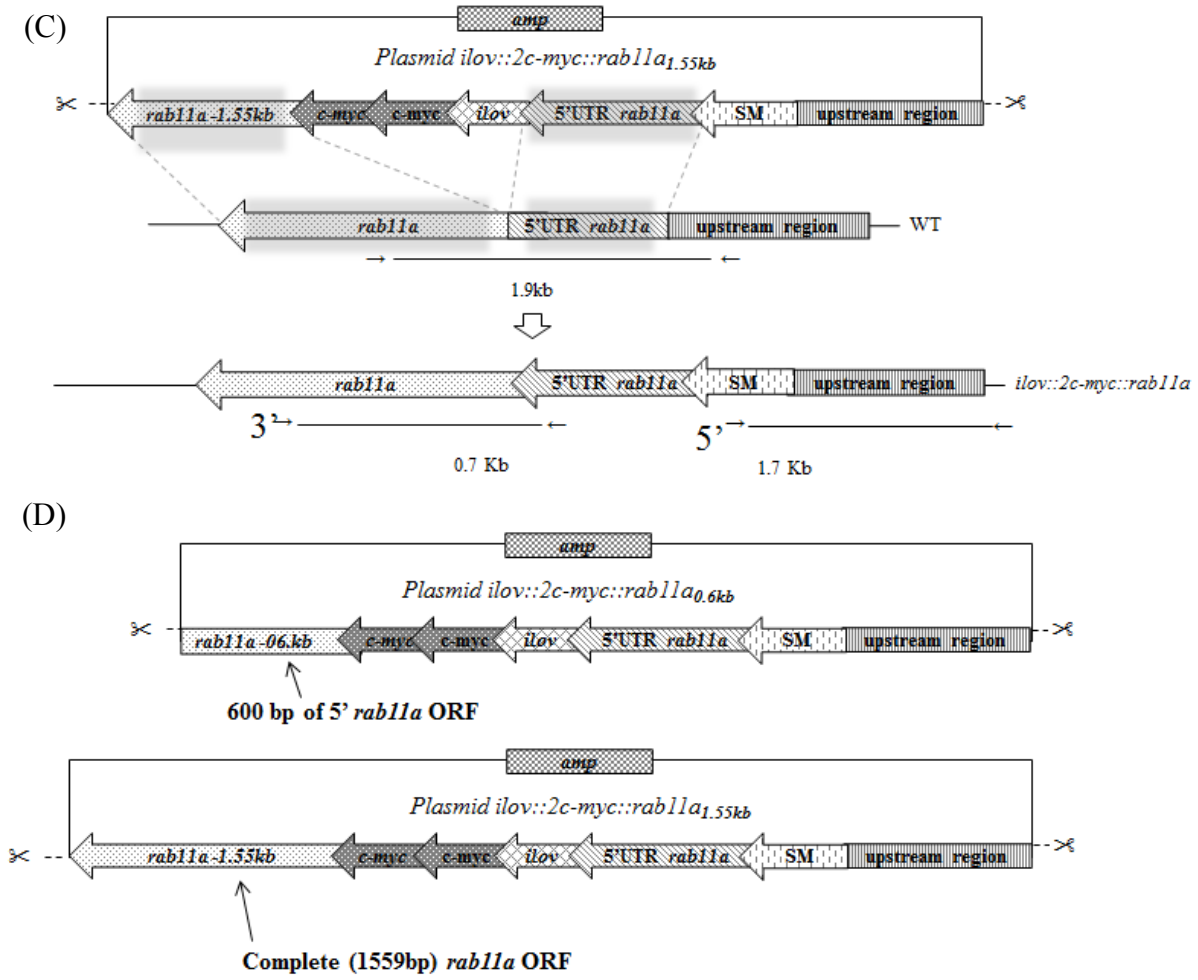

Figure 3.2.1 Approaches used for N-terminal tagging of Rab11A.

(A) Schematic representation of generation of *ilov::2c-myc::rab11a* parasites from *ilov* and *2cmyc* tagging construct containing 600bp of *5'rab11a* ORF. (B) Diagnostic PCR showing integration of selectable marker- human *dhfr/ts* and elimination of *ilov* and *2c-myc* and (C) its schematic representation. (D) Construct for *ilov* tagging using 600 *5'rab11a* ORF (*ilov::2c-myc::rab11a*$_{0.6kb}$) and complete (1559bp) *rab11a* ORF (*ilov::2c-myc::rab11a*$_{1.55kb}$).

(A)

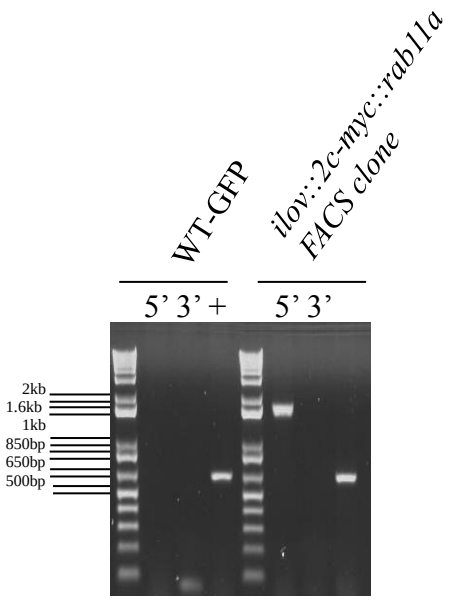

(B)

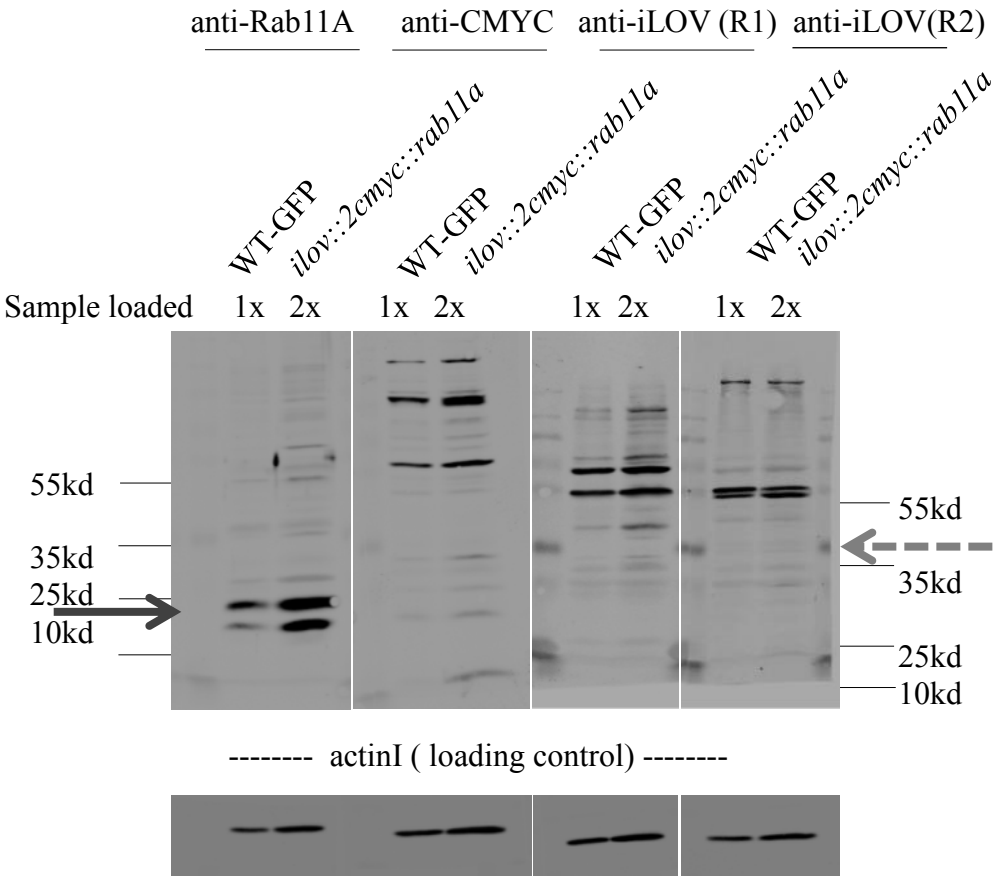

Protein sizes in kd

Rab11A	2CMYC	iLOV (without stop codon)	= iLOV::2CMYC::RAB11A
24.76	2.39	13.15	= 40.3

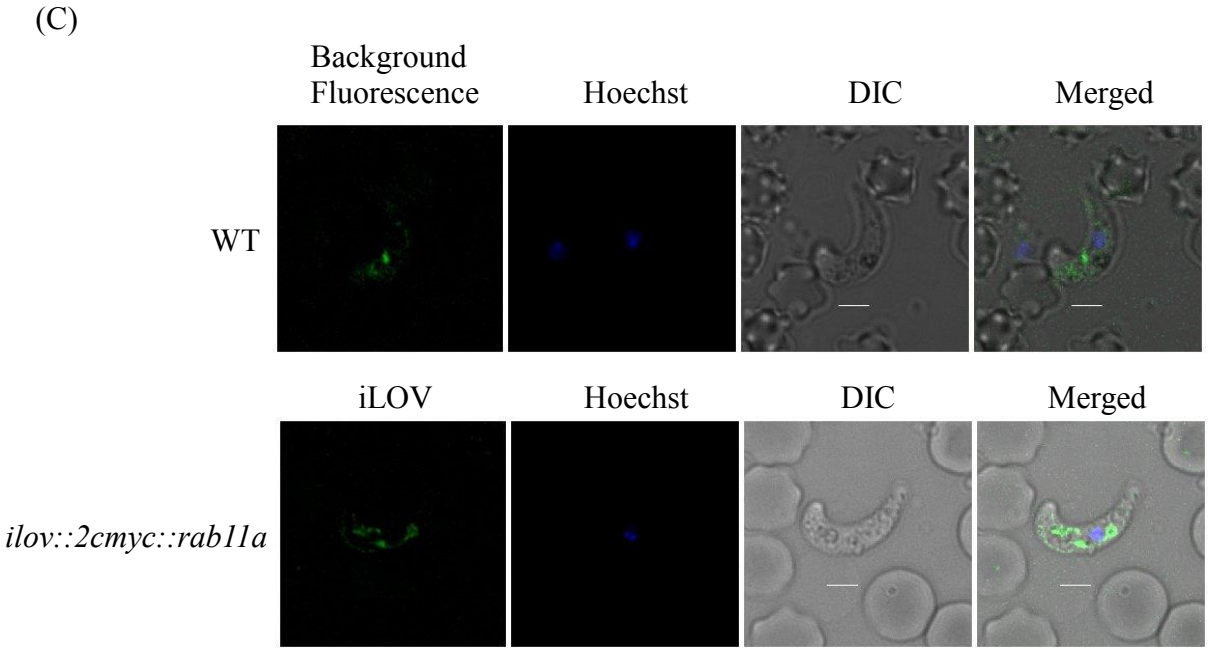

Figure 3.2.2: Analysis of iLOV tagged Rab11A parasites.

(A) Diagnostic PCR showing 5' integration of plasmid *ilov::2cmyc::rab11a*$_{1.55kb}$ in WT genome. Multiple attempts of diagnostic PCR for 3' integration failed. (B) Western blotting with anti-PbRab11A, anti-CMYC antibodies and anti-iLOV antibodies from rabbit 1 (R1) and 2 (R2) showing size of Rab11A in FACS cloned *ilov::2cmyc::rab11a*$_{1.55kb}$ parasites similar to WT. Black arrow shows WT protein i.e. RAB11A and dotted grey arrow suggest the area where recombinant protein i.e. iLOV::2CMYC::RAB11A (40.3Kd) might have been appeared. ActinI is a loading control. Double amount (2x) of *ilov::2cmyc::rab11a*$_{1.55kb}$ sample was loaded on the gel as compared to WT sample (1x). (C) Live images taken on Deltavision microscope (deconvoluted single slice) of FACS cloned *ilov::2cmyc::rab11a*$_{1.55kb}$ ookinetes showing background fluorescence as seen in WT ookinetes. Scale bar 3 µm.

3.3 Rab11A is crucial for ookinete morphology and is contributed by both male and female gamete

Rab11A mRNAs are more abundant in gametocytes (RNA-Seq data by A. Religa- Waters Group, Unpublished)(Otto, Böhme et al. 2014) (Results 3.1) and are translationally repressed (Mair, Braks et al. 2006, Guerreiro, Deligianni et al. 2014). Therefore, to determine the role of Rab11A during the development of the ookinete, a promoter swap approach has been used as *Pbrab11a* is refractory to deletion (Agop-Nersesian, Naissant et al. 2009). Both CLAG (PBANKA_140060) and AMA-1 (PBANKA_091500) promoters are known to remain silent in sexual stages while keeping expression level high during asexual blood stages (Laurentino, Taylor et al. 2011, Siden-Kiamos, Ganter et al. 2011, Otto, Böhme et al. 2014) (RNA-Seq data by A. Religa- Waters Group, Unpublished, figure 3.3.1 A). The 0.9 kb 5'UTR of *rab11a* were replaced by 2 kb 5'UTR of *clag* (promoter of *clag* referred as $_{p}$*clag*) or 1.7 kb 5'UTR of *ama-1* (promoter of *ama-1* referred as $_{p}$*ama-1*) and *2cmyc* in WT-GFP parasites (Franke-Fayard, Trueman et al. 2004) and cloned via serial dilution. Both independently generated Rab11A promoter-swap mutants: $_{p}$*clag:2cmyc::rab11a* and $_{p}$*ama-1:2cmyc::rab11a* (henceforth referred as $_{p}$*clag::rab11a* and $_{p}$*ama-1::rab11a* for simplicity) show appropriate genomic integration of respective plasmids ($_{p}$*clag::rab11a* and $_{p}$*ama-1::rab11a* plasmids)(Figure 3.3.1 B, C, D).

The two independently generated Rab11A promoter-swap mutants: $_{p}$*clag::rab11a* and $_{p}$*ama-1::rab11a* show no apparent growth defects during blood stages and gametogenesis, analysed by observation of morphology of $_{p}$*clag::rab11a* and $_{p}$*ama-1::rab11a* gametocytes and $_{p}$*clag::rab11a* and $_{p}$*ama-1::rab11a* male exflagellation as well as ratio of male gametocytes to female gametocytes in $_{p}$*clag::rab11a* and $_{p}$*ama-1::rab11a* parasites were comparable to WT-GFP blood stages (figure 3.3.2). However, *in vitro* ookinete cultures of $_{p}$*clag::rab11a* and $_{p}$*ama-1::rab11a* parasites show a severely impaired zygote to ookinete development by up to 99% and 98% respectively (figure 3.3.3 A). Ookinete cultures of $_{p}$*clag::rab11a* and $_{p}$*ama-1::rab11a* 24hpa shows spherical possibly arrested zygotes (referred as round/spherical ookinetes throughout this report) (figure 3.3.3 B). Due to the poorer ookinete conversion rate in $_{p}$*clag::rab11a* parasite line as compared to $_{p}$*ama-1::rab11a* parasite line, $_{p}$*clag::rab11a* line was chosen for further analysis.

Western analysis of $_{p}$*clag::rab11a* and $_{p}$*ama-1::rab11a* show normal expression of Rab11A in mixed asexual blood stages including schizonts, however, Rab11A is reduced in

gametocytes and *$_p$clag::rab11a* and *$_p$ama-1::rab11a* ookinetes (figure 3.3.4 A, B). Analysis of Rab11A post-fertilization shows continued absence of Rab11A in *$_p$clag::rab11a* from 2hpa (hours post activation) till 24hpa (figure 3.3.4 B). Immunofluorescence studies support the down-regulation of Rab11A in *$_p$ama-1::rab11a* ookinetes (figure 3.3.4 C). No expression defect was observed for the closely related Rab11B during zygote to ookinete development (figure 3.3.4 D, E). Activated-unfertilized 24h WT-GFP female gametes (AUFG - treated with 2-Deoxy-D-glucose, 2DG) show expression of Rab11A indicating activation of translationally stored Rab11A mRNAs (figure 3.3.4 B, C).

The large nucleus of the *$_p$clag::rab11a* and *$_p$ama-1::rab11a* spherical ookinetes indicate that *$_p$clag::rab11a* and *$_p$ama-1::rab11a* female gametocytes do fertilize and possibly undergo meiosis (figure 3.3.3 B and figure 3.3.4 C, E). The FACS pattern for DNA content of *$_p$clag::rab11a* zygotes 4hpa is similar to WT-GFP zygotes 4hpa (figure 3.3.5 A, B), suggesting meiosis has occurred; however, *$_p$clag::rab11a* zygotes fail to undergo morphological differentiation.

Next, we studied if the defect is gender-specific by performing genetic crosses between the *$_p$clag::rab11a* and male deficient (*p48/45*$^-$) (van Dijk, Janse et al. 2001) or female deficient (*p47*$^-$) gametocytes (van Dijk, van Schaijk et al. 2010). Cross fertilization of *$_p$clag::rab11a* female gametocytes where *$_p$clag::rab11a* male exflagellation is blocked with 100mM 2-Deoxy-D-glucose, a non-metabolizable analogue of D-glucose (K. Hughes, Waters group, unpublished data), with female deficient gametes (*p47*$^-$,male active) did rescue the phenotypes partially giving up to 10.1% ookinetes while cross fertilization of *$_p$clag::rab11a* male gametocytes (*$_p$clag::rab11a* female gametocytes are still active) with active female gametes (*p48/45*$^-$, male gamete deficient) rescued the phenotypes partially giving up to 10.7% ookinetes demonstrating that partial rescue was same for both the genders so the requirement for Rab11A is through both male and female gametes, is equivalent and likely to be a consequence of having two active *rab11a* alleles as opposed to one i.e. gene dose effect (figure 3.3.6 A, B).

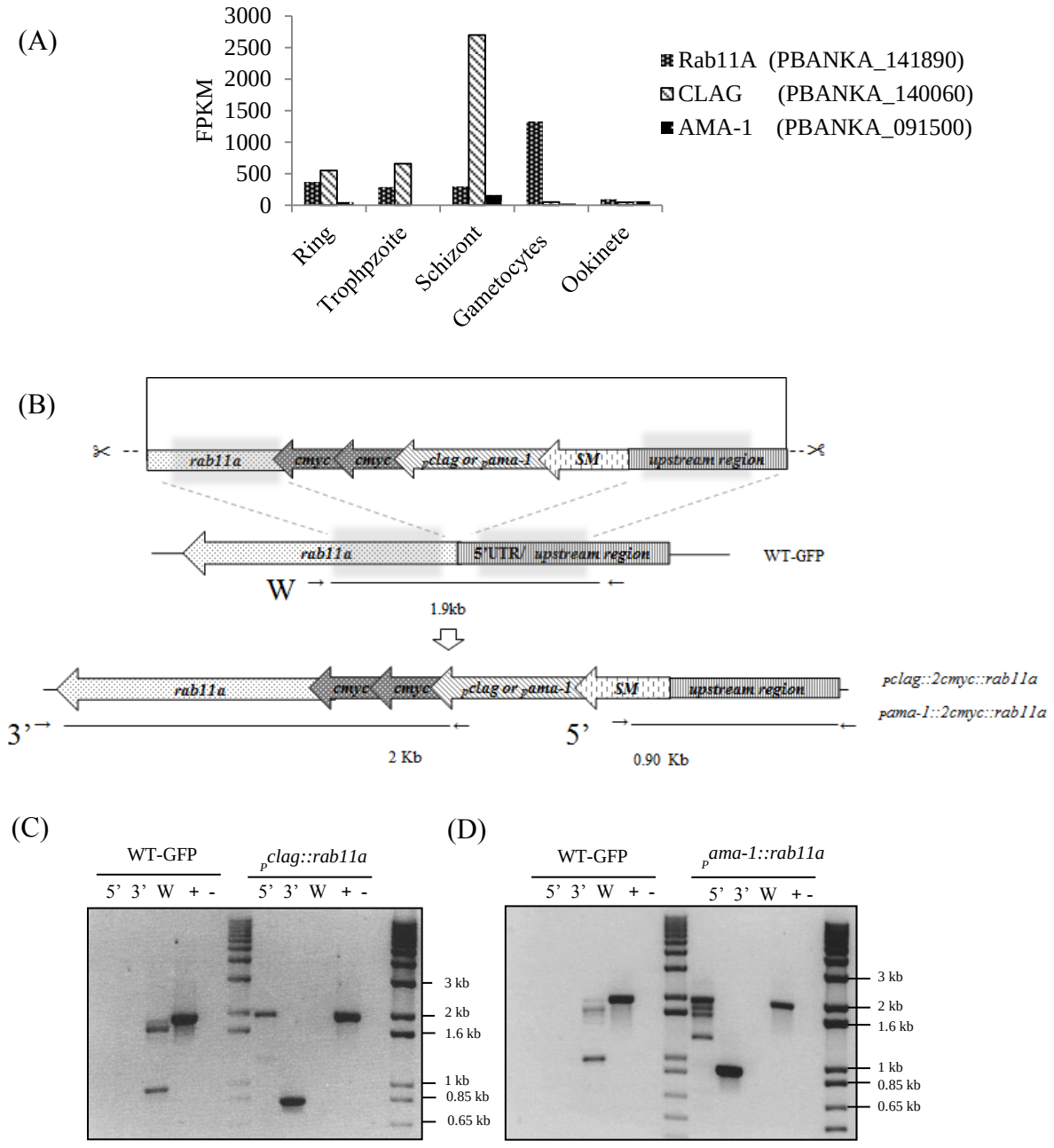

Figure 3.3.1 Generation of Rab11A promoter swap parasites.

(A) *P. berghei* RNA-Seq data for Rab11A, CLAG and AMA-1 with FPKM (fragments per Kb of open reading frame per million reads) values. (RNA-Seq data by A. Religa, Waters group, unpublished)(Otto, Böhme et al. 2014) (B) Schematic of the generation of *pclag::rab11a* and *pama-1::rab11a* parasites. (C and D) Diagnostic PCRs for integration of *pclag::rab11a* and *pama-1:: rab11a* plasmids into WT-GFP gDNA showing the 5' and 3' integration of respective constructs (PCR fragment as annotated in the schematic). W indicates a fragment present only in WT-GFP parasites. DNA '+' is an unrelated positive PCR control and '-' is a no DNA template negative PCR control.

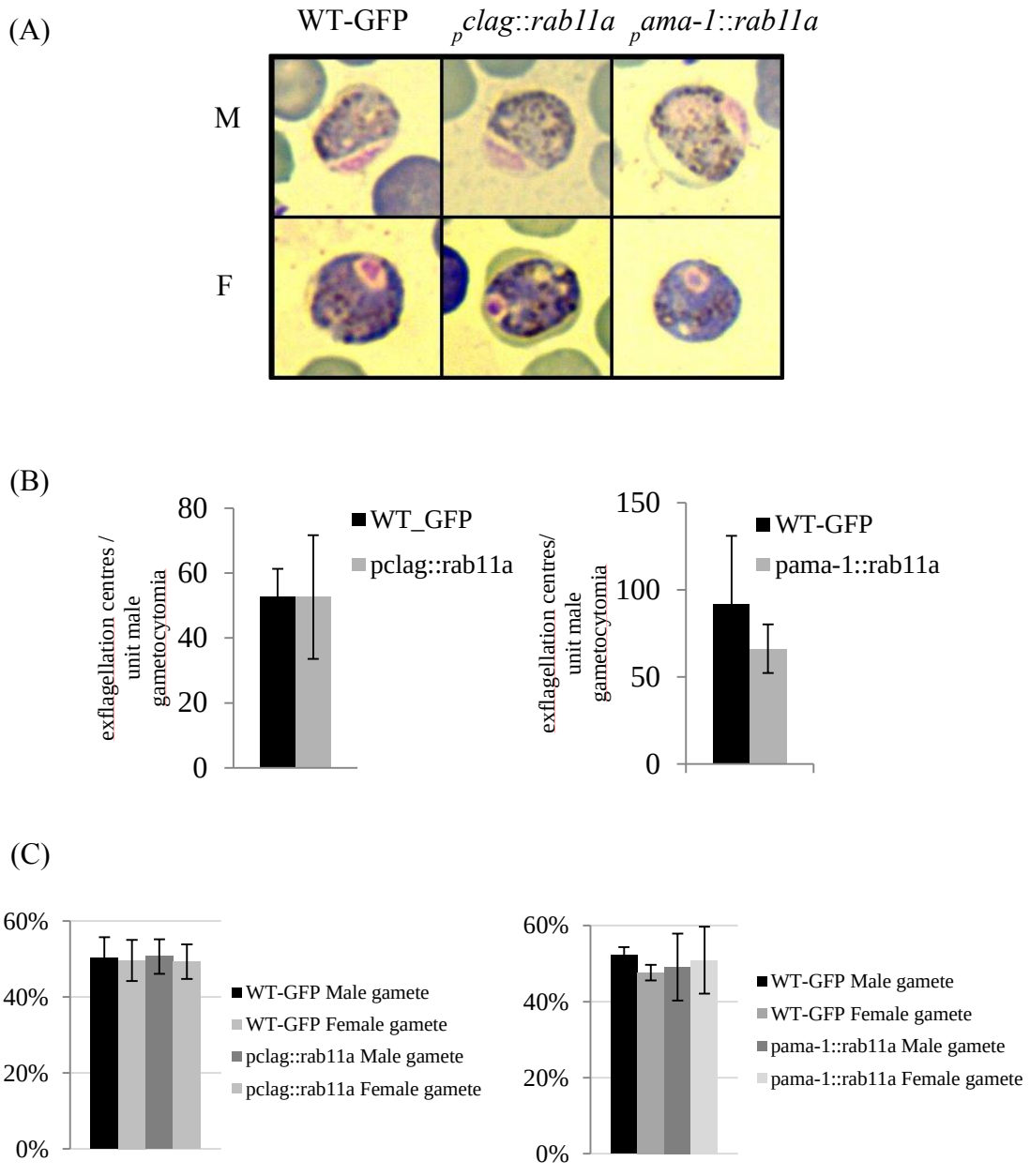

Figure 3.3.2 Development of asexual stages of *pclag::rab11a* and *pama-1::rab11a* parasites.

(A) Images of Giemsa stained *pclag::rab11a* and *pama-1::rab11a* gametocytes (B) *pclag::rab11a* (n=4, mean +/-SD, two tailed student t test, p-value 0.9891) and *pama-1::rab11a* (n=3, mean +/-SD, two tailed student test, p-value 0.4337) male gametocyte exflagellation count. (C) Ratio of *pclag::rab11a* (n=6, mean +/-SD, two tailed student t test, p value 0.00046) and *pama-1::rab11a* (n=3, mean +/-SD, two tailed student test, p-value 0.0111) male to female gametocytes.

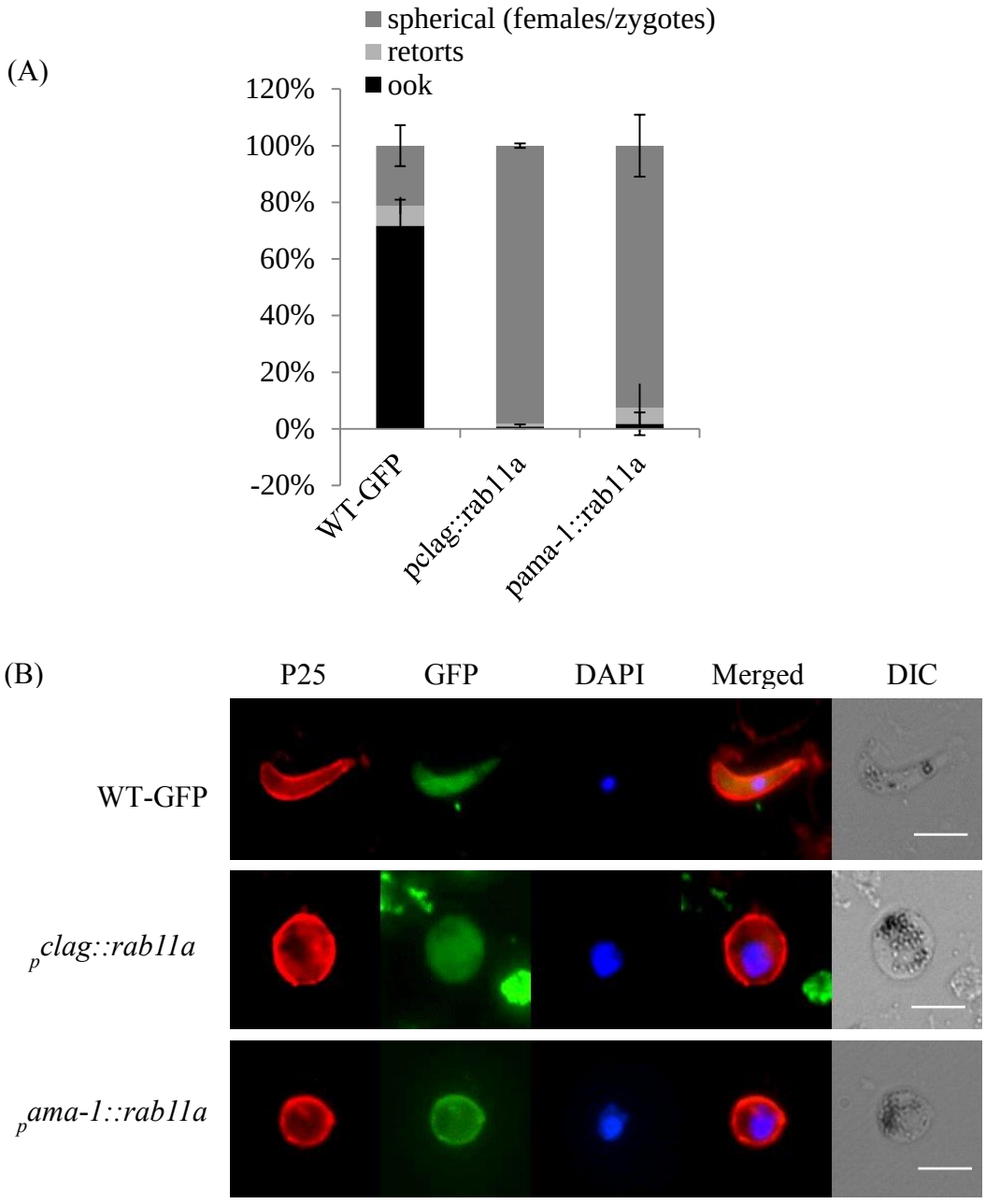

Figure 3.3.3 Spherical *pclag::rab11a* and *pama-1::rab11a* ookinetes.

(A) Plot of *pclag::rab11a* and *pama-1::rab11a* ookinete development (n=3, mean +/-SD, two tailed student t test, p-value 0.0001). (B) Fertilized *pclag::rab11a* and *pama-1::rab11a* spherical ookinetes i.e. 24h post-activation showing enlarged nucleus (Images taken on Axioplan). Scale bar 5 µm.

(A)

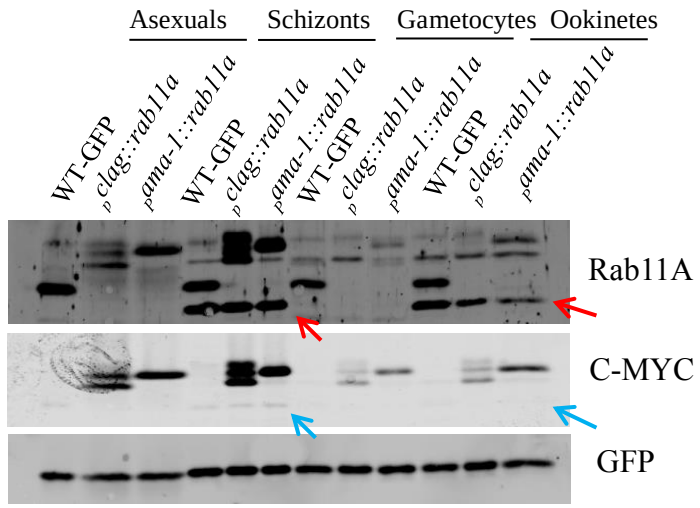
Asexuals
Schizonts
Gametocytes
Ookinetes
WT-GFP
pclag::rab11a
pama-1::rab11a
Rab11A
C-MYC
GFP

(B)

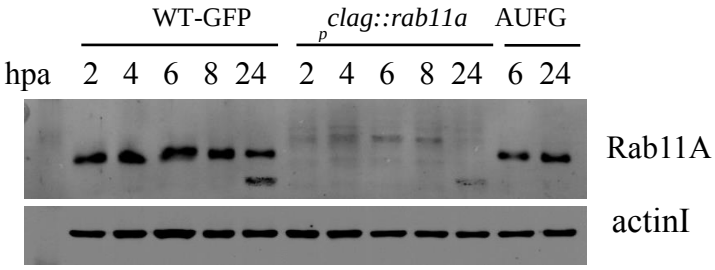
WT-GFP
pclag::rab11a
AUFG
hpa
2 4 6 8 24 2 4 6 8 24 6 24
Rab11A
actinI

(C)

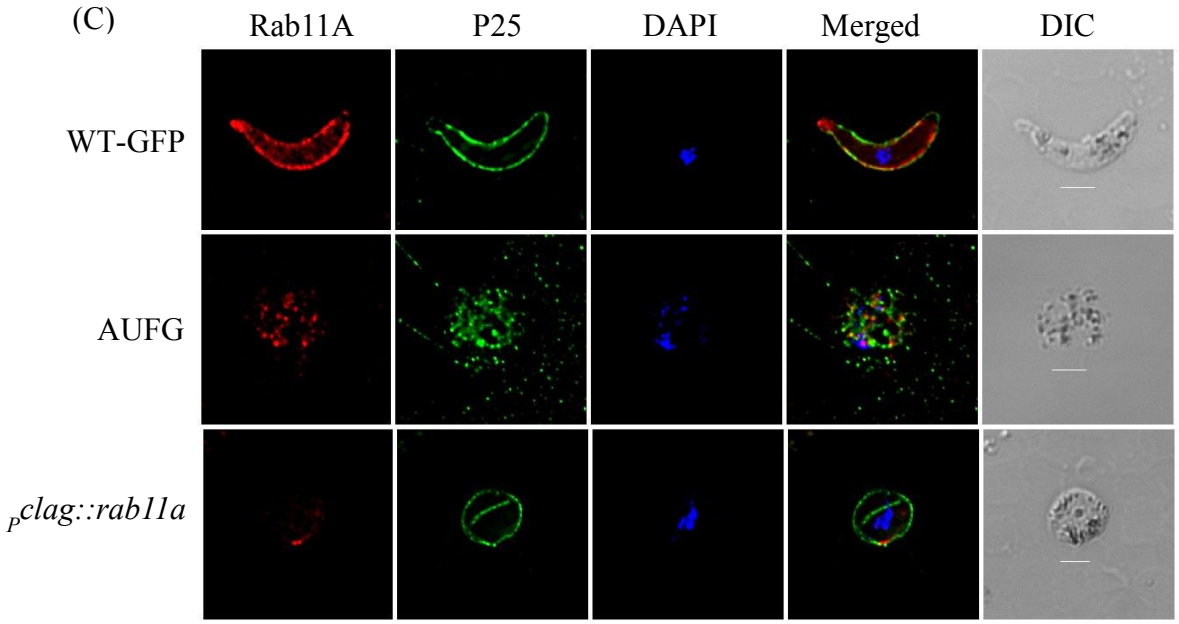
Rab11A
P25
DAPI
Merged
DIC
WT-GFP
AUFG
pclag::rab11a

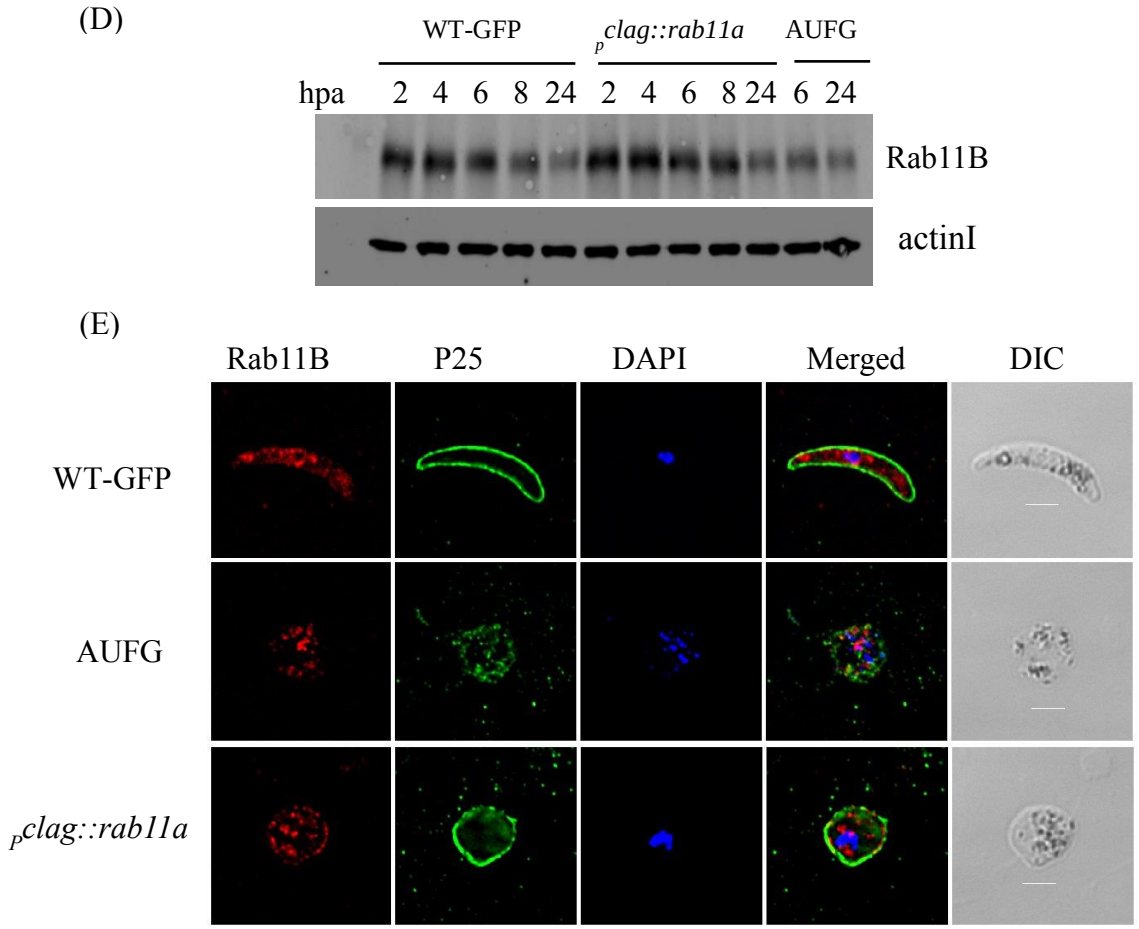

Figure 3.3.4 PbRab11A is down-regulated in *pclag::rab11a* and *pama-1::rab11a* ookinetes.

(A) Western blot for Rab11A in *pclag::rab11a* and *pama-1::rab11a* parasites at various life cycle stages probed with anti-PbRab11A, anti-CMYC antibody. GFP is a loading control. (B) Western blots showing the expression of Rab11A in *pclag::rab11a* at 2, 4, 6, 8 and 24hpa as well as in AUFG 6 and 24hpa. Red arrows show the presence of extra bands in schizont and ookinete stages when the blot is probed with anti-PbRab11A antibody. Blue arrows show the absence of these extra bands when probed with an anti-CMYC antibody. (C) Western blot showing expression of Rab11B in *pclag::rab11a* at 2, 4, 6, 8 and 24hpa as well as in unfertilized female gametes 6 and 24hpa. hpa-hours post-activation. PbRab11A is tagged to two copies *c-myc* (MW = 2.67 kd) in *pclag::rab11a* and *pama-1::rab11a* and not in WT-GFP. Western blots were scanned on Odyssey® Sa Infrared Imaging System (LI-COR Biosciences). (D) Microscopy images of immunofluorescence on fixed parasites using anti-RAB11A, anti-Rab11B, anti-P25 antibodies as indicated and DAPI as a nuclear stain. Image shown is a single slice of Deltavision deconvoluted Z stack, scale bar 3 μm.

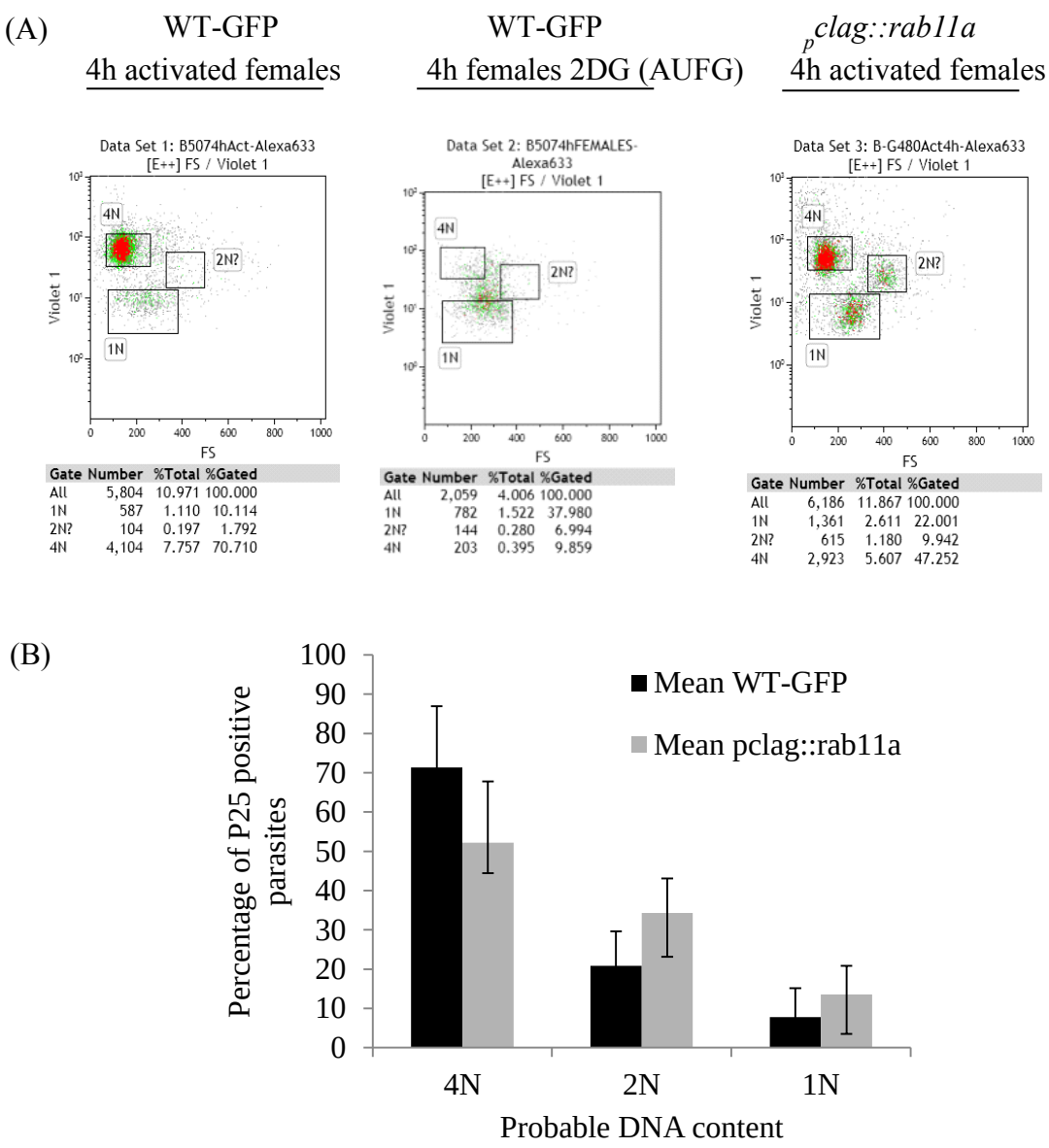

Figure 3.3.5 *pclag::rab11a* spherical ookinetes undergo meiosis.

(A) Flow cytometry analysis on FACsCYAN to illustrate DNA content of *pclag::rab11a* gametocytes 4hpa. Parasites stained with DNA stain Hoechst were gated for activation using anti-P25 antibody and DNA content in these compared to WT-GFP gametocytes 4hpa and WT-GFP unfertilized female gametes 4hpa. FACS plots showing results of one of three independent experiments while (B) bar graph shows percentage of 4N (zygotes underwent meiosis), 2N (fertilized female gametes, meiosis is incomplete or blocked) and 1N (gametocytes or asexual) parasites. Data from (activated) female gamete was used to verify the gating strategy (n=3, mean +/-SD, two tailed student t test, p-value 0.129292).

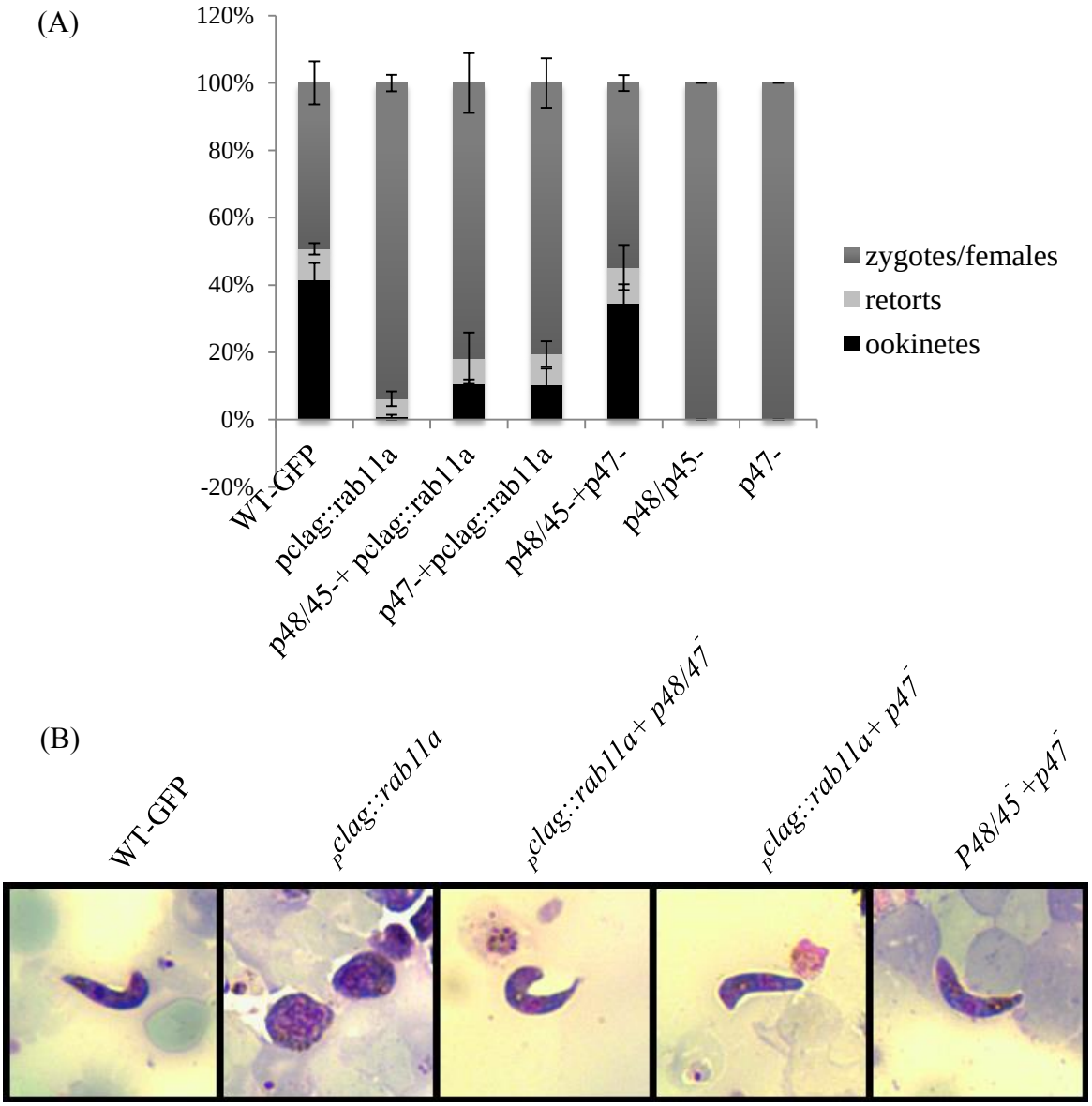

Figure 3.3.6 Rab11A is contributed by both male and female gametes.

(A) Cross-fertilization of *pclag::rab11a* with male defective (*P48/45*$^{-}$) and female defective (*p47*$^{-}$) mutants (n=3, mean +/- SD, p value 0.0001) and (B) Representative Giemsa images of ookinetes and zygotes obtained after cross fertilization .

3.4 Rab11A is essential for transmission of *P. berghei* through mosquitoes.

To determine if the spherical *$_p$clag::rab11a* and *$_p$ama-1::rab11a* ookinetes are able to complete the life cycle through invertebrate host, mosquito transmission experiments were performed. Female *Anopheles stephensi* mosquitoes were allowed to feed on WT-GFP, *$_p$clag::rab11a* or *$_p$ama-1::rab11a* infected mice. The resulting presence of oocysts in the mosquito midgut was examined on day 11 or 14. Mosquito midguts were also analysed on day 17, 18 or 22 assuming that *$_p$clag::rab11a* and *$_p$ama-1::rab11a* spherical ookinetes might have delayed midgut transversal and oocyst development. The WT-GFP showed normal oocyst development in mosquito midgut [median 150, mean 227.16 oocysts per midgut (n=3), mosquitoes infected with WT-GFP parasites were counted per experiment in 3 independent transmissions] while *$_p$clag::rab11a* (maximum of 4 oocysts per midgut with small size, mean 0.269, median 0 and n=3) or *$_p$ama-1::rab11a* (maximum of 5 oocysts per midgut with small size, mean 0.31, median 0, n=2) (independent WT-GFP control for *$_p$ama-1::rab11a* showed mean 83.66, median 130.47, n=2) showed greatly reduced numbers of oocysts (figure 3.4 A, B and D, E) and salivary gland analysis showed a complete absence of *$_p$clag::rab11a* and *$_p$ama-1::rab11a* sporozoites (figure 3.4 C,E). Upon feeding of infected mosquitoes on mice (bite-back) on day 18, 22 or 24, no parasites were observed in *$_p$clag::rab11a* (n=3) or *$_p$ama-1::rab11a* (n=2) infected mice monitored until day 14 post infection while WT-GFP parasites were observed on day 3 in all experiments. This effectively suggests that *$_p$clag::rab11a* and *$_p$ama-1::rab11a* spherical zygotes are unable to transmit through mosquitoes and therefore Rab11A is essential for the transmission of *P. berghei* and might have critical function during ookinete development.

Due to inability of *$_p$clag::rab11a* ookinetes to cross mosquito midgut and its spherical shape, we examined motility of *$_p$clag::rab11a* spherical ookinetes. Motility of *$_p$clag::rab11a* ookinetes were analysed with WT-mCherry ookinetes by embedding ookinete cultures in Matrigel (see 2.1.2 k in Chapter 2: Materials and Methods for details). WT-mCherry ookinetes showed normal corkscrew like movement with average speed of ~10µm/min whereas *$_p$clag::rab11a* spherical ookinetes were completely immobile (n=2). This indicates that *$_p$clag::rab11a* ookinetes are immobile due to spherical morphology caused by lack of Rab11A or probable lack of motility associated proteins and therefore transmission through mosquitoes is blocked.

(A)

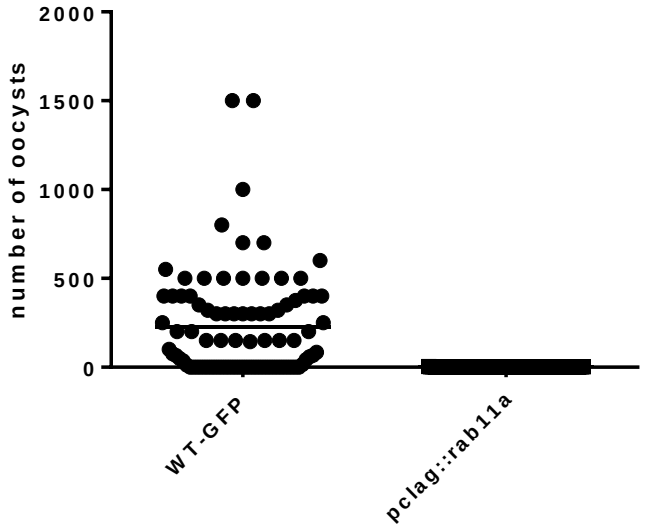
2000
1500
1000
500
0
number of oocysts
WT-GFP
pclag::rab11a

(B)

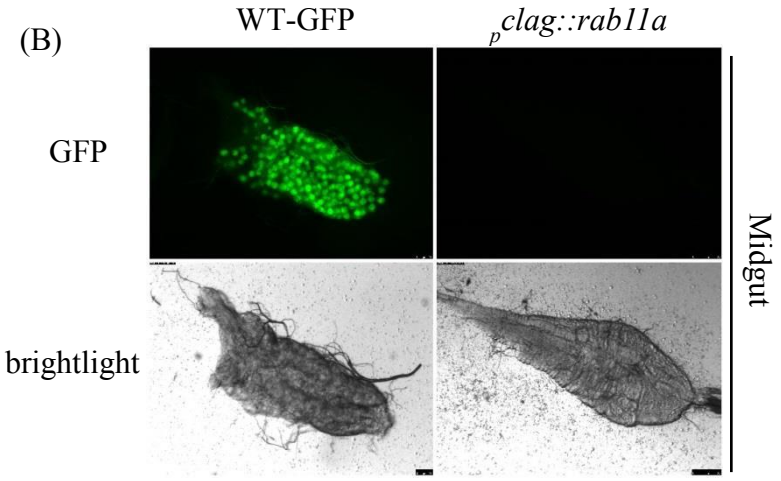
WT-GFP
pclag::rab11a
GFP
brightlight
Midgut

(C)

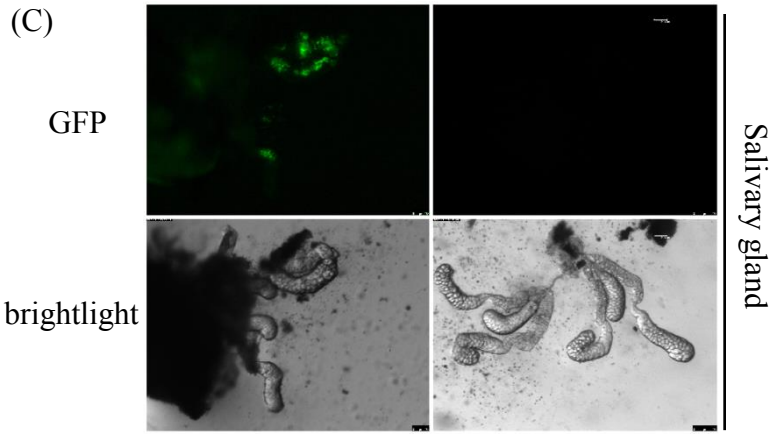
GFP
brightlight
Salivary gland

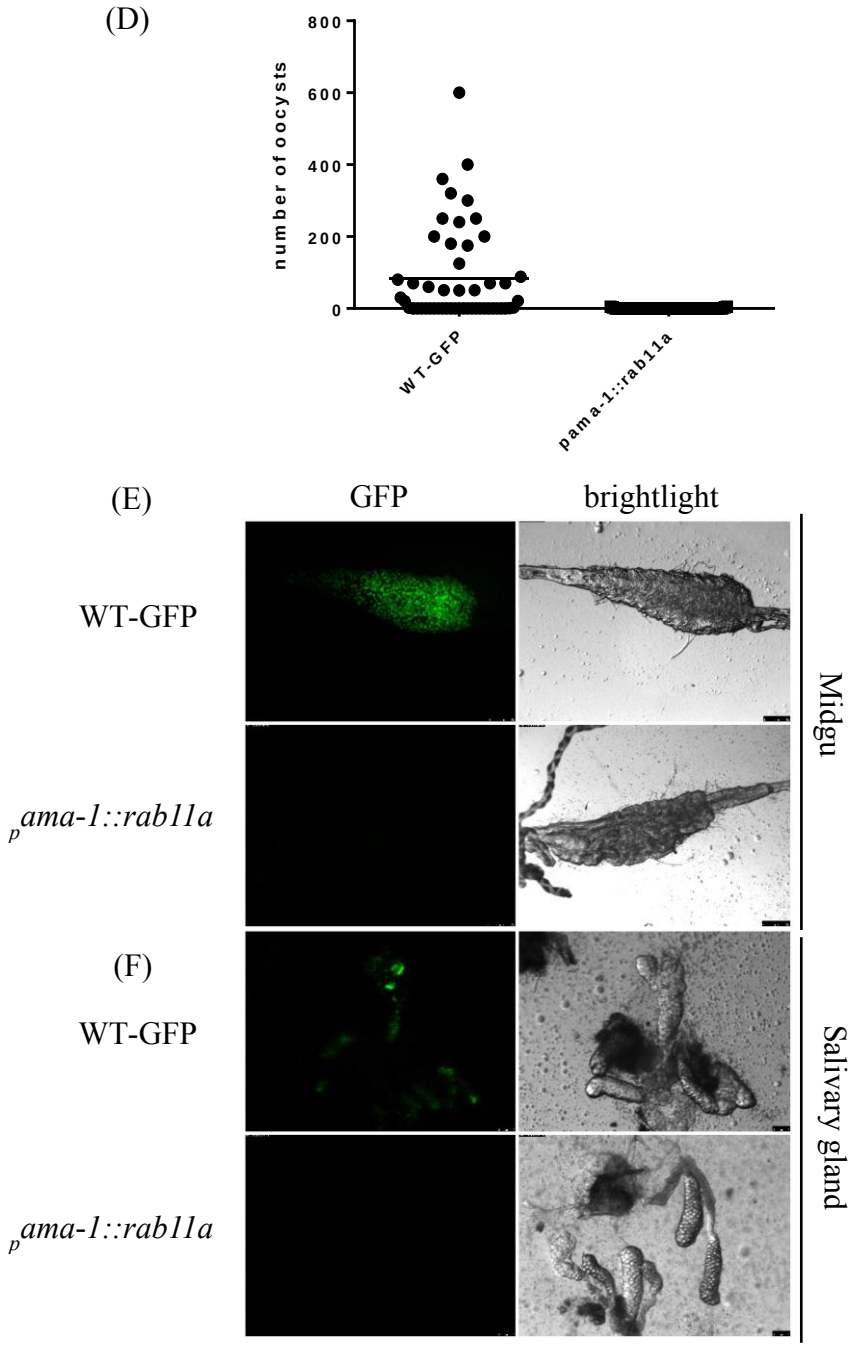

Figure 3.4.1 *pclag::rab11a* and *pama-1::rab11a* parasites are unable to transmit through mosquitoes

(A) Plot of oocyst load in dissected midguts of *pclag::rab11a* fed mosquitoes (n=3, two tailed student t test, p-value 0.0001). (B) Image of dissected midguts and (C) salivary glands from WT-GFP and *pclag::rab11a* parasites. (D) Plot of oocyst load in dissected midguts of *pama-1::rab11a* fed mosquitoes (n=2, two tailed student t test, p-value 0.0001). (E) WT-GFP and *pama-1::rab11a* infected midguts (E) and salivary glands.

(A)

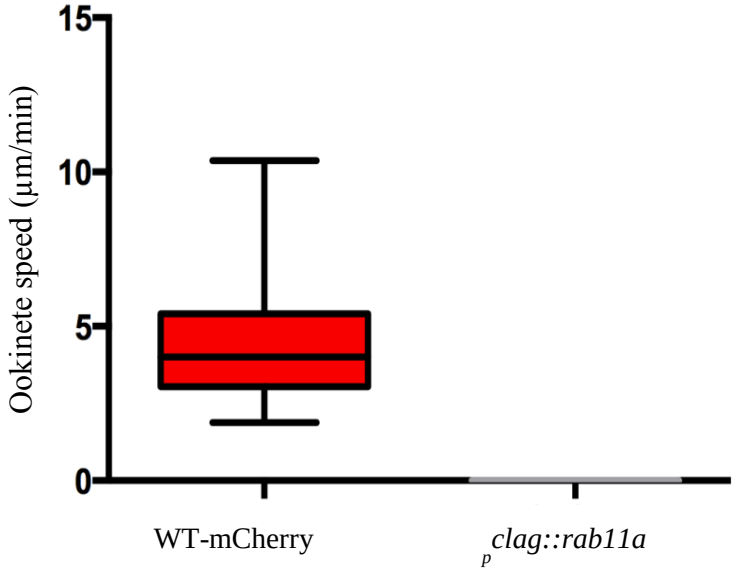

(B)

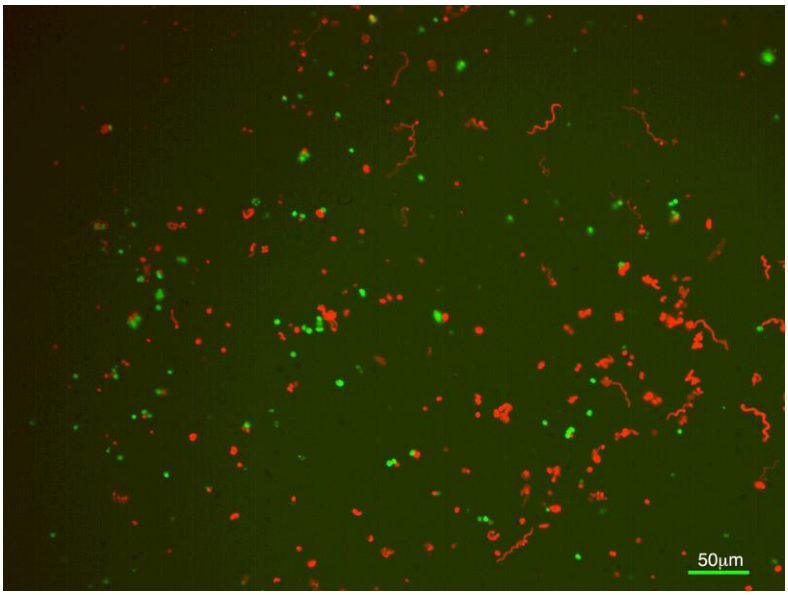

3.4.2 Motility of *pclag::rab11a* spherical ookinetes

(A) Speed of WT-mCherry and *pclag::rab11a* spherical ookinetes. For graph speed of 16 ookinetes for each genotype were measured; bottom and top boxes denote first and third quartiles respectively, whickers denote minimum and maximum. P<0.0001(B) Path of WT-mCherry and *pclag::rab11a* ookinetes for 10 minutes (n=2).

3.5 IMC and apical components are assembled in *$_p$clag::rab11a* zygotes

Rab11A is involved in protein trafficking and endocytic recycling therefore we questioned whether Rab11A is involved in the delivery of surface and IMC markers as predicted by (Agop-Nersesian, Naissant et al. 2009). To understand the role of Rab11A in the delivery of surface and IMC markers, immunofluorescence microscopy was performed for P25 - a surface marker of ookinete and GAP45 - an IMC marker, revealing that P25 is delivered to the plasma membrane and GAP45 underneath the plasma membrane indicating possible assembly of the IMC in 24h spherical *$_p$clag::rab11a* ookinetes (figure 3.5.1-C). Further analysis by time course GAP45 immunofluorescence studies on early and late zygotes show that 4h post-fertilization GAP45 is localized at a focal point which is then distributed into the emerging retort shape in WT-GFP retorts (6hpa). At 24hpa, GAP45 is localized throughout IMC of mature WT-GFP ookinetes (figure 3.5.1- A to C). *$_p$clag::rab11a* zygotes show similar localization of GAP45 at 4h post-fertilization compared to WT-GFP, which indicates an initial focal point or bud development site from which the leading apical end will emerge (figure 3.5.1 – A to C). However, although *$_p$clag::rab11a* 6h zygotes lack a prominent retort outgrowth, GAP45 is deposited along the IMC showing an arc-like localization and apparently bordering the whole IMC at 24h post fertilization. This indicates dynamic localization of GAP45, during zygote-to-ookinete development in WT-GFP parasites, initially at the apical bud (focal point) and then all over the developing IMC. Similarly, localization of GAP45 is observed in *$_p$clag::rab11a* parasites from focal point to possibly the complete IMC; however, *$_p$clag::rab11a* zygotes do not achieve the form of a mature ookinete even after 24h post fertilization.

The IMC and apical complex are important for the maintenance of *Plasmodium* cell structure and function therefore we performed ultrastructural analysis of *$_p$clag::rab11a* zygotes through scanning and transmission electron microscopy (SEM and TEM) to detect the integrity of the apical complex and IMC. SEM analysis shows 8h WT-GFP zygotes have noticeable retort outgrowth (now referred to as ‘retorts’ instead of ‘8h zygotes’) while 8h *$_p$clag::rab11a* zygotes have a small outgrowth of plasma membrane indicating a site for apical complex development (white arrow, figure 3.5.2).

TEM analysis shows integrity of IMC in 6h *$_p$clag::rab11a* zygotes and fully developed apical complex consisting collar (Co) with an aperture (Ap), micronemes (Mn), Inner membrane

complex (IMC) and subpellicular microtubules (Mt) in 8h $_{p}$*clag::rab11a* zygotes (figure 3.5.3 A,B). This suggests the likelihood that a full and functional apical complex is developed consisting of the IMC and internal organelles (e.g. micronemes shown by immunofluorescence of chitinase and CTRP, see section 3.10) in $_{p}$*clag::rab11a* ookinetes (Therefore, verifying that $_{p}$*clag::rab11a* 24h zygotes are indeed $_{p}$*clag::rab11a* ookinetes).

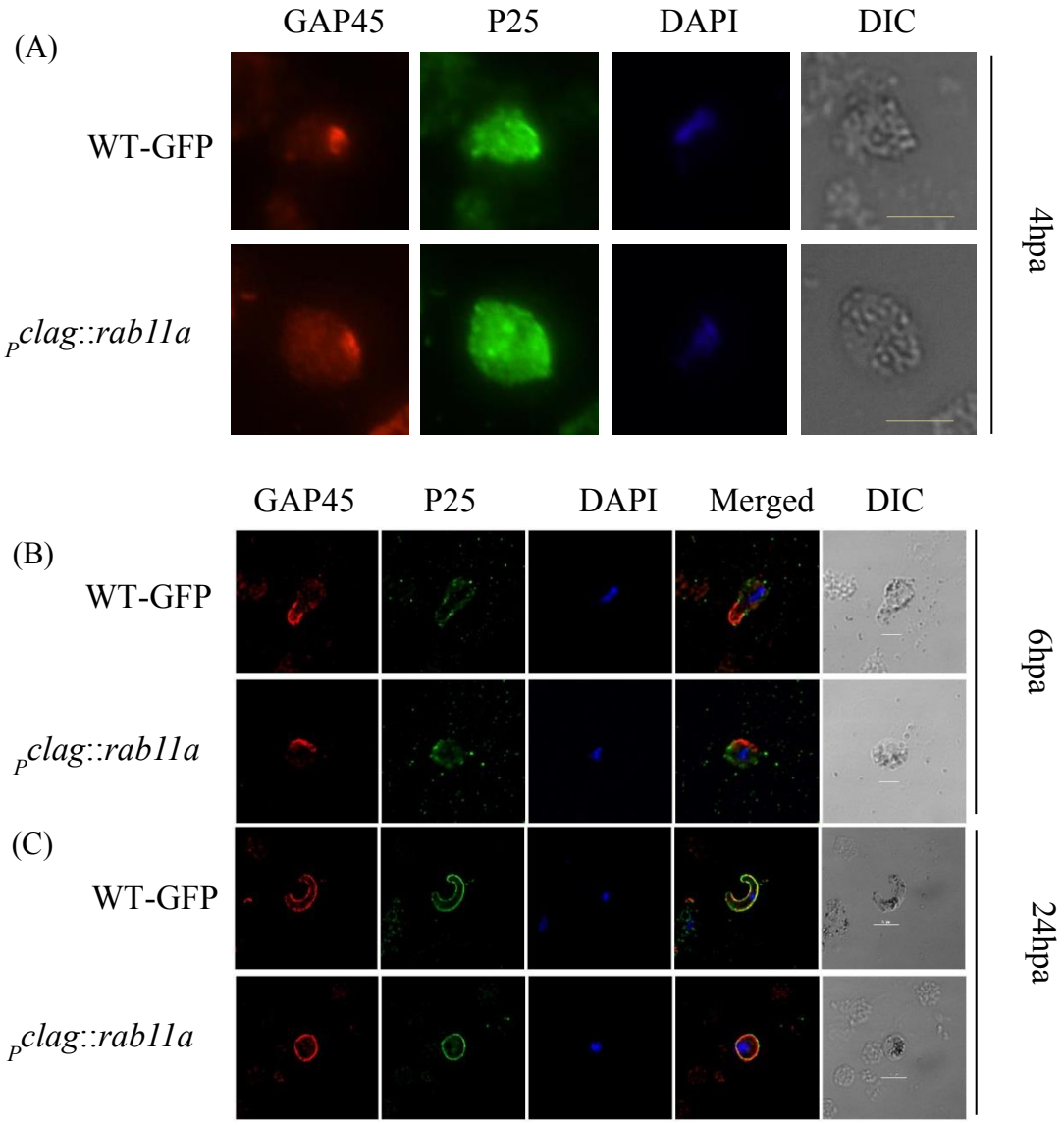

Figure 3.5.1 Dynamic localization of GAP45

Time course immunofluorescence of *pclag::rab11a* zygotes for P25 and GAP45 [images A are taken through Axioplan (Zeiss) and images B and C are taken via Deltavision, showing a single slice of a deconvoluted Z stack. Scale Bar for A and C=5 µm, B=3µm.

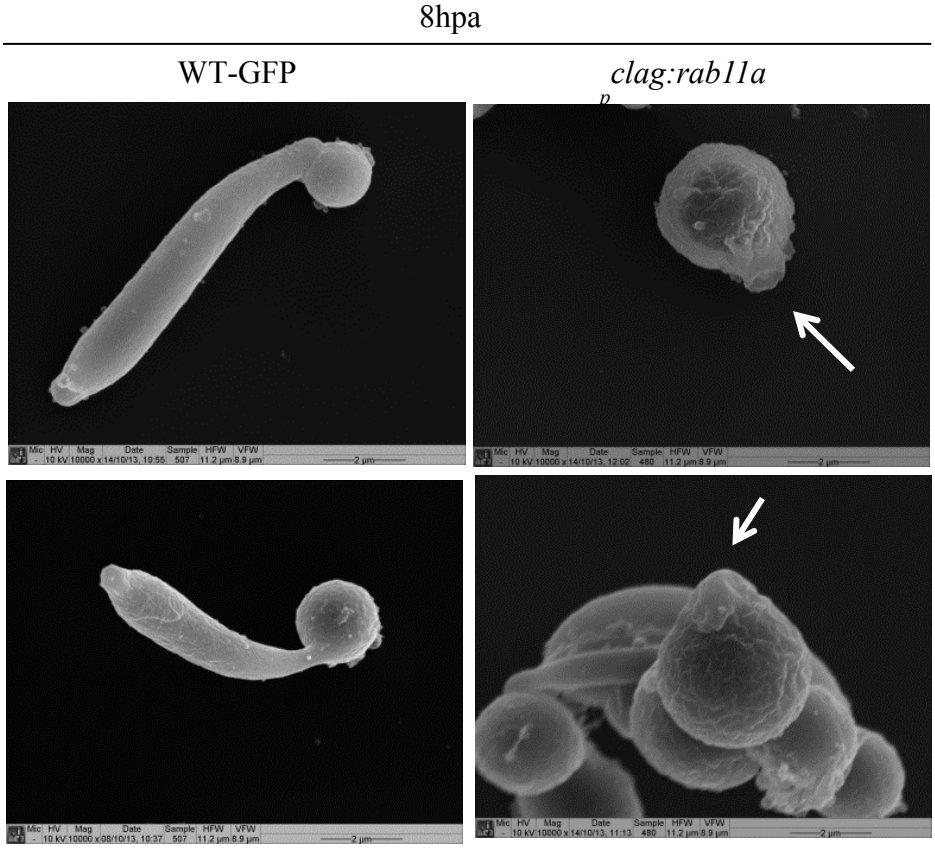

Figure 3.5.2: Ultrastructural analysis of *pclag::rab11a* 8h zygotes

SEM images of 8h *pclag::rab11a* zygotes showing the typical small yet specific membrane extension (see white arrow) as compared to retort outgrowth in WT-GFP 8h zygotes.

(A)

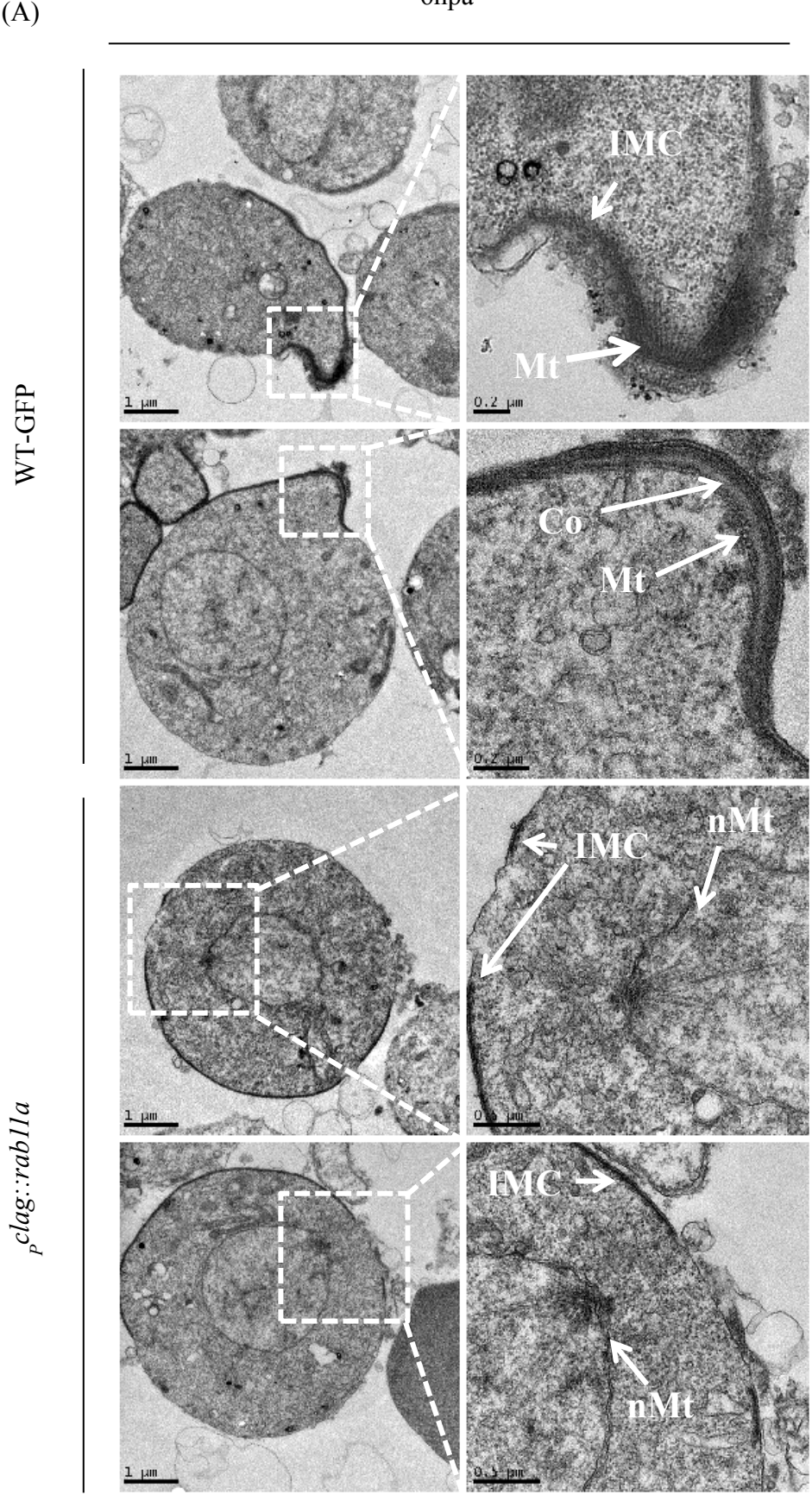
6hpa
WT-GFP
$_{P}$*clag::rab11a*
IMC
Mt
Co
Mt
IMC
nMt
IMC
nMt
1 µm
0.2 µm
0.5 µm

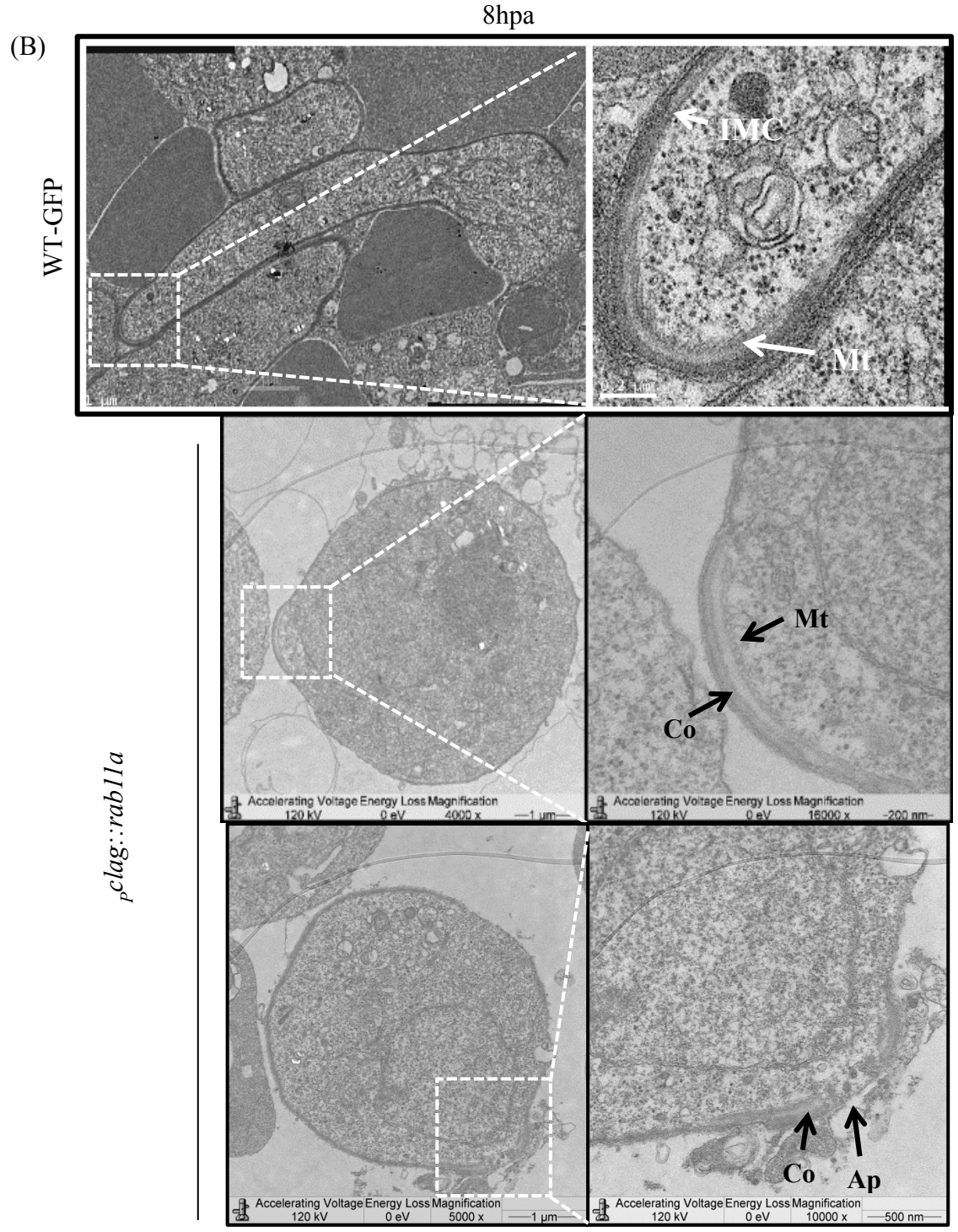

Figure 3.5.3: Ultrastructural analysis of *$_p$clag::rab11a* 8h zygotes.

(A) TEM images of *$_p$clag::rab11a* 6h and (B) 8h zygotes showing integrity of Collar (Co) with aperture (Ap), IMC and subpellicular microtubules (Mt) and nuclear microtubules (nMt)(Thickness of samples is 70nm). Images of *$_p$clag::rab11a* 8h zygotes taken on Leo 912 AB TEM running 120kV while rest of the images were taken though FEI Tecnai T20 running at 200kV.

3.6. Preparation of RNA samples for RNASeq

TEM and immunofluorescence analysis suggested assembly of apical complex and IMC in *$_p$clag::rab11a* zygotes (Results 3.5). Development of the zygote depends on translationally stored mRNAs in mRNPs. DOZI and CITH are the best characterised components of these mRNPs and deletion of either of them inhibits the zygote to ookinete transition in *P. berghei* although at different stages of that transition (Mair, Braks et al. 2006, Mair, Lasonder et al. 2010). Research from our group and others suggests that development of the zygote until retort stage (approximately 7 to 8hpa) is dependent on translationally stored mRNAs (i.e. DOZI/CITH stored mRNAs) while development of retort is exclusively dependent on further activation of transcription (A. Srivastava- Waters group, unpublished)(Guerreiro, Deligianni et al. 2014).

Therefore, to examine if PbRab11A is involved (at least partially) in the stabilization or deployment of translationally stored transcripts (i.e. DOZI/CITH stored transcripts) (Mair, Braks et al. 2006, Mair, Lasonder et al. 2010, Guerreiro, Deligianni et al. 2014) and/or re-initiation of transcription after meiosis (also referred as post-meiotic transcription), apparently to establish the coordination of cellular events during zygote to ookinete development which are already known to happen in WT, we performed RNA Sequencing (RNA-Seq) for total mRNAs of un-activated gametocytes and spherical ookinetes of *$_p$clag::rab11a* parasites. Total RNAs of *$_p$clag::rab11a* gametocytes (Question: are mRNAs translationally stored?) and spherical ookinetes (Questions: are the stored mRNAs translated? Is the post-meiotic transcription active?) were isolated. Along with WT-GFP un-activated gametocytes where mRNAs are translationally repressed and stored (Mair, Braks et al. 2006, Mair, Lasonder et al. 2010) and ookinetes which have active transcription as well as DOZI/CITH stored mRNAs (M. Stewart –Waters group, Unpublished data), two additional controls: Pre-activated WT-GFP gametocytes treated with 2-Deoxy-D-glucose (2DG- analogue of D-glucose) or WT-GFP gametocytes cultured into ookinete medium supplemented with actinomycinD (actD, a potent transcription blocking agent) were also included (figure 3.6 A) (see Materials and Methods 2.1.2 o for details of sample preparation). 2DG inhibits the activation of male gametocytes leaving female gametocytes activated and unfertilized (K. Hughes, Waters group-unpublished data) therefore translationally stored mRNAs might be stored or degraded 24hpa. ActD treated gametocytes are able to fertilize and grow until retort stage (approximately 7 to 8hpa), indicating utilization of pre-existing translationally stored mRNAs

to drive the growth until retort stage and further development is terminated due to the presumed transcriptional block (no mRNAs transcribed for further growth: A. Srivastava, Waters group-unpublished data)(Guerreiro, Deligianni et al. 2014) (figure 3.6 A).

Prior to RNA-Seq, total extracted RNAs were converted to cDNAs by reverse and transcriptase PCR and tested for possible gDNA contamination (occurrence of gDNA during RNA extraction) by PCR. Total RNA samples were deemed to be free of any detectable levels of gDNA (figure 3.6 B) therefore used for RNA-Sequencing (see Table 2.1.2.1 and Tables 2.1.2.2 in Chapter 2: Materials and Methods for parameters of RNA-Seq experiment). Three repetitions of each set of samples (each set consists of total six samples: $_{p}$*clag::rab11a* gametocytes, $_{p}$*clag::rab11a* spherical ookinetes, WT-GFP gametocytes, WT-GFP ookinetes, WT-GFP gametocytes treated with 2DG and actD, figure 3.6 A) were performed.

Our RNA-Seq experiment was designed to identify mRNAs, therefore only protein coding transcripts were analysed in this study. Recently, Otto et al has shown that, in an RNA-Seq study performed across various life cycle stage of *P. berghei*, the cut off FPKM values vary between 10 to 24 in various life cycle stages and even in the replicates of same life cycle stage (Otto, Böhme et al. 2014) (It depends on expression levels in introns and setting up limit assuming the top 10% of expression levels are real- personal communication with Dr. Thomos Otto, Wellcome Trust Sanger Institute, Cambridge). Therefore, mRNAs having FPKM value ≥10 were considered as 'significantly expressed transcripts' (to exclude scarce transcripts) in WT-GFP gametocytes and WT-GFP ookinetes. For drug treated WT-GFP parasites, $_{p}$*clag::rab11a* gametocytes and spherical ookinetes, transcripts having FPKM value ≥10 and significant Log2(fold_change) values where significance is shown by p-values were considered as 'significantly deregulated transcripts'.

To investigate whether or not a particular set of transcripts are deregulated, we performed gene ontology (GO) enrichment for significantly deregulated mRNAs of $_{p}$*clag::rab11a* gametocytes, $_{p}$*clag::rab11a* ookinetes and drug treated WT-GFP parasites. Initially 3276 significantly expressed transcripts (FPKM ≥10) in WT-GFP gametocytes (figure 3.7.1) and 3451 significantly expressed transcripts (FPKM ≥10) in WT-GFP ookinetes (figure 3.7.6) were distributed into four groups of percentile expression according to their rank order of abundance in the different stages: Group 1: Transcripts expressed in 100-75%, and similarly Group 2: 75-50%, Group 3: 50-25% and Group 4: 25-0%. Accordingly deregulated transcripts in $_{p}$*clag::rab11a* gametocytes, $_{p}$*clag::rab11a* ookinetes and drug treated WT-GFP parasites

were also distributed into percentile expression groups for further analysis. GO enrichment terms for deregulated transcripts were analysed manually (see Method 2.1.2 q in Chapter 2: Materials and Methods). For simplicity only GO- Biological Process terms are discussed for respective samples.

(A)

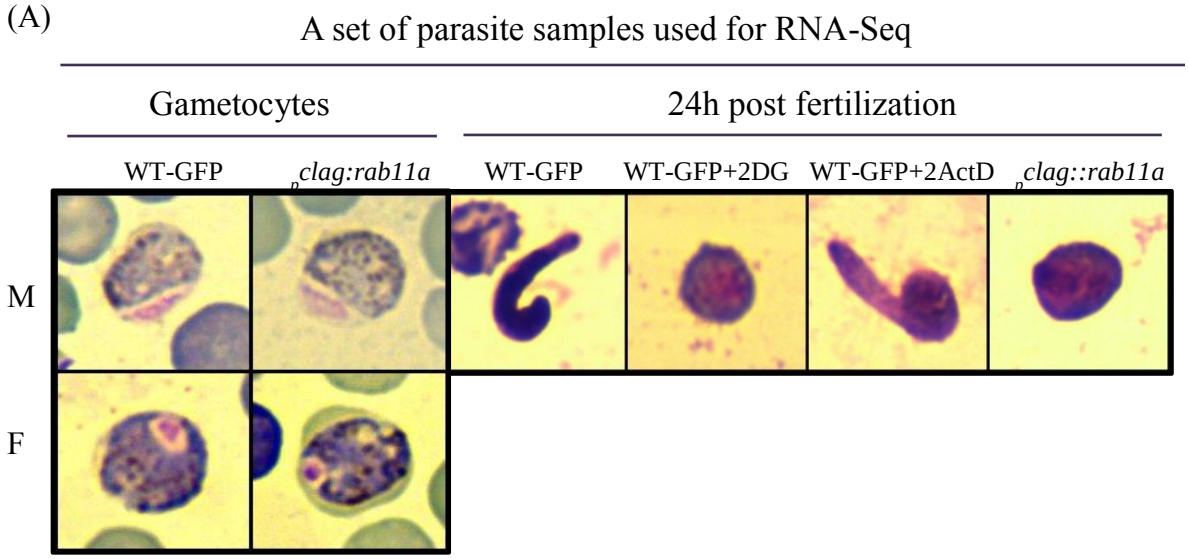

(B)

Gametocytes

	Gene IDs	PBANKA_112970	PBANKA_145120	PBANKA_134500
	Primer1	GU1948	GU1952	GU1950
	Primer2	GU1949	GU1953	GU1951
Expected size in base pairs	**gDNA**	646	606	1460
Expected size in base pairs	**cDNA**	404	410	572
		a	b	c

Ookinetes (24hpa)

	Gene IDs	PBANKA_131130	PBANKA_134500	PBANKA_010570
	Primer1	GU1948	GU1950	GU1935
	Primer2	GU1949	GU1951	GU1936
Expected size in base pairs	**gDNA**	623	1460	1015
Expected size in base pairs	**cDNA**	404	572	510
		x	y	z

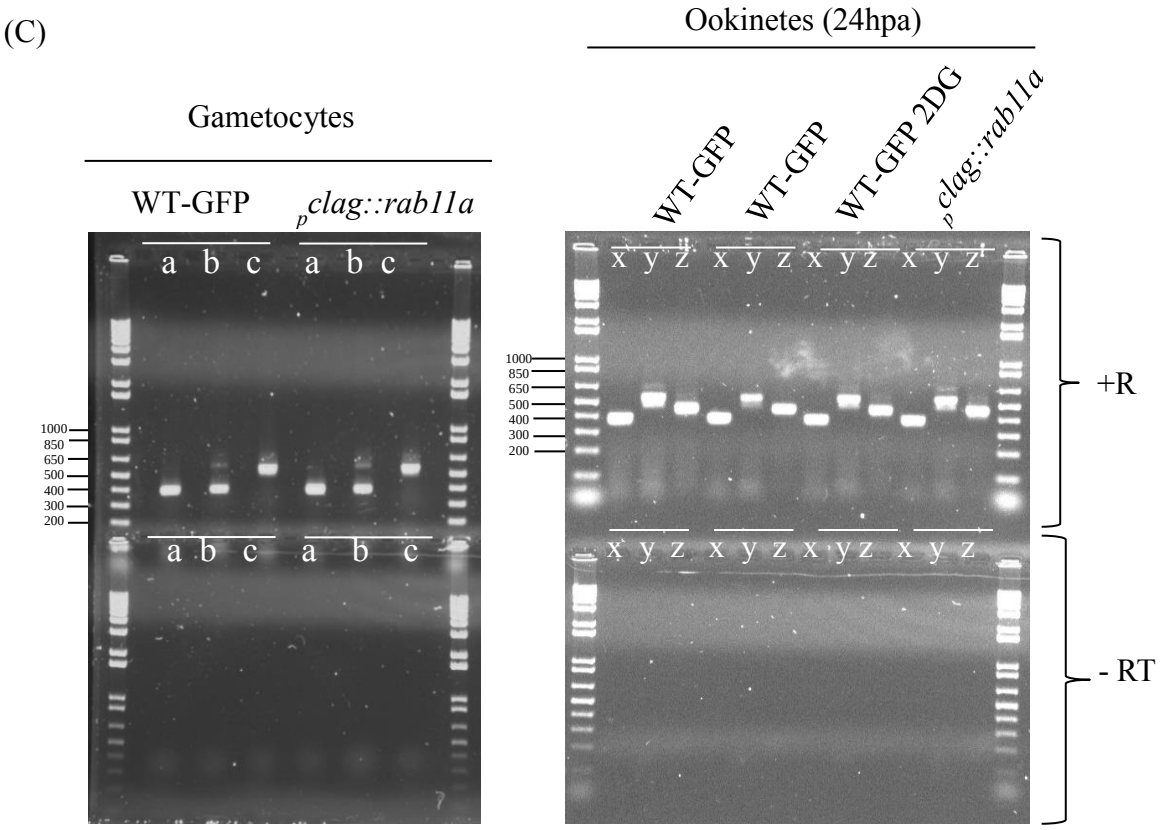

Figure 3.6 Sample preparations for RNA-Seq.

(A) Images of Giemsa stained *$_p$clag::rab11a* gametocytes, spherical *$_p$clag::rab11a* ookinetes (24hpa) and controls: mixed WT-GFP gametocytes, WT-GFP ookinetes (24hpa), WT-GFP 24h female gamete (treated with 2DG), WT-GFP 24h retorts (treated with actD) (B) Tables show primers used and expected PCR band sizes in reverse transcriptase PCR. See Appendix A, Table 1 for primer sequence. Colours indicate percentage expression values for respective transcripts as Red showing genes having percent RNA expression values in between 100 - 75%, Orange showing values in between 75-50% and Yellow showing values in between 50-25%. Reverse Transcriptase PCRs of total RNA isolated from above parasite preparations to check the purity of isolated total RNA. DNA ladder unit = base pairs (bp).

3.7 Analysis of RNA-Seq data

3.7. a) Comparison of transcriptome of *$_p$clag::rab11a* gametocytes with the transcriptome of WT-GFP gametocytes

The genome of *P. berghei* encodes 5020 protein coding genes out of total 5164 genes (www.plasmodb.org- PlasmoDB version 24). Out of total 5020 protein coding genes in *P. berghei* (PlasmoDB version 24, Gene type: protein coding, including pseudogenes), the transcriptome of WT-GFP gametocytes shows significant expression of 3276 protein coding transcripts (cut off FPKM values ≥10 to exclude scarce transcripts) (figure 3.7.1). Similarly, the transcriptome of *$_p$clag::rab11a* gametocytes shows that only 2834 protein coding transcripts are significantly expressed (with cut off FPKM ≥ 10) (figure 3.7.1). Therefore, the difference between the transcriptomes of WT-GFP gametocytes and that of *$_p$clag::rab11a* gametocytes is appears to be 542 transcripts (=3276-2834), however, significance shown by p-values suggests that only 368 protein coding transcripts (with cut off FPKM ≥ 10) are deregulated (119 are more abundant and 249 are less abundant) in *$_p$clag::rab11a* gametocytes as compared to WT-GFP gametocytes (see Appendix B - Table 1 for details of individual transcripts) i.e. *$_p$clag::rab11a* gametocytes transcriptome is 11.23% (368 out of 3276) variable from WT-GFP gametocyte transcriptome and these 368 deregulated transcripts includes Rab11A transcripts which is -3.4 fold less than that of WT-GFP gametocyte Rab11A transcripts (p-values 0.00005) (figure 3.7.2 A). This implies that almost 88.77% (except 368 transcripts out of 3276 transcripts in WT-GFP gametocytes) transcriptome of *$_p$clag::rab11a* gametocytes is similar to the transcriptome of WT-GFP gametocytes (figure 3.7.2 B). Additionally, the fold change values of most of the deregulated transcripts of *$_p$clag::rab11a* gametocytes are in between 2 and -2 (figure 3.7.2 A and Table 3.7.8).

Out of 119 significantly more abundant transcripts, four transcripts: PBANKA_020890 (StAR-related lipid transfer protein, putative), PBANKA_051900 (S-antigen, putative), PBANKA_114540 (Rodent Plasmodium exported protein, unknown function) and PBANKA_000480 (BIR protein) are exclusively more abundant in *$_p$clag::rab11a* gametocytes transcriptome and are not present in WT-GFP gametocyte transcriptome (Table 3.7.3). Out of these four transcripts, BIR protein and S-antigen are known to be associated with antigenic polymorphism (Mahajan, Farooq et al. 2005, Otto, Böhme et al. 2014) and therefore probably do not represent the real up-regulation. Similarly, out of 249 less abundant transcripts in *$_p$clag::rab11a* gametocytes, six transcripts are BIR proteins (PBANKA_040050,

PBANKA_114630, PBANKA_060030, PBANKA_080010, PBANKA_070020, PBANKA_120040) and two are Pb-fam-1 proteins (PBANKA_146570, PBANKA_000350) associated with antigenic variation (Otto, Böhme et al. 2014).

Recently, it had been shown that DOZI/CITH stored transcripts are essential for *P. berghei* zygote to ookinete transformation (Mair, Braks et al. 2006, Mair, Lasonder et al. 2010). Furthermore, it has been shown that *P. berghei* female gametocytes store 733 transcripts with DOZI/CITH (Guerreiro, Deligianni et al. 2014). Therefore, we looked at whether or not 368 significantly deregulated transcripts in $_{p}$*clag::rab11a* gametocytes share any of the 733 DOZI/CITH associated transcripts. Out of total 368 deregulated mRNAs (in $_{p}$*clag::rab11a* gametocytes), 19 are exclusively translationally stored with DOZI (Guerreiro, Deligianni et al. 2014) and 26 are translationally stored with CITH (Guerreiro, Deligianni et al. 2014) while 36 mRNAs are translationally stored with both DOZI as well as CITH (Guerreiro, Deligianni et al. 2014)(figure 3.7.2 A, C). In total, 81 out of 368 deregulated transcripts in $_{p}$*clag::rab11a* gametocytes are associated with DOZI/CITH.

In summary, the majority of significantly deregulated mRNAs in $_{p}$*clag::rab11a* gametocytes i.e. 287 (=368-81) are independent of translationally stored mRNAs. Additionally, out of total 733 DOZI/CITH stored transcripts (Guerreiro, Deligianni et al. 2014), 11.05% (i.e. 81 out of 733) are deregulated in the absence of Rab11A transcripts in $_{p}$*clag::rab11a* gametocytes. This suggests that Rab11A is partially associated with translational repression of mRNAs.

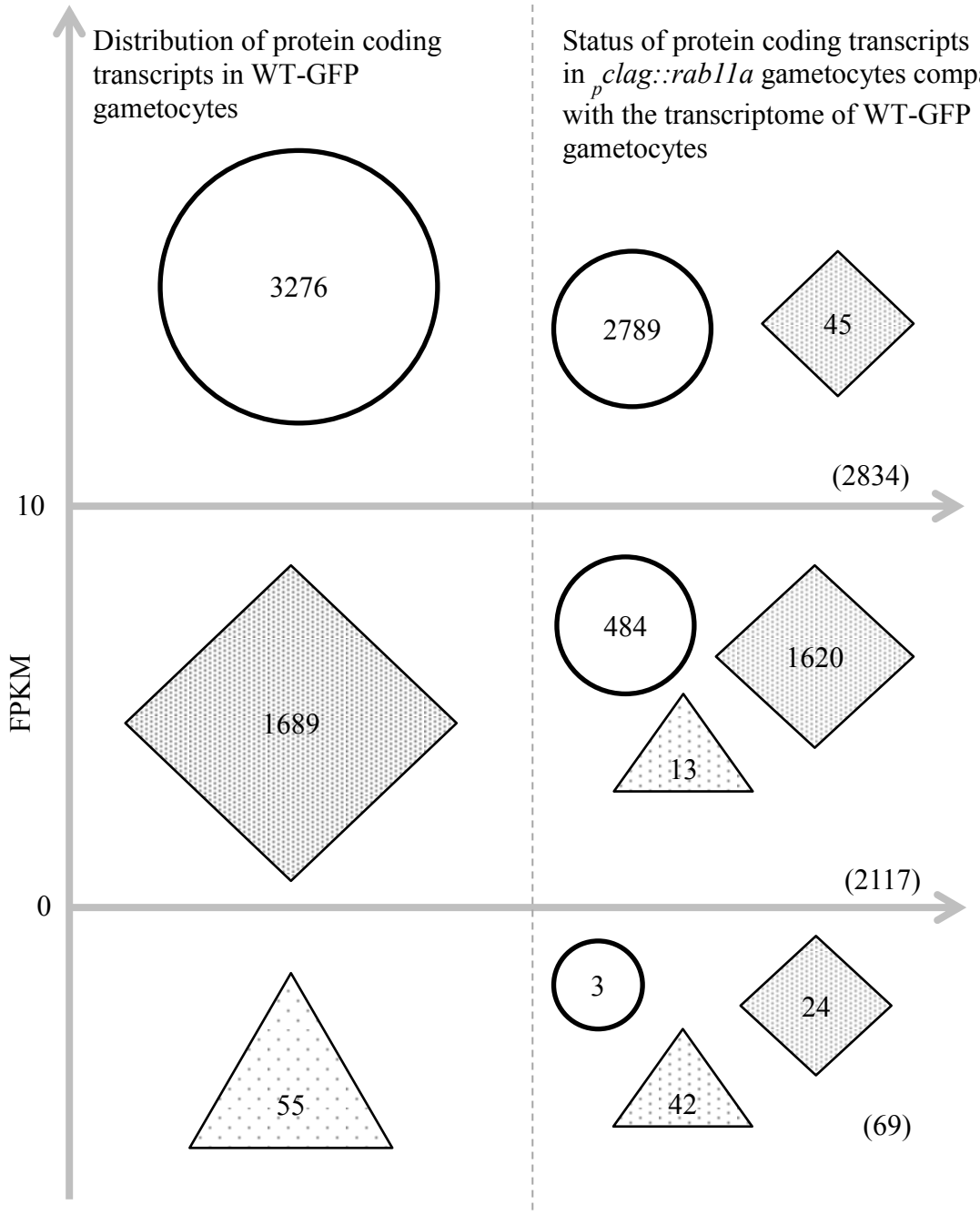

Figure 3.7.1 Distribution of total protein coding transcripts (5020) in WT-GFP gametocytes and their status in *pclag::rab11a* gametocytes.

Left side: Circle suggests transcripts having FPKM ≥ 10, Diamond suggests the transcripts having FPKM < 10 and > 0 whereas triangle suggests transcripts not detected in WT-GFP gametocytes. Right side: Status of identical transcripts of WT-GFP gametocytes in *pclag::rab11a* gametocytes. Brackets indicate the sum of respective sections.

(A)

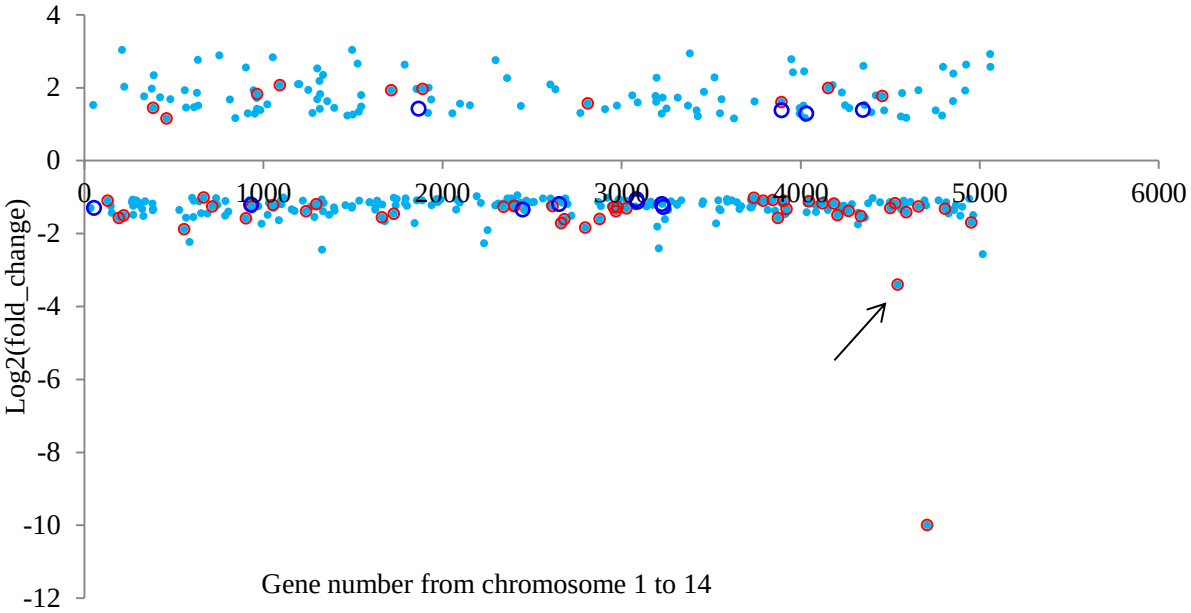

- Deregulated transcripts at gametocytes stage (WT-GFP v pclag::rab11a) (368 = 119 Up + 249 Down)
- Common transcripts (DOZI associated transcripts v deregulated in pclag::rab11a gametocytes) (45 = 10 Up + 45 Down)
- Common transcripts (CITH associated transcripts v deregulated in pclag::rab11a gametocytes) (62 = 17 Up + 45 Down)

(B)

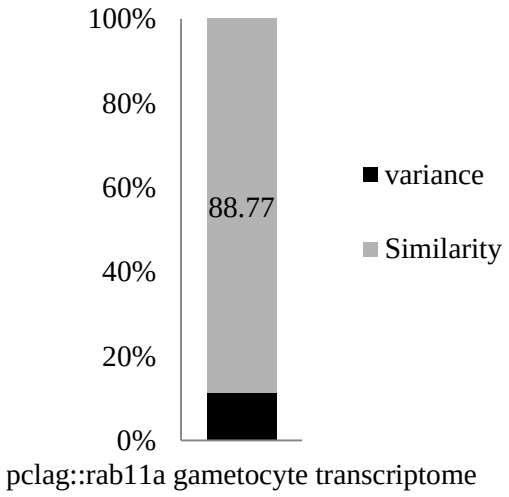

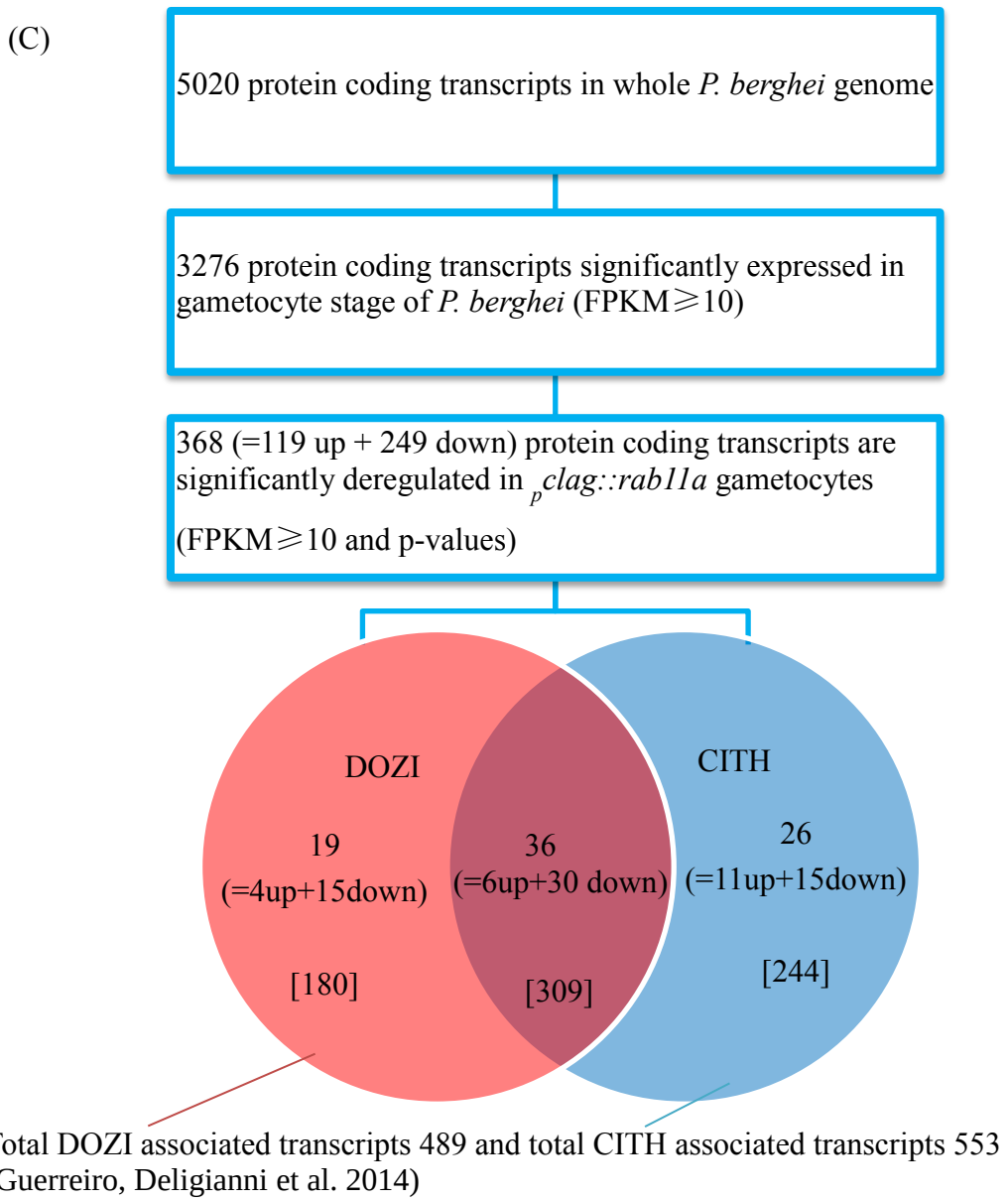

Figure 3.7.2 Comparison of *pclag::rab11a* gametocyte transcriptome with the translationally stored transcripts.

(A) Scatter plot showing fold change values of significantly deregulated 368 transcripts in *pclag::rab11a* gametocytes and common transcripts associated with DOZI and CITH. Arrow shows position of Rab11A (B) Bar graph showing the percent variance and similarity in between the transcriptome of WT-GFP gametocytes and the transcriptome of *pclag::rab11a* gametocytes. (C) Chart and Venn diagram showing common transcripts of 368 deregulated transcripts in *pclag::rab11a* gametocytes and DOZI/CITH stored transcripts. Square brackets represent the original DOZI/CITH associated transcript numbers from (Guerreiro, Deligianni et al. 2014).

3.7. b) Gene ontology enrichment for Gametocytes

Out of 119 more abundant (/up regulated) transcripts in $_{p}$*clag::rab11a* gametocytes, 112 transcripts have syntenic orthologues in *P. falciparum 3D7* and 114 have syntenic orthologues in *P. vivax Sal-1* (PlasmoDB, Version 24). These 119 more abundant transcripts are divided into four subgroups according to four percentile expression groups of WT-GFP gametocytes transcriptome, their distribution across annotated GO terms and DOZI/CITH association (Table 3.7.3). Out of these 119 significantly more abundant transcripts in $_{p}$*clag::rab11a* gametocytes, less than half i.e. only 57, 54 and 54 have annotations as GO- Molecular Function, Biological Process and Cellular Components respectively (Table 3.7.3). The majority of these 119 more abundant transcripts in $_{p}$*clag::rab11a* gametocytes (i.e. 83 out of 119) fall into the highly expressed percentile expression group of 100-75% (Table 3.7.3). Also, out of 119 more abundant transcripts, most of the DOZI/CITH associated transcripts (6 and15) come under the same percentage expression group of 100-75% (Table 3.7.3). GO Biological Process term analysis indicates a major up-regulation of 22 translation related biological processes followed by six transport, five transcription, four chromosome organization and three electron transport chain associated biological processes (figure 3.7.5 A). All the translation associated transcripts which are more abundant in $_{p}$*clag::rab11a* gametocytes are clustered into percentage expression group of 100-75% (figure 3.7.5 C). Most of them are 40s, 60s ribosomal proteins (see Appendix B, Table 1).

Out of 249 less abundant (/down regulated) transcripts in $_{p}$*clag::rab11a* gametocytes, 239 transcripts have syntenic orthologues in *P. falciparum 3D7* and 238 transcripts have syntenic orthologues in *P. vivax Sal-1* (PlasmoDB, Version 24). Like the 119 more abundant transcripts in $_{p}$*clag::rab11a* gametocytes, 249 less abundant transcripts (in $_{p}$*clag::rab11a* gametocytes) are divided into four percentile expression groups compared with the percentage expression groups of WT-GFP gametocytes, annotated GO and DOZI/CITH association (Table 3.7.4). These percentage expression groups (of 249 less abundant transcripts) and their GO analysis suggests that less than half i.e. 112, 80 and 52 have annotated GO- Molecular Function, Biological Process and Cellular Components respectively (Table 3.7.4). The majority of these 249 low abundant transcripts in $_{p}$*clag::rab11a* gametocytes i.e. 77+73 are grouped in the percentage expression group of 75-50% and 50-25% respectively , however, most of the DOZI/CITH associated transcripts (28 and 26) fall within 100-75% group (Table 3.7.4). GO- Biological process term analysis suggests that 14 transcripts associated with biosynthetic processes are majorly affected in $_{p}$*clag::rab11a* gametocytes and are distributed

among 100-75%, 75-50% and 50-25% percentage expression group (figure 3.7.5 C). Other significantly affected processes are protein modification and processing (10), transport (10) and metabolic processes (9) (figure 3.7.5 B). Some of the greatly affected (2 fold change) transcripts associated with these processes are Rab11B, MTIP, GAPM3, and enzymes involved in biosynthesis of cell constituents such as dihydrolipoamide dehydrogenase, putative GDP-mannose 4,6-dehydratase; putative aspartate carbamoyltransferase; putative pyridoxal 5'-phosphate synthase; putative phosphomannomutase and putative glutaminyl-peptide cyclotransferase. There are some transcripts associated with DNA replication and chromosome organization such as NEK2, putative chromatin assembly factor 1 P55 subunit are also less abundant in $_{p}$*clag::rab11a* gametocytes (Appendix B, Table 1).

This strongly suggests that in $_{p}$*clag::rab11a* gametocytes due to absence of Rab11A mRNAs, translation related transcripts are up-regulated while transcripts associated with biosynthetic processes, protein modification and processing, metabolic processes are hampered the most as compared to WT-GFP gametocytes. Down-regulation of various transport related processes in $_{p}$*clag::rab11a* gametocytes were expected as Rab11A is shown to be associated with various cellular transport mechanisms in many eukaryotic organisms. In addition, a significantly greater percentage of the down-regulated transcripts (81 out of 368) were associated with the conditional translation repression apparatus (DOZI/CITH associated). This is known to store transcripts that prepare the cell for its future development and it is perhaps not surprising that a general failure to activate (a subset of) these processes results in a defective zygote.

	100-75%	75-50%	50-25%	25-0%	Not expressed in WT-GFP gametocytes	Total
119 more abundant transcripts in *$_p$clag::rab11a* gametocytes (112 Pf and 114 Pv orthologues)	83	23	6	3	4	119
DOZI associated	6	2	2	-	-	10
CITH associated	15	1	1	-	-	17
Annotated GO Term - Molecular Function	49	5	2	-	1	57
Annotated GO Term - Biological Process	44	7	2	-	1	54
Annotated GO Term - Cellular Component	44	7	1	-	2	54

Table 3.7.3 Table showing distribution of 119 more abundant transcripts in *$_p$clag::rab11a* gametocytes across translationally stored transcripts as well as annotated GO terms. Pf- *P. falciparum 3D7* and Pv – *P. vivax Sal-1*.

	100-75%	75-50%	50-25%	25-0%	Total
249 less abundant transcripts in *$_p$clag::rab11a* gametocytes (239 Pf and 238 Pv orthologues)	53	77	73	46	249
DOZI associated	28	9	5	3	45
CITH associated	26	12	6	1	45
Annotated GO Term - Molecular Function	21	37	35	19	112
Annotated GO Term - Biological Process	15	26	23	16	80
Annotated GO Term - Cellular Component	10	16	14	12	52

Table 3.7.4 Table showing 249 less abundant transcripts in *$_p$clag::rab11a* gametocytes and their distribution across translationally stored transcripts as well as annotated GO term. Pf- *P. falciparum 3D7* and Pv – *P. vivax Sal-1*.

(A)

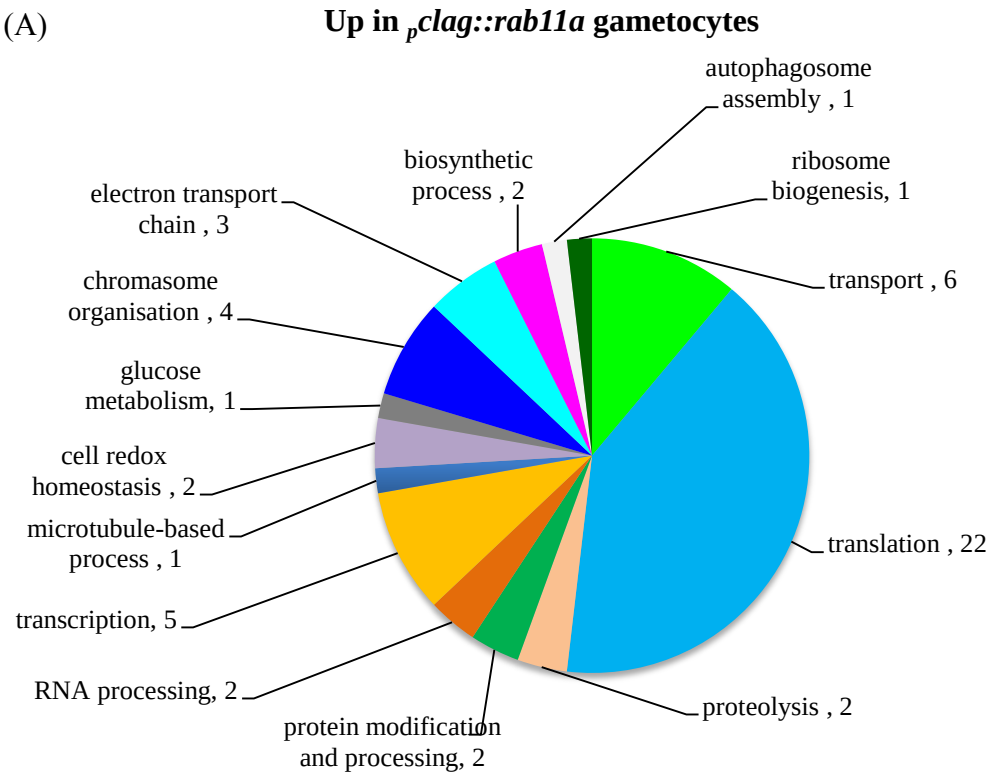
Up in pclag::rab11a gametocytes
autophagosome assembly , 1
ribosome biogenesis, 1
transport , 6
translation , 22
proteolysis , 2
protein modification and processing, 2
RNA processing, 2
transcription, 5
microtubule-based process , 1
cell redox homeostasis , 2
glucose metabolism, 1
chromasome organisation , 4
electron transport chain , 3
biosynthetic process , 2

(B)

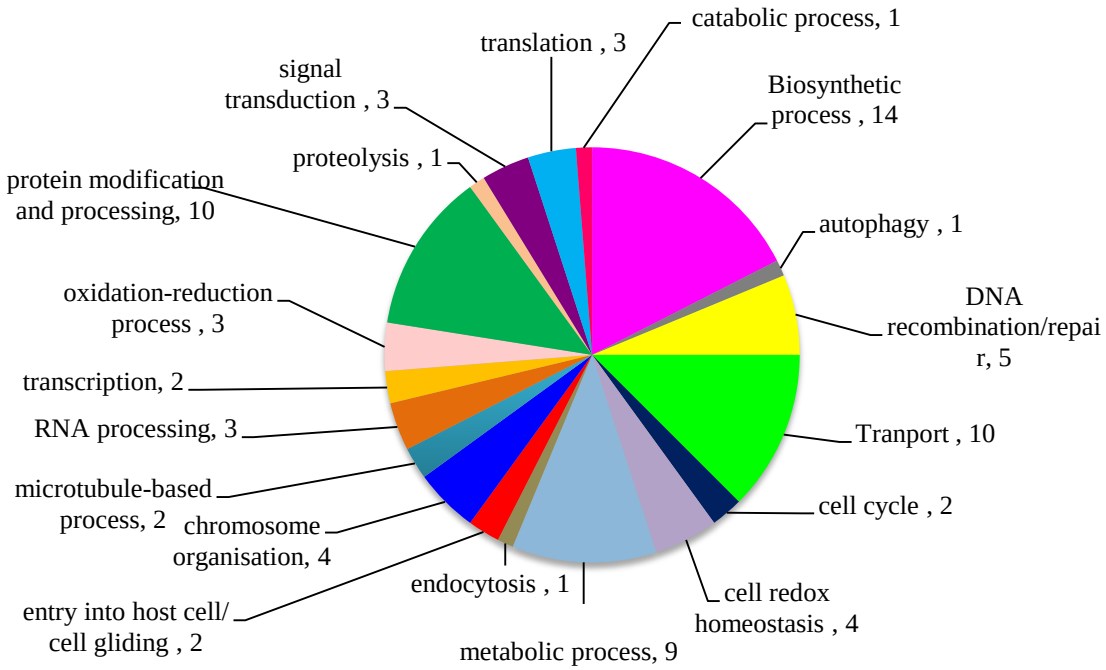
Down in pclag::rab11a gametocytes
catabolic process, 1
translation , 3
signal transduction , 3
Biosynthetic process , 14
proteolysis , 1
protein modification and processing, 10
autophagy , 1
oxidation-reduction process , 3
DNA recombination/repair, 5
transcription, 2
Tranport , 10
RNA processing, 3
cell cycle , 2
microtubule-based process, 2
chromosome organisation, 4
cell redox homeostasis , 4
endocytosis , 1
entry into host cell/ cell gliding , 2
metabolic process, 9

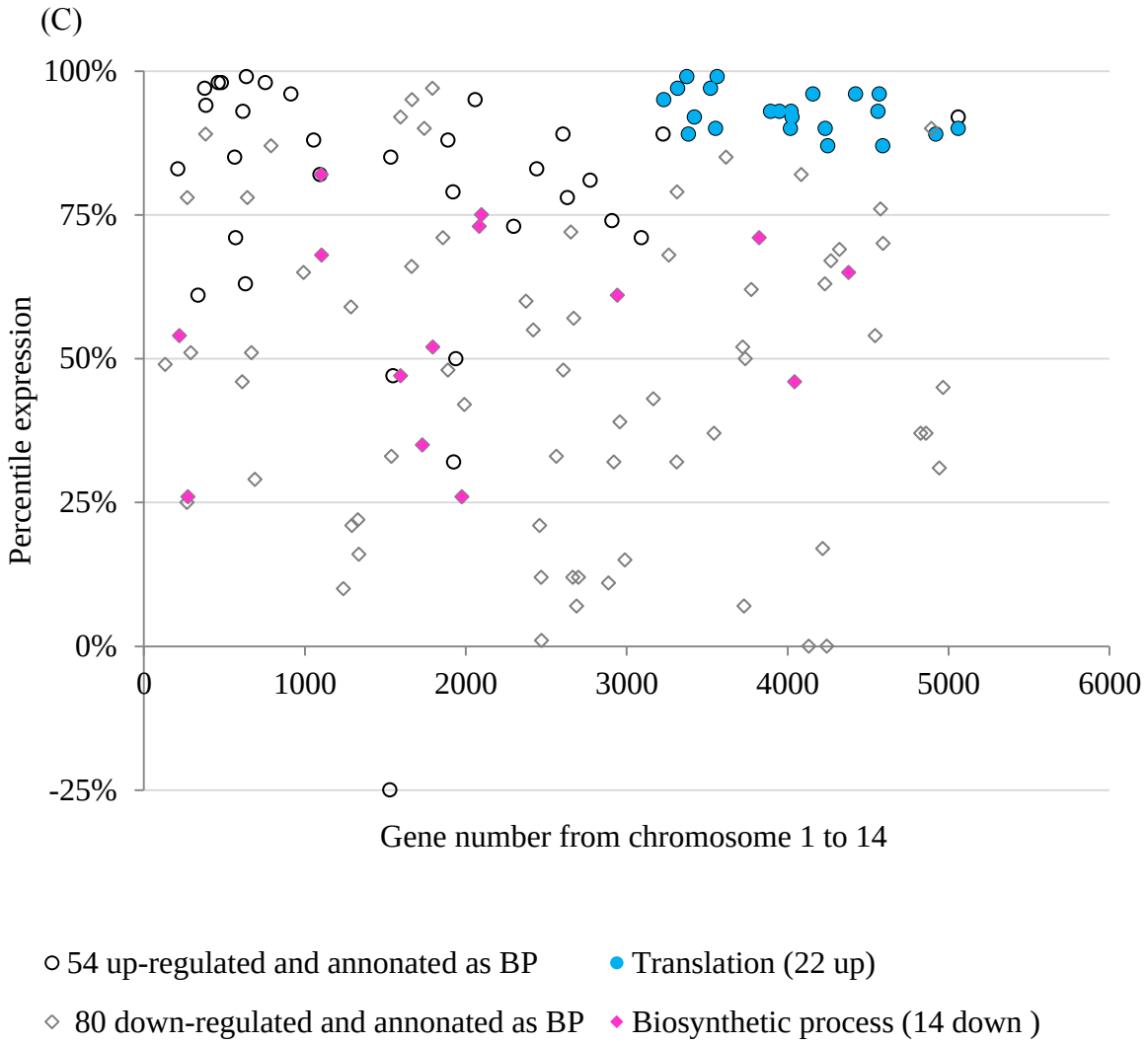

Figure 3.7.5 GO- (Biological Process) term analysis for deregulated transcripts in *$_p$clag::rab11a* gametocytes.

(A) Pie chart showing GO (Biological Process) term enrichment for more abundant/up regulated transcripts and (B) less abundant/ down regulated transcripts in *$_p$clag::rab11a* gametocytes. (C) Deregulated transcripts of *$_p$clag::rab11a* gametocytes having GO annotated as Biological Process (BP) and their distribution across percentile expression groups compared to the percentile expression groups of WT-GFP gametocytes transcriptome. Most up-regulated and most down-regulated transcripts in *$_p$clag::rab11a* gametocytes are colour coded as per pie charts A and B. Up-regulated transcripts in *$_p$clag::rab11a* gametocytes which are not detected in the transcriptome of WT-GFP gametocytes were given an arbitrary percentage expression value of -25%.

3.7. c) Comparison of transcriptome of $_{p}$*clag::rab11a* ookinetes, AUFG and TAR with the transcriptome of WT-GFP ookinetes

Out of total 5020 protein coding genes in *P. berghei* (PlasmoDB version 24, Gene type protein coding, including pseudogenes), WT-GFP ookinetes transcriptome identifies 3451 protein coding transcripts expressed above the chosen cut-off value (FPKM ≥10) (figure 3.7.6 A). Similarly, transcriptome of $_{p}$*clag::rab11a* ookinetes identifies 3489 protein coding transcripts (FPKM ≥10) (figure 3.7.6 A). Despite the difference of 38 transcripts (=3489-3451) in between the transcriptome of WT-GFP ookinetes and the transcriptome of $_{p}$*clag::rab11a* ookinetes, significance shown by p-values suggest that 144 transcripts are significantly deregulated in $_{p}$*clag::rab11a* ookinetes (FPKM ≥10) (figure 3.7.6 A) (see Appendix B- Table 2 for details of individual transcripts). Therefore, it appears that out of these 3451 significantly expressed transcripts in WT-GFP ookinetes, 4.17 % i.e. 144 transcripts are significantly deregulated (40 are significantly more abundant while 104 are significantly less abundant) in $_{p}$*clag::rab11a* ookinetes (figure 3.7.6 A, D). Out of these 40 more abundant transcripts only one might be associated with antigenic variation (PBANKA_000480, BIR protein) and out of 104 less abundant transcripts only one might be associated with antigenic variation (PBANKA_062340, Pb-fam-1 protein) (See Appendix B, Table 2 for details).

Compared to the transcriptome of WT-GFP ookinetes (Significantly expressed 3451 protein coding transcripts), in AUFG 3063 transcripts are significantly expressed (FPKM ≥ 10) (figure 3.7.6 B). There is difference of 388 transcripts (=3451-3063) in between the transcriptomes of WT-GFP ookinetes and that of AUFG ,however, significance shown by p-values suggests that in AUFG 1637 i.e. 47.43% transcripts (1637 out of 3451 of WT-GFP ookinetes) are significantly deregulated (638 more abundant, 999 less abundant) (figure 3.7.7 B, D) (Appendix B- Table 3 for details).

Likewise, as compared to the transcriptome of WT-GFP ookinetes where significantly expressed transcripts are 3451, the transcriptome of TAR shows significant expression of 3498 transcripts (FPKM ≥ 10) (figure 3.7.6 C). Although, the difference between the transcriptome of WT-GFP ookinetes and TAR is 47 transcripts (=3498-3451), the significance shown by p-values suggests that in TAR 977 i.e. 28.31% transcripts (977 out of 3451 of WT-GFP ookinetes) are significantly deregulated (453 more abundant, 524 less abunadant) (figure 3.6.7 C, D) (Appendix B- Table 4 for details).

In other words, the transcriptome of AUFG and TAR which are 52.57% and 71.69% similar respectively to the transcriptome of WT-GFP ookinetes are nevertheless less similar than the that of *$_p$clag::rab11a* ookinetes (which is almost 95.83% similar) and that of WT-GFP ookinetes (figure 3.6.7 D).

Additionally, the fold changes of 99.30% (143 out of 144) deregulated transcripts of *$_p$clag::rab11a* ookinetes are not more than 2 and -2, whereas the fold changes of the 48.69% (797 out of 1637) deregulated transcripts in AUFG and 28.86% (282 out of 977) deregulated transcripts in TAR are above 2 and -2 (Table 3.7.8). This clearly signifies that, with the exception of 144 deregulated mRNAs, the rest of the *$_p$clag::rab11a* ookinete transcriptome appears to be similar with WT-GFP ookinetes and the fold changes of 144 deregulated transcripts of *$_p$clag::rab11a* ookinetes are not large and the impact of Rab11A upon transcription during the zygote-ookinete transition is not great and apparently less than the effect on the steady state mature gametocyte.

Out of 144 significantly deregulated transcripts in *$_p$clag::rab11a* ookinetes (compared to WT-GFP ookinete transcriptome), the majority (60.41%, 87 out of 144) transcripts are common with the deregulated transcripts of both AUFG as well as TAR (compared to WT-GFP ookinete transcriptome), whereas 11.80% (17 out of 144) are common only with AUFG, 13.19% (19 out of 144) are common only with TAR and 14.58% (21 out of 144) are exclusively deregulated in *$_p$clag::rab11a* ookinetes (figure 3.7.9 A). Interestingly, the pattern of significantly up/down regulation of the 144 deregulated *$_p$clag::rab11a* ookinete transcripts is similar to AUFG and TAR (figure 3.7.9 B).

(A)

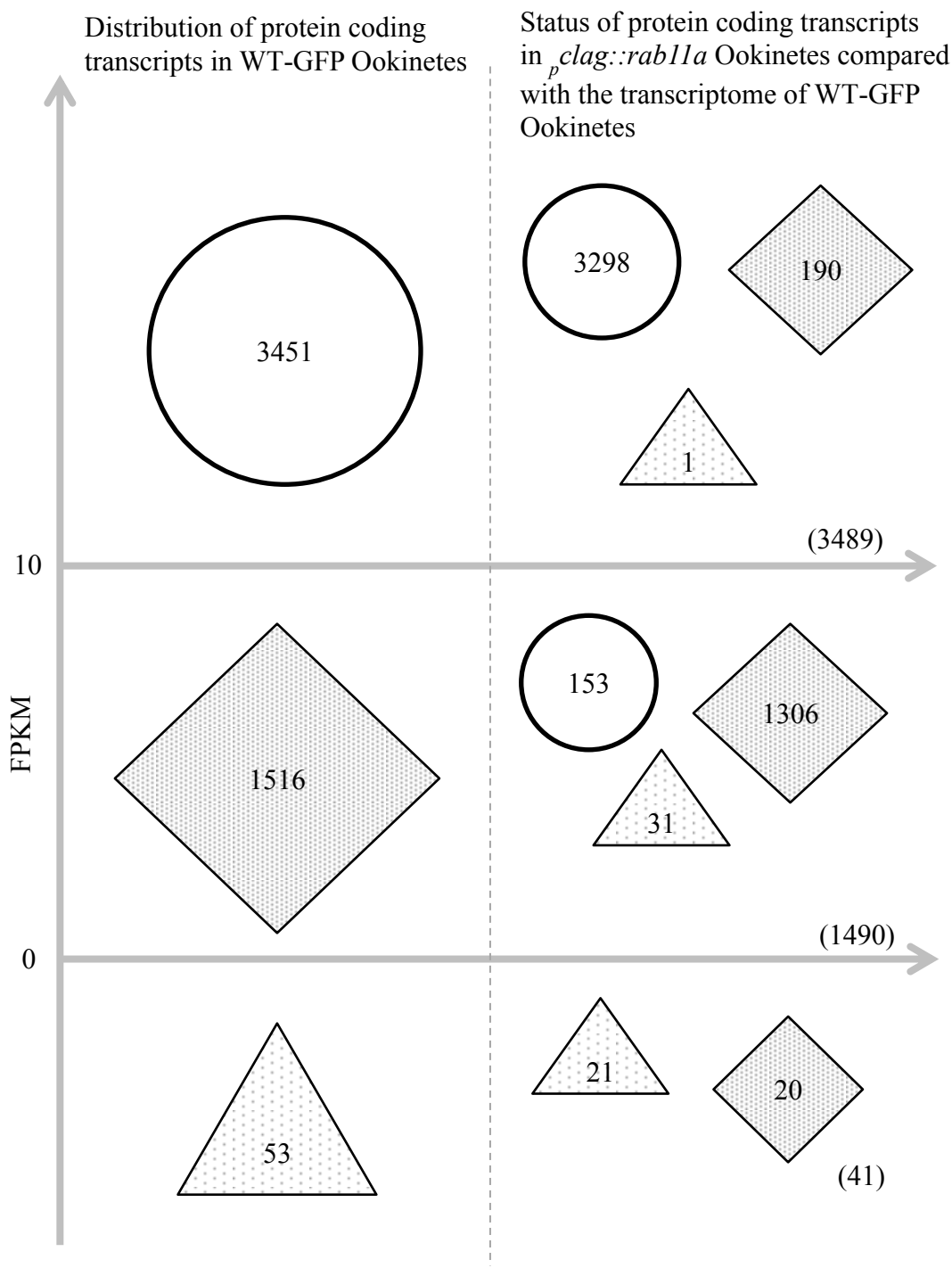
Distribution of protein coding transcripts in WT-GFP Ookinetes
Status of protein coding transcripts in pclag::rab11a Ookinetes compared with the transcriptome of WT-GFP Ookinetes
3451
3298
190
1
(3489)
10
FPKM
153
1306
1516
31
(1490)
0
21
20
53
(41)

(B)

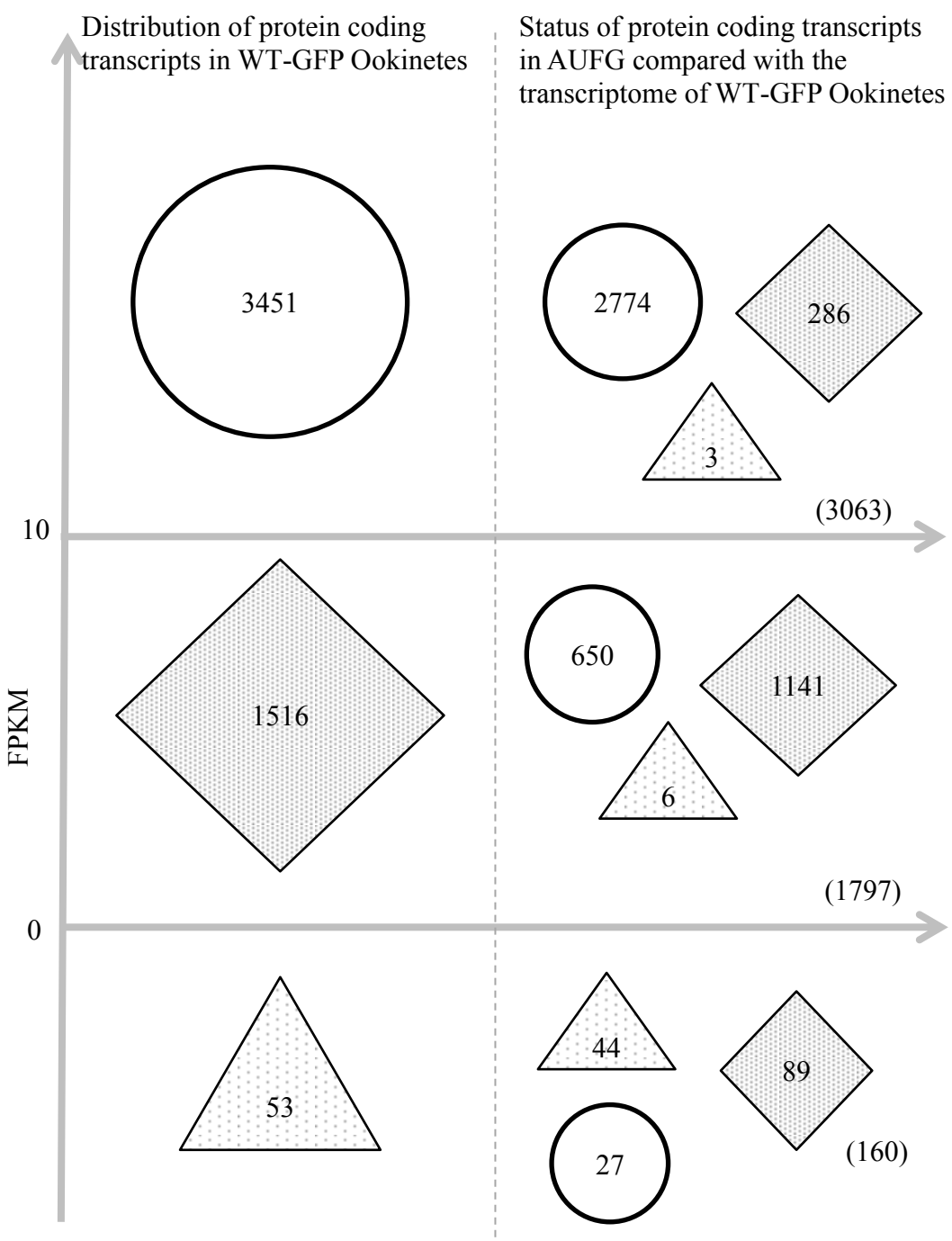
Distribution of protein coding transcripts in WT-GFP Ookinetes
Status of protein coding transcripts in AUFG compared with the transcriptome of WT-GFP Ookinetes
3451
2774
286
3
(3063)
10
FPKM
1516
650
1141
6
(1797)
0
53
44
89
27
(160)

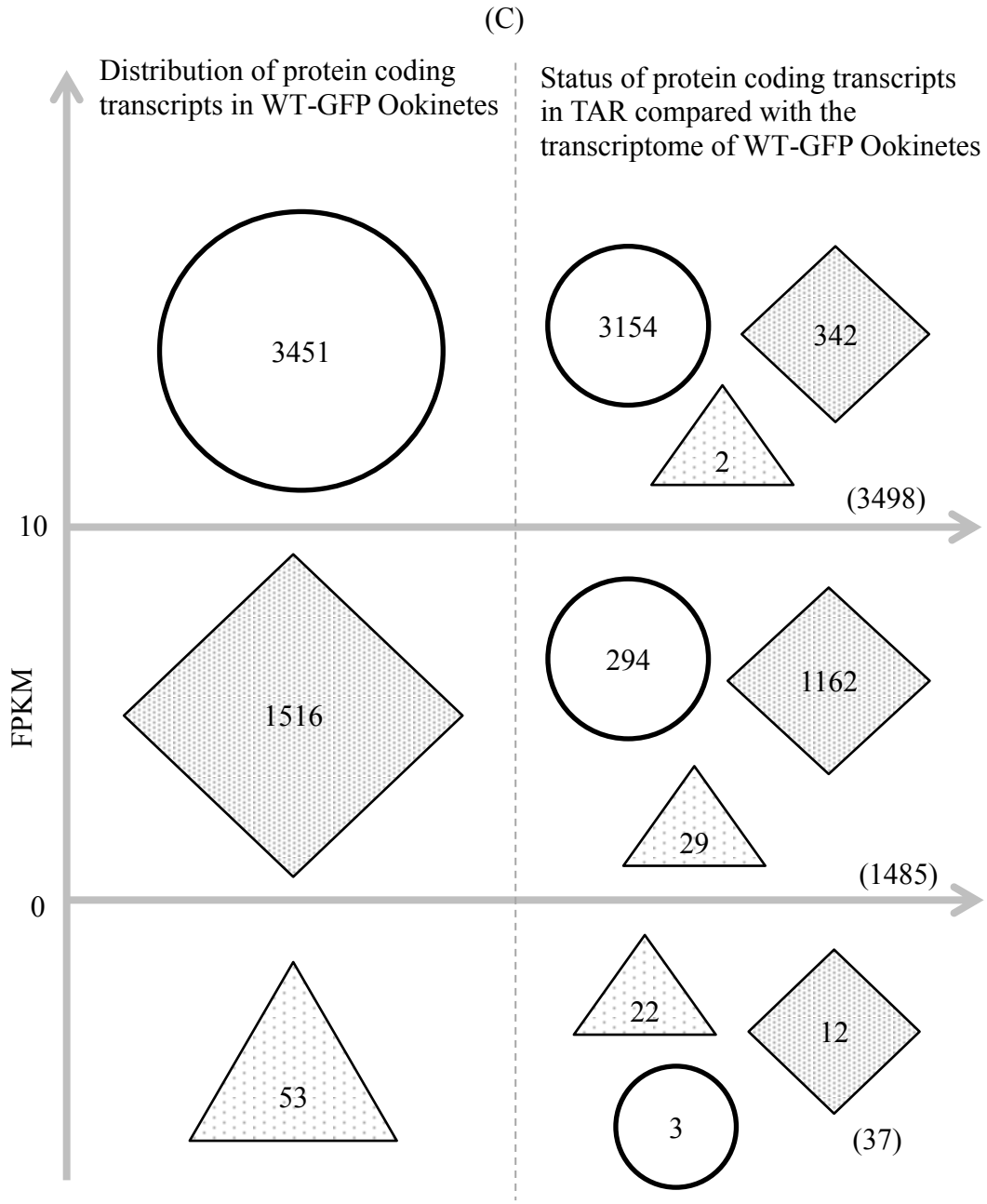

Figure 3.7.6 Distribution of total protein coding transcripts (5020) in WT-GFP ookinetes and their status AUFG, TAR and *$_p$clag::rab11a* ookinetes.

(A) Distribution of total protein coding transcripts in WT-GFP ookinetes and their status in *$_p$clag::rab11a* ookinetes or (B) in AUFG or (C) in TAR. Left side: Circle suggests transcripts having FPKM ≥ 10, Diamond suggests the transcripts having FPKM < 10 and > 0 whereas triangle suggests transcripts not detected in WT-GFP ookinetes. Right side: Status of identical transcripts of WT-GFP ookinetes in *$_p$clag::rab11a* ookinetes, AUFG and TAR respectively. Brackets indicate the sum of respective sections.

(A)

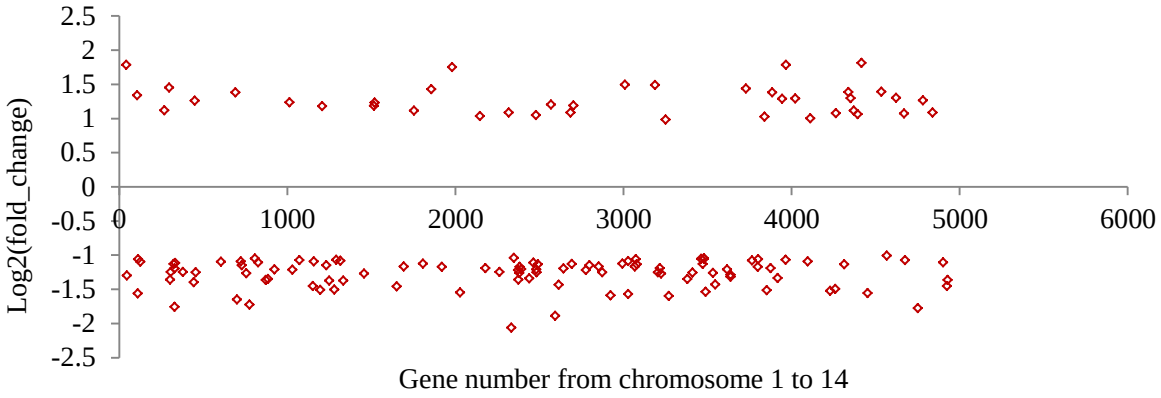

◇ 144 deregulated (40 up, 104 down) in the transcriptome of (WT-GFP Ookinetes v pclag::rab11a Ookinete)

(B)

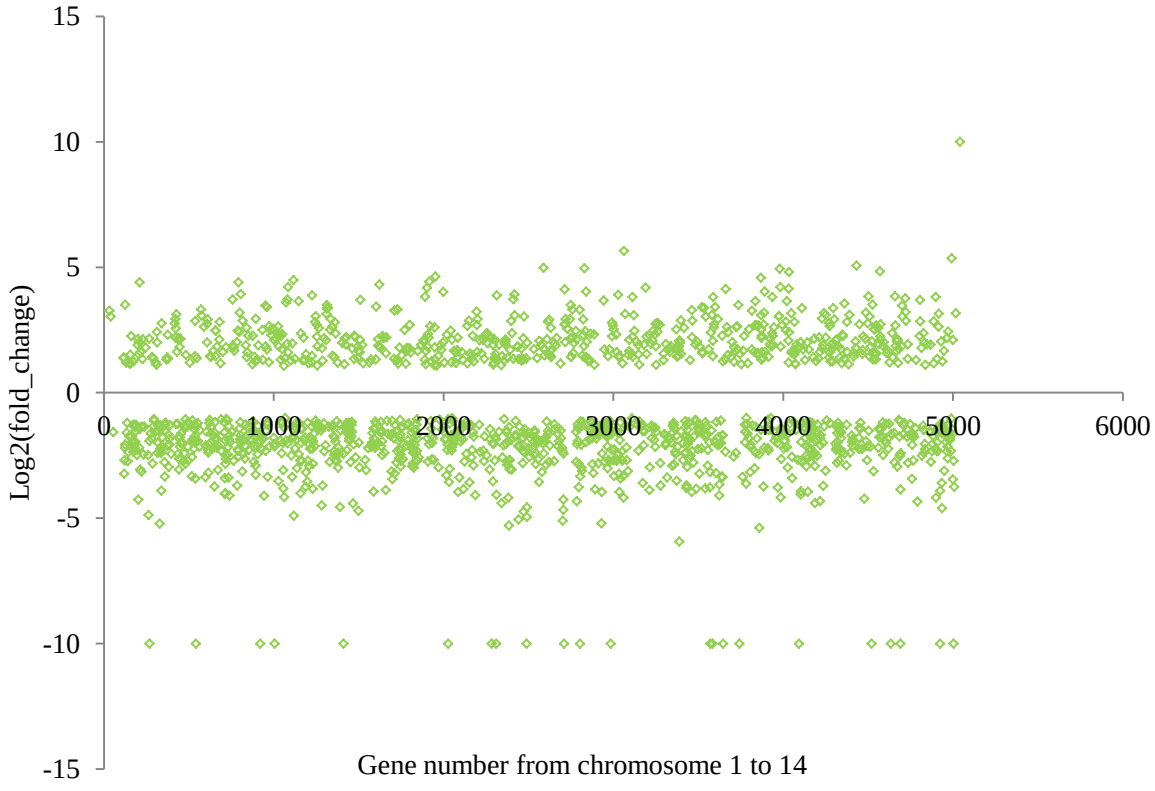

◇ 1637 deregulated (638 up, 999 down) in the transcriptome of (WT-GFP Ookinetes v AUFG)

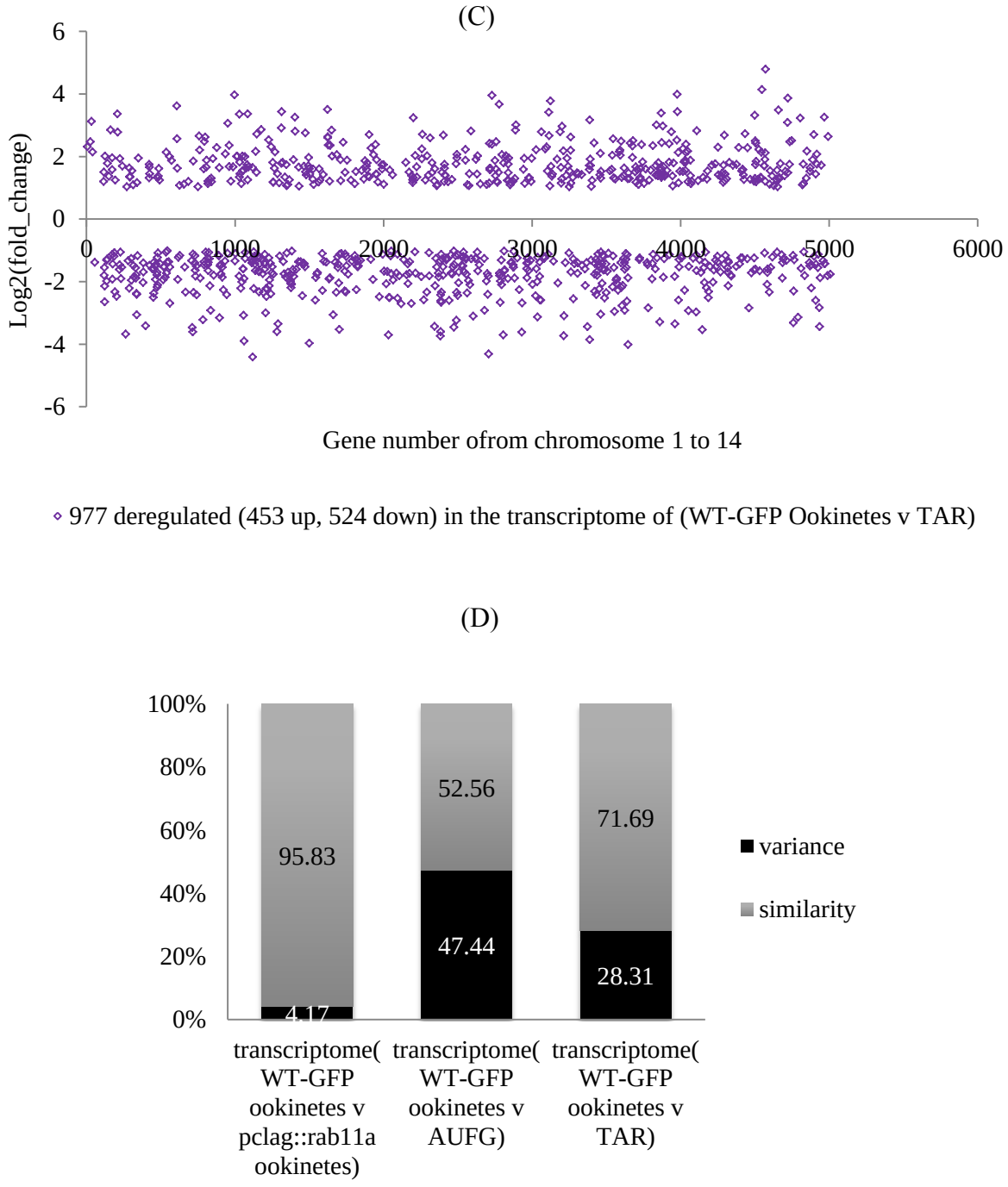

Figure 3.7.7 Comparison of transcriptome of *$_p$clag::rab11a* ookinetes, AUFG, TAR and WT-GFP ookinetes.

(A) Scatter plots showing fold changes of deregulated transcripts of *$_p$clag::rab11a* ookinetes or (B) AUFG or (C) TAR as compared to the transcriptome of WT-GFP ookinete. (D) Bar graph showing percent similarity and variance between the transcriptomes of *$_p$clag::rab11a* ookinete or AUFG or TAR with the transcriptome of WT-GFP ookinete.

Comparison of transcriptome	Number of deregulated transcripts (Cut off FPKM ≥10)	Distribution of Log2(fold_Change)	
		Number of transcripts within the range of fold change ≤ 2 and -2 ≥	Number of transcripts within the range of fold change > 2 and -2 <
WT-GFP gametocytes v *$_p$clag::rab11a* gametocytes	368 (=119Up+249Down)	329 (=87Up+242Down)	39 (=32Up+7Down)
WT-GFP ookinetes v *$_p$clag::rab11a* ookinetes	144 (=40Up+104Down)	143 (=40Up+103Down)	1 (Down)
WT-GFP ookinetes v AUFG	1637 (=638Up+999Down)	840 (=316Up+524Down)	797 (=322Up+475Down)
WT-GFP ookinetes v TAR	977 (=453Up+524Down)	695 (=319Up+376Down)	282 (=134Up+148Down)

Table 3.7.8 Table showing distribution of deregulated transcripts across fold changes.

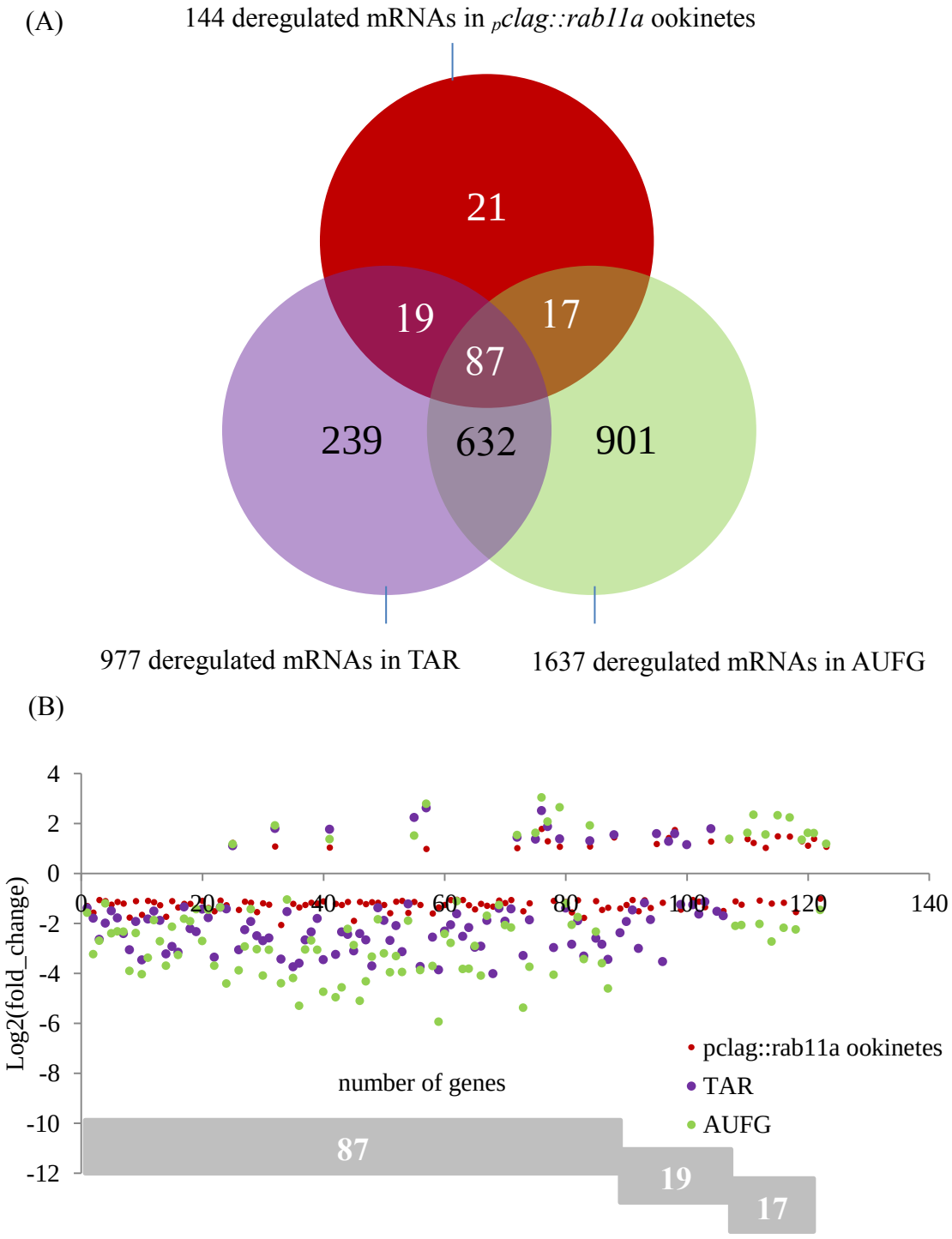

Figure 3.7.9 Pattern of the 144 deregulated transcripts in *pclag::rab11a* ookinetes

(A) Venn diagram showing the overlap of significantly deregulated transcripts in *pclag::rab11a* ookinetes, AUFG and TAR transcriptome. (B) Scatter plot showing fold changes of the 144 deregulated transcripts in *pclag::rab11a* ookinetes and fold changes of common deregulated transcripts of AUFG (87+17) and TAR (87+19).

3.7. d) Gene ontology enrichment for ookinetes

Thus, compared to the transcriptome of WT-GFP ookinetes, that of *$_p$clag::rab11a* ookinetes showed deregulation of 144 transcripts (40 more abundant and 104 less abundant). These 144 deregulated transcripts were divided into four percentile expression group according to the percentage expression groups of the transcriptome of WT-GFP ookinetes (Table 3.7.10 and Table 3.7.11).

Out of 40 more abundant transcripts of *$_p$clag::rab11a* ookinetes, only 21, 16 and 13 are annotated as GO - Molecular Function, Biological Process and Cellular Components respectively. Most of the 40 more abundant transcripts of *$_p$clag::rab11a* ookinetes i.e. 11 out of 40 are associated with the percentile expression group of 100-75% (Table 3.7.10). The GO Biological Process terms indicate that four DNA replication and four proteolysis associated biological processes are the most significantly up-regulated in *$_p$clag::rab11a* ookinete (figure 3.7.12 A), however, the four DNA replication associated transcripts fall in the WT-GFP ookinete 25% percentile and may be marginal and prior analysis indicated no apparent defect. Three out of four proteolysis associated transcripts are above the 25% percentile and may represent noteworthy up-regulation (figure 3.7.12 C). Some of the transcripts associated with the proteolysis are proteasome subunit beta type 7 precursor (putative), 26S proteasome regulatory subunit (putative) and aspartyl protease (putative) (Appendix B, Table 2). This might suggest that protein degradation might be involved in cellular remodelling associated with the morphological development of the ookinete from the zygote.

Out of 104 less abundant transcripts of *$_p$clag::rab11a* ookinete distributed across four percentile expression groups, less than half the transcripts (50 Molecular Function, 31 Biological Process, 19 Cellular Components) have annotated GO-terminologies (Table 3.7.11). GO Biological Processes suggest that six biosynthetic processes, five ribosome biogenesis, three transport and three proteolysis are majorly down-regulated biological processes (Table 3.7.12 B). Out of six down-regulated biosynthetic processes, four are above 50% percentile and therefore suggests notable down-regulation (figure 3.7.12 C). However they do not form a coherent pathway that might indicate a specific biological process was being affected. Transcripts associated with ribosome biogenesis involve rRNA processing protein which might be affected in a non-growing cell (Appendix B, Table 2).

	100-75%	75-50%	50-25%	25-0%	not expressed in WT-GFP ookinetes	Total
40 more abundant transcripts in *$_p$clag::rab11a* ookinetes (39 Pf and 43 Pv orthologues)	11	7	9	7	6	40
Annotated GO - Molecular Function	5	2	5	5	4	21
Annotated GO - Biological Process	4	0	4	5	3	16
Annotated GO - Cellular Components	6	0	2	2	3	13

Table 3.7.10 Table showing distribution of 40 more abundant transcripts in *$_p$clag::rab11a* ookinetes across annotated GO terms. Pf- *P. falciparum 3D7* and Pv – *P. vivax Sal-1.*

	100-75%	75-50%	50-25%	25-0%	Total
104 less abundant transcripts in *$_p$clag::rab11a* ookinetes (98 Pf and 100 Pv orthologues)	38	30	22	14	104
Annotated GO - Molecular Function	14	16	10	10	50
Annotated GO - Biological Process	13	9	5	4	31
Annotated GO - Cellular Components	10	5	1	3	19

Table 3.7.11 Table showing 104 less abundant transcripts in *$_p$clag::rab11a* ookinetes and their distribution across annotated GO terms. Pf- *P. falciparum 3D7* and Pv – *P. vivax Sal-1.*

(A)

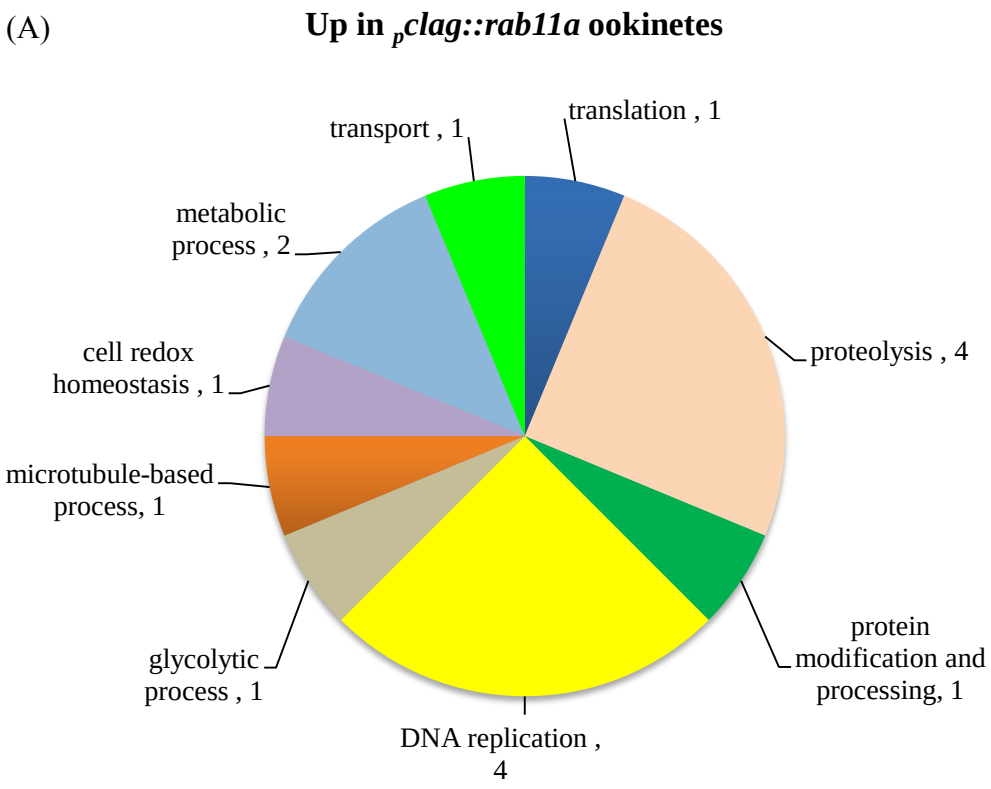
Up in pclag::rab11a ookinetes
translation , 1
transport , 1
metabolic process , 2
proteolysis , 4
cell redox homeostasis , 1
microtubule-based process, 1
protein modification and processing, 1
glycolytic process , 1
DNA replication , 4

(B)

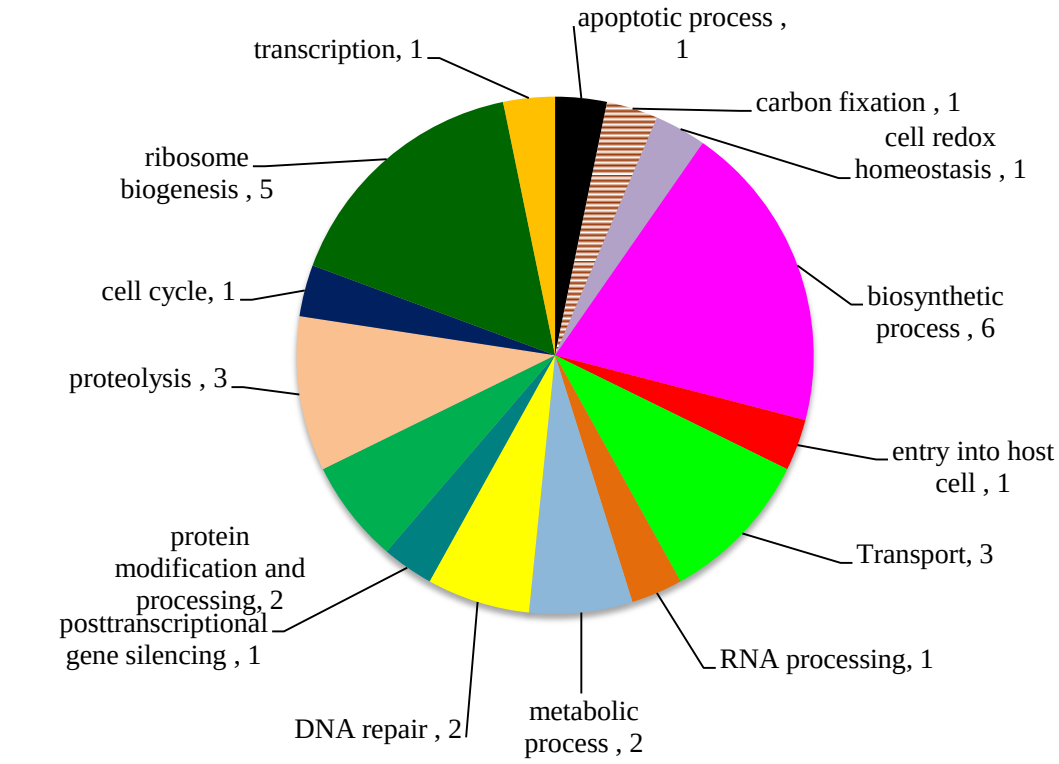
Down in pclag::rab11a ookinete
apoptotic process , 1
transcription, 1
carbon fixation , 1
cell redox homeostasis , 1
ribosome biogenesis , 5
biosynthetic process , 6
cell cycle, 1
proteolysis , 3
entry into host cell , 1
Transport, 3
protein modification and processing, 2
posttranscriptional gene silencing , 1
RNA processing, 1
DNA repair , 2
metabolic process , 2

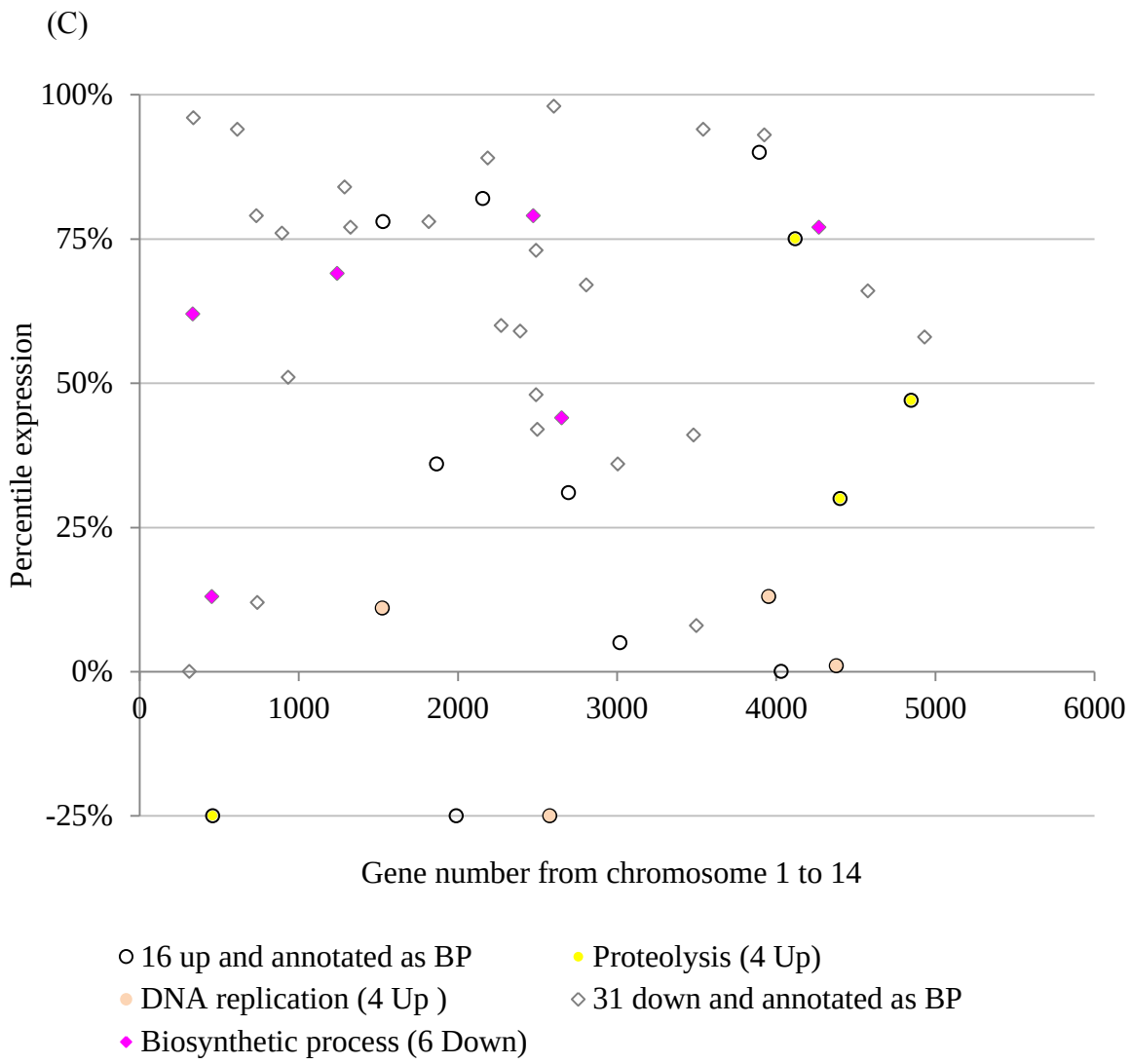

Figure 3.7.12 GO- (Biological Process) term analysis for deregulated transcripts in *$_p$clag::rab11a* ookinetes.

(A) Pie chart showing GO (Biological Process) term enrichment for more abundant (up regulated) transcripts and (B) less abundant (down regulated) transcripts in *$_p$clag::rab11a* ookinetes. (C) Deregulated transcripts of *$_p$clag::rab11a* ookinetes having GO annotated as Biological Process (BP) and their distribution across percentile expression groups compared to the percentile expression groups of WT-GFP ookinete transcriptome. Most up regulated and most down regulated transcripts in *$_p$clag::rab11a* ookinete are colour coded as per pie charts A and B. Up regulated transcripts in *$_p$clag::rab11a* ookinete which are not detected in the transcriptome of WT-GFP ookinetes were given an arbitrary percentile expression value of -25%.

3.7. e) The transcriptome of AUFG is completely different to the transcriptome of TAR

The transcriptome of AUFG and TAR are compared with the transcriptome of WT-GFP ookinetes, and not with the transcriptome of WT-GFP gametocytes, as AUFG and TAR samples used for RNA-Seq were collected at the same time point as for the samples of WT-GFP ookinetes i.e. 24hpa and the number of deregulated transcripts were analysed.

Compared to the transcriptome of WT-GFP ookinetes (3451 protein coding transcripts expressed), that of TAR is 71.69% similar and AUFG is 52.56% similar (figure 3.7.7 D)(See Appendix B, Table 3 and 4 for details of transcripts). This indicates that the transcriptome of TAR is more similar to the transcriptome of WT-GFP ookinetes than that of AUFG. When the transcriptome of AUFG is compared with the transcriptome of TAR, they show almost 75% similarity with each other and therefore 25% difference (figure 3.7.13), although very different processes have been blocked experimentally (transcription in TAR and fertilization in AUFG). This shows that only 25% of the transcriptome is essentially deregulated when fertilization is blocked and transcription is arrested and this 25% of the transcriptome appear to be essential for the development of zygote into ookinete.

Since destabilisation of translationally repressed/ stored (i.e. DOZI/CITH associated) transcripts gives a similar phenotype (Mair, Braks et al. 2006, Mair, Lasonder et al. 2010) , the transcriptome of AUFG and TAR were analysed in detail. The transcriptome of AUFG and TAR were compared with that with WT-GFP ookinetes but referred to the catalogue of 733 DOZI/CITH associated transcripts in WT-GFP gametocytes (Guerreiro, Deligianni et al. 2014), to assess if gametocyte stored transcripts were stabilised and to assess the further development of the experimentally manipulated parasites (TAR & AUFG).

The comparison of the transcriptome of AUFG with that of the transcriptome of WT-GFP ookinetes, indicates significantly more abundance of 638 transcripts and significantly less abundance of 999 transcripts. Out of these 638 more abundant transcripts, 222 transcripts are associated with DOZI/CITH i.e. 30.28% (222 out of 733) and out of 999 down regulated transcripts 119 are associated with DOZI/CITH i.e. 16.28% (119 out of 733) (figure 3.7.14 A). This suggests that significant amount (30.28% i.e. 222 out of 733) of the translationally stored mRNAs (which remain less abundant in WT-GFP ookinetes) remain more abundant, stable and possibly untranslated after the activation of female gametocytes when fertilization

is inhibited and withheld (DOZI/CITH stored) from mRNA degradation mechanisms in AUFG even at 24hpa (figure 3.7.14 B).

The comparison of the transcriptomes of WT-GFP ookinetes and TAR revealed 453 transcripts to be significantly more abundant and 524 transcripts are significantly less abundant. Of the 453 more abundant transcripts, 173 are common with DOZI/CITH i.e. 23.74% (174 out of 733) and out of 524 less abundant transcripts, 67 are common with DOZI/CITH i.e 9.17% (67 out of 731) (figure 3.7.15 A). Retention of a subset of DOZI/CITH stored mRNAs i.e. 23.74% (174 out of 733) in TAR, and the same subset of transcripts remain less abundant in WT-GFP ookinetes, indicates the utilization of most of the DOZI/CITH stored mRNAs (Guerreiro, Deligianni et al. 2014) and perhaps explains why the partial outgrowth of apical complex is achieved (figure 3.7.15 B).

Compared to the transcriptome of WT-GFP ookinetes, that of AUFG shows significant deregulation of 1637 transcripts and that of TAR shows deregulation of 977 transcripts. Out these 1637 deregulated transcripts of AUFG and 977 deregulated transcripts of TAR, 719 transcripts are common (figure 3.7.14 A). Out of these 719 transcripts, 285 transcripts are more abundant in both AUFG and TAR, 433 transcripts are less abundant in both AUFG and TAR and only 1 transcript is less abundant in AUFG yet more abundant in TAR. 353 transcripts are exclusively more and 565 are exclusively less abundant in AUFG whereas 167 are exclusively more and 91 are exclusively less abundant in TAR (figure 3.7.13 B). Altogether, the data from figure 3.7.14 A and B suggest that more transcripts are deregulated in AUFG as compared to TAR. This indicates the importance of fertilization process and activation of post-meiotic transcription to co-ordinate cellular events for zygote development in *P. berghei.*

(A)

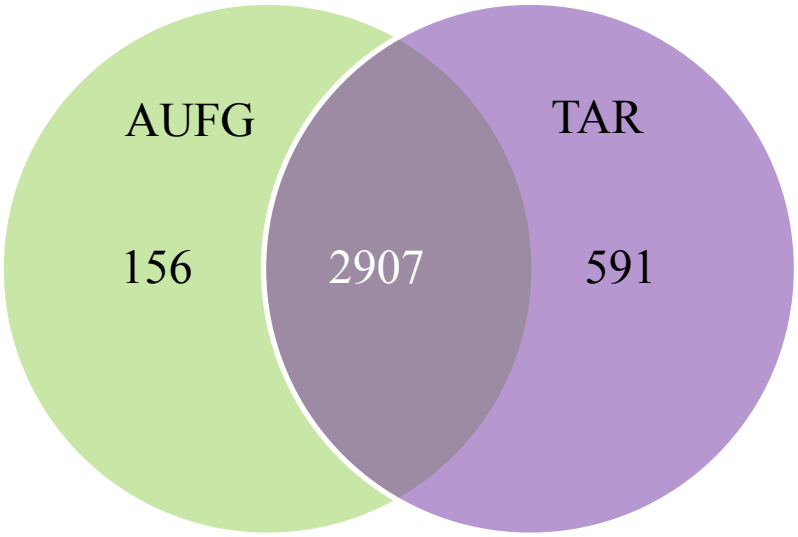

(B)

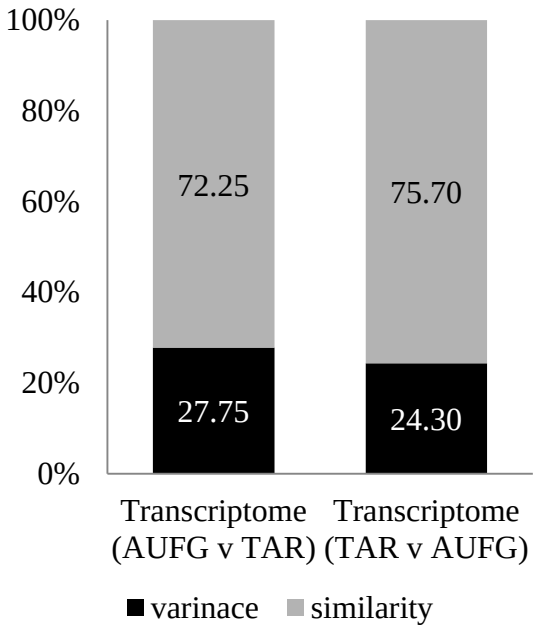

Figure 3.7.13 Similarity of AUFG and TAR transcriptome.

(A) Venn diagram showing common transcripts in AUFG and TAR (B) percentage similarity and variance of AUFG and TAR transcripome with each other.

(A)

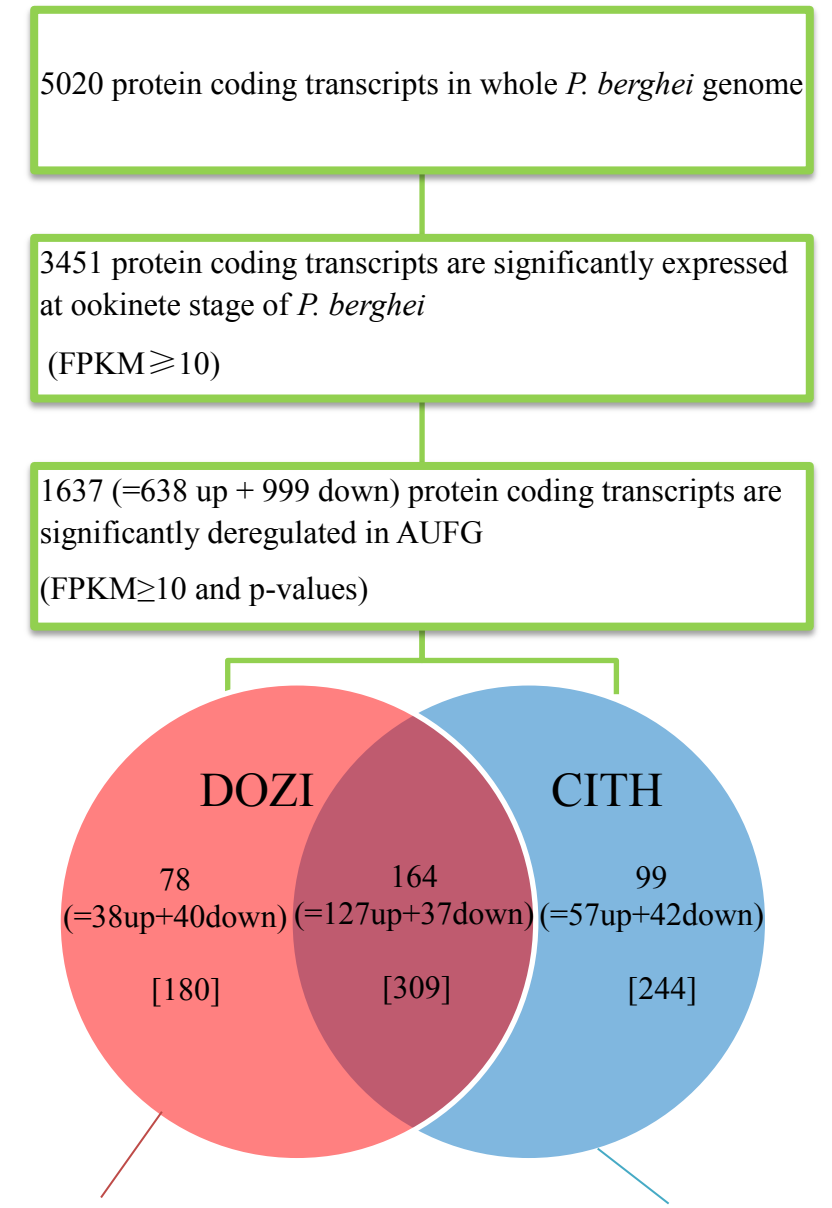

Total DOZI associated transcripts 489 and total CITH associated transcripts are 553(Guerreiro, Deligianni et al. 2014)

(B)

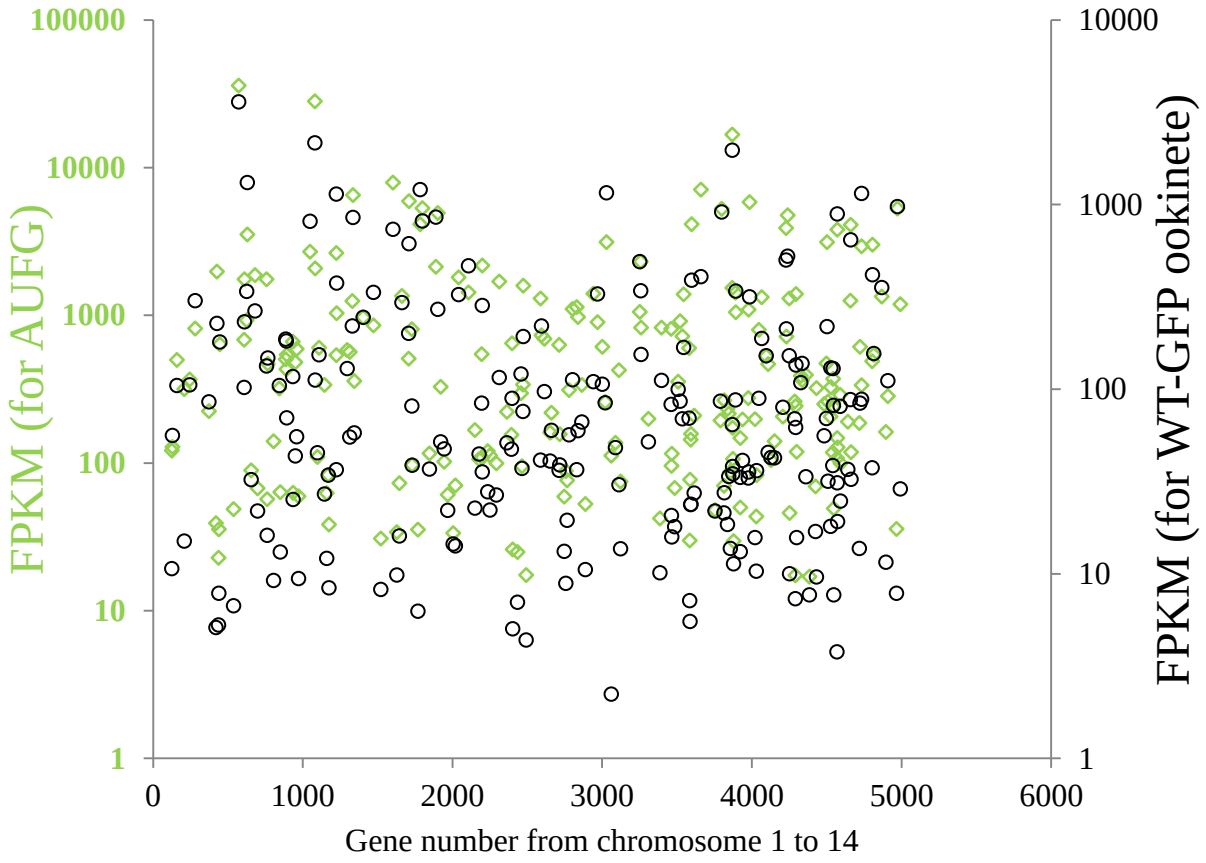

Figure 3.7.14 Comparison of the AUFG transcriptome with translationally stored transcripts.

(A) Chart and Venn diagram showing common transcripts of deregulated transcripts in AUFG and translationally stored transcripts (Guerreiro, Deligianni et al. 2014). (B) Scatter plot showing FPKM values of 222 common transcripts of 638 more abundant and 733 DOZI/CITH associated transcripts (Guerreiro, Deligianni et al. 2014) in AUFG. Y axis shows log scale.

(A)

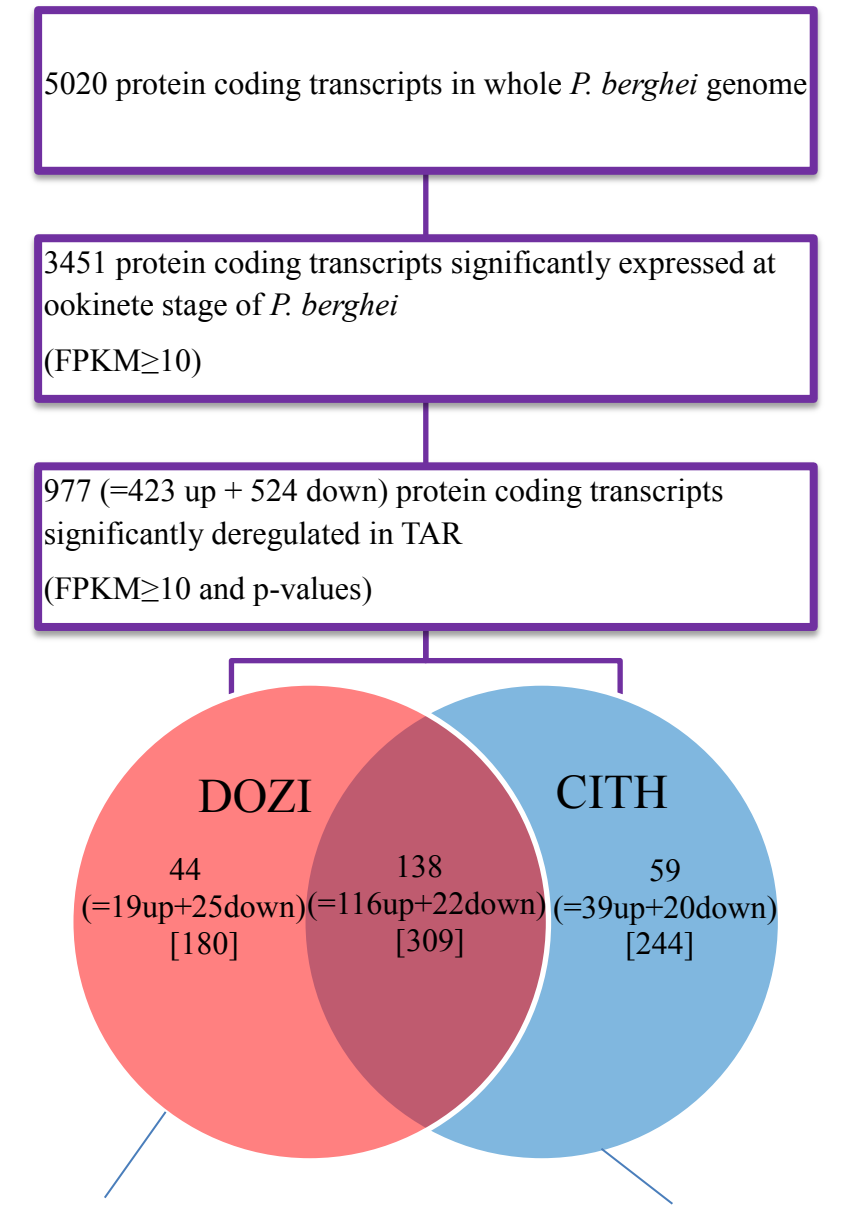

Total DOZI associated transcripts 489 and total CITH associated transcripts are 553(Guerreiro, Deligianni et al. 2014)

(B)

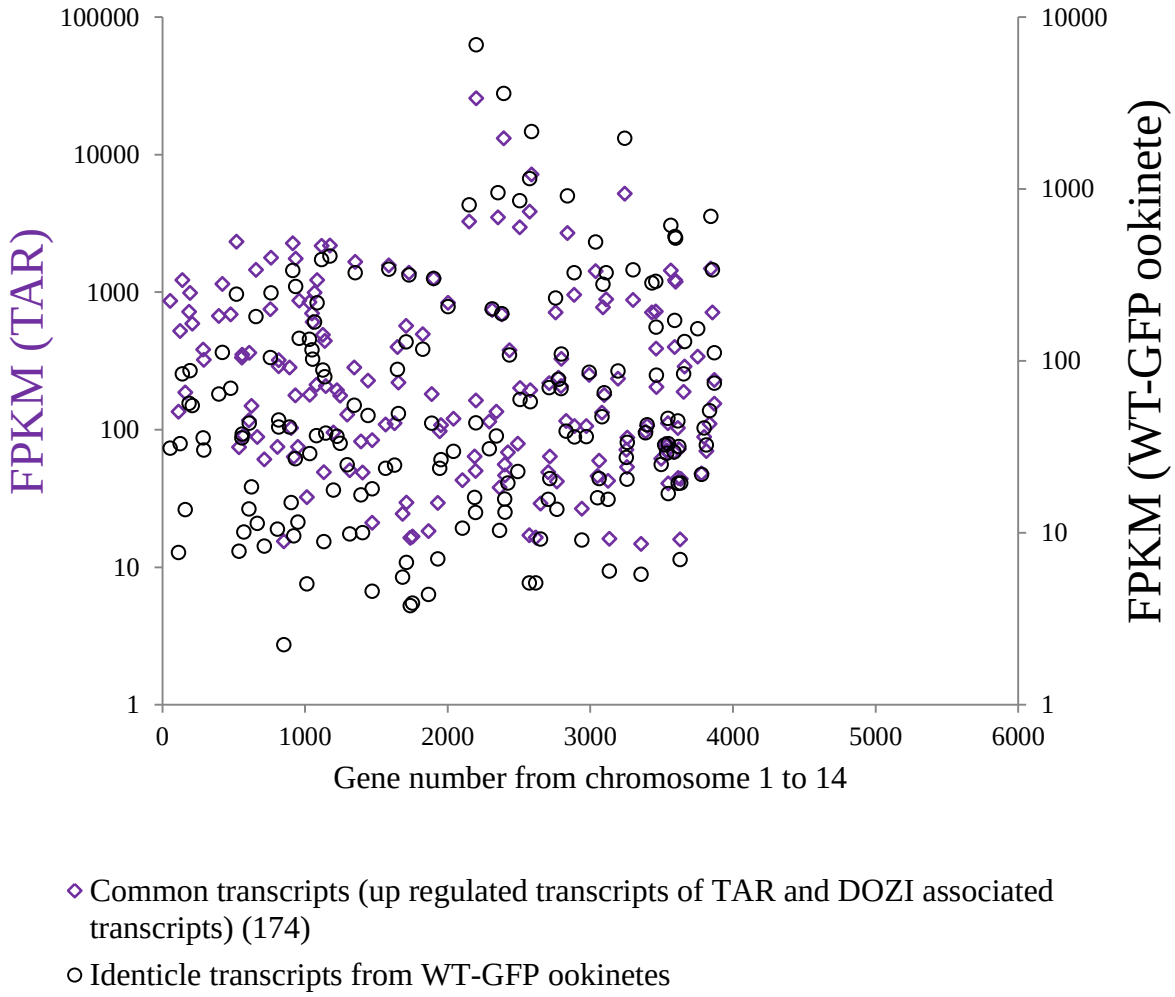

Figure 3.7.15 Comparison of the TAR transcriptome with translationally stored transcripts.

(A) Chart and Venn diagram showing common transcripts of deregulated transcripts in TAR and translationally stored transcripts. Square brackets represent the original DOZI/CITH associated transcripts numbers from (Guerreiro, Deligianni et al. 2014). (B) Scatter plot showing FPKM values of 174 common transcripts of 423 more abundant and 733 DOZI/CITH associated transcripts (Guerreiro, Deligianni et al. 2014) in TAR. Y axis shows log scale.

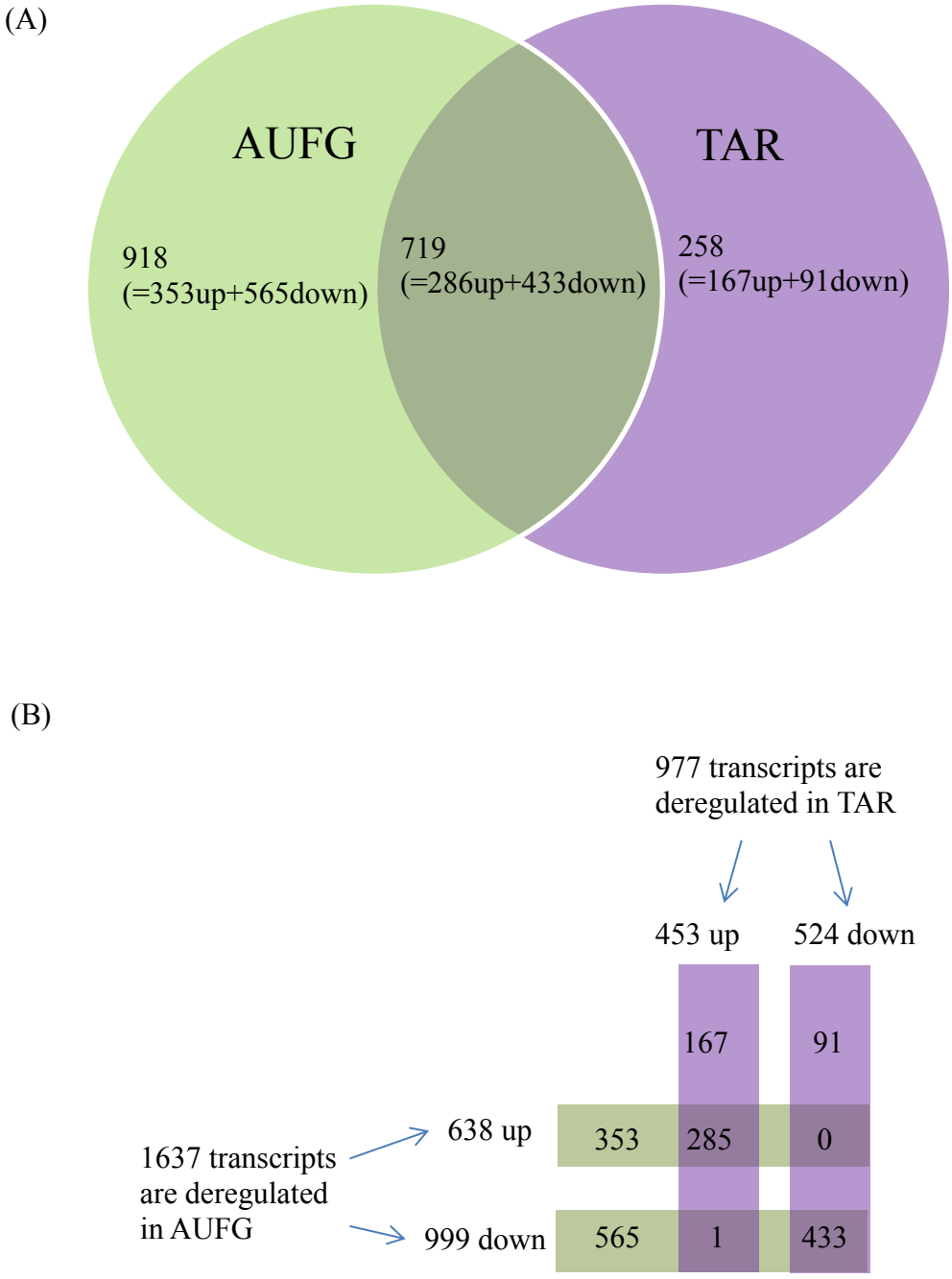

Figure 3.7.16 Overlap of deregulated transcripts of the drug treated WT-GFP parasites transcriptome.

(A) Venn diagram showing common deregulated transcripts in AUFG and TAR (B) and details of up and down regulation.

3.7. f) Gene ontology enrichment for AUFG

The distribution of the 638 more abundant transcripts in AUFG transcriptome across the four WT-GFP percentile expression groups and compared to those of WT-GFP ookinete transcriptome (because AUFG samples were collected at 24hpa) and the distribution across DOZI/CITH and GO terms examined (Table 3.7.17). Out of 638 more abundant transcripts, almost 33% (229 Molecular Function, 171 Biological Process, 134 cellular components) have annotated GO terms (Table 3.7.17). The majority of the more abundant transcripts (221 out of 638) of AUFG fall in 25-0% percentile (Table 3.7.17). Common transcripts of 638 more abundant transcripts and 733 DOZI/CITH associated transcripts (65 and 64) come under 100-75% percentile (Table 3.7.17). The GO-Biological Process terms analysis indicates that 28 protein modification and processing, 22 transport, 18 translation, 15 DNA repair/replication and 14 proteolysis related biological processes are the most up-regulated (figure 3.7.19 A). The most up-regulated protein modification and processing related transcripts are spread across the entire percentiles (figure 3.7.19 C) (See Appendix B, Table 3 for details about transcripts).

The 999 less abundant transcripts in AUFG transcriptome were also classified according to the WT-GFP ookinete percentile groups and distribution of these 999 down regulated transcripts in AUFG across DOZI/CITH and GO were shown in table 3.7.18. Of these 999 down regulated transcripts in AUFG, only half of them have GO annotation (489 Molecular Function, 354 Biological Process and 262 Cellular Component). Most of the less abundant transcripts (438 out of 999) fall into 25-0% WT-GFP ookinete percentile whereas the most of the shared DOZI/CITH transcripts (35 and 36 transcripts) fall under 100-75% percentile (Table 3.7.18). The biological process GO indicates major down-regulation of transport (56), protein modification and processing (43), translation associated biological processes (38) (figure 3.7.19 B). The most affected transport related transcripts are spread across all the percentage expression groups above 0% (figure 3.7.19 C) (See Appendix B, Table 3 for details about transcripts).

In summary, the same general biological processes appear to be deregulated although the direction of deregulation can be either up or down. Those that are up-regulated may be further stabilised due to remaining associated with the translation repression apparatus. The extent of the deregulation is profound affecting almost 25% of the parasite transcriptome (figure 3.7.13 B).

	100-75%	75-50%	50-25%	25-0%	Not expressed in WT-GFP ookinetes	Total
638 more abundant transcripts in AUFG (Pf 603, Pv 594)	145	130	-	221	142	638
DOZI	65	39	-	49	11	164
CITH	64	39	-	61	19	183
Annotated GO - Molecular Function	56	50	-	74	49	229
Annotated GO - Biological Process	42	41	-	51	37	171
Annotated GO - Cellular Component	43	30	-	41	20	134

Table 3.7.17 Table showing distribution of 638 more abundant transcripts in AUFG across translationally stored transcripts as well as annotated GO terms. Pf- *P. falciparum 3D7* and Pv – *P. vivax Sal-1*.

	100-75%	75-50%	50-25%	25-0%	Total
999 less abundant transcripts in TAR (Pf 993, Pv 984)	285	276	-	438	999
DOZI	35	26	-	16	77
CITH	36	26	-	17	79
Annotated GO - Molecular Function	128	147	-	214	489
Annotated GO - Biological Process	109	110	-	135	354
Annotated GO - Cellular Component	90	71	-	101	262

Table 3.7.18 Table showing distribution of 999 less abundant transcripts in AUFG across translationally stored transcripts as well as annotated GO terms. Pf- *P. falciparum 3D7* and Pv – *P. vivax Sal-1*.

Up in AUFG

(A)

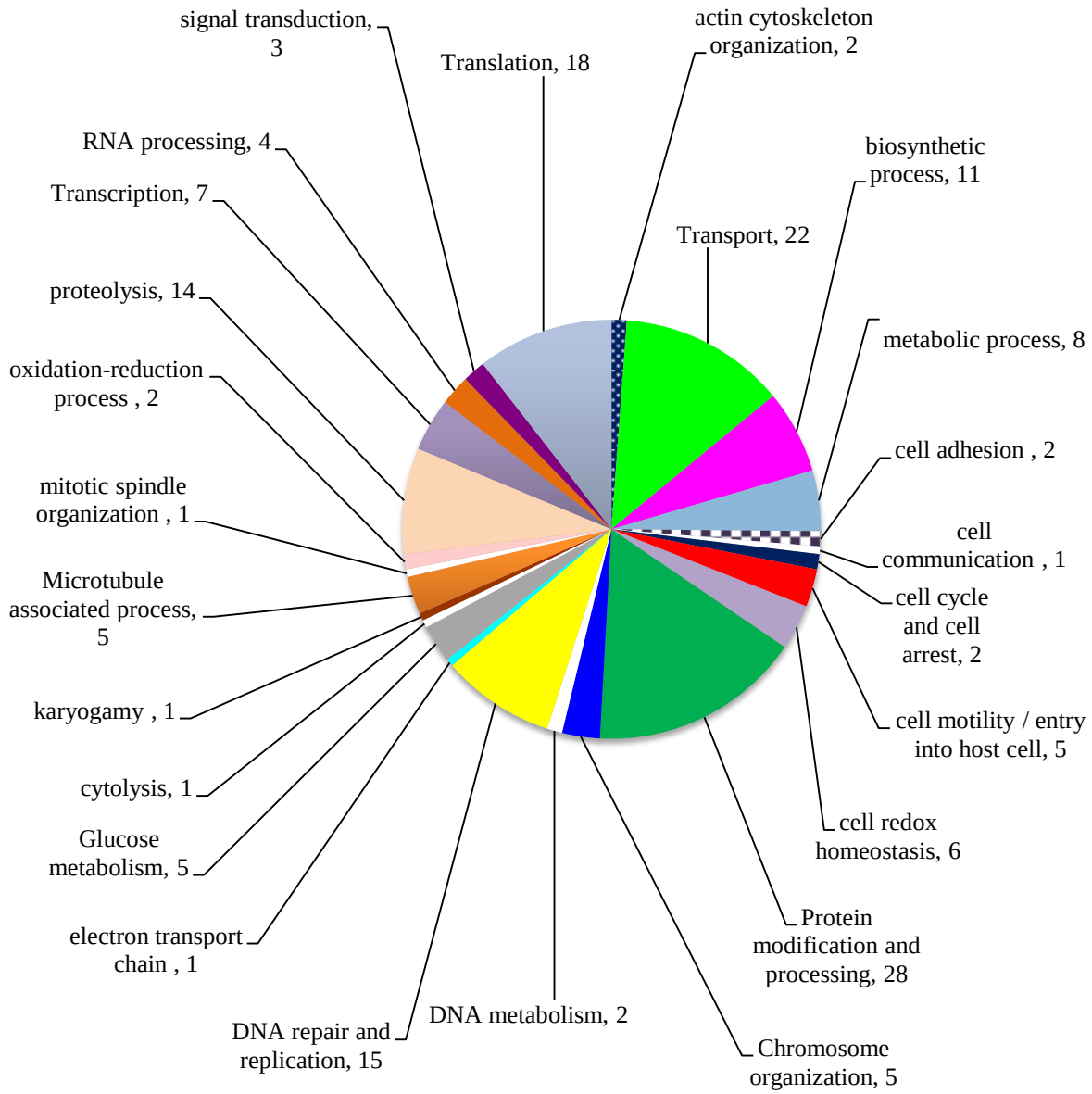
signal transduction, 3
Translation, 18
actin cytoskeleton organization, 2
RNA processing, 4
biosynthetic process, 11
Transcription, 7
Transport, 22
proteolysis, 14
metabolic process, 8
oxidation-reduction process , 2
cell adhesion , 2
mitotic spindle organization , 1
cell communication , 1
Microtubule associated process, 5
cell cycle and cell arrest, 2
karyogamy , 1
cell motility / entry into host cell, 5
cytolysis, 1
cell redox homeostasis, 6
Glucose metabolism, 5
Protein modification and processing, 28
electron transport chain , 1
DNA repair and replication, 15
DNA metabolism, 2
Chromosome organization, 5

Down in AUFG

(B)

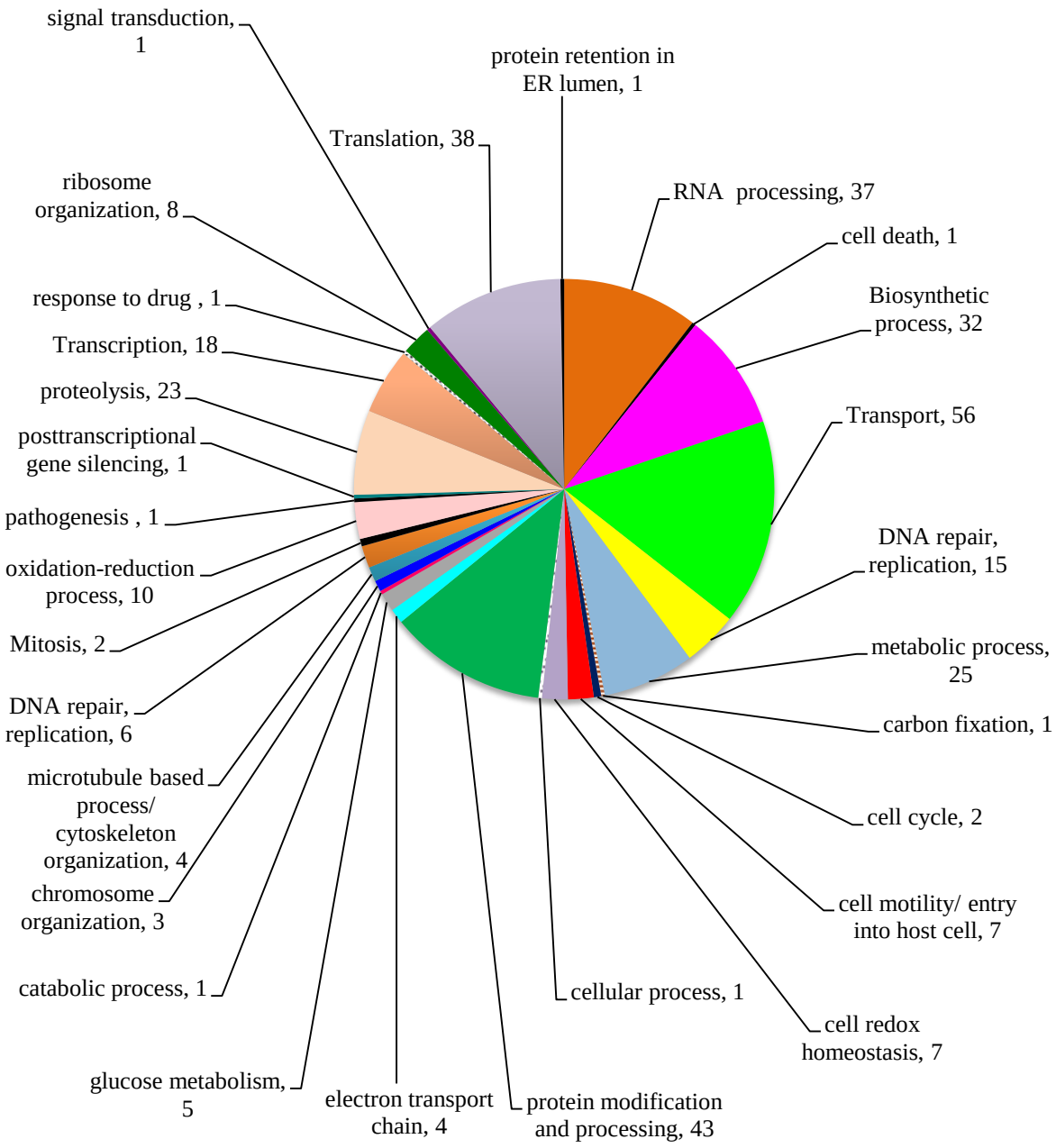

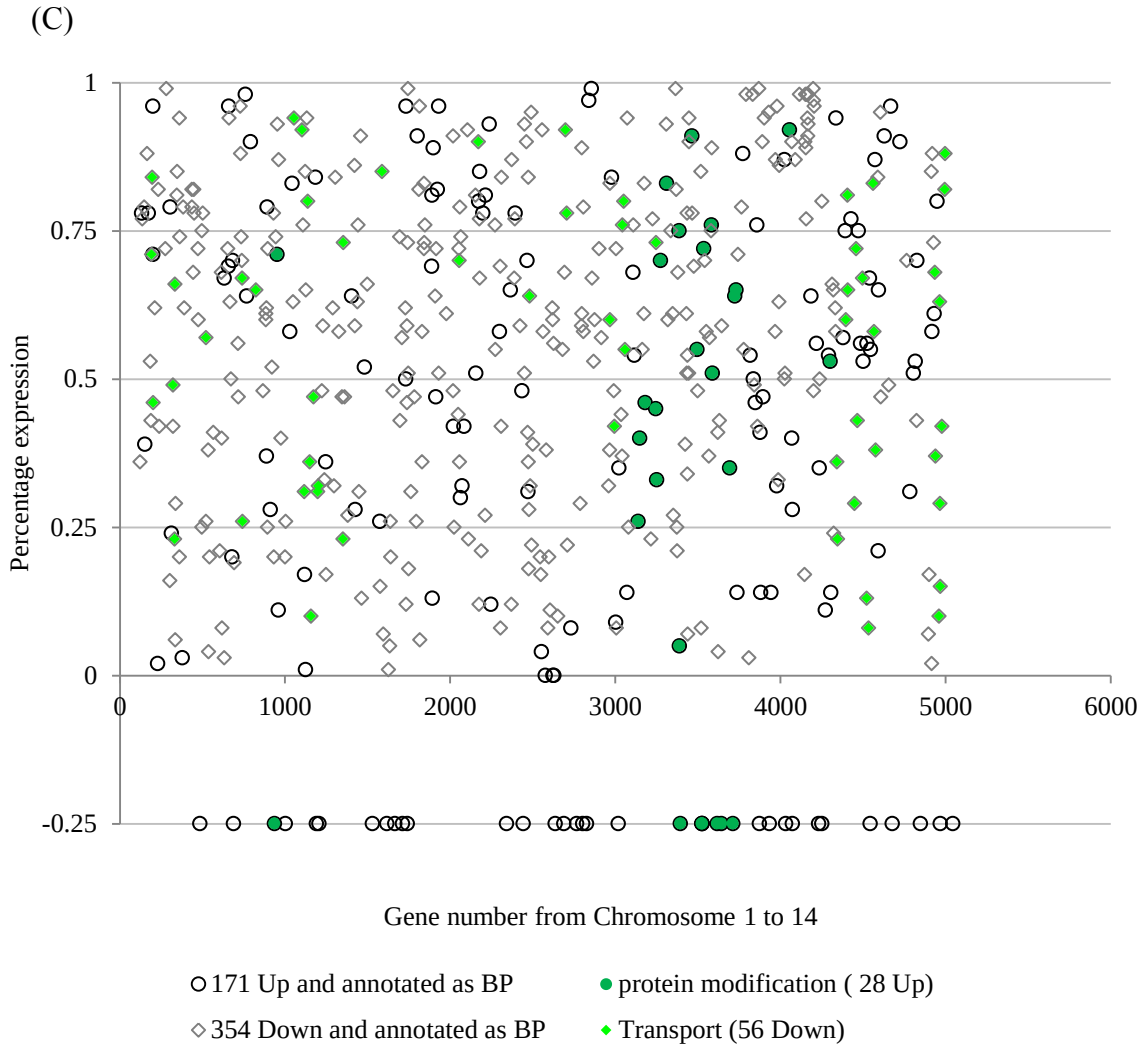

Figure 3.7.19 GO- (Biological Process) term analysis for mis-regulated transcripts in AUFG.

(A) Pie chart showing GO (Biological Process) term enrichment for more abundant transcripts and (B) less abundant transcripts in AUFG. (C) Deregulated transcripts of AUFG having GO annotated as Biological Process and their distribution across percentile expression groups compared to the percentile expression groups of WT-GFP ookinete transcriptome. Most up-regulated and most down-regulated transcripts in AUFG are colour coded as per pie charts A and B. Up-regulated transcripts in AUFG which are not detected in the transcriptome of WT-GFP ookinetes were given an arbitrary percentile expression value of -25%.

3.7. g) Gene ontology enrichment for TAR

The most abundant 423 transcripts in the TAR transcriptome (when compared to the transcriptome of WT-GFP ookinete), were examined for their distribution across the WT-GFP ookinete percentile expression groups and for their predicted association with DOZI/CITH and GO terminology. 33% have annotated GO terms (151-Molecular Function, 115 Biological Process and 105 Cellular Components) (Table 3.7.20). Most of these 423 more abundant transcripts come under the percentage expression group of 50-25% and most of the shared transcript with DOZI/CITH (46 and 45) fall under 100-75% (Table 3.7.20). Interestingly a large number of transcripts which are exclusively more abundant in TAR are not present in the WT-GFP ookinete transcriptome (103 out of 423) implying that they would normally be degraded in the WT-GFP parasite. GO- Biological Process term enrichment suggests that 21 transport, 15 protein modification and processing, 14 DNA replication/repair and 8 biosynthetic processes related transcripts are the majorly affected (figure 3.7.22 A). The up-regulated 21 transport related transcripts are spread across all the percentiles (figure 3.7.22 C) (See Appendix B, Table 4 for details of transcripts).

The less abundant 524 transcripts in TAR were examined for their distribution across the WT-GFP ookinete percentile expression groups; for their predicted association with DOZI/CITH and their GO terminology and shown in Table 3.7.21 and almost half of the less abundant transcripts (267 Molecular Function, 180 Biological Process and 125 Cellular Components) have annotated GO. Most of the less abundant transcripts (185 out of 524) and most of the DOZI/CITH associated transcripts (29 and 22) fall in 100-75% percentile expression group (Table 3.17.21). GO biological process term enrichment suggest that 29 transport, 28 protein modification and processing, 25 RNA processing and 21 biosynthetic processes are the most affected processes (figure 3.7.22 B). The down regulated transport related biological processes are also spread across all the percentage expression groups above 0% (figure 3.7.22 C) (See Appendix B, Table 4 for details of transcripts).

In summary transport, protein modification and processing are the two most up/down regulated biological processes in TAR compared to WT-GFP ookinetes.

	100-75%	75-50%	50-25%	25-0%	Not expressed in WT-GFP ookinetes	Total
453 more abundant transcripts in AUFG **(Pf 423, Pv 419)**	77	76	103	94	103	453
DOZI	46	26	30	21	11	134
CITH	45	30	34	26	19	154
Annotated GO - Molecular Function	17	34	31	39	30	151
Annotated GO - Biological Process	17	28	26	22	22	115
Annotated GO - Cellular Component	21	17	30	16	21	105

Table 3.7.20 Table showing distribution of 453 more abundant transcripts in TAR transcriptome distributed across translationally stored transcripts as well as annotated GO terms. Pf- *P. falciparum 3D7* and Pv – *P. vivax Sal-1*.

	100-75%	75-50%	50-25%	25-0%	Total
524 less abundant transcripts in TAR **(Pf 524, Pv 519)**	185	150	130	59	524
DOZI	29	13	3	2	47
CITH	22	11	6	3	42
Annotated GO - Molecular Function	81	86	64	36	267
Annotated GO - Biological Process	64	55	39	22	180
Annotated GO - Cellular Component	50	37	24	14	125

Table 3.7.21 Table showing distribution of 524 less abundant transcripts in the transcriptome of TAR distributed across translationally stored transcripts as well as annotated GO terms. Pf- *P. falciparum 3D7* and Pv – *P. vivax Sal-1*.

(A)

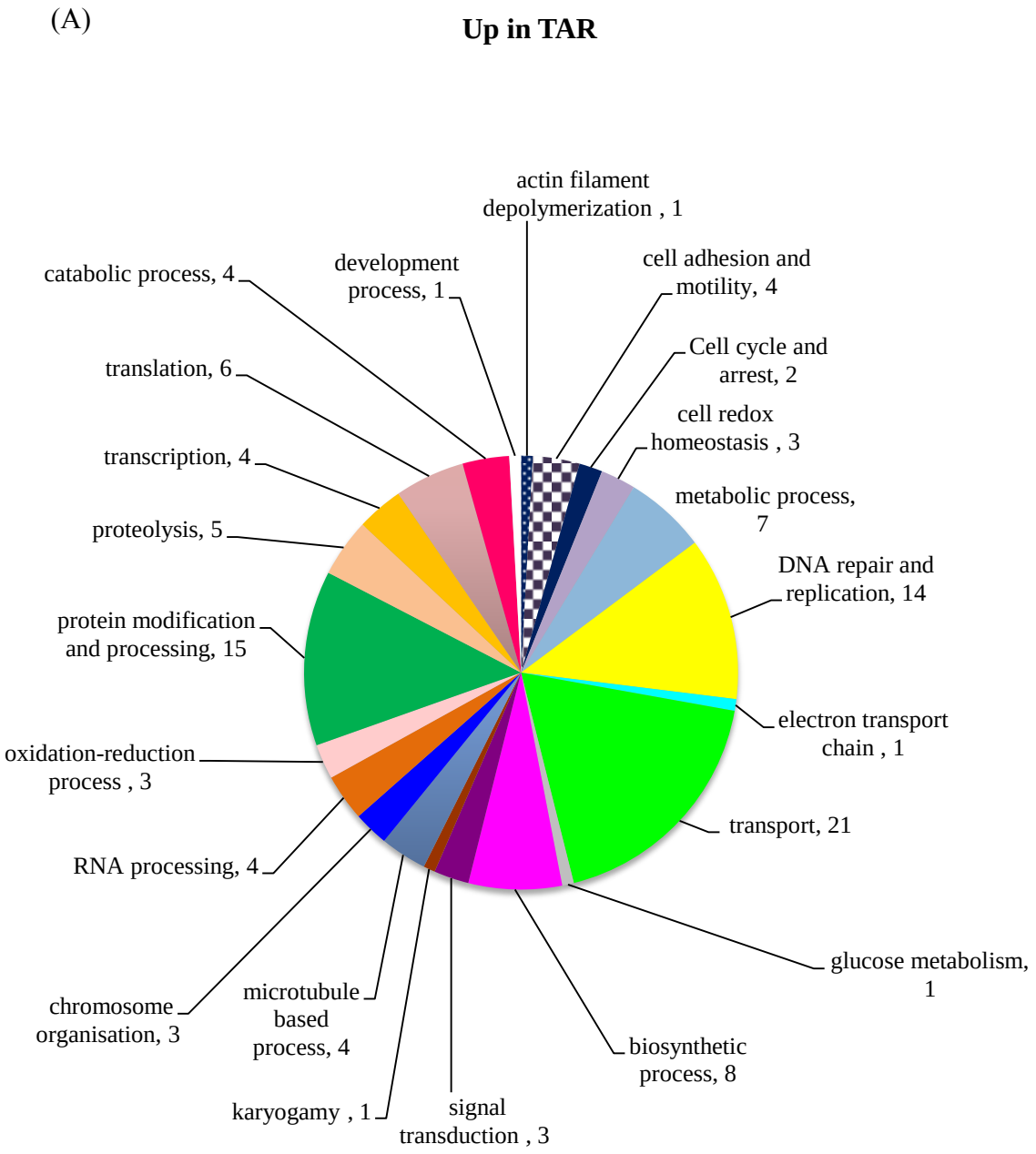
Up in TAR
actin filament depolymerization , 1
development process, 1
cell adhesion and motility, 4
catabolic process, 4
Cell cycle and arrest, 2
translation, 6
cell redox homeostasis , 3
transcription, 4
metabolic process, 7
proteolysis, 5
DNA repair and replication, 14
protein modification and processing, 15
electron transport chain , 1
oxidation-reduction process , 3
transport, 21
RNA processing, 4
glucose metabolism, 1
chromosome organisation, 3
microtubule based process, 4
biosynthetic process, 8
karyogamy , 1
signal transduction , 3

(B)

Down in TAR

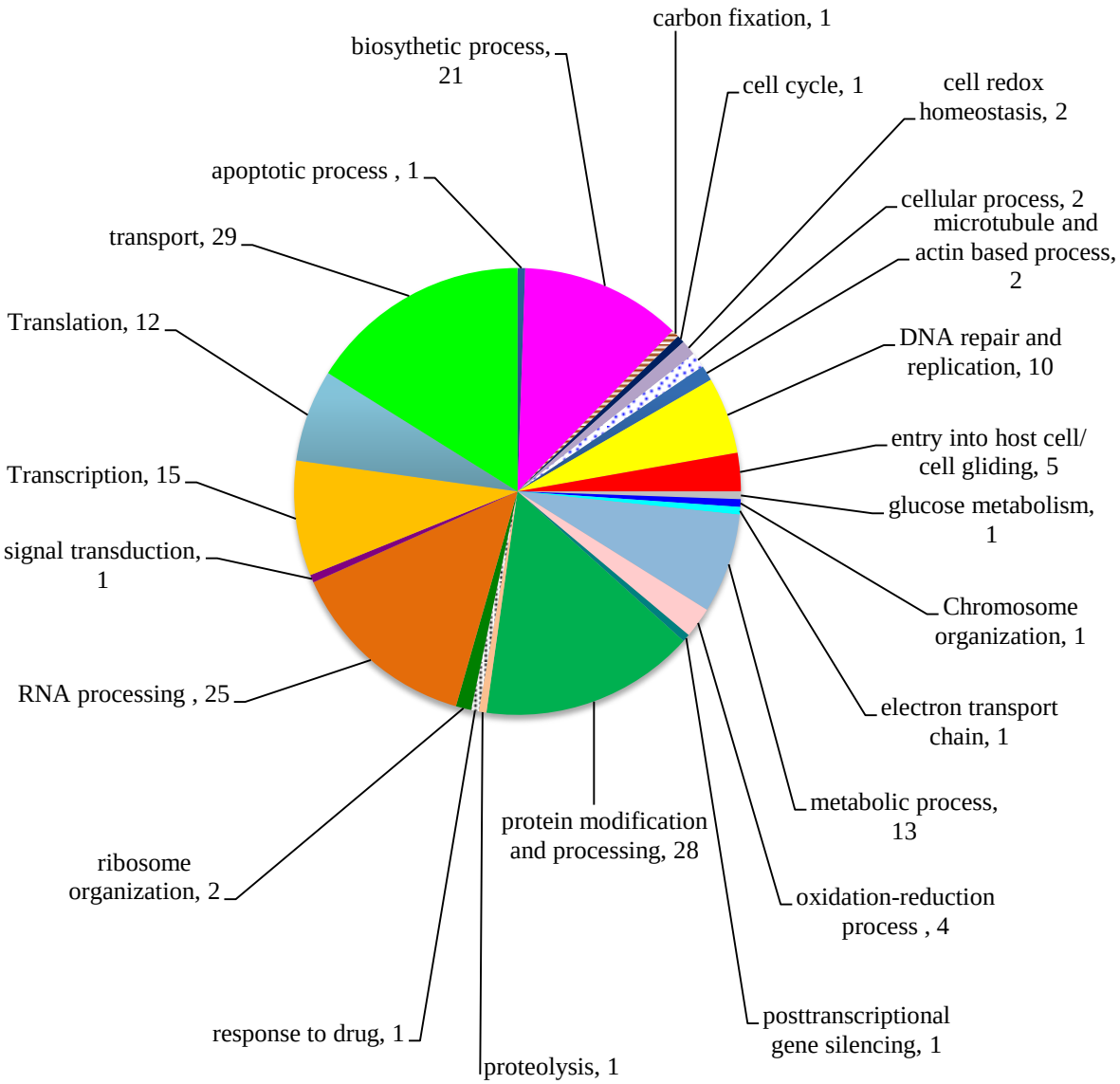
carbon fixation, 1
biosythetic process, 21
cell cycle, 1
cell redox homeostasis, 2
apoptotic process , 1
cellular process, 2
microtubule and actin based process, 2
transport, 29
Translation, 12
DNA repair and replication, 10
entry into host cell/ cell gliding, 5
Transcription, 15
glucose metabolism, 1
signal transduction, 1
Chromosome organization, 1
electron transport chain, 1
RNA processing , 25
metabolic process, 13
protein modification and processing, 28
ribosome organization, 2
oxidation-reduction process , 4
posttranscriptional gene silencing, 1
response to drug, 1
proteolysis, 1

(C)

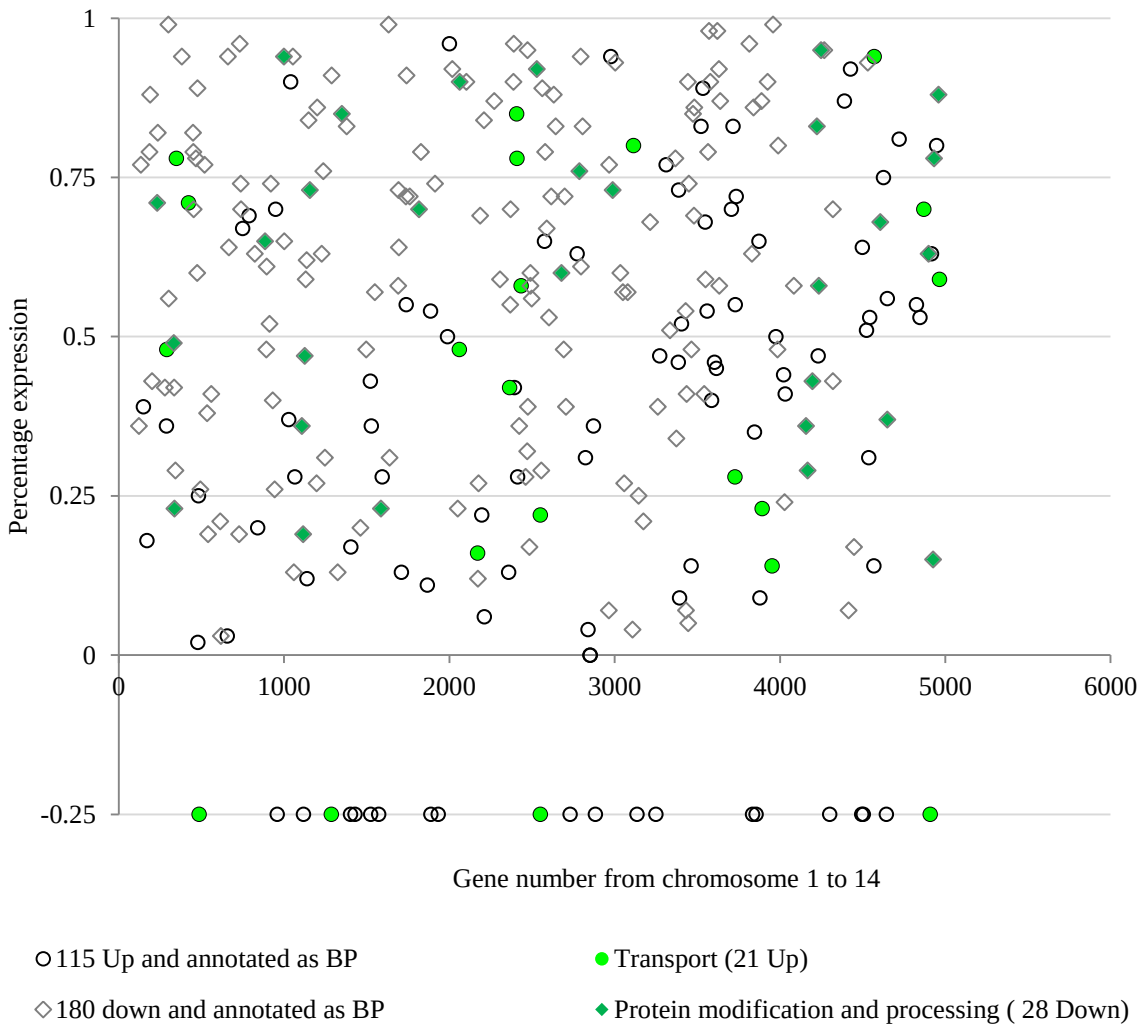

Figure 3.7.22 GO- (Biological Process) term analysis for mis-regulated transcripts in AUFG.

(A) Pie chart showing GO (Biological Process) term enrichment for up regulated transcripts and (B) down regulated transcripts in TAR. (C) Deregulated transcripts of TAR having GO annotated as Biological Process (BP) and their distribution across percentile expression groups compared to the percentage expression groups of WT-GFP ookinete transcriptome. Most up regulated and most down regulated transcripts in TAR are colour coded as per pie charts A and B. Up regulated transcripts in TAR which are not detected in the transcriptome of WT-GFP ookinetes were given an arbitrary percentile expression value of -25% .

3.7. h) Summary of RNA-Seq results

Comparative transcriptome analysis demonstrated that eleven biological processes are mainly affected when $_{p}$*clag::rab11a* gametocytes were compared to WT-GFP gametocytes and when $_{p}$*clag::rab11a* ookinetes, AUFG and TAR were compared to WT-GFP ookinetes. Out of these 11 affected biological processes, cellular transport, protein modification and processing, translation, biosynthetic processes and proteolysis were common across all samples (figure 3.7.20).

Figure 3.7.23 also suggested that $_{p}$*clag::rab11a* gametocytes are more affected than $_{p}$*clag::rab11a* ookinetes despite the fact that $_{p}$*clag::rab11a* gametocytes are able to fertilize and internal structural development is achieved with only a slight delay/reduction in protein synthesis being evident (see Results 3.10 for delay/reduction in protein synthesis). In absence of Rab11A transcripts, most affected biological processes are translation, biosynthetic processes, transport and some metabolic processes. Furthermore, deregulation of these processes is only up to 2 fold (Table 3.7.8).

AUFG shows more severe deregulation of various but similar biological processes than TAR (figure 3.7.23). Most affected biological processes 24hpa in absence of fertilization (in AUFG) and transcriptional block (TAR) are transport, RNA processing and translation. Other major processes affected in AUFG and TAR are proteolysis and biosynthetic processes. This suggests that cellular transport system is most affected biological process in absence of fertilization as well as in presence of transcriptional block in *P. berghei* 24hpa. Deregulation of these biological processes in AUFG and TAR is more severe than in $_{p}$*clag::rab11a* parasites (figure 3.7.23).

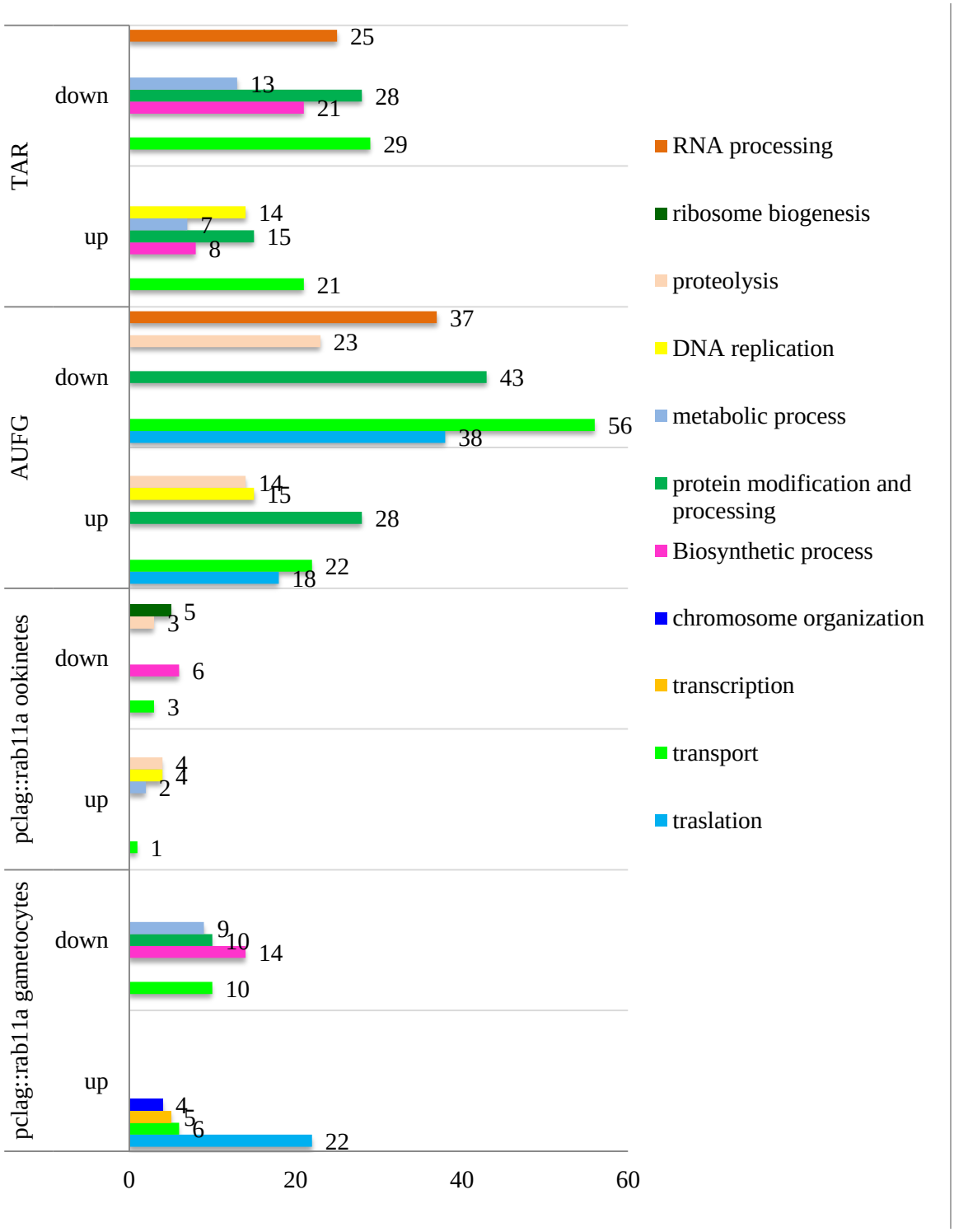

Figure 3.7.23 Major deregulated biological processes.

Graph showing 11 major up and down-regulated biological processes in $_{p}$*clag::rab11a* gametocytes (as compared to WT-GFP gametocytes) and in $_{p}$*clag::rab11a* ookinetes, AUFG and TAR (as compared to WT-GFP ookinetes).

3.8 The trend of gametocyte to ookinete transition in *$_p$clag::rab11a* is comparable to WT-GFP *P. berghei.*

When the significantly deregulated 368 transcripts from *$_p$clag::rab11a* gametocyte and significantly deregulated 144 transcripts of *$_p$clag::rab11a* ookinetes are combined, only 18 transcripts were found shared at gametocyte and ookinete stage leading to 350 transcripts exclusively and significantly deregulated in *$_p$clag::rab11a* gametocyte and 126 solely in *$_p$clag::rab11a* ookinetes (figure 3.8.1). This again suggests that *$_p$clag::rab11a* gametocytes are more severely affected as compared to *$_p$clag::rab11a* ookinetes in absence of Rab11A.

Upon comparing the transcriptome of WT-GFP gametocytes to that of WT-GFP ookinetes, it looks like that these transcriptomes are almost similar (figure 3.8.2 A), however, significant fold change (shown by p-values) suggests that only 2011 transcripts are regulated during WT-GFP gametocyte to ookinete development (cut off FPKM >0). Out of these 2011 significantly regulated transcripts, 953 are more abundant and 1058 are less abundant in WT-GFP ookinetes as compared to WT-GFP gametocytes (figure 3.8.3 A) (Appendix B, Table 5).

Similarly, during transition of *$_p$clag::rab11a* gametocytes to ookinetes, where the transcriptome of these two appears almost similar (figure 3.8.2 B) (cut off FPKM >0), instead of 2011 transcripts in WT-GFP parasites only 1651 transcripts are significantly regulated (significance shown by p-values). Of these 1651, 1071 are more abundant and 580 are less abundant in *$_p$clag::rab11a* ookinetes as compared to *$_p$clag::rab11a* gametocytes (figure 3.8.3 B)(Appendix B, Table 6).

To compare the pattern of transcriptional regulation during gametocyte to ookinete development in WT-GFP and *$_p$clag::rab11a* parasites, 2011 significantly regulated transcripts in WT-GFP parasites and 1651 significantly regulated transcripts in *$_p$clag::rab11a* parasites were compared to each other. These two sets of transcripts show 1212 common transcripts while 799 transcripts are exclusively significantly (significance shown by p-values) regulated only in WT-GFP parasites and 439 in *$_p$clag::rab11a* parasites (figure 3.8.4 A). The common 1212 transcripts have more or less similar fold changes during gametocytes to ookinete development in both WT-GFP and *$_p$clag::rab11a* parasites (figure 3.8.4 B). This suggest that though the transcripts of most of the protein coding genes are present at gametocytes and ookinetes stages, not all of them significantly regulated during this transition and not all of

them are translated in gametocytes and ookinetes (see section 3.9 for details of stage specific transcript analysis).

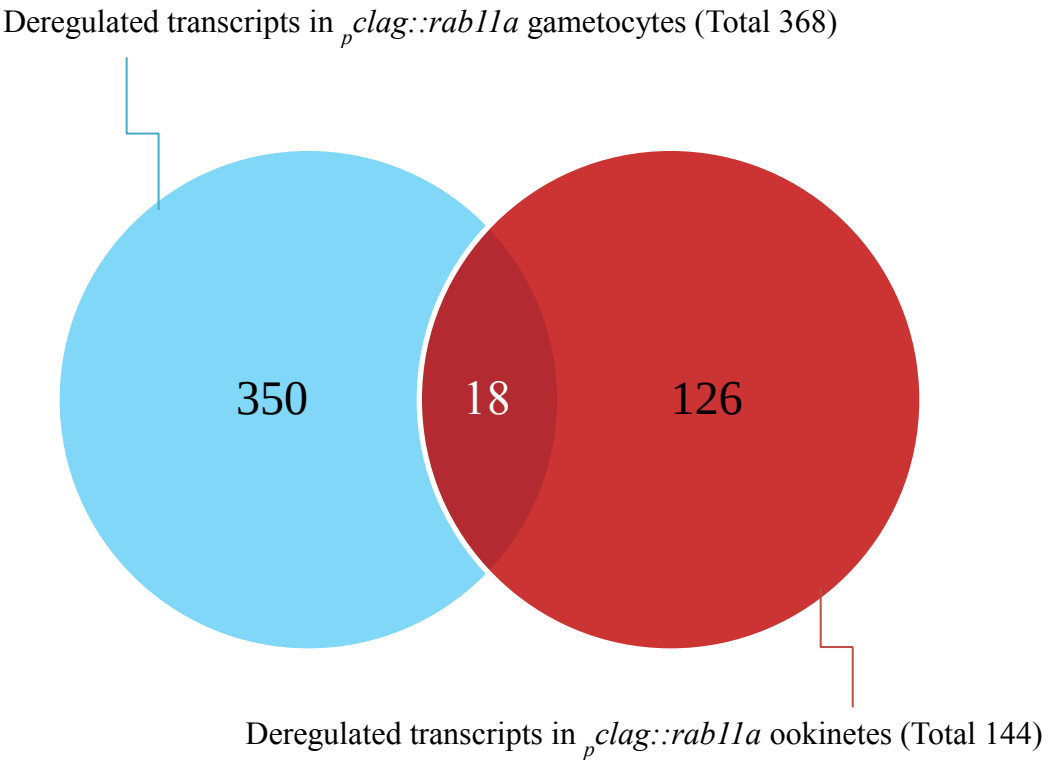

Figure 3.8.1 Venn diagram showing overlap of deregulated transcripts in *pclag::rab11a* gametocytes and *pclag::rab11a* ookinetes.

(A)

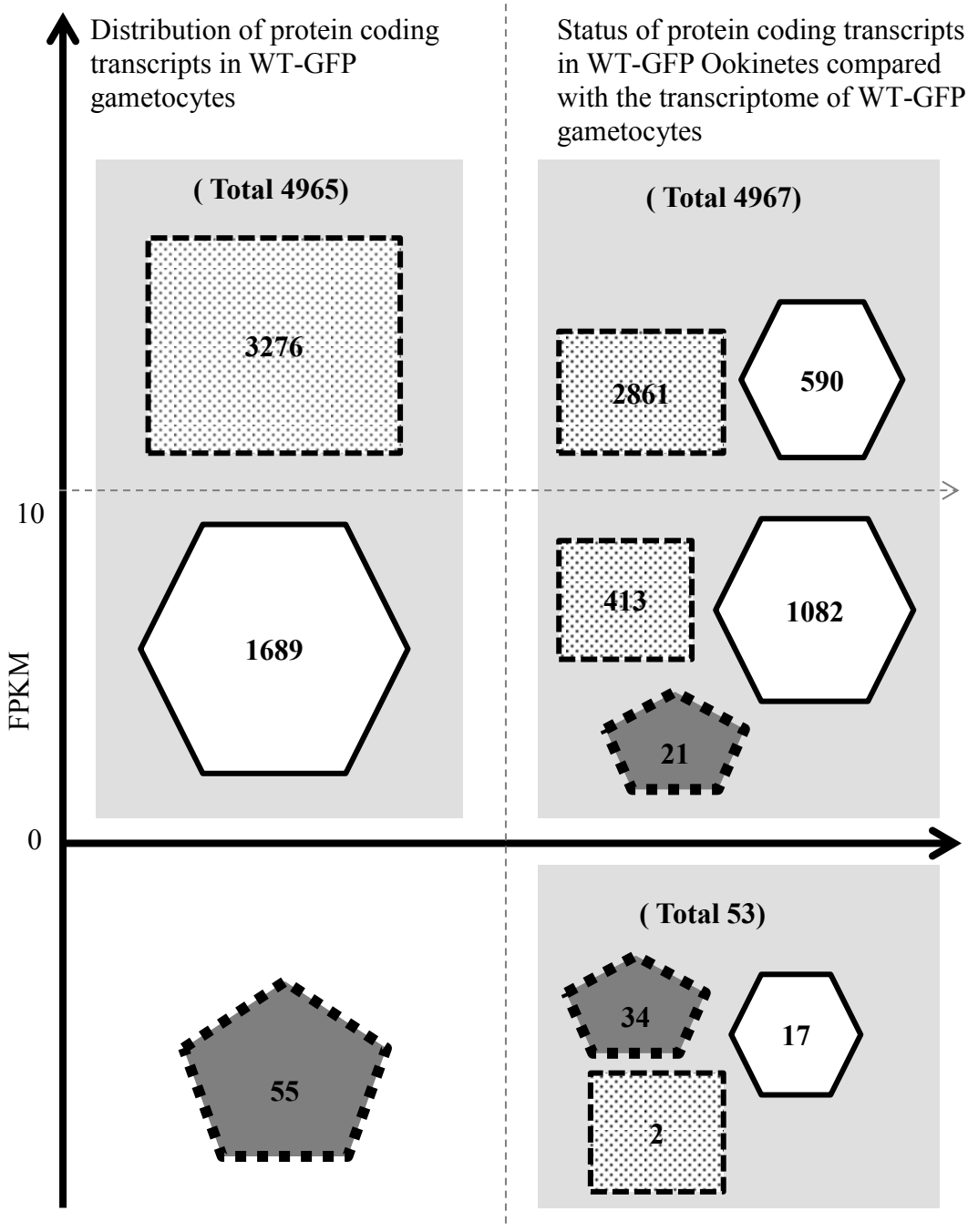
Distribution of protein coding transcripts in WT-GFP gametocytes
Status of protein coding transcripts in WT-GFP Ookinetes compared with the transcriptome of WT-GFP gametocytes
(Total 4965)
(Total 4967)
3276
2861
590
10
1689
413
1082
21
FPKM
0
(Total 53)
34
17
55
2

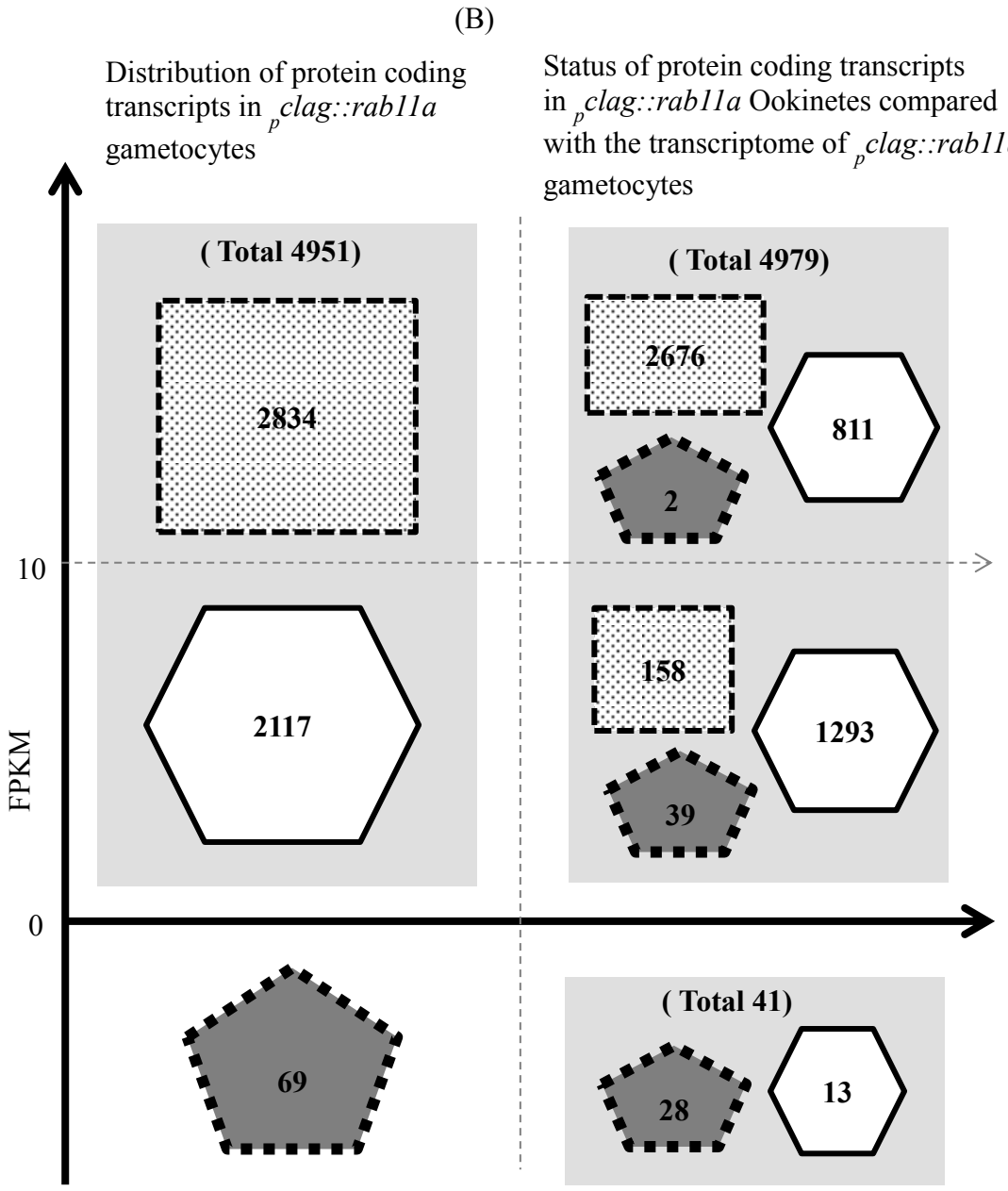

Figure 3.8.2 Distribution of total protein coding transcripts (5020) in gametocytes and ookinetes.

(A) Distribution of total protein coding transcripts in WT-GFP gametocytes and their status in WT-GFP ookinetes (B) Distribution of total protein coding transcripts in *pclag::rab11a* gametocytes and their status in *pclag::rab11a* ookinetes. Left side: Rectangle suggests transcripts having FPKM ≥ 10, hexagon suggests the transcripts having FPKM < 10 and > 0 whereas pentagon suggests transcripts not detected in gametocyte stage. Right side: Status of identical transcripts at ookinete stage. Blue area and brackets indicates the sum of respective sections.

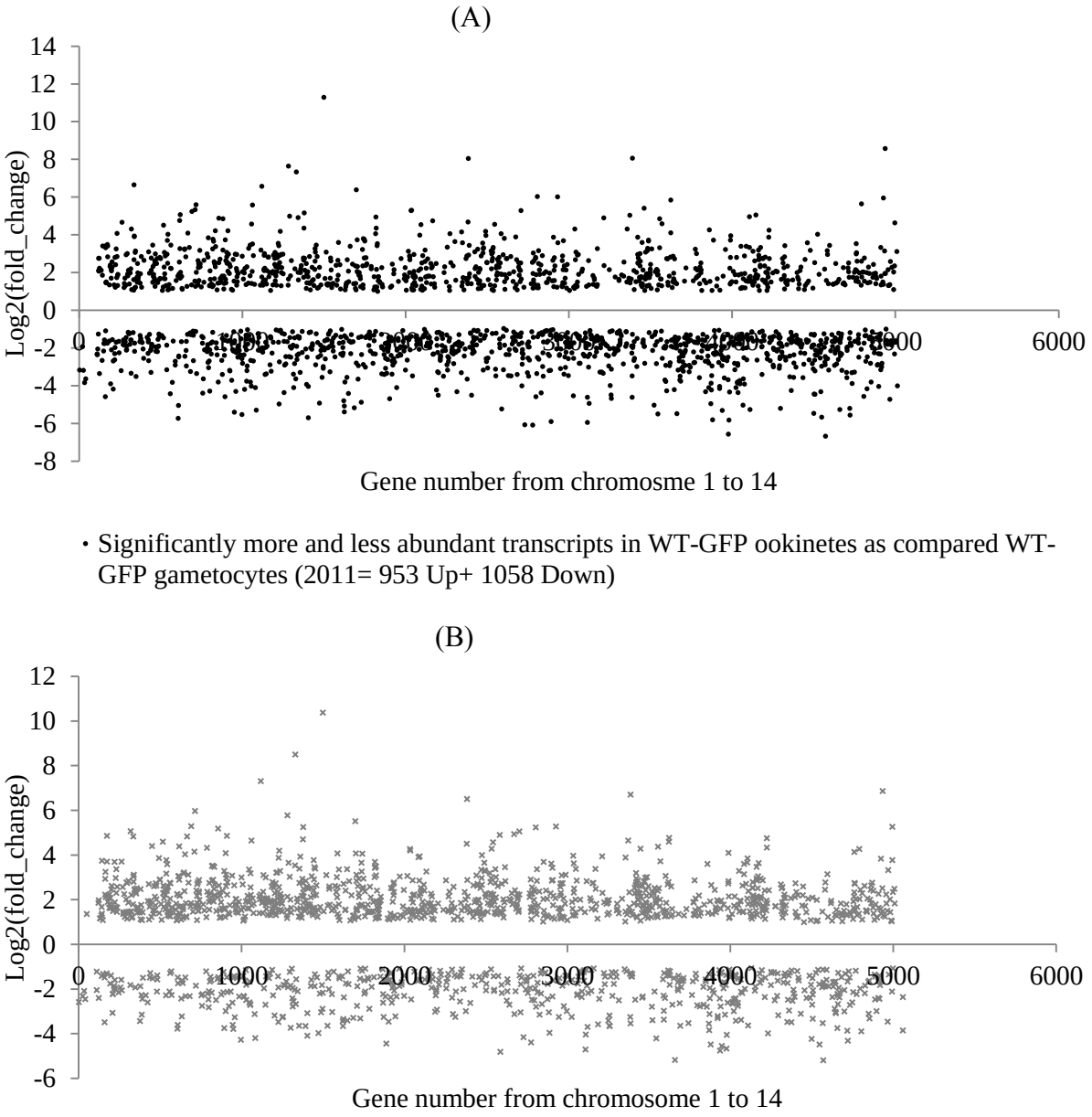

Figure 3.8.3 Significantly regulated transcripts during gametocytes to ookinete development.

(A) Significantly regulated 2011 transcripts during gametocytes to ookinete development in WT-GFP parasites (B) Significantly regulated 1651 transcripts during gametocytes to ookinete development in *$_p$clag::rab11a* parasites.

(A)

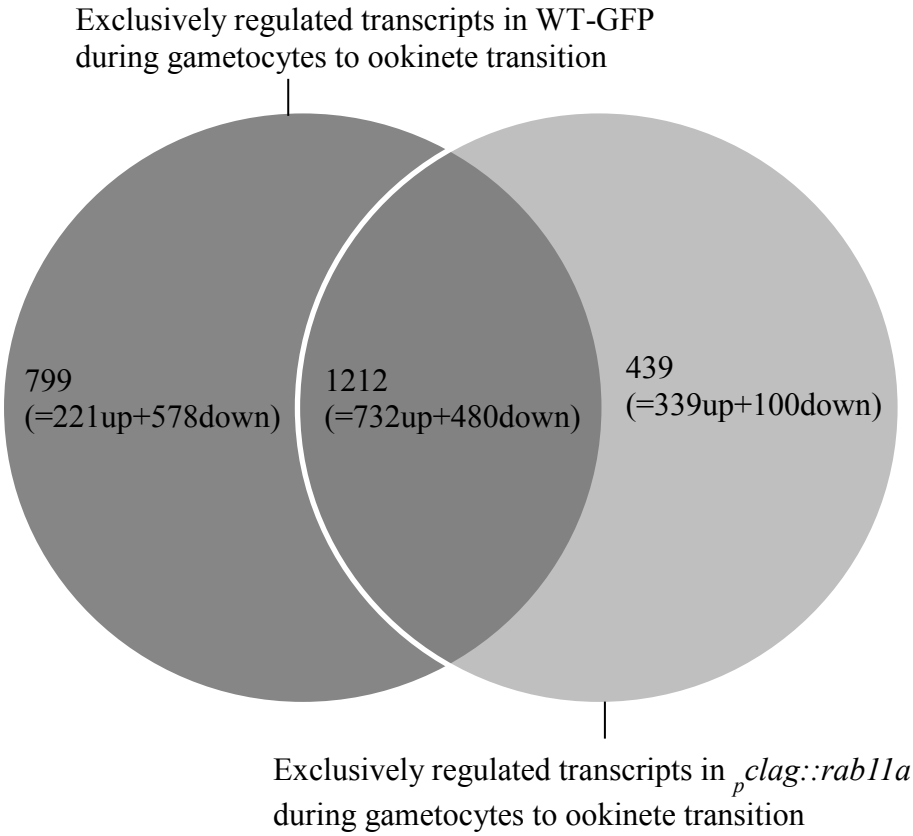

(B)

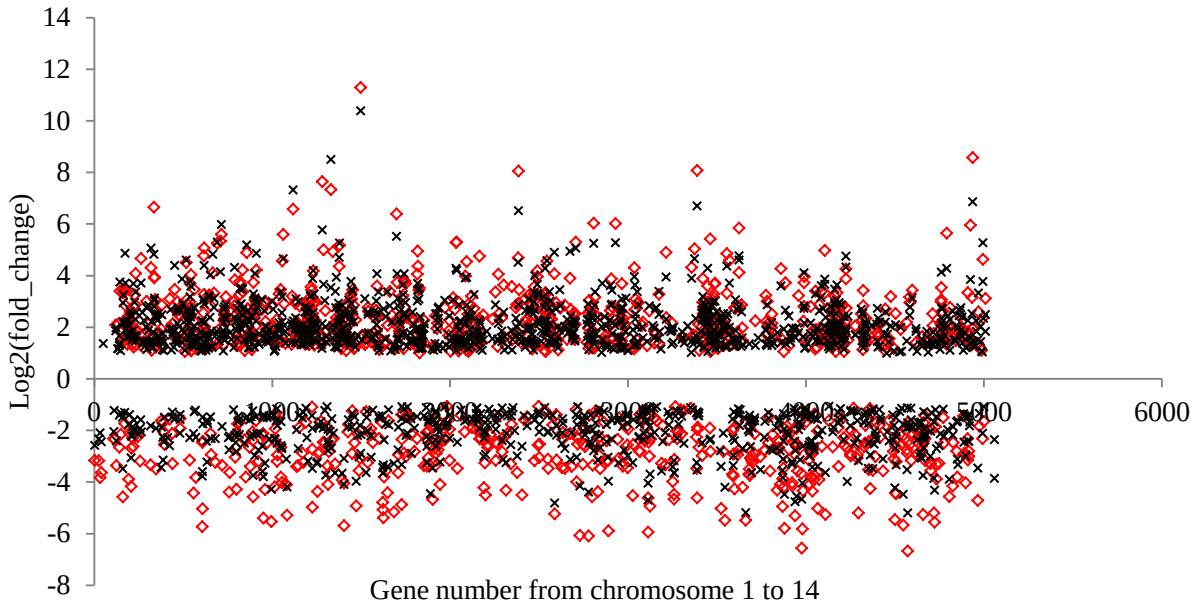

◇ Common 1212 transcripts (down 480, up 732)during gametocytes to ookinete transition in pclag::rab11a

× Common 1212 transcripts (down 480 and up 732) during gametocyte to ookinete transition in WT-GFP

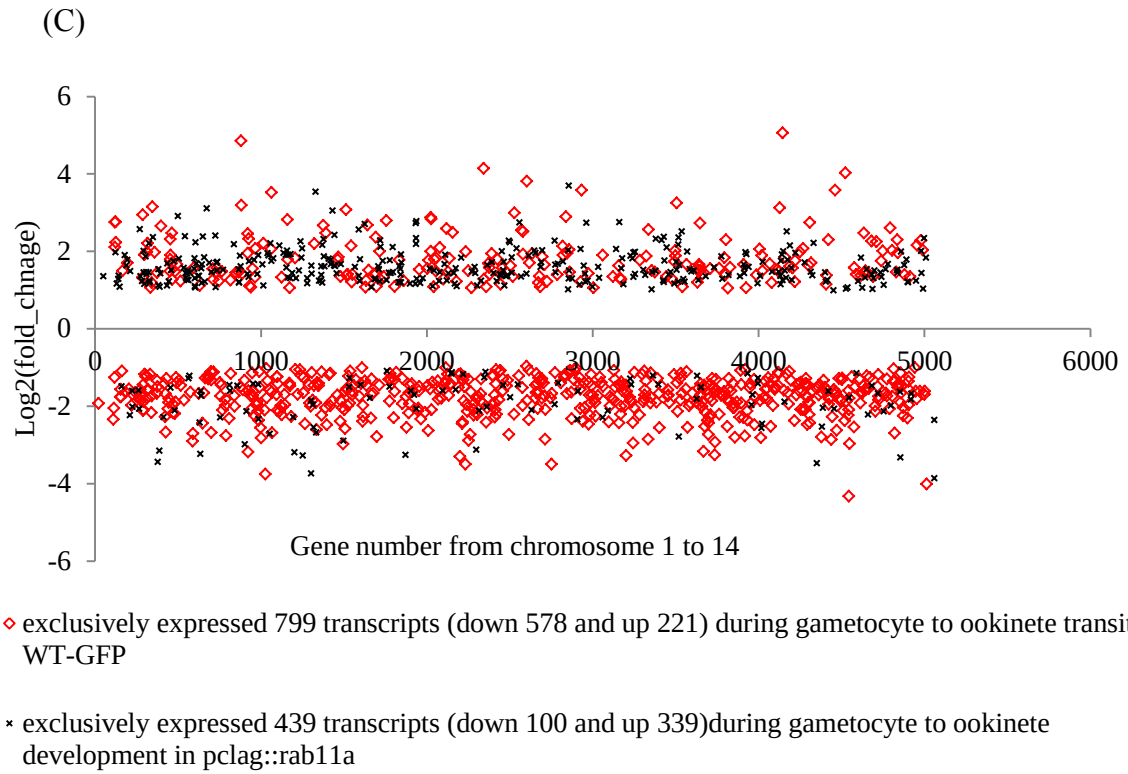

Figure 3.8.4 Trend of significantly regulated transcripts during gametocytes to ookinete transition in WT-GFP and *$_p$clag::rab11a* parasites.

(A) Venn diagram showing overlap of more and less abundant transcript during gametocyte to ookinete transition in WT-GFP and *$_p$clag::rab11a* parasites. (B) Scatter plot showing fold changes of common 1212 transcripts during gametocytes to ookinete transition in WT-GFP and *$_p$clag::rab11a* parasites. (C) Scatter plot showing fold changes of 799 exclusively significantly regulated transcripts during gametocytes to ookinete development in WT-GFP parasites and 439 exclusively significantly regulated transcripts during gametocytes to ookinete development in *$_p$clag::rab11a* parasites.

3.9 Determining the cut of FPKM in RNA-Seq is difficult.

Next, we looked at some of the transcripts and their fold changes during gametocytes to ookinete transition in WT-GFP as well as *$_p$clag::rab11a* parasites. These transcripts were selected according to their biological role in the development of WT ookinetes such as structural and developmental markers of ookinete development including surface markers, IMC components/glideosome associated proteins and Rabs where already published data is available. Some of these selected transcripts also include the genes where time-course of transcription and translation is already published. The structural and developmental markers analysed in this study, through western or immunofluorescence microscopy (see section 3.10), in *$_p$clag::rab11a* parasites (and compared with WT-GFP parasites) were also included in the list of selected transcripts and apparently 45 transcripts were selected (see Appendix A- Table 2).

Out of total selected 45 transcripts of *P. berghei*, transcripts of 43 genes were detected in gametocyte stages and 44 were detected at ookinete stage (Appendix A- Table 2). Out of these 45 selected transcripts, eight transcripts show significant deregulation at *$_p$clag::rab11a* gametocytes (as compared to WT-GFP gametocyte transcriptome) and only one transcript is significantly affected at *$_p$clag::rab11a* ookinetes (as compared to WT-GFP ookinete transcriptome). No deregulation was found for surface markers P25 and P28 at *$_p$clag::rab11a* gametocytes and ookinetes stage. Therefore, we looked at the FPKM values of 8 (out of 45) deregulated transcripts in *$_p$clag::rab11a* gametocytes (Table 3.9.1). Table 3.9.1 shows that the FPKM values of IMC1a, Conserved Plasmodium protein -unknown function, CDPK3 and CTRP are very low in WT-GFP gametocytes, also CDPK3 is expressed (as protein) 16hpa (Li, Baker et al. 2000, Ishino, Orito et al. 2006) and CTRP is expressed (as protein) 10hpa of gametocytes (Dessens, Beetsma et al. 1999) and therefore not considered for further analysis.

Out of the remaining four transcripts, low abundance of Rab11A transcripts was expected as promoter swap strategy was designed to knockdown Rab11A post-activation of gametocytes. Rest of the three transcripts - MTIP, GAPM3 and Rab11B have a very high to considerable amount of difference in the FPKM values in *$_p$clag::rab11a* gametocytes as compared to WT-GFP gametocytes. However, we did not detect a significant amount of down-regulation of MTIP and Rab11B at protein level (see figure 3.10.1 E and figure 3.3.4 D, No western was performed for GAPM3). Therefore, it is assumed that despite of a very high down-regulation of mRNAs, no significant expression defect is observed at protein level (e.g. MTIP and

Rab11B). In addition, MTIP and Rab11B mRNAs are DOZI/CITH stored (Table 3.9.1)(Guerreiro, Deligianni et al. 2014). Therefore, it further supports the notion that lack of Rab11A mRNAs cause partial deregulation of some of the DOZI/CITH stored transcripts.

Despite of arbitrarily setting the cut off FPKM to 10 to determine the number of 'significantly expressed transcripts' and to minimize the number of scarce transcripts in all the samples studied along with setting up the cut off FPKM to 10 and with significant fold change values (where significance is shown by p-values) to establish the numbers of 'significantly deregulated transcripts' in *$_p$clag::rab11a* and WT-GFP drug treated parasite samples, still the noise of some of low expressing transcripts were noticed in the list of 'significantly deregulated transcripts' as well as 'significantly expressed transcripts' e.g. occurrence of CTRP, CDPK3 and IMC1a in the list of 368 'significantly deregulated transcripts' in *$_p$clag::rab11a* gametocytes and occurrence of same transcripts in the list of 3276 'significantly expressed transcripts' of WT-GFP gametocytes (when cut off FPKM ≥10 was used).

CTRP mRNAs are low expressing and still present in gametocytes while CTRP (protein) is expressed only 10hpa (Dessens, Beetsma et al. 1999). Despite of poor mRNA expression of IMC1a and CDPK3 in gametocytes and even in asexual stages, IMC1a and CDPK3 proteins are expressed only at ookinete-sporozoite stage and 16hpa respectively (Li, Baker et al. 2000, Ishino, Orito et al. 2006). Therefore, to minimize the occurrence of such poorly expressed transcripts (in gametocytes and ookinete stage), which also show significant fold change (shown by p-values), however actually do not get translated in respective stages and hence need to be ignored from the list of 'significantly deregulated transcripts' as well as 'significantly expressed transcripts'.

For this reason, increasing the FPKM cut off from 10 to higher values would minimize the low expressing noise from 'significantly expressed transcripts' in WT-GFP parasites e.g. At cut off FPKM ≥10, WT-GFP gametocytes show significant expression of 3276 transcripts, however, at the cut off FPKM of ≥50 WT-GFP gametocytes show significant expression of top 1634 transcripts (figure 3.9.2). Increasing the cut off FPKM to higher values will also reduce the number of 'significantly deregulated transcripts' in *$_p$clag::rab11a* and WT-GFP drug treated parasites compared to respective controls e.g. At cut off FPKM ≥10, *$_p$clag::rab11a* gametocytes show significant deregulation of 368 transcripts (as compared to the transcriptome of WT-GFP gametocytes), however, increasing the FPKM cut off to ≥50 the

list of 368 deregulated *$_p$clag::rab11a* gametocytes reduces to top 235 deregulated transcripts (figure 3.9.3).

Therefore, cut off FPKM value is further increased from 10 to 50 and 100; and accordingly the number of 'significantly expressed transcripts' in WT-GFP, WT-GFP drug treated and *$_p$clag::rab11a* parasites were recalculated (figure 3.9.2). Additionally, the number of 'significantly deregulated transcripts' in WT-GFP drug treated and *$_p$clag::rab11a* parasites were also reanalysed (figure 3.9.3).

In summary, in RNA-Seq study setting up the lower limit to determine whether a particular gene is expressed at given stage is difficult and therefore considering only top 10% to 25% of deregulated transcripts would give more realistic results. Although, the cut off FPKM of 10 was used in this study, the emphasis was given to top 25% deregulated transcripts.

Gene ID	Description	Log2(fold change) at gametocytes stage (WT-GFP v *$_p$clag::rab11a*)	FPKM in WT-GFP gametocytes	FPKM in *$_p$clag::rab11a* gametocytes	DOZI associated	CITH associated
PBANKA_041290	circumsporozoite- and TRAP-related protein (CTRP)	-1.26508	14.913	6.20493	YES	YES
PBANKA_136440	conserved Plasmodium protein, unknown function	-1.53257	50.7001	17.5251	YES	NO
PBANKA_103540	glideosome associated protein with multiple membrane spans 3, putative (GAPM3)	-1.61416	4590.64	1499.56	YES	YES
PBANKA_040260	inner membrane complex protein 1a (IMC1a)	-1.55766	43.7192	14.8515	NO	NO
PBANKA_145950	myosin light chain 1, putative,myosin A tail domain interacting protein MTIP, putative (MTIP)	-1.70637	7418.04	2273.11	YES	YES
PBANKA_141890	Rab GTPase 11a (Rab11a)	-3.40816	2592.69	244.226	YES	YES
PBANKA_135410	Rab GTPase 11b	-1.26062	577.033	240.834	NO	YES
PBANKA_040820	calcium-dependent protein kinse 3 (CDPK3)	-1.02298	39.3438	19.361	YES	NO

Table 3.9.1 Eight deregulated transcripts in *$_p$clag::rab11a* gametocytes as compared to WT-GFP gametocytes.

All of the eight transcripts were deregulated in *$_p$clag::rab11a* gametocytes and only one (CDPK3) was deregulated in *$_p$clag::rab11a* ookinete.

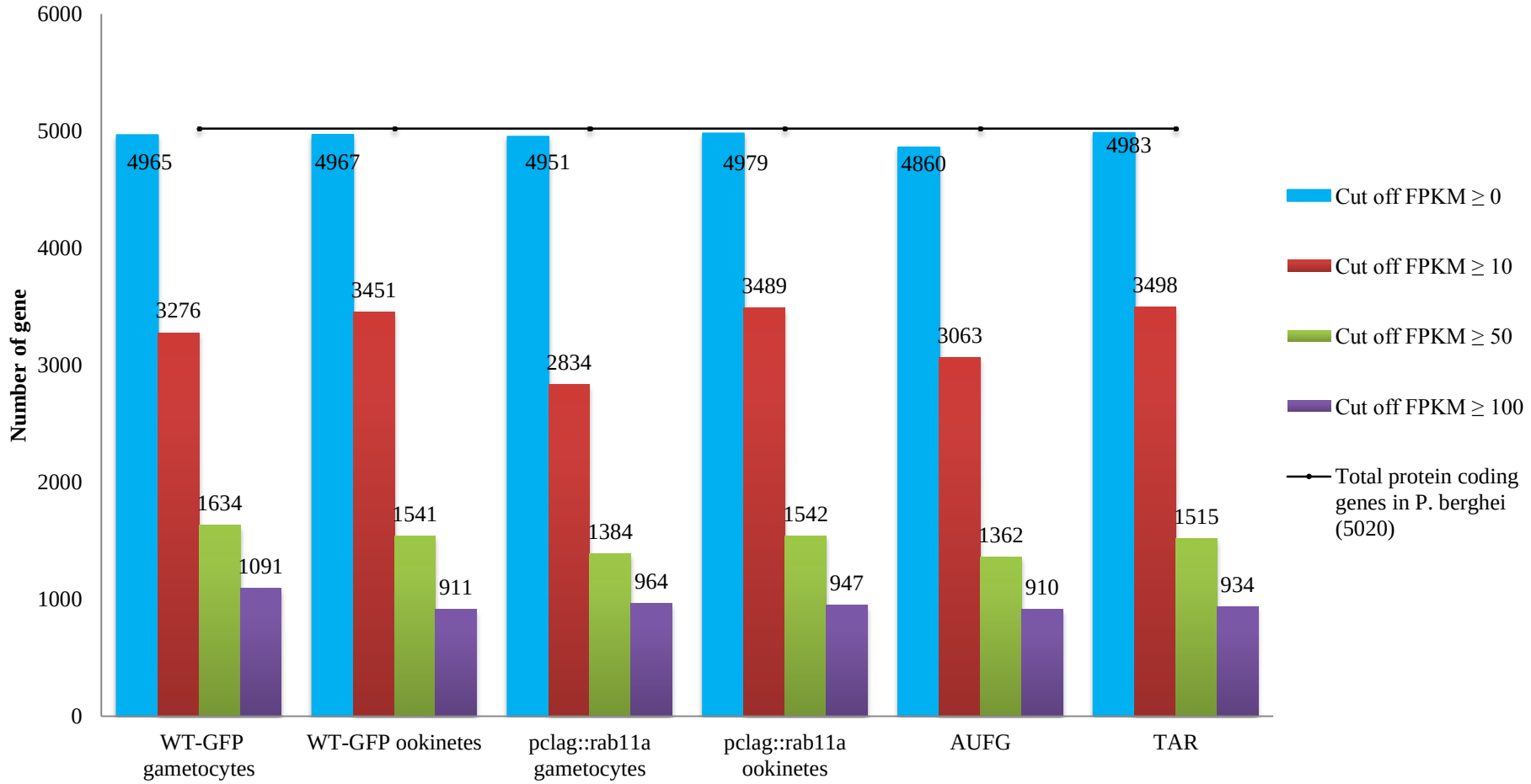

Table 3.9.2 Number of significantly expressed transcripts in given samples with various FPKM cut offs.

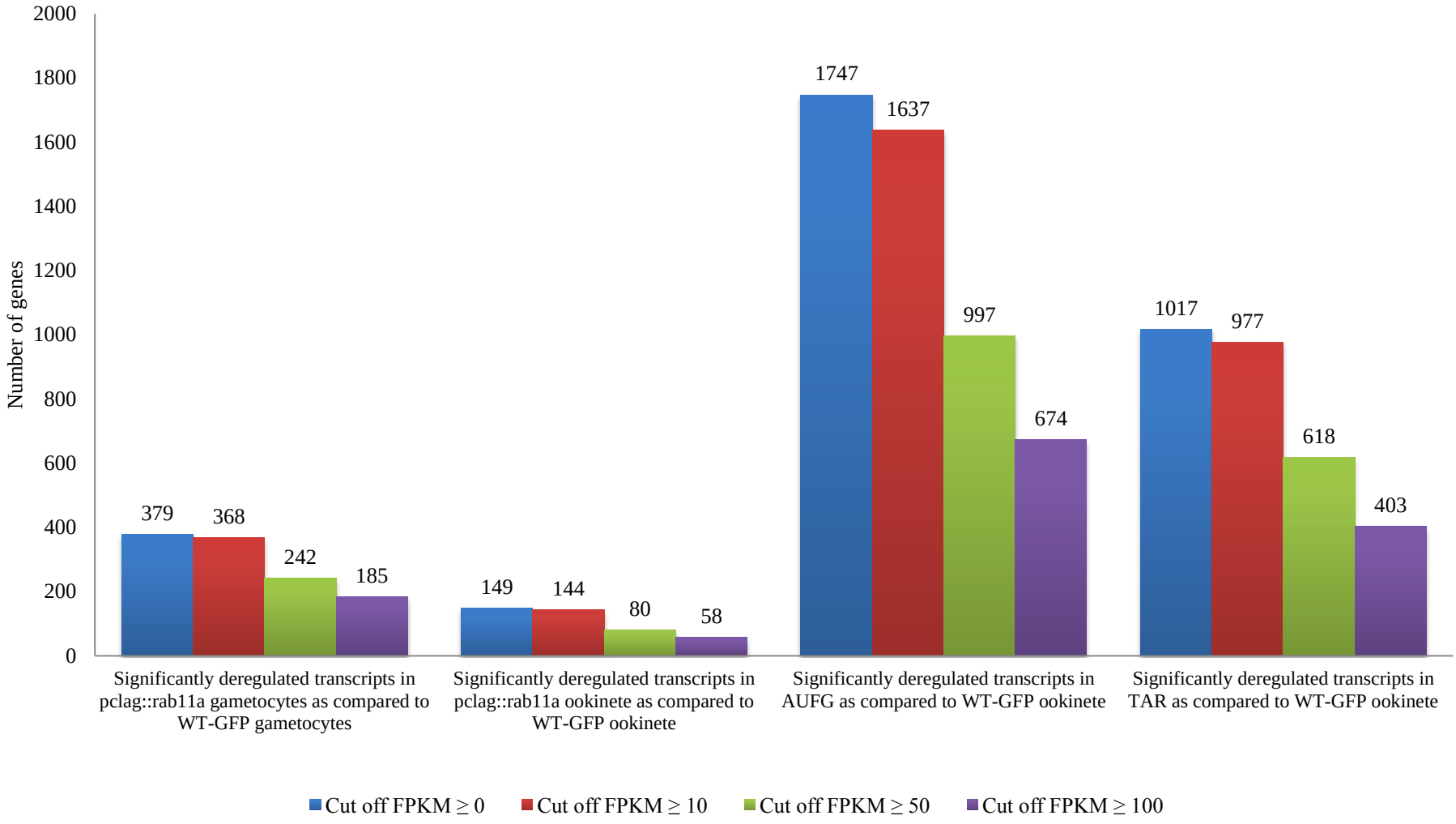

Table 3.9.3 Number of significantly deregulated transcripts with various FPKM cut offs.

3.10 The expression and distribution of most developmental marker proteins remain unaffected in *$_p$clag::rab11a* spherical ookinetes

Ultrastructural analysis and GAP45 immunofluorescence microscopy had suggested no apparent defects in IMC and apical complex assembly in 6 to 8h *$_p$clag::rab11a* zygotes in absence of Rab11A. RNA-Seq of *$_p$clag::rab11a* gametocytes suggests significant deregulation of 11.23% (368 out of 3276) of total gametocyte stage transcriptome and nearly similar percentage (11.05% i.e. 81 out of 733) of DOZI/CITH stored transcripts, and RNA-Seq of *$_p$clag::rab11a* ookinete suggests deregulation of 4.17% (144 out of 3451) of total ookinete stage transcripts. These deregulated transcripts (in *$_p$clag::rab11a* gametocytes and ookinete stage) are majorly associated with translation, transcription, transport, protein modification and processing, biosynthetic processes and metabolic processes. Therefore, to investigate the expression and localization defects, we used western and immunofluorescence to study 12 and 16 of the structural and developmental markers respectively where antibodies were available.

3.10.1 Western analysis shows delayed/reduced expression of some of the developmental and structural markers

Expression of two glideosome associated proteins: GAP45 and GAP50, motility protein MyoA suggest possible marginal reduction of protein level at 6 to 8h *$_p$clag::rab11a* zygotes, however, no significant change was observed at *$_p$clag::rab11a* ookinetes (figure 3.10.1 A, B and D). Similarly, the ookinete surface marker P28 expression seems to be delayed/ reduced at 6 and 8h in *$_p$clag::rab11a* zygotes but not at 24hpa (figure 3.10.1 C). Expression of another motility marker –MTIP shows single band during 2 to 8hpa and two bands at 24hpa in WT-GFP. In *$_p$clag::rab11a,* MTIP expression was similar to WT-GFP during 2 to 8hpa, however, only one band was identified at 24hpa (figure 3.10.1 E). Expression of the RNA helicase DOZI and another RNA binding protein CITH, responsible for storage of mRNAs in female gametocytes (Mair, Braks et al. 2006, Mair, Lasonder et al. 2010) seemed to be normal in *$_p$clag::rab11a* zygotes and ookinetes as compared to WT-GFP zygotes and ookinetes respectively (figure 3.10.1 F, G). On the other hand, whereas the protein phosphatase

containing kelch-like domains (PPKL) which is essential for ookinete development, motility and mosquito invasion (Guttery, Poulin et al. 2012, Philip, Vaikkinen et al. 2012), appeared to show normal expression levels analysed by western blot during *$_p$clag::rab11a* zygote to ookinete development (figure 3.10.1 H), ookinete secretory proteins chitinase and CTRP appeared slightly down-regulated in *$_p$clag::rab11a* ookinetes (figure 3.10.1 I and J).

3.10.2 Immunofluorescence microscopy suggest normal localization of some of the developmental and structural markers

Localization of GAP45 is dynamic from 4hpa till 24hpa and appeared to be normal in *$_p$clag::rab11a* zygotes and ookinetes (figure 3.5.1). Despite of detection of a clear band in GAP50 western (figure 3.10.1 B), anti-GAP50 antibody does not show the ookinete peripheral localization of GAP50 (figure 3.10.2 A) as seen by protein tagging studies by K. Hughes -Waters group (unpublished data) and our GAP50::mCherry results (Chapter 4- figure 4.4.2 I) (figure 3.10.2 A). Expression of motility marker- MyoA was detected at 8hpa in WT-GFP but not in *$_p$clag::rab11a* 8h zygotes supporting the reduced/delayed expression levels seen by Western analysis yet MyoA appears to be localized at the apical complex as well as towards the periphery of WT-GFP ookinete and similar localization was detected in *$_p$clag::rab11a* ookinetes (figure 3.10.1 D and figure 3.10.2 B). Despite of absence of upper MTIP band at *$_p$clag::rab11a* ookinetes (24hpa) as seen in WT-GFP ookinetes, we could detect normal localization of MTIP by immunofluorescence in *$_p$clag::rab11a* ookinetes (figure 3.10.2 C). Immunofluorescence shows weak polarization of Chitinase possibly towards apical end and peripheral-cum-cytoplasmic localization of CTRP, therefore, CTRP localization mostly appeared to be variable in *$_p$clag::rab11a* ookinetes as compared to WT-GFP ookinetes (figure 3.10.2 D, E). Localization of RNA helicase DOZI (figure 3.10.2 F) and other protein involved in storage of mRNAs in female gametocytes – CITH (figure 3.10.2 G), IMC markers: IMC1a, IMC1b and IMC1h (figure 3.10.2 H, I, J), cytoskeletal components actin-I (figure 3.10.2 K) and α-tubulin (component of microtubules) (figure 3.10.2 L, M, N) and MTOC marker SPBP seem typical (figure 3.10.2 L). However, as opposed to a punctate apical localisation of PPKL (Philip, Vaikkinen et al. 2012), the *$_p$clag::rab11a* ookinetes do not contain a punctate spot of PPKL but just show a diffuse cytoplasmic localisation of the protein (figure 3.10.2 M, N).

3.10.3 Expression and distribution of structural and developmental markers is variable in AUFG

We also studied the expression and localization of ookinete development and structural markers in activated-unfertilized female gamete (AUFG) 24hpa. Expression of DOZI, CITH, PPKL, actinI and α-tubulin was normal as they are expected to be present in un-activated female gametocytes (figure 3.10.1 and figure 3.10.2). Surprisingly, we could detect the normal expression of translationally stored small GTPase Rab11A, motility protein MTIP and reduced expression of glideosome protein GAP50, small GTPase Rab11B at 6 and 24hpa and ookinete surface marker P28 at 24hpa in AUFG by Western which we assumed to be expressed only in fertilized female gametes (i.e. zygotes) and ookinetes, however, we could not detect expression of other translationally stored proteins: motility protein MyoA and glideosome protein GAP45 and late zygote development markers: chitinase and CTRP in AUFG by western. Immunofluorescence studies show the presence of Rab11A, Rab11B, MTIP, GAP50, PPKL, DOZI, CITH, actinI and α-tubulin in AUFG 24hpa, but most of them are not localized to their appropriate cell organelles as compared to WT-GFP ookinetes (figure 3.10.1 and figure 3.10.2). This implies that some of the translationally stored mRNAs are activated to undergo translation in absence of fertilization and remains mis-localized. Sometimes, the nucleus of the AUFG itself looks disintegrated after 24hpa (figure 3.10.2 and figure 3.3.4 C, E).

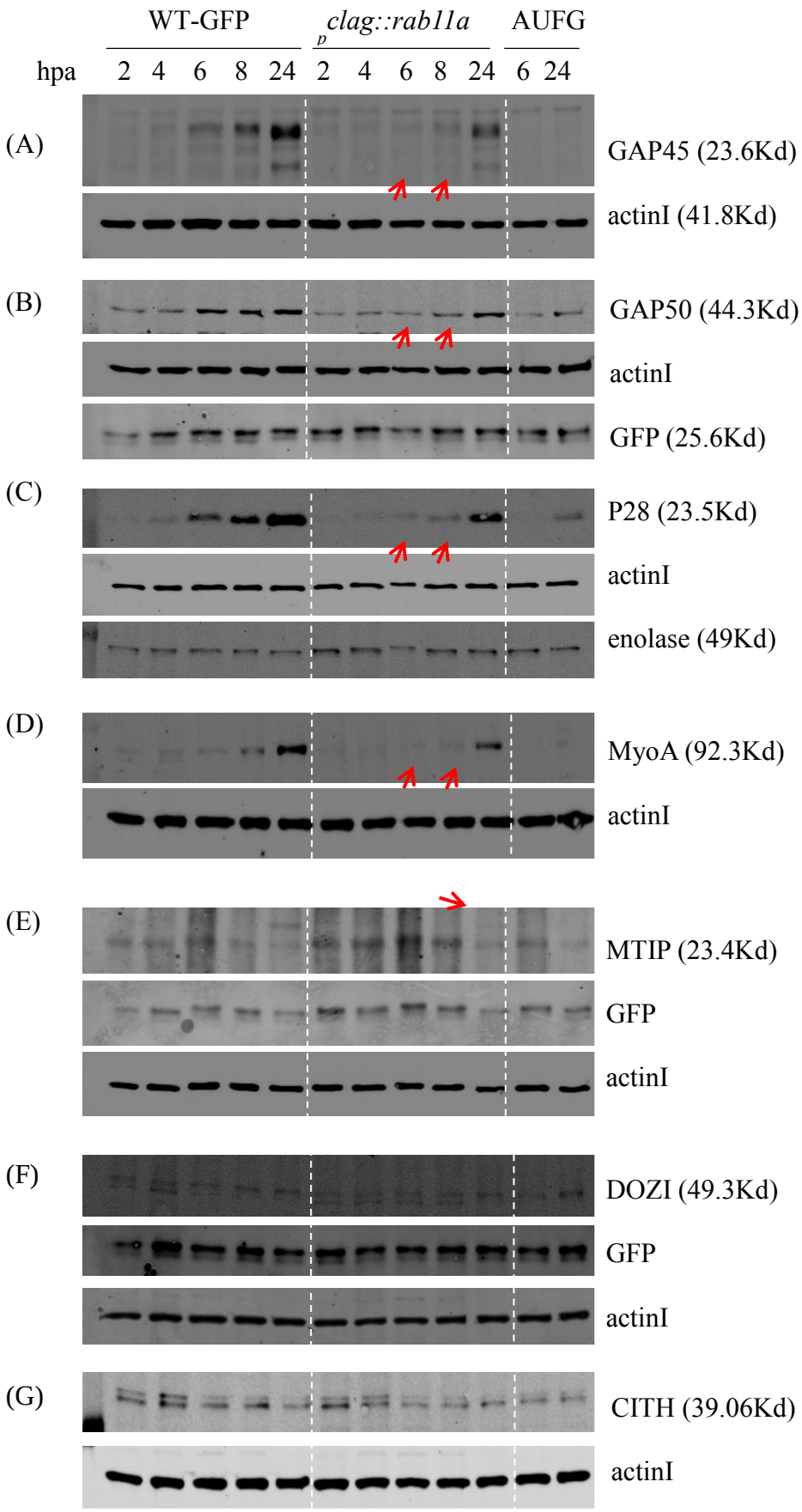
WT-GFP
clag::rab11a
p
AUFG
hpa
2 4 6 8 24 2 4 6 8 24 6 24
(A)
GAP45 (23.6Kd)
actinI (41.8Kd)
(B)
GAP50 (44.3Kd)
actinI
GFP (25.6Kd)
(C)
P28 (23.5Kd)
actinI
enolase (49Kd)
(D)
MyoA (92.3Kd)
actinI
(E)
MTIP (23.4Kd)
GFP
actinI
(F)
DOZI (49.3Kd)
GFP
actinI
(G)
CITH (39.06Kd)
actinI

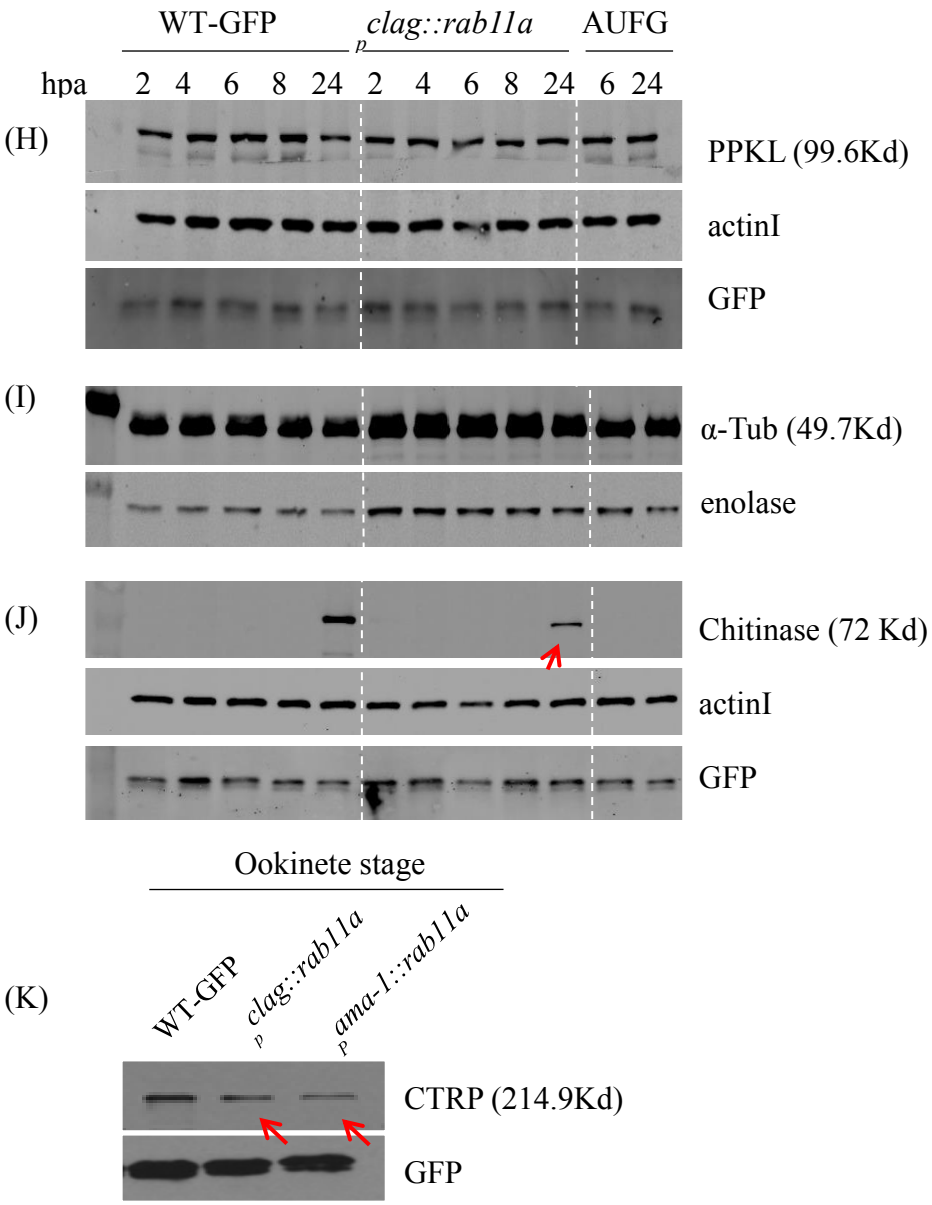

Figure 3.10.1 Western analysis of ookinete development and structural markers.

Western blots for WT-GFP and *pclag::rab11a* gametocytes at 2,4,6,8 and 24hpa, and for AUFG at 6 and 24hpa using (A) anti-GAP45, (B) anti-GAP50, (C) anti-P28, (D) anti-MyoA, (E) anti-MTIP, (F) anti-DOZI, (G) anti-CITH, (H) anti-PPKL (I) anti-Tubulin (J) anti-chitinase and (K) anti-CTRP antibodies. Blots were stripped and reproved with either anti-enolase, anti-actinI and/or anti-GFP antibodies as loading controls. All the blots were scanned on Odyssey® Sa infrared Imaging System (LI-COR biosciences) except for anti-CTRP antibody. Anti-CTRP antibody blot was treated with ECL and a film was developed (conventional method) (for details see Chapter 2- section 2.1.2 n). Red arrows show down-regulation or delay in respective bands.

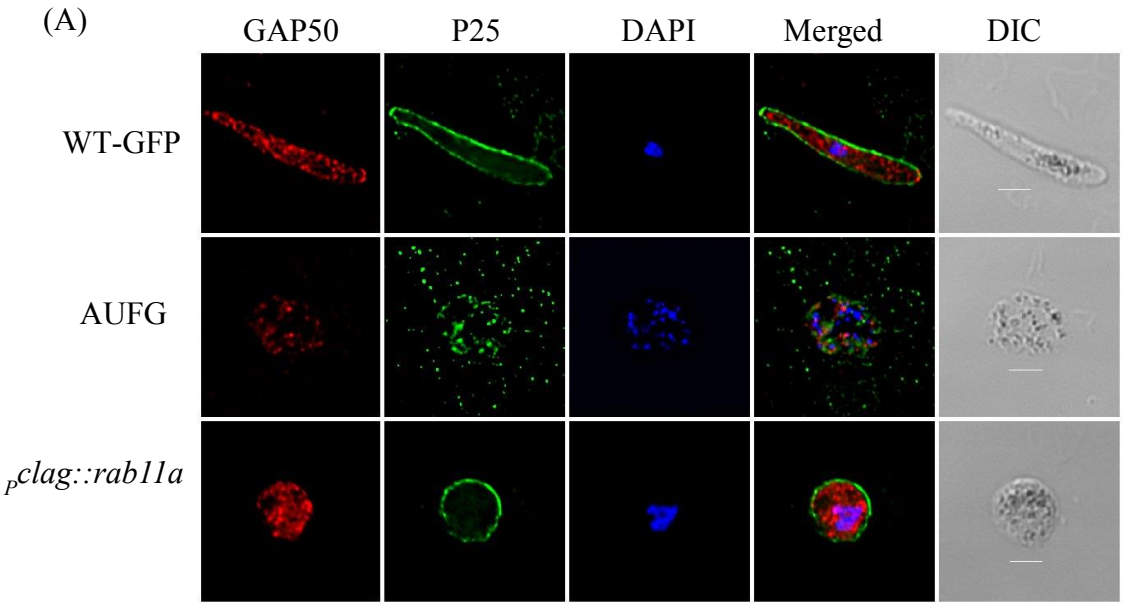
(A)
GAP50
P25
DAPI
Merged
DIC
WT-GFP
AUFG
PclagrabA1a

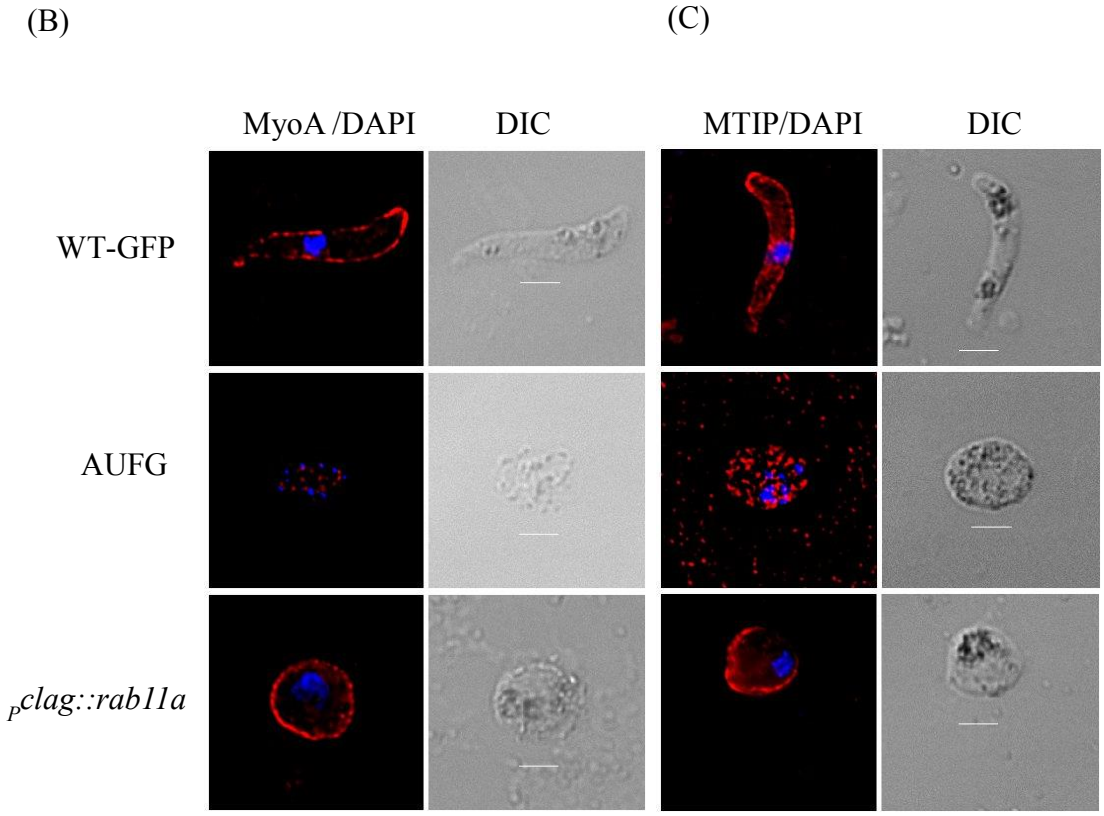
(B)
(C)
MyoA /DAPI
DIC
MTIP/DAPI
DIC
WT-GFP
AUFG
PclagrabA1a

(D)

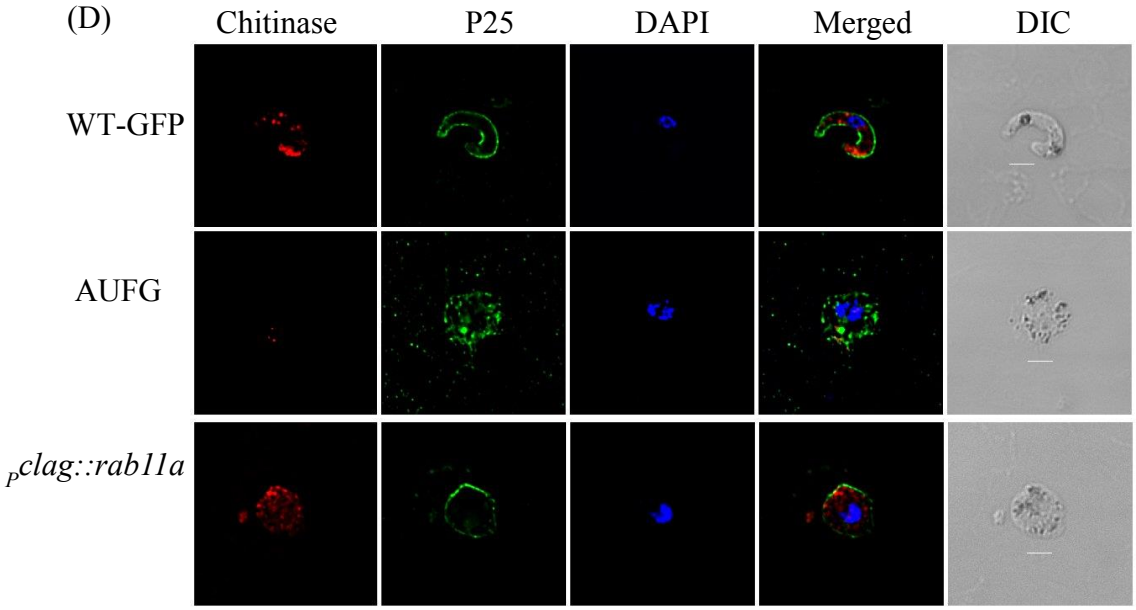
Chitinase
P25
DAPI
Merged
DIC
WT-GFP
AUFG
pclag::rab11a

(E)

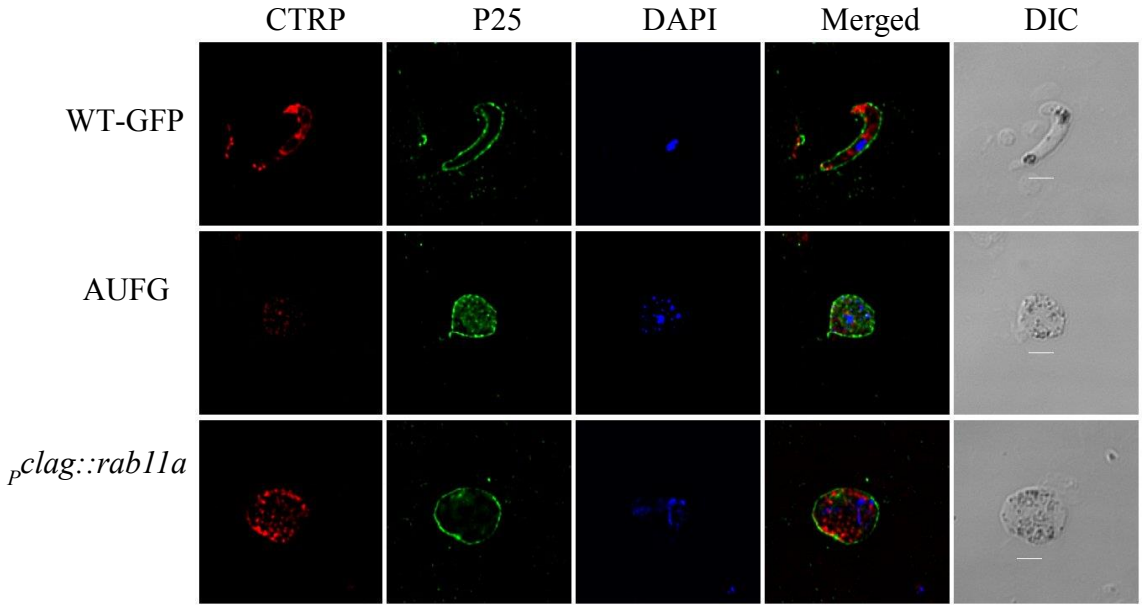
CTRP
P25
DAPI
Merged
DIC
WT-GFP
AUFG
pclag::rab11a

(F)

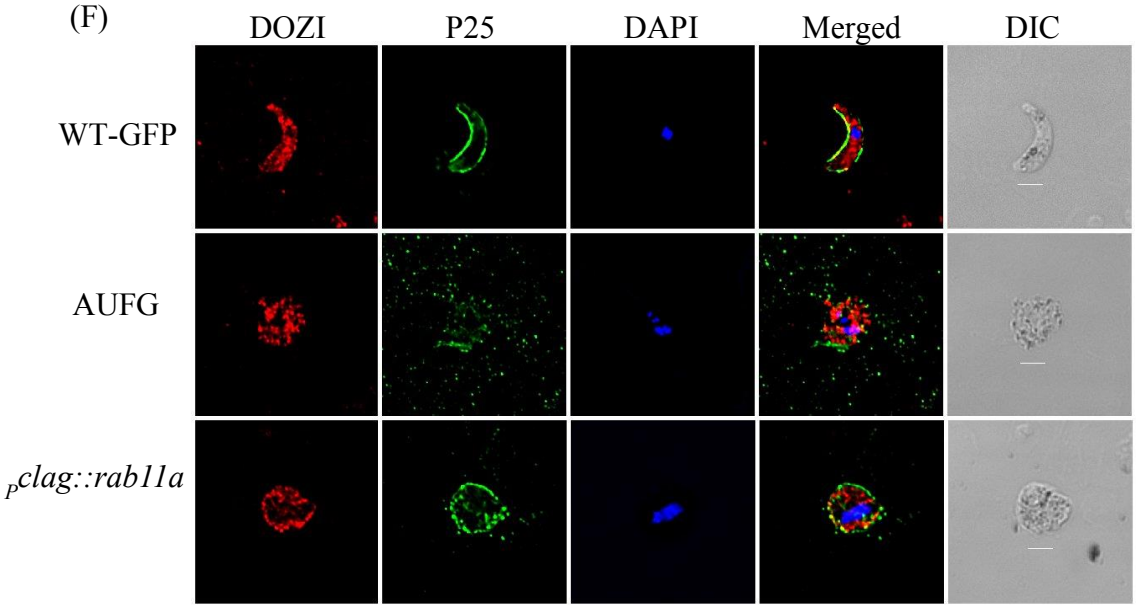
DOZI
P25
DAPI
Merged
DIC
WT-GFP
AUFG
$_{P}$clag::rab11a

(G)

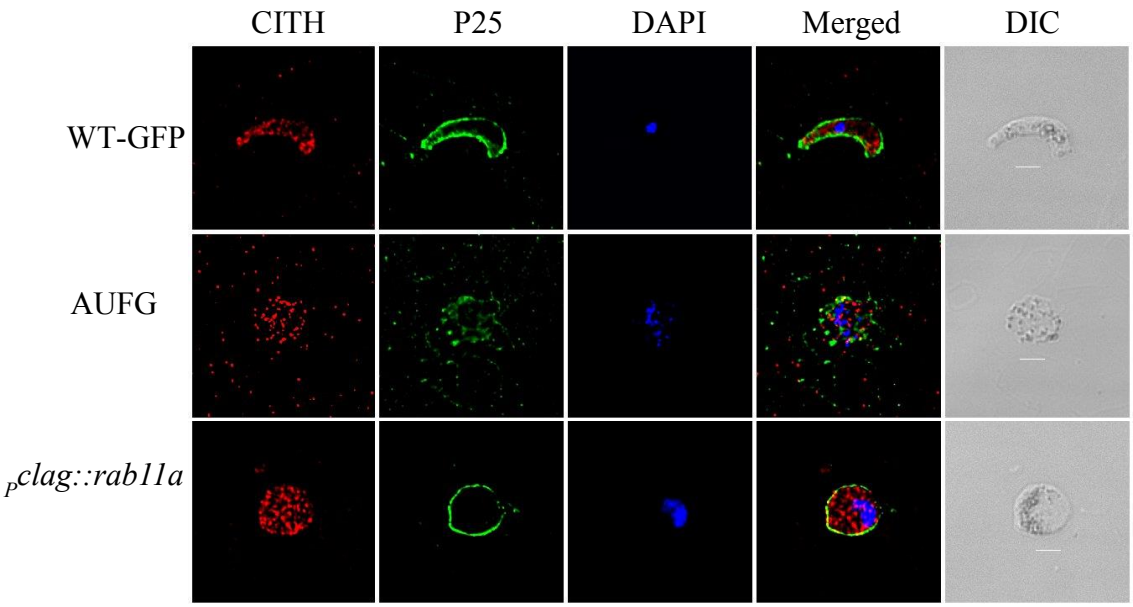
CITH
P25
DAPI
Merged
DIC
WT-GFP
AUFG
$_{P}$clag::rab11a

(H)

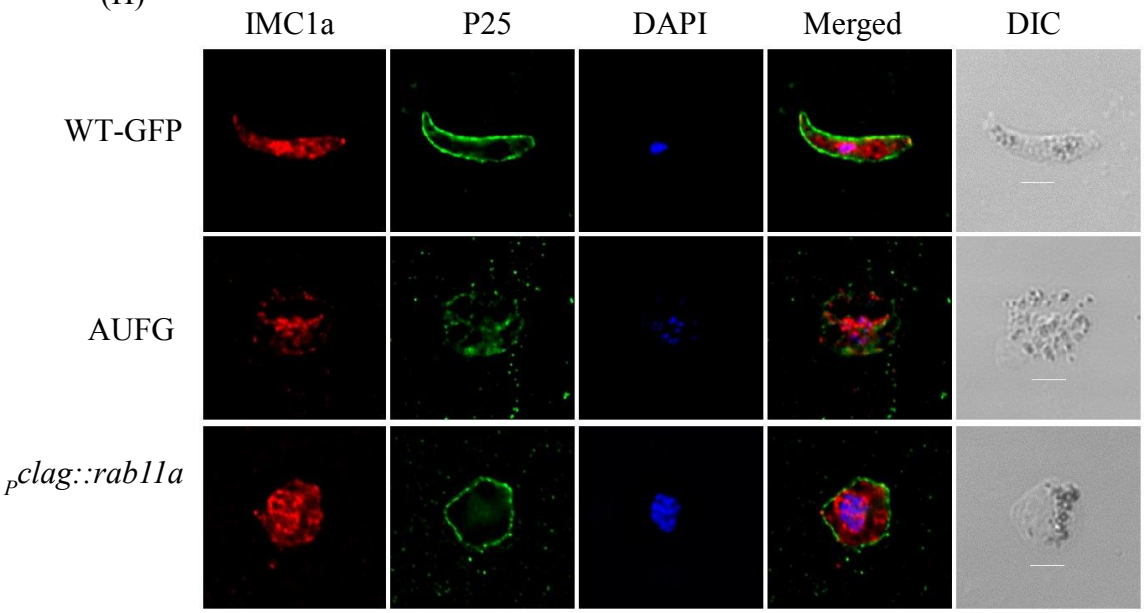
IMC1a
P25
DAPI
Merged
DIC
WT-GFP
AUFG
pclag::rab11a

(I)

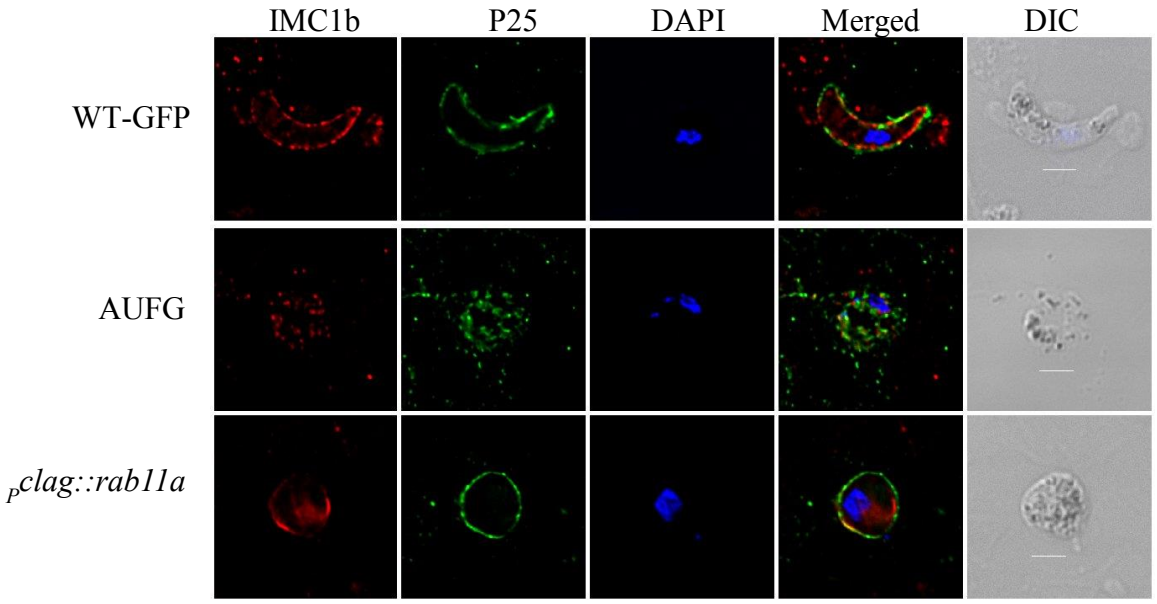
IMC1b
P25
DAPI
Merged
DIC
WT-GFP
AUFG
pclag::rab11a

(J)

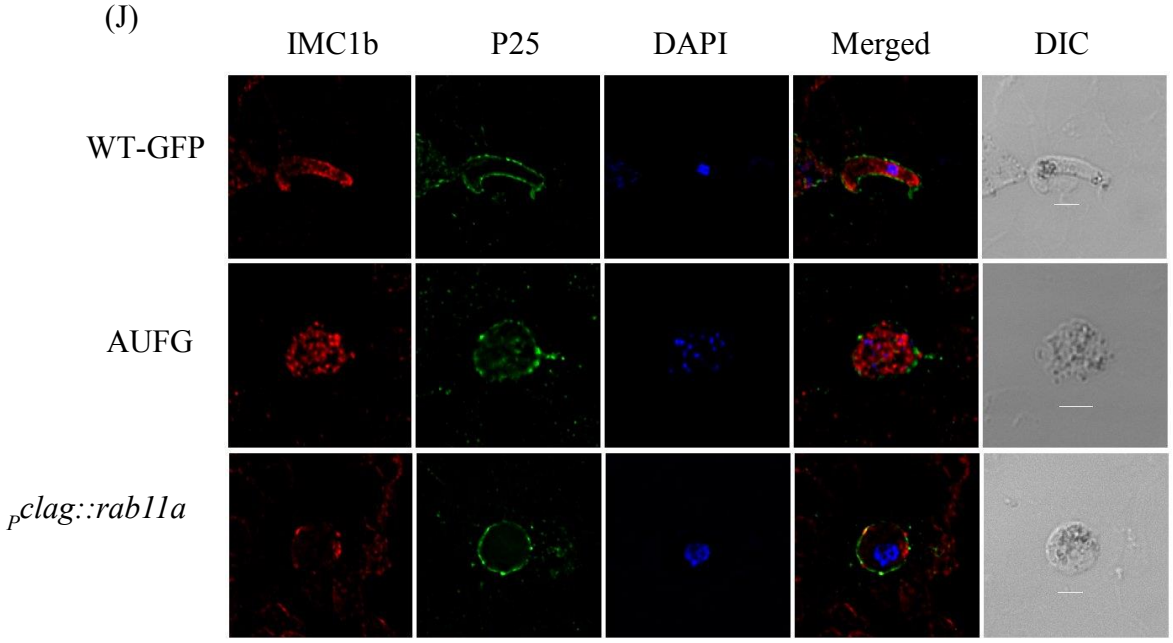
IMC1b
P25
DAPI
Merged
DIC
WT-GFP
AUFG
Pclag::rab11a

(K)

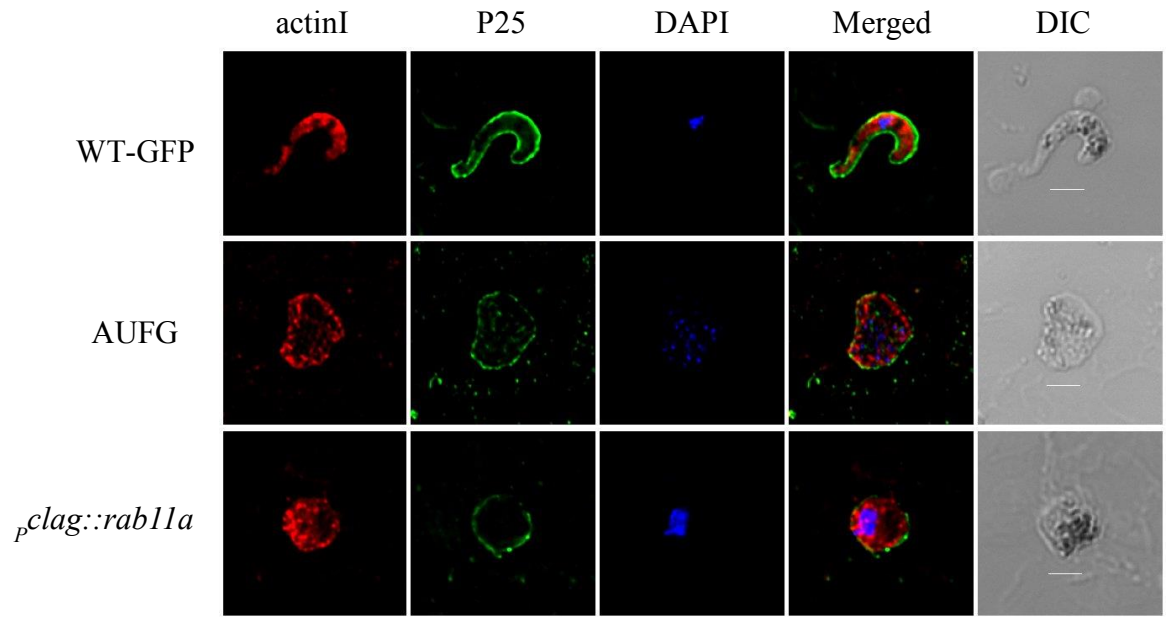
actinI
P25
DAPI
Merged
DIC
WT-GFP
AUFG
Pclag::rab11a

(L)

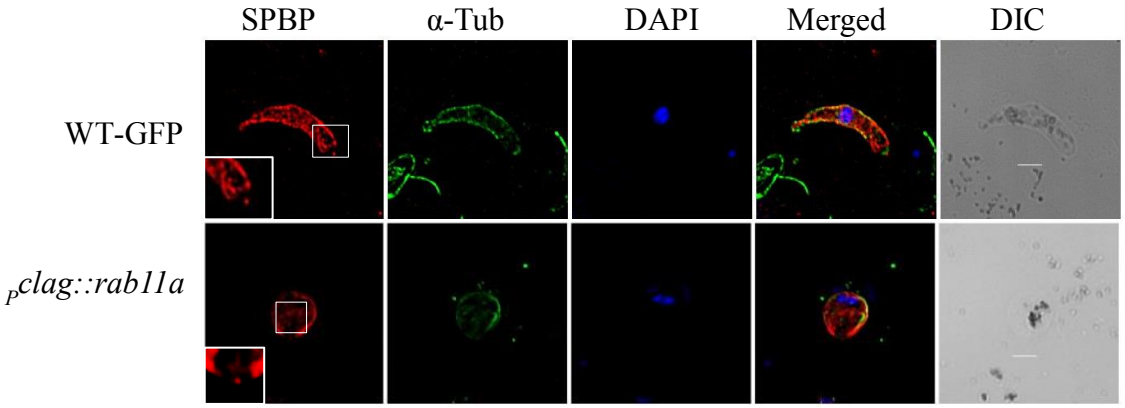
SPBP
α-Tub
DAPI
Merged
DIC
WT-GFP
Pclag::rab11a

(M)

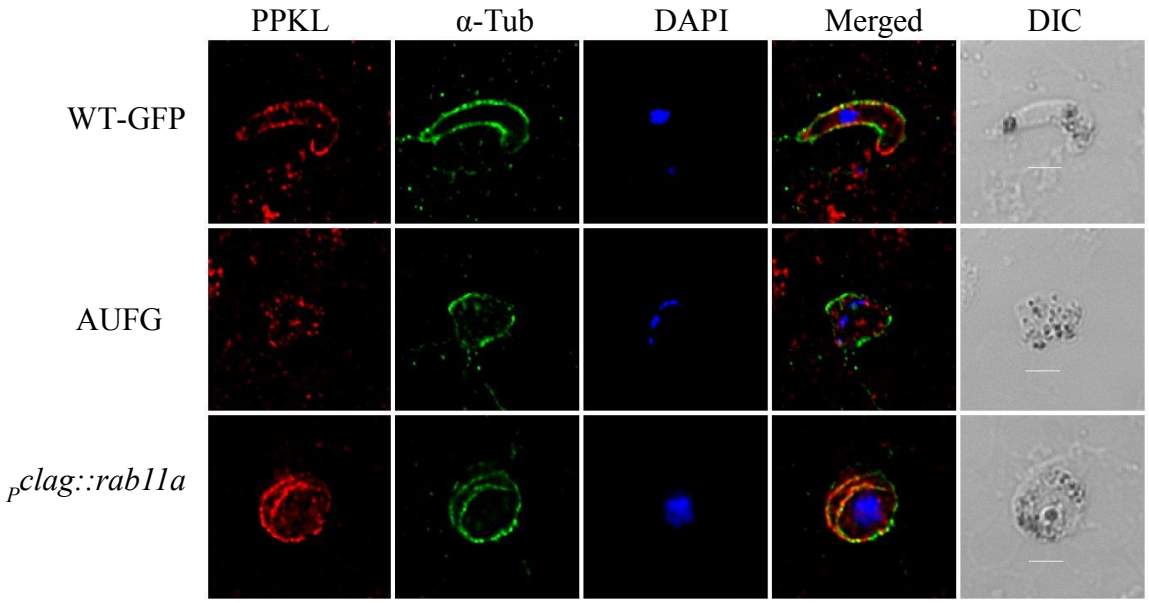
PPKL
α-Tub
DAPI
Merged
DIC
WT-GFP
AUFG
Pclag::rab11a

(N)

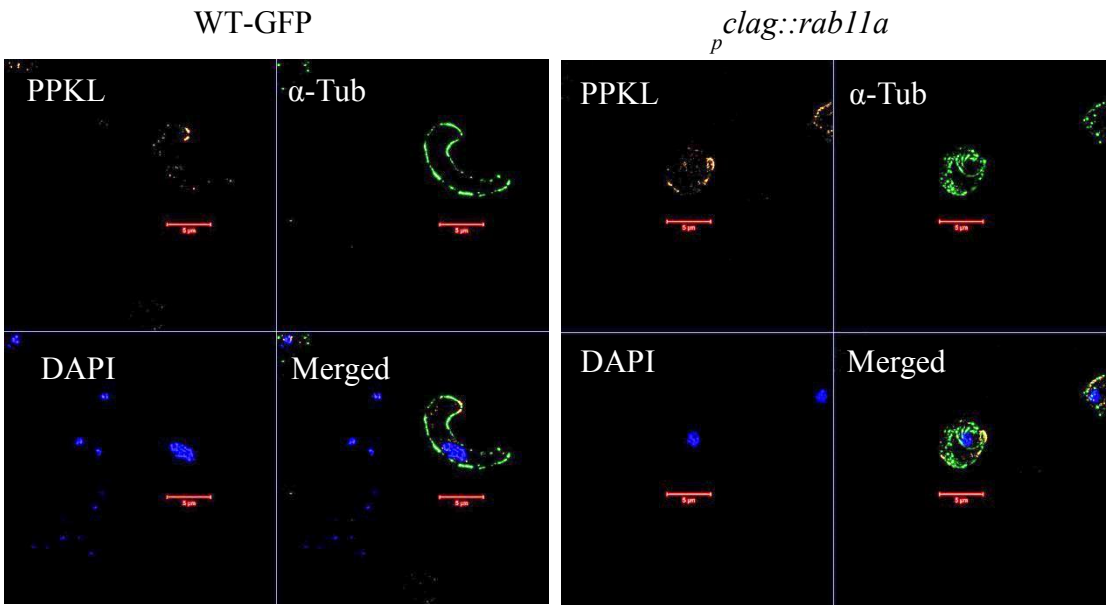

Figure 3.10.2 Immunofluorescence microscopy for ookinete development and structural markers

Fixed WT-GFP ookinetes, *$_p$clag::rab11a* spherical ookinetes and AUFG were probed with primary antibodies (A) anti-GAP50, (B) anti-MyoA, (C) anti-MTIP, (D) anti-chitinase, (E) anti-CTRP, (F) anti-DOZI, (G) anti-CITH, (H) anti-IMC1a, (I) anti-IMC1b, (J) anti-IMC1h (K) anti-actinI (L) anti-SpindlePoleBodyProtein (M) anti-PPKL antibodies dilution mixed with either FITC-tagged anti-P25 or anti-tubulin antibodies. Images shown are single slice of Deltavision deconvoluted Z stack. (N) Single slice images of Z stacks obtained from ELYRA 3D SIM microscope of fixed parasite preparation using anti-PPKL antibody mixed with α-tubulin antibody (For details see Chapter 2- section 2.1.2 l). Scale bar 5 µm.

3.11 Discussion

Previous attempts to delete PbRab11A in haploid blood stages of *P. berghei* were unsuccessful indicating its essentiality (Agop-Nersesian, Naissant et al. 2009). The abundance of Rab11A mRNA in gametocytes (Otto, Böhme et al. 2014) (RNASeq data by A. Religa, Waters group, unpublished data, figure 3.1.1 A) and its translational repression (Mair, Braks et al. 2006) suggested a role for Rab11A in ookinete development. Our results validated the expression of PbRab11A throughout the *P. berghei* lifecycle (figure 3.1.1 and 3.1.2). Western analysis suggested two bands of Rab11A in schizonts as well as in ookinetes (figure 3.1.1 C, D and 3.3.4 A, B) but the significance of the observation remains unclear. Rab11A has been previously predicted to be involved in the cytokinesis of *Plasmodium* (Agop-Nersesian, Naissant et al. 2009, McNamara, Lee et al. 2013) therefore one possibility is that Rab11A might be more active than normal and possibly undergo differential (post-translational) regulation during zoite development enabling detection of additional band in schizont and mature ookinetes (figure 3.1.1 C, D).

Rab11A localization is dynamic at different stages of lifecycle from cytoplasmic to peripheral (figure 3.1.2). In ookinetes, Rab11A mostly remains peripheral and also appears to localise to the apical complex (figure 3.1.2) like SPBP, a marker of MTOC, localization (figure 3.10.2 L) suggesting by analogy with other systems (Gnazzo and Skop 2014, Hehnly and Doxsey 2014) Rab11A and SPBP might have important functions at the apical complex and probably at MTOC, possibly transport of microtubule nucleation components, cell membrane synthesis components, cell surface markers and adhesin proteins and/or in secretion (Prekeris, Klumperman et al. 2000, Dollar, Struckhoff et al. 2002, Jing and Prekeris 2009, Lapierre, Avant et al. 2012, Takahashi, Kubo et al. 2012, Burke, Inglis et al. 2014, Chutna, Goncalves et al. 2014, Hehnly and Doxsey 2014, Welz, Wellbourne-Wood et al. 2014). However, due to the rabbit origin of both anti-Rab11A and anti-SPBP antibodies, we were unfortunately unable to perform co-localization studies. In segmented schizonts/merozoites, we detected a cytoplasmic localization of PbRab11A by immunofluorescence and not the apically punctate shown by GFP-tagged and immunofluorescence microscopy in *P. berghei* and *P. falciparum* (Agop-Nersesian, Naissant et al. 2009, McNamara, Lee et al. 2013). This might suggest that the GFP-tagged PbRab11A is mis-localised, however this appeared to have little effect on function as the parasite behaved as wild type, and the other possible explanation of the data is the difference between the imaging of live and fixed parasites.

Despite of three independent attempts of N-terminal tagging, Rab11A failed to tag with small green fluorescent protein iLOV (Chapman, Faulkner et al. 2008, Christie, Hitomi et al. 2012) and two copies of C-MYC when constructed to express under PbRab11A endogenous 5'UTR and targeted to the endogenous *rab11a* (figure 3.2.1 and 3.2.2). This clearly implied that PbRab11A endogenous 5'UTR participate in recombination. Alternatively, expression of N-terminal tagged copy of *rab11a* (with endogenous 5'UTR and 3'UTR) inserted as a transgene at a redundant location followed by deletion of endogenous *rab11a* may be useful to tag Rab11A with fluorescent protein without the concern of overexpression. In another approach, the use of a different 5'UTR with a similar expression profile to *rab11a* 5'UTR might be useful to fluorescently tag the endogenous copy of *rab11a* as shown by (McNamara, Lee et al. 2013). C-terminal tagging of Rab11A was not attempted as it would be predicted to interfere with the conserved C-terminal geranylgeranylation in a similar way discussed by (Pereira-Leal, Hume et al. 2001, Chakrabarti, Da Silva et al. 2002, Agop-Nersesian, Naissant et al. 2009).

Our inability to delete PbRab11A in haploid blood stages (Agop-Nersesian, Naissant et al. 2009) meant that it was not possible to generate a conventional gene-deletion knock out in order to examine the role of PbRab11A during asexual parasite development therefore we used a promoter swap strategy (Laurentino, Taylor et al. 2011, Siden-Kiamos, Ganter et al. 2011) in order to study PbRab11A during sexual stages. To examine the function of PbRab11A in zygote to ookinete development, we generated two independent mutant parasite lines: $_{p}$*clag:rab11a* and $_{p}$*ama-1:rab11a* (figure 3.3.1 B, C, D). CLAG and AMA-1 promoters were shown to control the expression of protein to normal level and therefore showing no obvious growth defect during blood stage and remain silent during sexual stage and therefore reducing the protein levels producing phenotype (Laurentino, Taylor et al. 2011, Siden-Kiamos, Ganter et al. 2011, Sebastian, Brochet et al. 2012). As it is not possible to delete *Pbrab11a* at haploid blood stages (Agop-Nersesian, Naissant et al. 2009), CLAG and AMA-1 promoters were used to drive the expression of Rab11A in *P. berghei* parasite to study its function during sexual stage development whilst ensuring correct asexual blood stage development. Indeed development of asexual stages, morphology and ratio of gametocytes along with gametogenesis observed by male gamete exflagellation and fertilization remain normal in $_{p}$*clag:rab11a* and $_{p}$*ama-1:rab11a* (figure 3.3.2), however, ookinete development was almost completely blocked (figure 3.3.3). Fertilized $_{p}$*clag:rab11a* female gametes remain spherical after 24hpa (figure 3.3.3B) yet appear to undergo meiosis (figure 3.3.5). Expression

and localization of PbRab11A is normal in blood stages and reduced only in *$_p$clag:rab11a* and *$_p$ama-1:rab11a* parasites as early as from 2h post-fertilization of gametocytes (figure 3.3.4 A, B) while closely related Rab11B is unaffected showing that PbRab11A is specifically depleted by the promoter swap strategy (figure 3.3.4 D).

Genetic crossing of *$_p$clag::rab11a* gametocytes with male deficient (*p48/45*$^-$) (van Dijk, Janse et al. 2001) or female deficient (*p47*$^-$) gametocytes (van Dijk, van Schaijk et al. 2010) demonstrated that expression of PbRab11A occurs from both male and female gamete alleles (figure 3.3.6).

The ability of *$_p$clag:rab11a* and *$_p$ama-1:rab11a* ookinetes to transmit through mosquito was prevented as extremely low amount of oocysts and no sporozoites were observed (figure 3.4.1) indicating major role of PbRab11A during transmission through mosquito midgut and possibly in oocyst development as Rab11A is also expressed in oocysts (figure 3.1.2). Upon feeding of *$_p$clag:rab11a* and *$_p$ama-1:rab11a* infected mosquitoes on naïve mice, *$_p$clag:rab11a* (n=3) and *$_p$ama-1:rab11a* (n=2) infections were unsuccessful indicating an absolute role of Rab11A in transmission (figure 3.4.1).

Like *$_p$clag::rab11a* and *$_p$ama-1::rab11a* spherical ookinetes, similarly spherical (and developmentally arrested) 20h zygotes were obtained when GAP45 was specifically down regulated post-fertilization in *P. berghei* using a similar promoter swap strategy. The spherical cell was at least in part due to the IMC floating inside the cytoplasm of the *gap45* promoter swap zygotes suggesting that GAP45 is involved in attaching the IMC to the cell membrane and is also essential for *P. berghei* retort formation (Sebastian, Brochet et al. 2012). GAP45 is believed to be delivered to the IMC by Rab11A-mediated vesicles (Agop-Nersesian, Naissant et al. 2009). Localization studies of GAP45 suggest the selection of a focal point in *$_p$clag:rab11a* 4h zygotes which then grows along the membrane of *$_p$clag:rab11a* 6h zygotes lacking the WT retort outgrowth and lays down the IMC across the entire cytoplasmic side of the plasma membrane of the spherical *$_p$clag:rab11a* ookinete (24hpa) indicating the assembly of IMC (figure 3.5.1). Our data however, suggest that delivery of GAP45 does not depend on Rab11A mediated vesicles. SEM analysis also suggest appearance of a small, cone-like outgrowth in 8h *$_p$clag:rab11a* zygotes (figure 3.5.2). TEM analysis of 6h and 8h *$_p$clag:rab11a* zygotes strongly suggest the outgrowth is associated with the assembly of the collar with an aperture, apical microtubules and the IMC (figure 3.5.3). Therefore, assembly of complete set of internal organelles such as IMC, apical complex and micronemes (shown by

immunofluorescence studies for Chitinase and CTRP, Results 3.10) is expected in spherical *$_p$clag:rab11a* ookinetes and is comparable with the morphology of round dedifferentiated PDEδ KO *P. berghei* ookinetes which do form apical organelles, however possess an incomplete IMC (Moon, Taylor et al. 2009). These round dedifferentiated PDEδ KO *P. berghei* ookinetes rotate rapidly and have little or no forward motility. Since the external morphology of our *$_p$clag:rab11a* ookinete is similar to round PDEδ KO *P. berghei* zygotes also IMC and apical complex are assembled, *$_p$clag:rab11a* spherical ookinetes were anticipated to have little motility or rotational movement. However, motility assays suggest that *$_p$clag:rab11a* spherical ookinetes do not have little motility or even rotational movement (figure 3.4.2).)

Translationally stored mRNAs are stored in mRNP complexes (with DOZI and CITH) which are translated in a coherent and phased programme following activation and/or fertilization for zygote development. Despite substantial mRNA loss, DOZI and CITH gene deletion mutants remain fertile and ookinete development is terminated early in zygote development (Mair, Braks et al. 2006, Mair, Lasonder et al. 2010). This prompted us to speculate that PbRab11A might have some role in regulating the expression or stability of DOZI/CITH with a further effect on the stabilization and deployment of translationally repressed transcripts (Mair, Braks et al. 2006, Mair, Lasonder et al. 2010). However, our western blots showed normal or slightly delayed expression of some of the ookinete developmental and structural components in *$_p$clag:rab11a* zygotes and ookinetes which are stored translationally in DOZI/CITH complex demonstrating translation of at least some DOZI/CITH stored mRNAs is possible in *$_p$clag:rab11a* zygotes and ookinetes (Results 3.5 and 3.10). To investigate in-depth, the fate of DOZI/CITH stored (translationally stored) mRNAs and reactivation of post-meiotic transcription in *$_p$clag:rab11a* gametocytes and spherical ookinetes respectively, we performed RNA-Seq and compared their transcriptomes to those of WT-GFP gametocytes and ookinetes, AUFG and TAR respectively (figure 3.6). RNA-Seq data suggest that down-regulation of Rab11A transcript (in *$_p$clag:rab11a* gametocytes due to the promoter swap strategy) majorly affects the gametocytes than ookinetes, and causes deregulation of almost 11% of the total (*$_p$clag:rab11a*) gametocyte transcriptome up to 2 folds including the same percentage and fold change of translationally stored (DOZI/CITH associated) transcripts (figure 3.7.2 and Table 3.7.3 and 3.7.4).Taken together the data suggest that the protein coding potential of the transcriptome that is sequestered by the DOZI/CITH apparatus in

gametocytes is fully realised although the timing of expression of some elements might be somewhat delayed/ reduced.

GO- Biological Process - term analysis of the transcriptome of *$_p$clag:rab11a* gametocytes revealed less than half of deregulated transcripts have annotated GO terms (Table 3.7.3 and Table 3.7.4). GO- Biological Process – term enrichment suggested gross defects and significant up-regulation of translation associated transcripts which consists of ribosomal proteins, and down-regulation of various biosynthetic processes, protein modification and processing, cellular transport and metabolic processes which comprises of various enzymes involved in biosynthesis of cellular components, protein modification/processing, metabolism and some of the known transcripts associated with zygote development (Rab11B involved in the biogenesis of IMC in *T. gondii*), zygote DNA replication (NEK2), ookinete invasion and motility (CTRP, MTIP, PSOP2, PSOP6, PSOP12, CDPK3, SUB2), sporozoite development (TRAP, IMC1a) (figure 3.7.4) (Appendix B- Table 1). However, despite the significant down-regulation of NEK2 associated with zygote DNA replication (Reininger, Tewari et al. 2009), DNA contents of *$_p$clag:rab11a* 4h zygotes analysed by FACS were found to be similar to WT-GFP 4h zygotes (figure 3.3.5). Similarly, no reduction in protein levels of Rab11B was detected despite the reduced amounts of *rab11b* steady state transcript. Rab11B is associated with IMC biogenesis *in T. gondii* (Agop-Nersesian, Egarter et al. 2010) which appears to be normal (figure 3.3.4 D, E). However expression of microneme proteins CTRP (also associated with ookinete motility) and chitinase appears to be slightly less in *$_p$clag:rab11a* ookinetes than WT-GFP ookinetes (figure 3.10.1 J) although micronemes are formed. We were unable to perform the expression and localization studies of other significantly up/down-regulated transcripts due to unavailability of respective antisera but the cross-section of candidates analysed in this study shows that down regulation of steady state transcript levels might not accompanied by a similar down regulation of protein abundance. GO (Biological Process) enrichments suggested the significant up-regulation of some of the biological processes associated with chromosome organization and DNA replication (in *$_p$clag:rab11a* gametocytes and spherical ookinetes, respectively) and this could account for enlarged nucleus seen in immunofluorescence images of most of the *$_p$clag:rab11a* ookinetes as compared to WT-GFP ookinetes (figure 3.3.3 B, figure 3.3.4 C, E, figure 3.5.1 C and 3.10.2).

Similar to the deregulated transcripts in *$_p$clag:rab11a* gametocytes stage, almost half of the deregulated transcripts in *$_p$clag:rab11a* ookinetes have annotated GO (Table 3.7.10 and Table 3.7.11). GO (Biological Process) enrichment suggested major up regulation of proteolysis

associated biological processes and down regulation of a variety of transcripts in *$_p$clag:rab11a* ookinetes (figure 3.7.12) consisting of transcripts of genes associated with proteolysis, biosynthetic processes, ribosome biogenesis and transport including some of the transcripts associated with sporozoite development such as thrombospondin related sporozoite protein (TRSP), sporozoite invasion-associated protein 1 (SIAP1) and up-regulated in infective sporozoites (UIS4) (Appendix B – Table 2). The appearance of sporozoite stage transcripts is not unexpected as the ookinete appears to re-establish the DOZI/CITH translational repression apparatus with a different cohort of mRNA cargo and largely similar protein components (M. Stewart- Waters group, unpublished data). Therefore, it appears that the ookinete, like the gametocyte, prepares stocks of stored mRNA to be deployed later in development. The down-regulation of Rab11A in the *$_p$clag:rab11a* parasites appear to affect transcripts in gametocytes more than *$_p$clag:rab11a* ookinetes (figure 3.7.2 A, figure 3.7.7 A and figure 3.8.1).

A very high number of transcripts are deregulated 24hpa when fertilization is inhibited (i.e. in AUFG) than 24hpa when transcription is arrested (i.e. in TAR) (figure 3.7.7). Transcriptome of AUFG and TAR show almost 75% similarity with each other and, therefore, approximately 25% variance (figure 3.7.13). This indicates that only 25% of transcriptome is important for development from gametocytes to ookinete stage. Additionally, AUFG also shows almost 30.28% of DOZI/CITH stored transcripts indicating that RNA degradation mechanisms are inactive in absence of fertilization (figure 3.7.14). Withholding of small subgroup (i.e. 23.74%) of DOZI/CITH stored transcripts in TAR suggests that most of the DOZI/CITH stored transcripts are consumed until retort growth takes place (figure 3.7.15). Our western also suggest that some of the translationally stored transcripts are also translated in absence of fertilization. GO- Biological Process enrichment suggested up and down regulation of a variety of biological processes (figure 3.7.19 and figure 3.7.22).

Also *$_p$clag:rab11a* ookinetes show a very small number of deregulated transcripts (144) as compared to AUFG (1637) and TAR (977) (when all these three samples are compared to the transcriptome of WT-GFP ookinetes) indicating that the transcriptome of *$_p$clag:rab11a* ookinetes is more similar to WT-GFP ookinetes rather than transcriptome of AUFG and TAR (figure 3.7.7)., however, 144 of deregulated transcripts in *$_p$clag:rab11a* ookinetes mirrors the transcriptome pattern of AUFG (figure 3.7.9).

The transcriptome pattern during gametocyte to ookinete development in *$_p$clag:rab11a* and WT-GFP parasites is generally similar for 1212 transcripts having more or less similar fold changes (figure 3.8.4). These 1212 common transcripts have generally similar expression profile to their respective WT-GFP transcripts during gametocytes to ookinete development (figure 3.8.4). However, during the same developmental transition a set of 439 transcripts is exclusively and significantly regulated in *$_p$clag:rab11a* parasites rather than 799 transcripts in WT-GFP parasites (figure 3.8.4).

Also, we tried to use several FPKM cut off values to enrich the top 'significantly expressed transcripts' in WT-GFP parasites and 'significantly deregulated transcripts' in *$_p$clag::rab11a* and drug treated WT-GFP parasites (figure 3.9.2 and figure 3.9.3). Therefore, it is expected that determining cut off FPKM in RNA-Seq analysis is not robust tool and for that reason considering <25% more or less abundant transcripts in *$_p$clag::rab11a* and drug treated WT-GFP parasites (compared to respective controls) would provide a more reasonable results.

PPKL, essential for ookinete development, motility and mosquito transmission (Guttery, Poulin et al. 2012, Philip, Vaikkinen et al. 2012), was expressed normally throughout post-activation of *$_p$clag:rab11a* female gametocytes, however, localization of PPKL appear to be cytoplasmic in *$_p$clag:rab11a* ookinetes rather than focused at apical collar as in WT-GFP ookinetes (figure 3.10.3). Deletion of *ppkl*, causes defect in apical complex integrity (Philip, Vaikkinen et al. 2012), however, the apical complex and IMC appear normal in *$_p$clag::rab11a* 8h zygotes (Results 3.5). Therefore, PPKL appears to be at least partially functional in *$_p$clag::rab11a* ookinetes and our analysis might imply additional functions for this protein phosphatase.

3.11.1 Conclusion

Together, these results illustrate that *$_{p}$clag:rab11a* zygotes are morphologically arrested and remain spherical. Furthermore, the expression of many of the zygote-to-ookinete development and structural markers is unaltered in timing, localisation and extent and therefore uncoupled from ookinete morphology. This independent repertoire of cellular events includes meiosis as the *$_{p}$clag:rab11a* mutant showed no defect in DNA replication, however its chromosomes appear to remain decondensed 24 hours after fertilisation. Formation and organisation of the apical organelles as well as the IMC appeared to be unaffected by the absence of PbRab11A indicating no role for this protein in the establishment of zygote polarity in *P. berghei* as well as meiosis. Instead the defect most obviously manifests itself at the level of a failure to mature morphologically.

Transcriptome data suggests that *$_{p}$clag:rab11a* "ookinetes" are generally similar to WT-GFP ookinetes more so than AUFG and TAR. In absence of Rab11A mRNAs, there is slight but significant reduction of various transcripts having role at either ookinete maturation or at later stages (e.g. sporozoites) and no absolute reduction of any particular transcript or set of transcripts associated with ookinete development except Rab11A itself. Most of the significantly deregulated transcripts in *$_{p}$clag:rab11a* gametocytes and ookinetes are not translationally stored. Therefore, I predict that cumulative effect of all the minor defects associated with either expression, delay, localization or reduction of variety of transcripts (and proteins) in absence of Rab11A causes morphological arrest of *$_{p}$clag:rab11a* ookinetes. The *$_{p}$clag:rab11a* "ookinetes" undertake the early landmarks of zygote development such as meiosis and P25/28 expression even in the absence of PbRab11A but ultimately the morphological transformation is not possible. Therefore, I propose that PbRab11A is required for morphological transformation and not for the establishment of zygote polarity in *P. berghei*.

3.11.2 Proposed model for role of Rab11A in *P. berghei* zygote development

Based on current results and past studies, I propose a model for developmental block of *$_p$clag:rab11a* spherical ookinetes (figure 3.11 A). ISP1 is polarised in late female zygote indicating pre-selection of the focal point of ookinete and deletion of ISP1 was unsuccessful in seven independent experiments suggesting the essentiality of ISP1 during asexual stages of *P. berghei* (Poulin, Patzewitz et al. 2013). Published data (Sebastian, Brochet et al. 2012) and our results (figure 3.5.1) suggest that GAP45 is also important for further development of the focal point, however, we assume that along with GAP45, Rab11A is critical for the retort outgrowth of *P. berghei* zygote. Once the focal point is marked through ISP1, GAP45 might start assembling at the focal point 4h post-fertilization along with as yet unknown focal point markers but which might include components of IMC, collar, MTOC (Mahajan, Selvapandiyan et al. 2008, Tran, de Leon et al. 2010, Francia and Striepen 2014) through which microtubules extend. Subsequently, Rab11A along with cytoskeletal components such as actin as well as microtubules assist in the retort shape formation. Specifically, Rab11A endosomes might provide plasma membrane to the growing tip or to the joint of the retort and the main body of the zygote (here I refer to it as the 'neck' region) (figure 3.11 B) and anticipate a role for Rab11A in the secretion, delivery of membrane synthesis components e.g. PI4K (McNamara, Lee et al. 2013) and other necessary proteins while donating plasma membrane to assist the intended morphological transformation. Along with plasma membrane, the Rab11A endosome might help directly or indirectly in the incorporation of marker(s) at the neck region (referred to here as 'neck marker(s)') forming a transition point segregating the main spherical body of the zygote from the retort outgrowth. Forces might be generated at the transition point that pushes the growing apical complex outwards by donating plasma membrane. Furthermore the transition point 'neck marker/s' may act as a centre for pulling the plasma membrane during ookinete development, possibly during late hours to reorganize the last bulge of zygote and apparently to form complete a banana shape ookinete. In *$_p$clag::rab11a* zygotes, developmental and structural markers are formed normally however, due to a lack of Rab11A mediated endosomes no plasma membrane is available for the growing apical complex and 'neck marker/s' are probably mis-localized and thus no forces are generated and the apical bud is formed but not moved. In *$_p$clag::rab11a*, GAP45 delivered to the focal point and in the absence of a retort shape and/or absence of the transition point (and unknown 'neck marker/s' responsible for pull and push mechanism of

plasma membrane or deposition of GAP45 into the retort outgrowth), GAP45 is distributed all over the spherical $_{p}$*clag::rab11a* zygotes (figure 3.5.1).

It has been observed that retort outgrowth extends immediately after 6h post-fertilization in WT *P. berghei*. Hence, any membrane delivery machinery must be extremely active during 6hpa and thus, Rab11A assisted endosomes involved in the delivery of plasma membrane and probably 'neck marker/s'. And our zygote time course western results show that Rab11A is expressed as early as 2h post-fertilization (figure 3.1.1). This suggests PbRab11A might have other function(s) in addition to membrane delivery in the early hours of post-fertilization plausibly preparation for deposition of cell membrane synthesis machinery or microtubule nucleation components, as shown recently in human cells (Hehnly and Doxsey 2014), which might acts as 'neck marker/s' involved in pull and push mechanism. In addition to acts as a source of plasma membrane and force generation, PbRab11A vesicles might play part in the delivery of mRNAs to the apical complex for on-site translation (Dollar, Struckhoff et al. 2002, Januschke, Nicolas et al. 2007). .

(A)

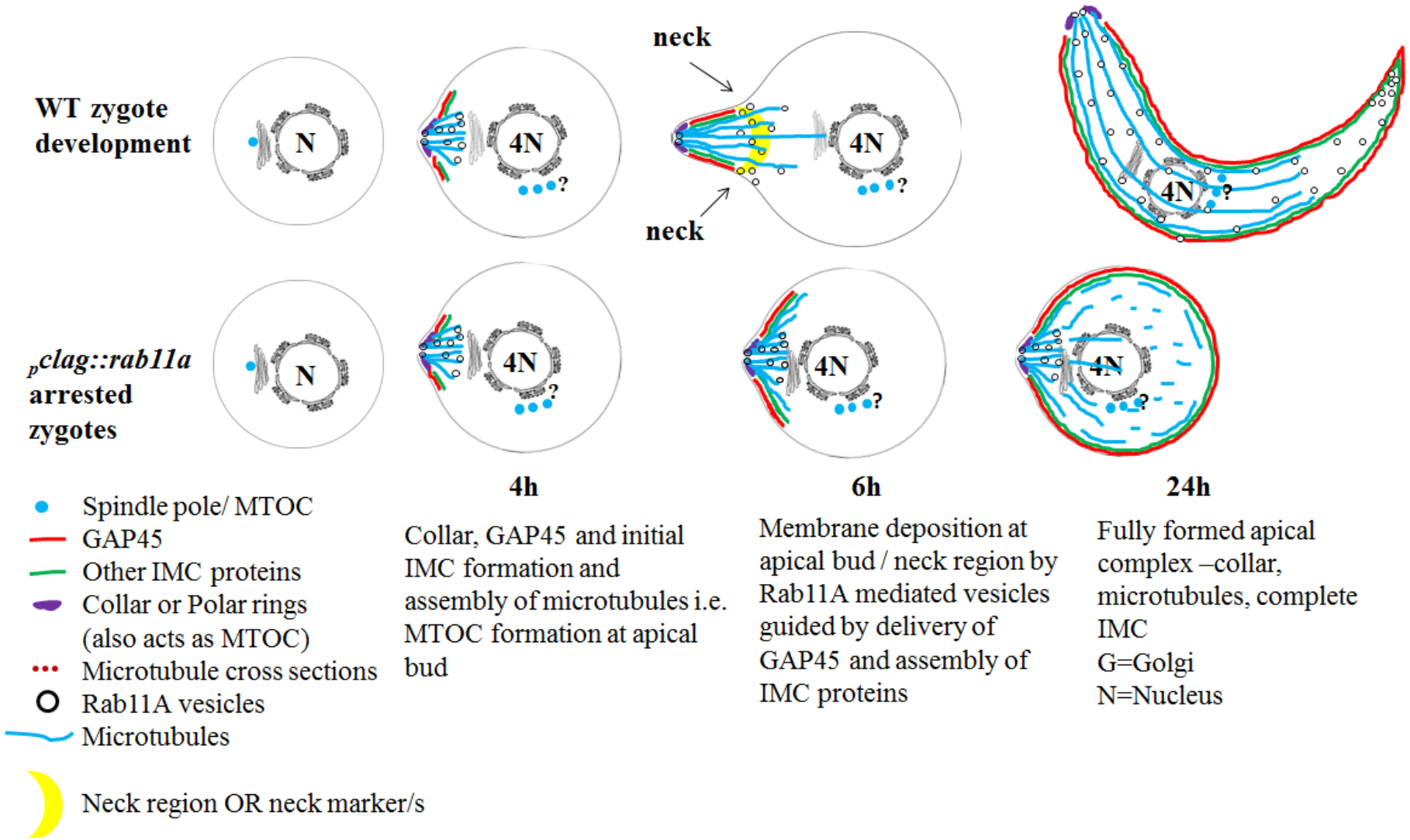
WT zygote development
N
4N
?
neck
neck
4N
?
4N
?
pclag::rab11a arrested zygotes
N
4N
?
4N
?
4N
?
4h
6h
24h
Spindle pole/ MTOC
GAP45
Other IMC proteins
Collar or Polar rings (also acts as MTOC)
Microtubule cross sections
Rab11A vesicles
Microtubules
Neck region OR neck marker/s
Collar, GAP45 and initial IMC formation and assembly of microtubules i.e. MTOC formation at apical bud
Membrane deposition at apical bud / neck region by Rab11A mediated vesicles guided by delivery of GAP45 and assembly of IMC proteins
Fully formed apical complex –collar, microtubules, complete IMC
G=Golgi
N=Nucleus

(B)

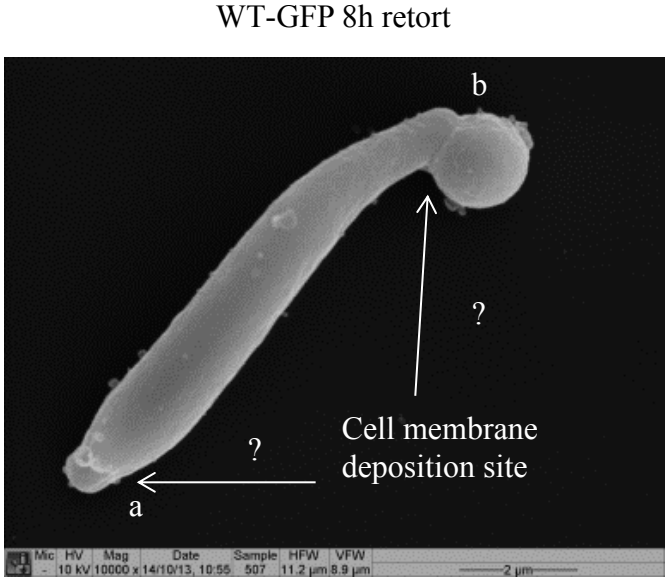

Figure 4: Proposed model Rab11A mediated delivery of plasma membrane in *P. berghei*.

(A) Rab11A mediated vesicles are involved in the delivery the plasma membrane and transmembrane proteins to the growing tip or to the neck region of retort / zygote. These are also possibly involved in secretion, development and maintenance of cell shape, protein trafficking coordinating with cytoskeletal components. 'Four blue dots with ?' suggest possible numbers of spindle poles in a zygote (B) WT-GFP 8h retort showing possible site for membrane expansion either apical tip 'a' or neck region 'b'.

Chapter 4: Results and Discussion – Gamete fusion approach

4.0 Introduction: Fertilization and establishment of polarity

Fertilization is a very important phenomenon of living organisms which provides opportunity for genetic recombination for a new life. Generally, fertilization is a multistep complex process and generally involves a cascade of cell signalling events comprising Cdcs, Cdks, protein kinases and MAP kinases as well as calcium signalling and a number of other cell components (Sato 2014), merging of cytoplasm, genetic recombination and the emergence of the new fertilised entity. In humans, (male gamete) spermatozoa need to travel through a long distance through the female reproductive tract and have to cross a number of barriers to fertilize with oocyte (female gamete) which is covered by cumulus cells embedded in a cumulus matrix (containing proteins and carbohydrates and rich in no-sulfated glycosaminoglycan known as hyaluronan) and the zona pellucida (ZP) (Anifandis, Messini et al. 2014, Gupta 2014). Sperm penetrates extracellular cumulus matrix via hyaluronidase (Martin-Deleon 2011) and ZP with numbers of acrosomal proteins (sp56 and zonadhesin) and enzymes such as acrosin protease, GPI-anchored serine protease-TESP and the multi-subunit proteasome having proteolytic activities which interacts with ZP markers (Anifandis, Messini et al. 2014). The adhesion of sperm and oocyst plasma membranes is mediated by various membrane molecules expressed on the surface of sperm (CD46, ADAM2) as well as oocyst (CD9, CD81, CD11b/CD18). Sperm surface markers IZUMO1 and SPESP1 have been studied in a fusion pore formation where IZUMO1 pairs with Juno on oocysts surface and assists in the fusion process (Anifandis, Messini et al. 2014, Bianchi, Doe et al. 2014, Klinovska, Sebkova et al. 2014). Similarly, in *Xenopus laevis* (and other invertebrates and amphibians) oocyst are surrounded by two glycol-protein rich membranes known as vitelline envelope (equivalent to ZP in mammals) made up of glycoproteins such as gp37, gp41, gp80 and gp120, gp69/64 and a jelly layer of J1, J2, J3 and allurin which is responsible for the chemotactic movement of sperm towards the oocyte. The feature of an oocyte being surrounded by multiple layers is conserved in many species e.g. nematodes *C. elegans* (Johnston and Dennis 2012). Sperm surface glycoproteins interacts with oocyte membrane associated Src family Kinase (P57 kinase in *Xenopus* and Fyn, Yes and Fgr in mice) and activates the downstream phosphorylation and calcium signalling events for fusion to take place. In mice, inhibition or deletion of Fyn kinase disrupts oocyst polarity but not the fusion process (Luo, McGinnis et al. 2009). The exact mechanism of these events is not well understood, however, similar mechanisms are functional in rat, frog, sea urchin and mouse eggs (Sato 2014).

In general, fertilization in *Plasmodium* comprises of interactions between male and female gamete surface molecules, membrane fusion, nuclear fusion, and meiosis followed by development of the resulting zygote. Some of the molecules involved in gamete interactions and fusion have been studied and they appear to be physically if not necessarily functionally conserved, although the exact mechanisms of interactions remain poorly understood. Some of the molecules from either of the gametes are essential or nearly essential in fertilization. P48/45 (van Dijk, Janse et al. 2001) and P230 surface protein of male gametes and P47 surface marker of female gametes (van Dijk, van Schaijk et al. 2010) play a major role in *P.* berghei gamete fertility. Although the roles of Pf230 (*P. falciparum* 230) and Pf48/45 appear to be conserved in *P. falciparum*, Pf47 however seems dispensable for gamete fertility (van Schaijk, van Dijk et al. 2006) and has instead been shown to be involved in evasion of the mosquito innate immune system (Molina-Cruz, Garver et al. 2013) a mechanism that engages the Jun-N-terminal kinase (JNK) pathway (Ramphul, Garver et al. 2015). One of the well-studied molecules in plants and a number of other lower eukaryotic organism fertilization is GSC1 (generative cell-specific) also known as HAP2 has been described and shown to be essential for *Plasmodium* male gamete fusion to the female gamete (Mori, Kuroiwa et al. 2006, Liu, Tewari et al. 2008, Orias 2014).

The oocytes of some of the ascidian species are polarised along the animal–vegetal axis and sperm entry makes significant changes to the embryo (zygote) architecture. For example, sperm derived centrosomes may define the posterior pole of the embryo (Sardet, Paix et al. 2007). Likewise, in *C. elegans*, the sperm entry site determines the axis of polarity. A guanosine tri-phosphate activating protein (GAP)-CYK-4 donated by sperm, guanosine nucleotide exchange factor (GEF)- ect-2 and rho-1 signal for the establishment of single celled embryonic polarity related to the sperm entry site. CYK-4 orthologues are found in the sperm of other species (e.g. MgcRacGAP in Drosophila) which indicates that this phenomenon might be conserved (Sardet, Prodon et al. 2004, Jenkins, Saam et al. 2006). However, in the Drosophila embryo the axis of polarity is established before fertilization as sperm entry is guided by egg's micropyle (Sardet, Prodon et al. 2004, Jenkins, Saam et al. 2006). In the rice zygote, establishment of the axis of polarity was studied with respect to the site of male gamete fusion. *In vitro*, the zygote to two cell embryo development suggests that male gamete fusion and surrounding environmental clues are necessary for the zygote to embryo development, however, the establishment of asymmetry (polarity) seems to be independent of the site of male gamete fusion (Okamoto 2010).

As an alternative approach to study the development of polarity in *P. berghei* ookinete, we assumed that the point of male gamete fusion would be the same as the point of emergence of the apical complex in *P. berghei* zygote (we call it 'the point of fusion' hypothesis) (see Chapter 1: General Introduction 1.7 for details about the hypothesis). To study this hypothesis, multiple fluorescently tagged *P. berghei* parasite lines were generated and analysis of these lines is ongoing. Therefore, data presented in this chapter is preliminary but details the generation of the necessary lines and the establishment of the experimental approach, however multiple repeats are important to conclude the results.

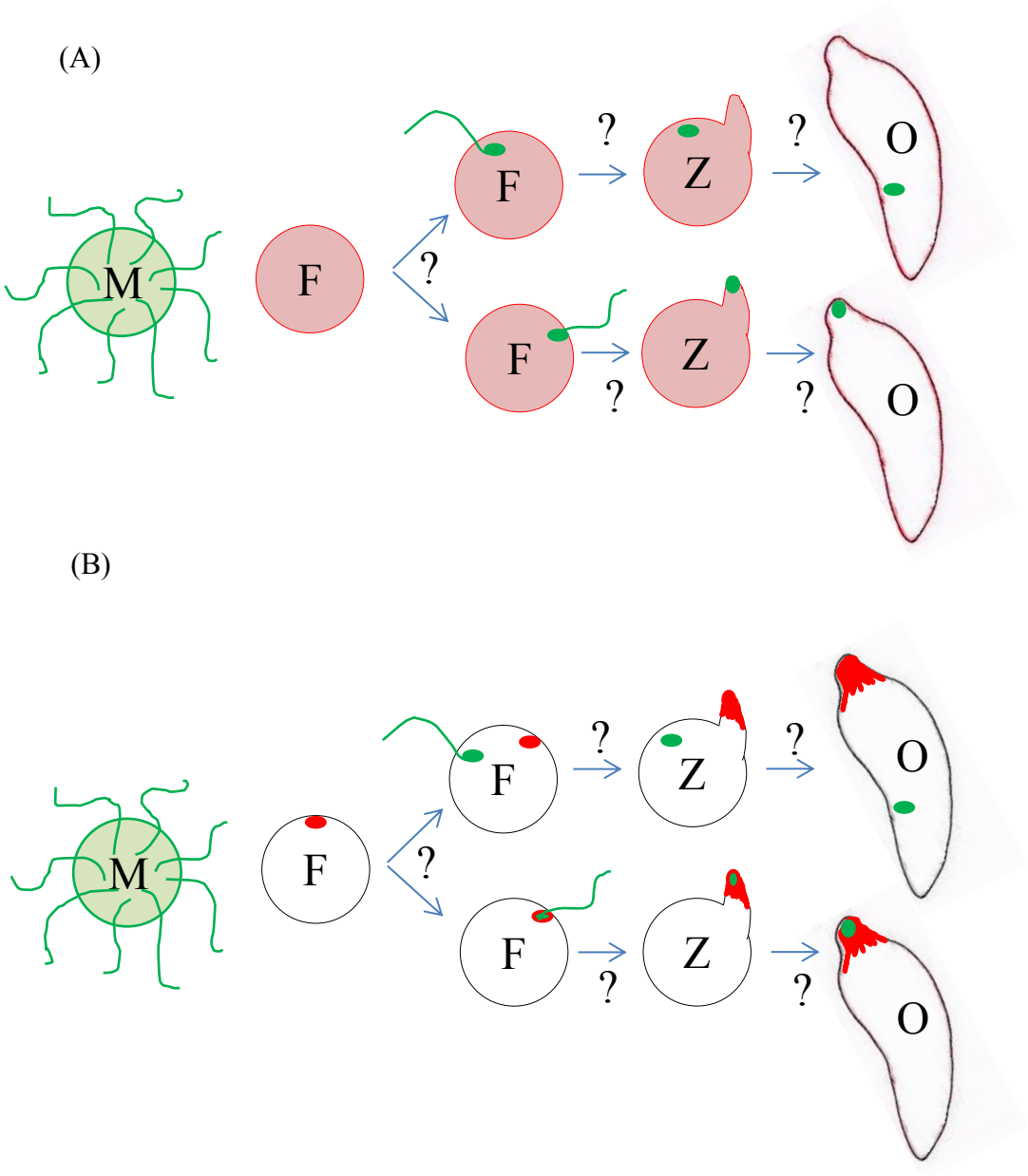

Figure 4.0 Hypothesis of point of gamete fusion and the point of emergence of apical bud in *P. berghei* zygotes.

(A) Schematic of fertilization and zygote to ookinete development using membrane localized GFP (green fluorescent protein) male gametocytes and membrane localized mCherry female gametocyte producer *P. berghei* parasites. (B) Schematic of fertilization and zygote to ookinete development using membrane localized GFP male gametocytes and mCherry tagged to female specific marker (PPKL/ISP1/SPBP/GAP50) producer *P. berghei* parasite lines. M- male gametocyte, F- female gametocyte, Z-zygote and O- ookinete. See text for details.

4.1 Generation of membrane localized green male gametocyte producer parasites.

A construct to generate GFP targeted to the parasite membrane under the control of a male specific promoter [5'UTR of PBANKA_041610, based on the 820 line by (Ponzi, Sidén-Kiamos et al. 2009, Mair, Lasonder et al. 2010)] was generated (see Methods 2.1.1 f for plasmid details) and transfected into the WT *P. berghei* HPTBB strain to generate green male gametocyte producer (GMGP) parasites (figure 4.1.1 A). It has been confirmed by live fluorescence microscopy that GMGP generates green gametocytes and green fluorescence appears to be located in the parasite membrane (figure 4.1.1 B). These green gametocytes undergo exflagellation to give green microgametes therefore green gametocytes deemed to be male gametocytes (also referred as membrane localized green male gamete producer) (figure 4.1.1 B, C) and no green fluorescence was observed in other developmental stages (not shown). The GMGP was cloned by limiting dilution into 10 mice and four clones were obtained (see Method 2.1.2 i for cloning procedure). Diagnostic PCRs on gDNA isolated from clone 2 of GMGP (GMGPcl2) show appropriate integration at 5' and 3' end of plasmid targeted at P230p locus (figure 4.1.2 A). GMGPcl2 was used for further examination and was able to exflagellate normally (not shown) and generate a normal amount of ookinetes (figure 4.1.2 C, D).

After confirming membrane localised green male gametocytes, GMGPcl2 was negatively selected to permit further genetic modification (Braks, Franke-Fayard et al. 2006, Maier, Braks et al. 2006, Orr, Philip et al. 2012). A mouse was infected with GMGPcl2 and parasitemia was monitored daily by Giemsa smears and prodrug 5-fluorocytosine (5FC) was given through drinking water to remove the selectable markers (yFCU and human *dhfr/ts*) when parasites were visible (parasitemia 0.156%) (See Method 2.1.2 i for negative selection). The mixed population of parental GMGPcl2 and negatively selected and recombined GMGPcl2 (GMGPcl2n) was further cloned by serial dilution. Diagnostic PCRs shows appropriate bands showing removal of selectable markers (yFCU and human *dhfr/ts*) in GMGPcl2ncl1, GMGPcl2ncl2 and GMGPcl2ncl3 (figure 4.1.3).

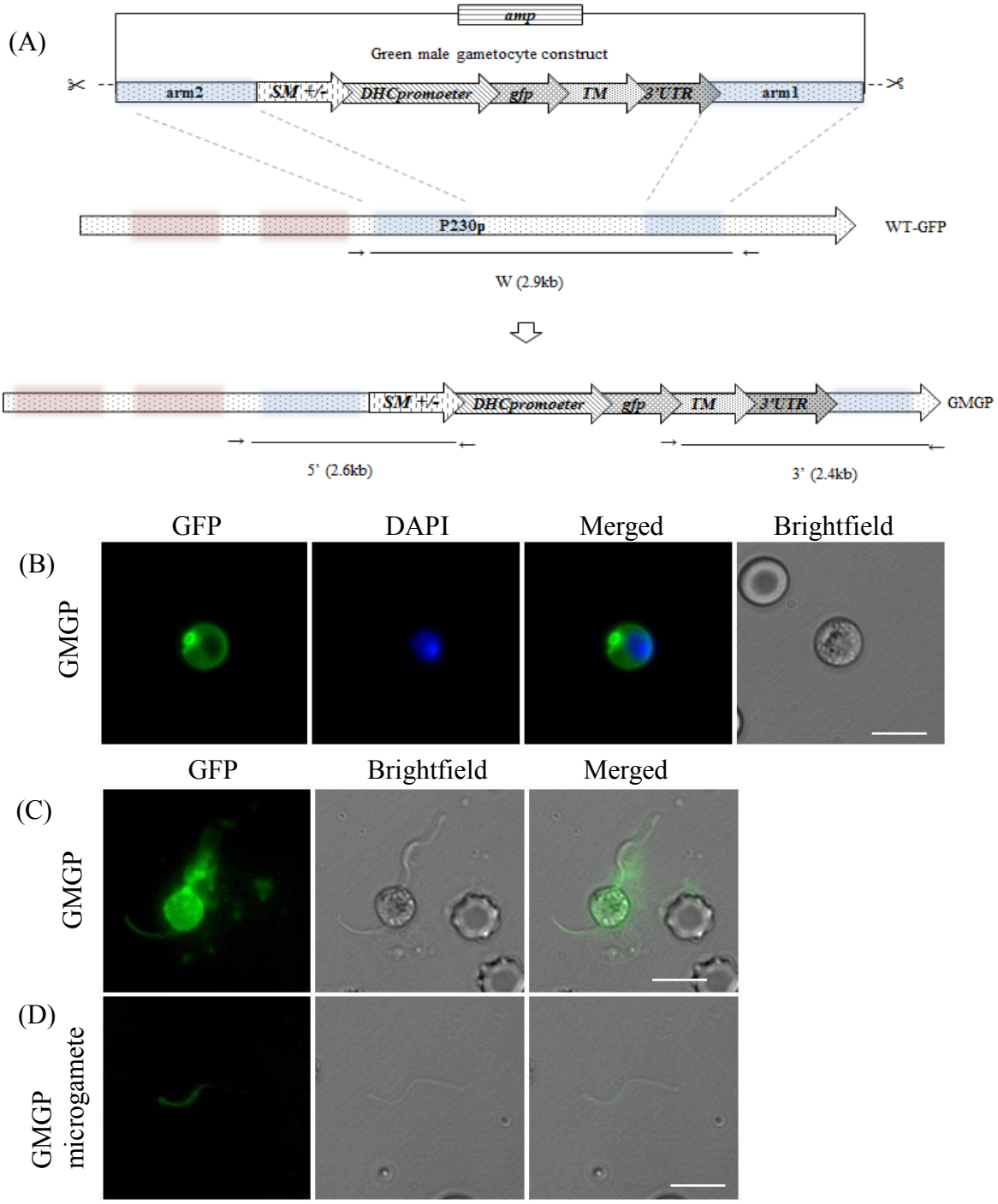

Figure 4.1.1 Generation of green male gametocyte producer *P. berghei* parasites. (A) Schematic representation of the generation of green male gametocyte producer (GMGP) parasite as described in text (B) Representative image of live fluorescence microscopy of membrane localized GFP in an un-activated male gametocyte (C) male gamete exflagellation showing green microgametes moving out of the cell body (C) Individual microgamete showing green fluorescence. Live images were taken on Axioplan as given in methods 2.1.2 m. Scale bar 5 µm.

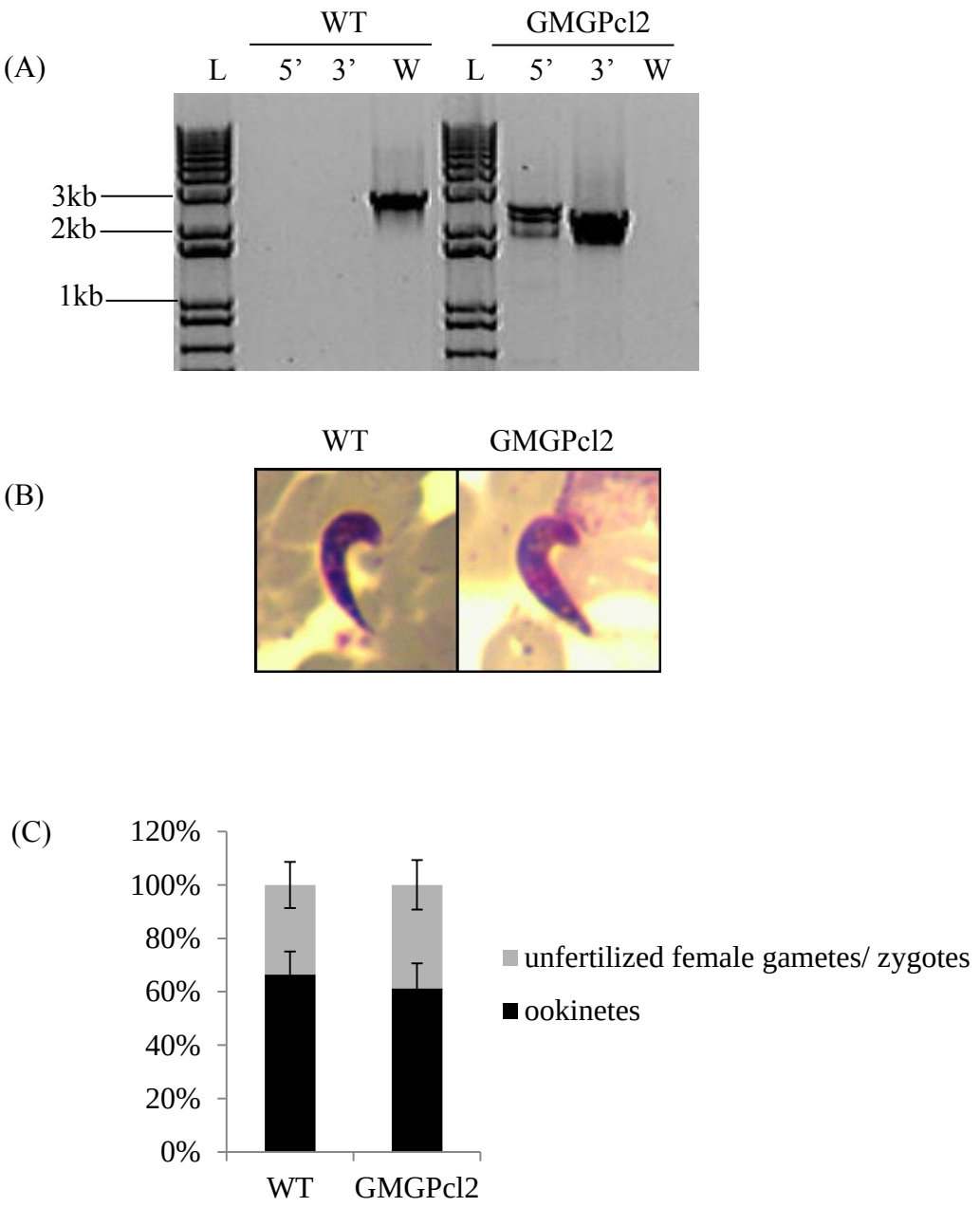

Figure 4.1.2 Diagnostic PCR and ookinete conversion of green male gametocyte producer *P. berghei* parasites.

(A) Diagnostic PCR of the green male gametocyte producer-clone2 (GMGPcl2) confirming the appropriate integration of 5' and 3' end of the green male construct in WT *P. berghei* genome and absence of band corresponding to wild-type (W). (B) Giemsa images of the ookinete morphology of green male gametocyte producer-clone2 (GMGPcl2) and wild type parasites (C) Ookinete conversion rate of GMGPcl2 (n=3, mean +/-SD, two tailed student t test, p-value 0.505).

(A)

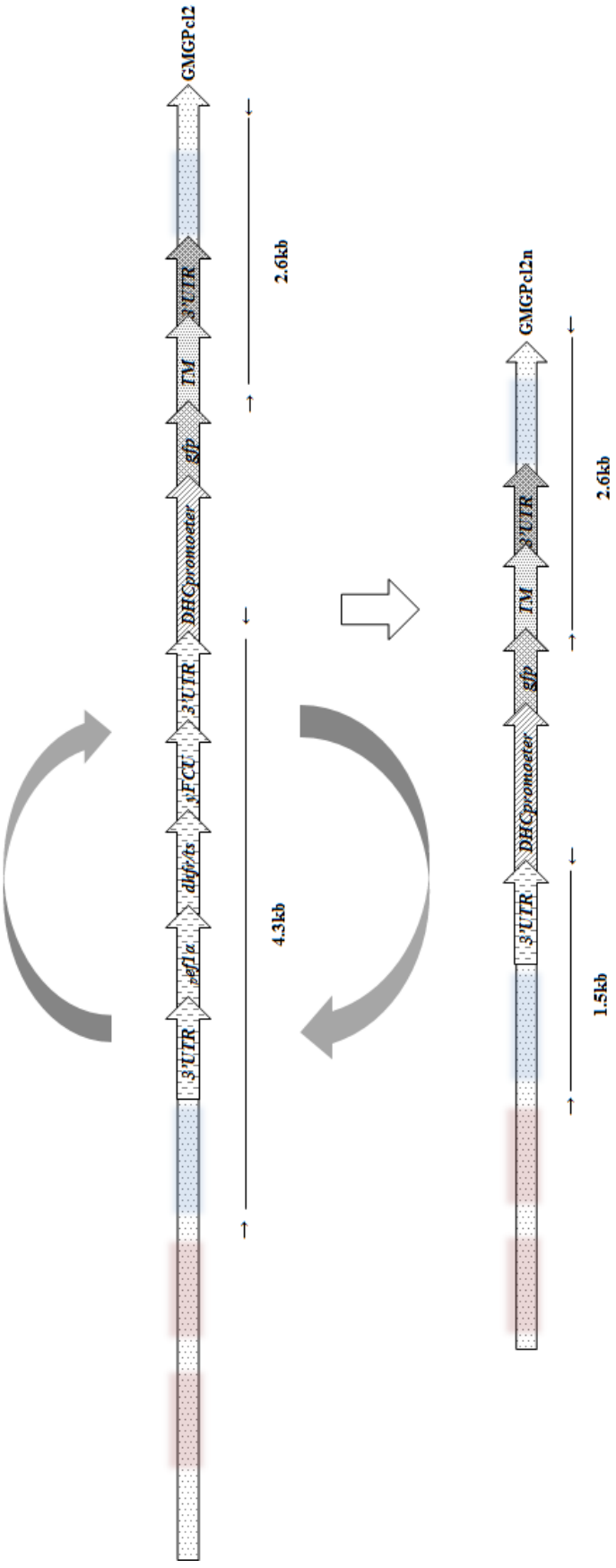
GMGPcl2
3'UTR
TM
gfp
DHCpromoter
3'UTR
yFCU
dapb/ts
eef1α
3'UTR
2.6kb
4.3kb
GMGPcl2n
3'UTR
TM
gfp
DHCpromoter
3'UTR
2.6kb
1.5kb

(B)

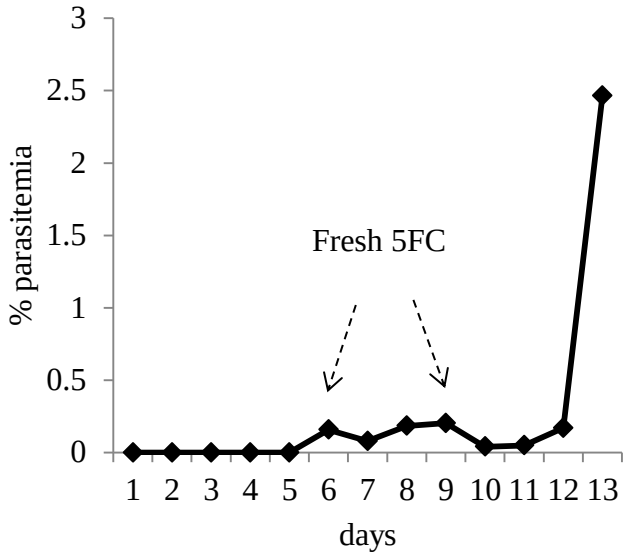

(C)

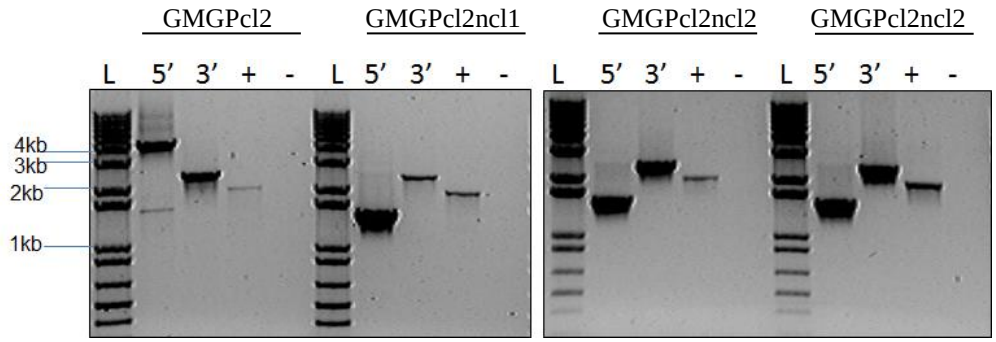

Figure 4.1.3 Negative selection of green male gametocyte producer *P. berghei* parasites.

(A) Schematic representation of negative selection of green male gametocyte producers where prodrug 5FC selects for parasites that have removed the selectable markers yFCU and human *dhfr/ts* (B) Graph of increasing parasitemia after initial decline post-application of fresh 5FC in drinking water (C) PCR analysis of clones of negatively selected green male gametocyte producers showing correct 5' and 3' integration. DHC – Dynein heavy chain.

4.2 Generation of membrane localised green male and red female gametocyte producer line.

A construct to express mCherry targeted to the parasite membrane under the regulation of a female specific promoter [5'UTR of PBANKA_130070, based on the 820 line by (Ponzi, Sidén-Kiamos et al. 2009, Mair, Lasonder et al. 2010)] was generated (see Methods 2.1.1 g for plasmid details) and transfected into GMGPcl2ncl2. Diagnostic PCRs show appropriate integration of red female construct at 5' and 3' end (figure 4.2 A, B). The presence of green and red gametocytes has been confirmed by fluorescence microscopy where green and red fluorescence is located in the membrane of male and female gametocytes respectively (figure 4.2 C, D). Parasites with mCherry localised to the membrane, visualised through fluorescence microscopy of gametocyte enriched culture, do not exflagellate and therefore are deemed to be female gametocytes (Therefore, the negatively selected green male gametocyte producer clone2 with red female gametocyte producer is referred as GMGPcl2ncl2-RFGP or membrane localized green male gametocyte:: membrane localized red female gametocyte producer). Further, ookinetes obtained from red-green parasite show red fluorescence therefore confirming that the female gametocytes membrane is red and that there is little turnover of the female gamete membrane by the developing zygote (figure 4.2 E).

(A)

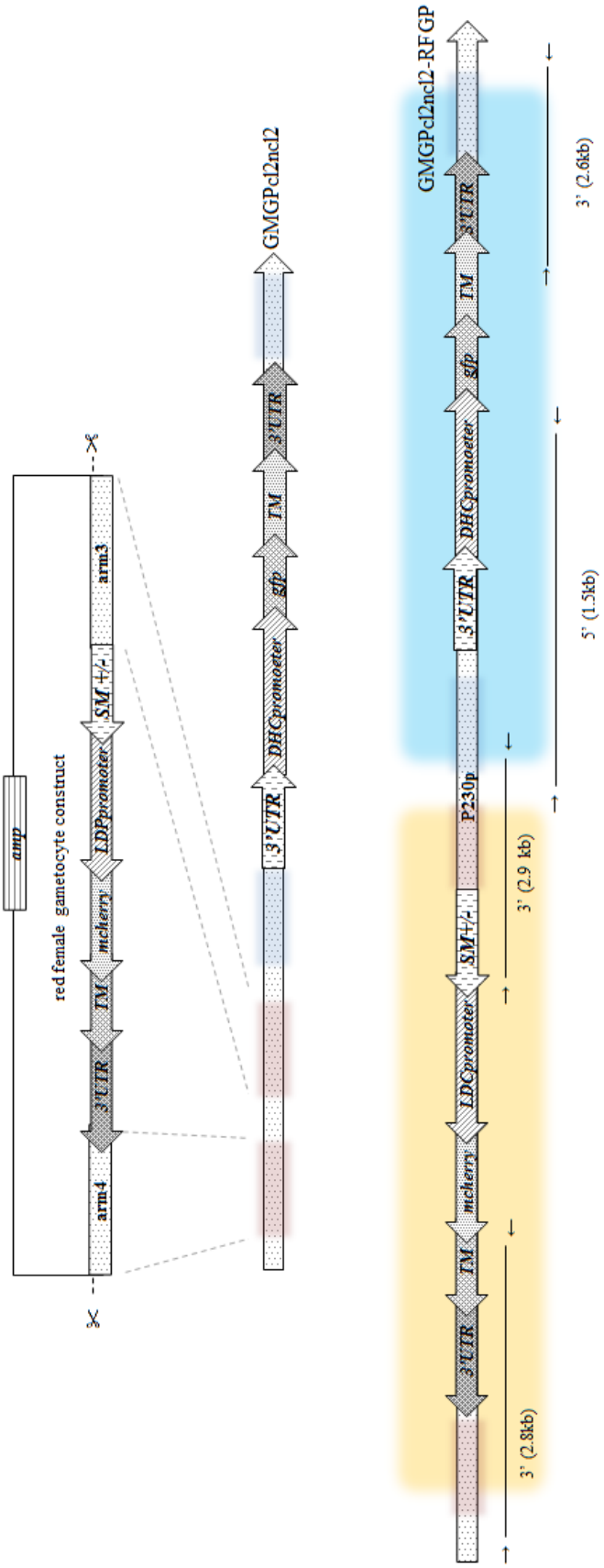
red female gametocyte construct
amp
arm3
SM +/-
LDPpromoter
mcherry
TM
3'UTR
arm4
GMGPcl2ncl2
3'UTR
TM
sfp
DHCpromoter
3'UTR
GMGPcl2ncl2-RFGP
3'UTR
TM
sfp
DHCpromoter
3'UTR
P230p
SM+/-
LDCpromoter
mcherry
TM
3'UTR
3' (2.6kb)
5' (1.5kb)
3' (2.9 kb)
3' (2.8kb)

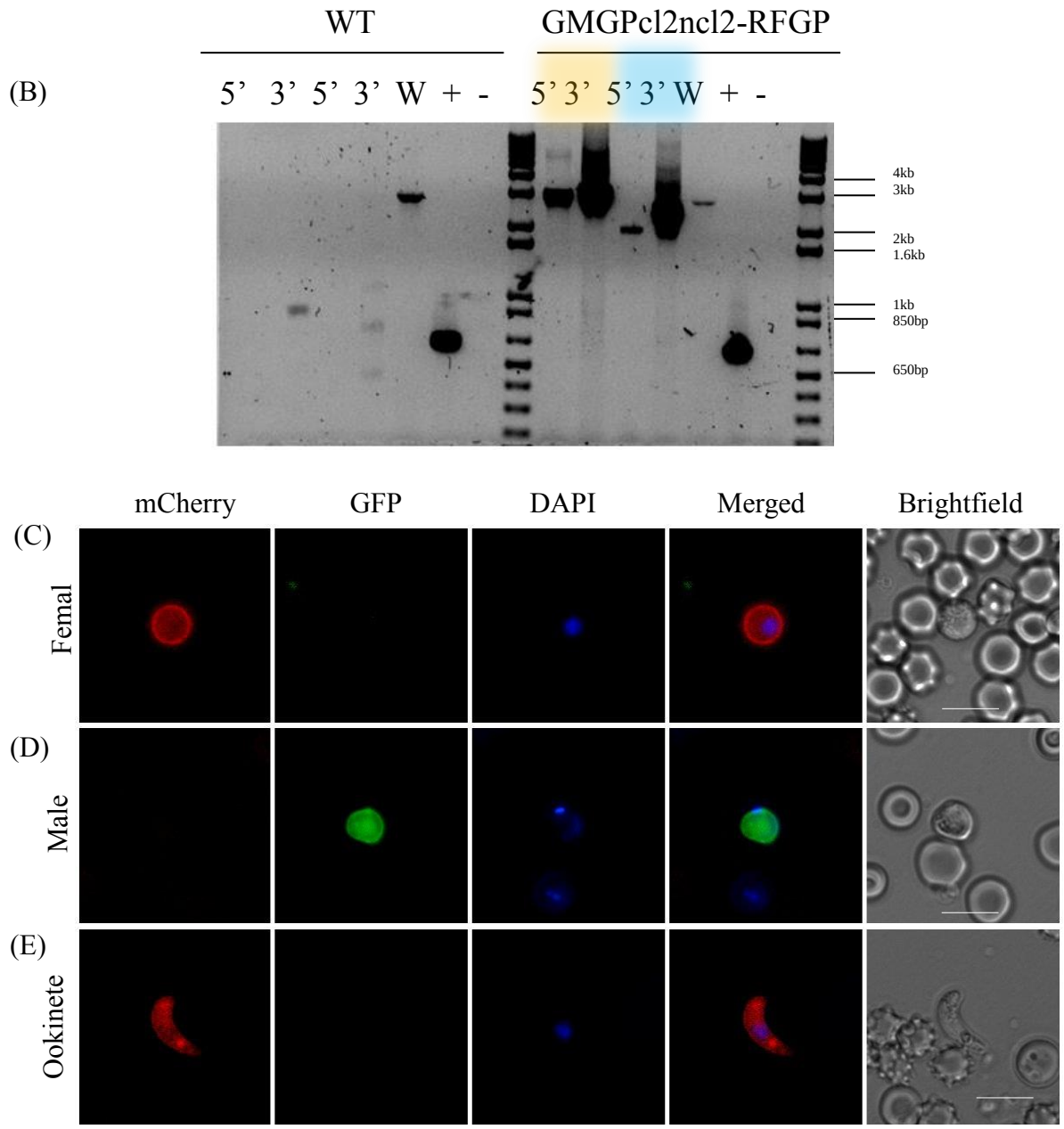

Figure 4.2 Generation of membrane localized green male red female *P berghei* parasites.

(A) Schematic of the generation of membrane localized green male-red female *P berghei* parasites. (B) Diagnostic PCRs of (pre-cloned) green male-red female gametocyte producers (GMGPcl2ncl2-RFGP) showing 5’ and 3’ integration of red female and green male constructs (C) Membrane localised red female gametocytes after transfection of red female construct in GMGPcl2ncl2 and (D) membrane localized green male gametocytes in the same parasite line. (E) Ookinete obtained from GMGPcl2ncl2-RFGP *P. berghei* parasites is red. Deltavision deconvoluted single slice live images taken on Axioplan (see Methods 2.2.2 m for details). Scale 5μm.

4.3 Generation of fluorescently tagged polarity marker lines

Recently, it has been shown that IMC sub-compartment protein 1 (ISP1) localizes to the periphery of late female gametocytes (Poulin, Patzewitz et al. 2013). Also, a protein phosphatase PPKL (PBANKA_132950) localises to the apical prominence in the zygote as the retort stage is initiated (Guttery, Poulin et al. 2012, Philip, Vaikkinen et al. 2012). Furthermore, research within our group has suggested the localisation of GAP50 at the apical bud of the developing zygote (K. Hughes - Waters' group, unpublished). The apical polar ring of the zygote/ookinete acts as an MTOC, therefore, to assess the delivery/development of the MTOC during the zygote to ookinete transition, we attempted to fluorescently tag C-terminal of Spindle Pole body protein (SPBP, PBANKA_040210), a marker of MTOC (Communication with Dr. O. Billker, Wellcome Trust Sanger Institute, Cambridge). Localization of ISP1, GAP50, PPKL and SPBP during zygote to ookinete development would be correlated along with the distribution of the male gamete membrane signal to examine the point of male gamete fusion and the characteristics of the emergence of the retort in the zygotes (figure 4.0). The constructs for *isp1::mcherry*, *ppkl::mcherry*, *gap50::mcherry* and *spbp::mcherry* have been generated (see Methods 2.1.1 h) and transfected into GMGPcl2ncl2 to generate following fluorescent *P. berghei* lines (figure 4.3 A) to study the hypothesis that the point of male gamete fusion defines the point of emergence of apical bud from the zygote. The following *P. berghei* lines were created: 1) *isp1::mcherry* in GMGPcl2ncl2 background (GMGPcl2ncl2-*isp1::mcherry*) 2) *ppkl::mcherry* in GMPcl2ncl2 background (GMGPcl2ncl2-*ppkl::mcherry*) 3) *gap50::mcherry* in GMPcl2ncl2 background (GMGPcl2ncl2-*gap50::mcherry*) 4) *spbp::mcherry* in GMPcl2ncl2 background (GMGPcl2ncl2-*spbp::mcherry*). The diagnostic PCRs performed on above fluorescent parasites (pre-cloned) confirm the integration of *isp1::mcherry*, *ppkl::mcherry*, *gap50::mcherry* and *spbp::mcherry* constructs into genome of independent GMPcl2ncl2 (figure 4.3 A to E).

However, we could not detect mCherry via fluorescence microscopy in the schizonts, gametocytes, zygotes or ookinetes obtained from three independently generated (pre-cloned) GMGPcl2ncl2-*spbp::mcherry* and GMGPcl2ncl2-*isp1::mcherry* enriched with pyrimethamine. Due to my inability to detect *spbp::mcherry* or *isp1::mcherry* (in GMGPcl2ncl2 background), we studied the point of male gamete fusion and the point emergence of apical bud hypothesis by recently FACS cloned (see Methods 2.1.2 s for FACS cloning) GMGPcl2ncl2-*gap50::mcherry* parasite line (Western blotting was still to be performed to detect the tagging of GAP50 with mCherry).

(A)

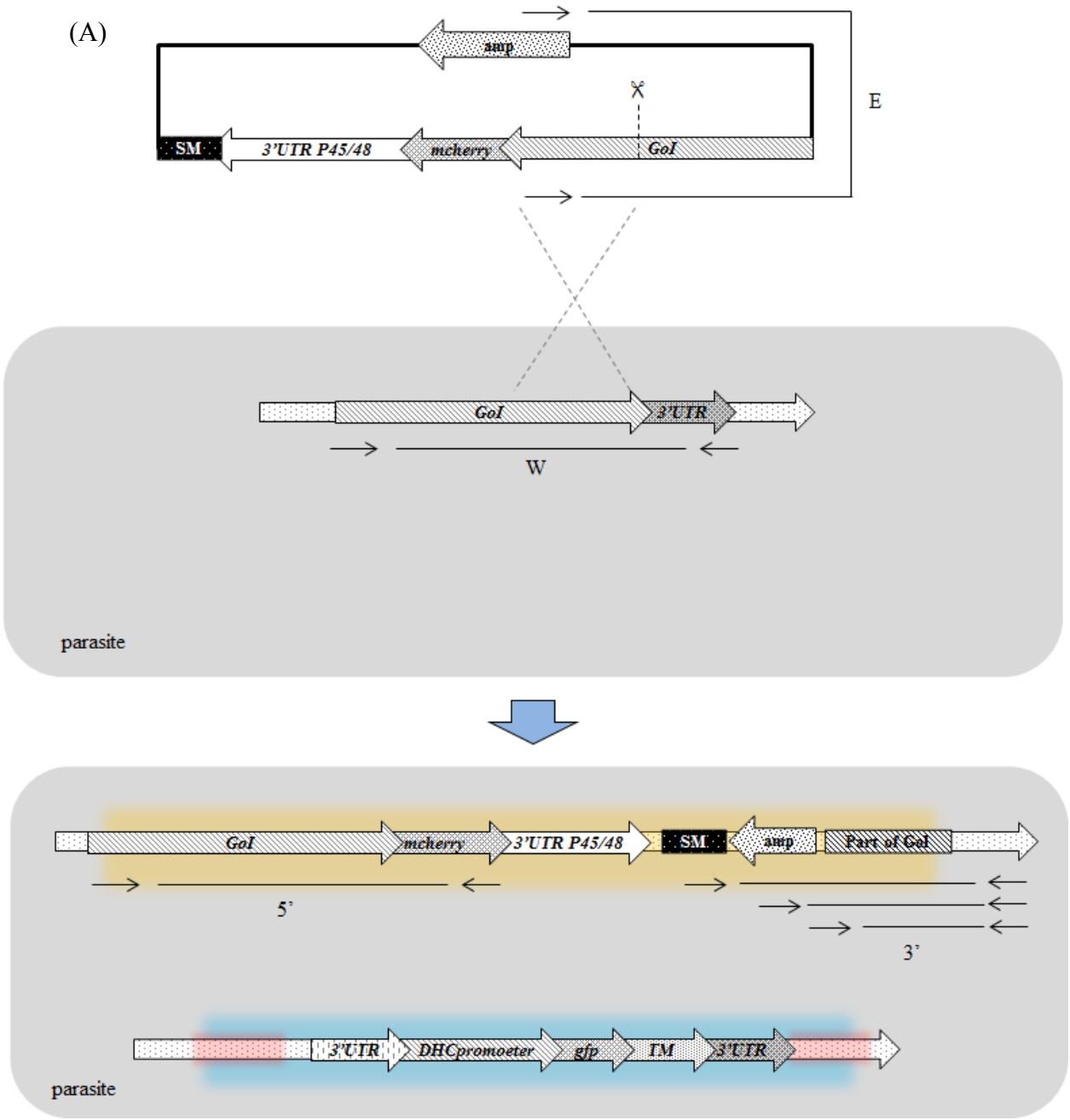

(B)

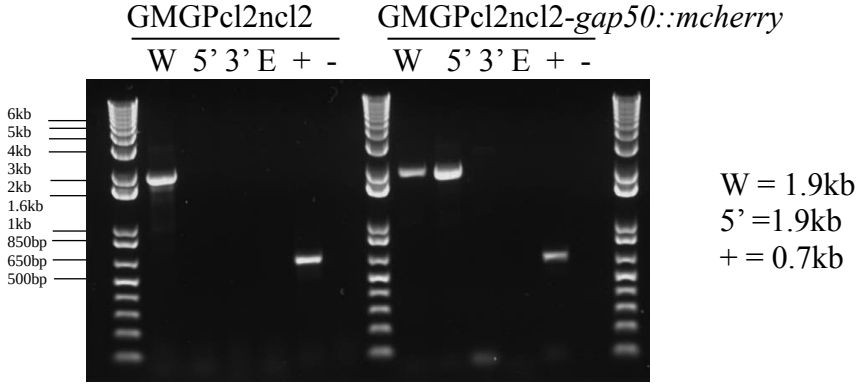

W = 1.9kb
5' =1.9kb
+ = 0.7kb

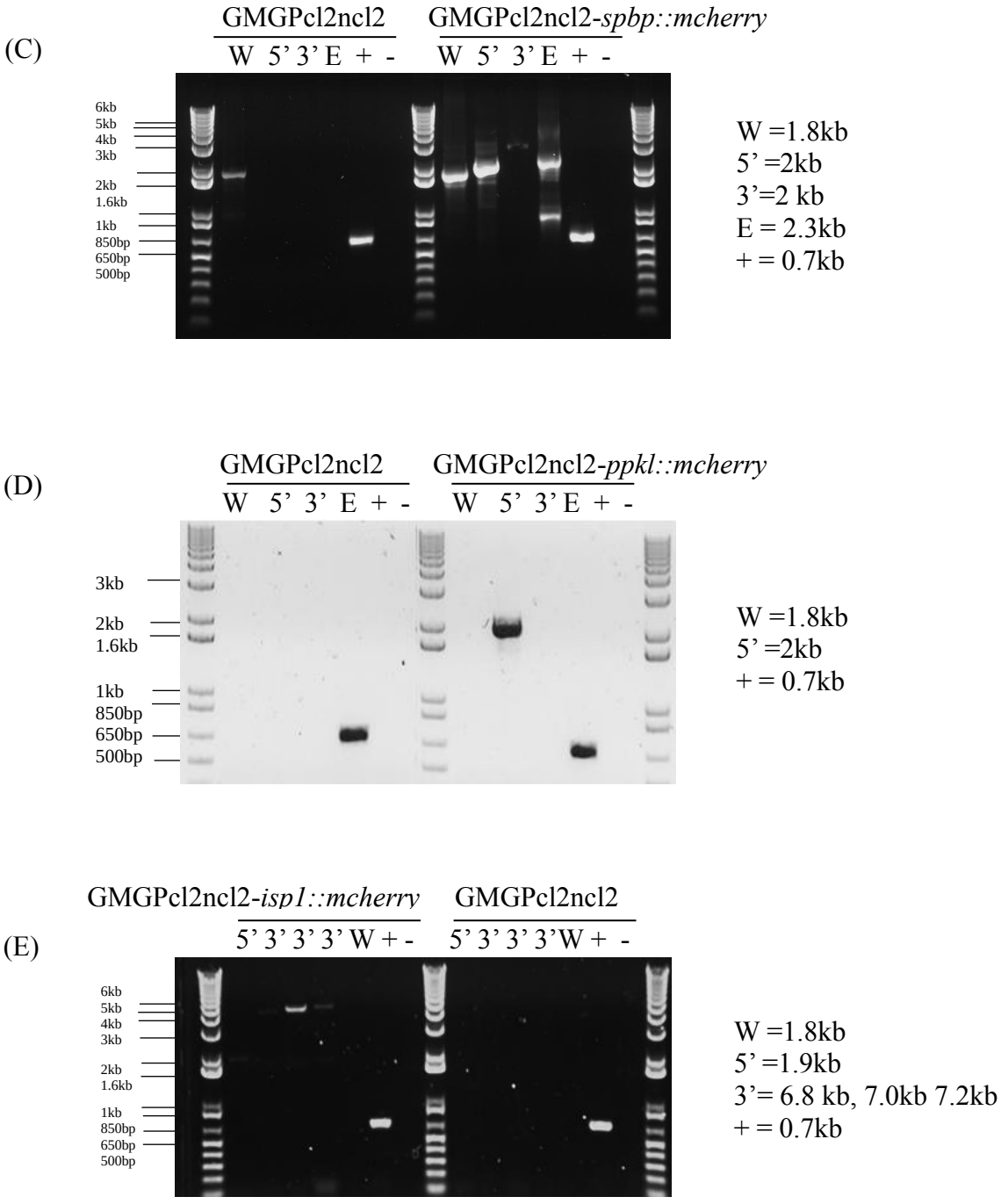

Figure 4.3: Generation of polarity markers *P. berghei* parasites.

(A) Schematic representation of the generation of polarity marker *P. berghei* parasites as described in text. (B) Diagnostic PCR showing integration of the *gap50::mcherry* construct at the 5' end (C) the *spbp::mcherry* construct as the 5' end (D) the *ppkl::mcherry* construct at the 5' end (E) *isp1::mcherry* construct as 5' and 3' end in the genome of GMGPcl2ncl2 parasites. W- Wild type, E- Episome

4.4 Analysis of the point of male gamete fusion hypothesis

To assess the hypothesis that the point of male gamete fusion is the point of emergence of apical bud in developing ookinetes, live fluorescent microscopy was performed. Live fluorescence microscopy verified the apical localization of PPKL::mCherry in the ookinetes obtained from pre-cloned GMGPcl2ncl2-*ppkl::mcherry* parasites with cytoplasmic green fluorescence possibly coming from the green male gamete (figure 4.4.1 A).

Live fluorescence microscopy performed on gametocytes enriched GMGPcl2ncl2-*gap50::mcherry* parasite suggests the presence of GAP50::mCherry in un-activated male gametocytes (figure 4.4.1 B), however, female gametocytes can be clearly differentiated from male gametocytes as they (female gametocytes) do not show green fluorescence. Localization of GAP50 in GMGPcl2ncl2-*gap50::mcherry* female gametocytes approximately within 30 minutes of activation suggesting polar localization of GAP50::mCherry and a small nucleus associated with green fluorescence on the surface (figure 4.4.2 A to C), probably identifying fusion of a green microgamete with the activated red female gamete. At 1.5 hpa, a point of microgamete fusion (a green dot) is clearly visible on the surface of red zygote (figure 4.4.2 D, E). At 5hpa, 6hpa and 8hpa, a point of microgamete fusion (a green dot) is generally noticeable on the surface of red zygotes and retorts (figure 4.4.2 F-i, F-ii, F-iii, G-ii, H-i), however, occasionally green fluorescence appears to be distributed over the surface of zygote as a smear/ multiple points (figure 4.4.2 F-iv, G-i, G-iii and H-ii, H-iii). At 24hpa, multiple green points were observable on the surface of ookinete (figure 4.4.2 I) unlike the green cytoplasmic fluorescence as in GMGPcl2ncl2-*ppkl::mcherry* ookinetes (figure 4.4.1 A).

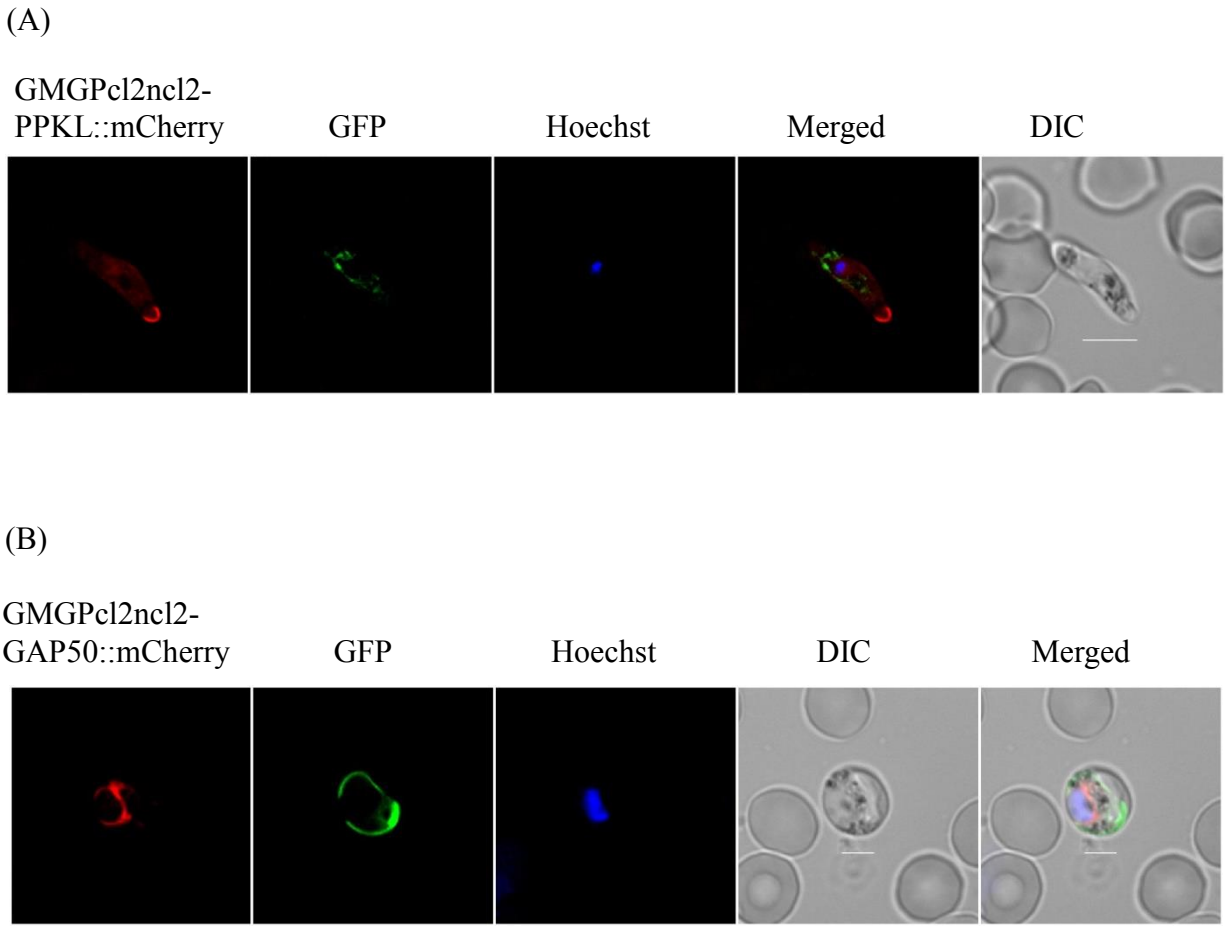

Figure 4.4.1 Localization of mCherry tagged ookinete development markers.

(A) Ookinetes of GMGPcl2ncl2-*ppkl::mcherry* showing PPKL localization at the apical bud. Live images of parasites, obtained from non-phenyhydrazine treated mouse, taken on Deltavision microscope - deconvoluted single slice. (B) Un-activated male gametocyte of GMGPcl2ncl2-*gap50::mcherry* parasites. Deconvoluted single slice images taken on deltavision. Scale bar 3 μm.

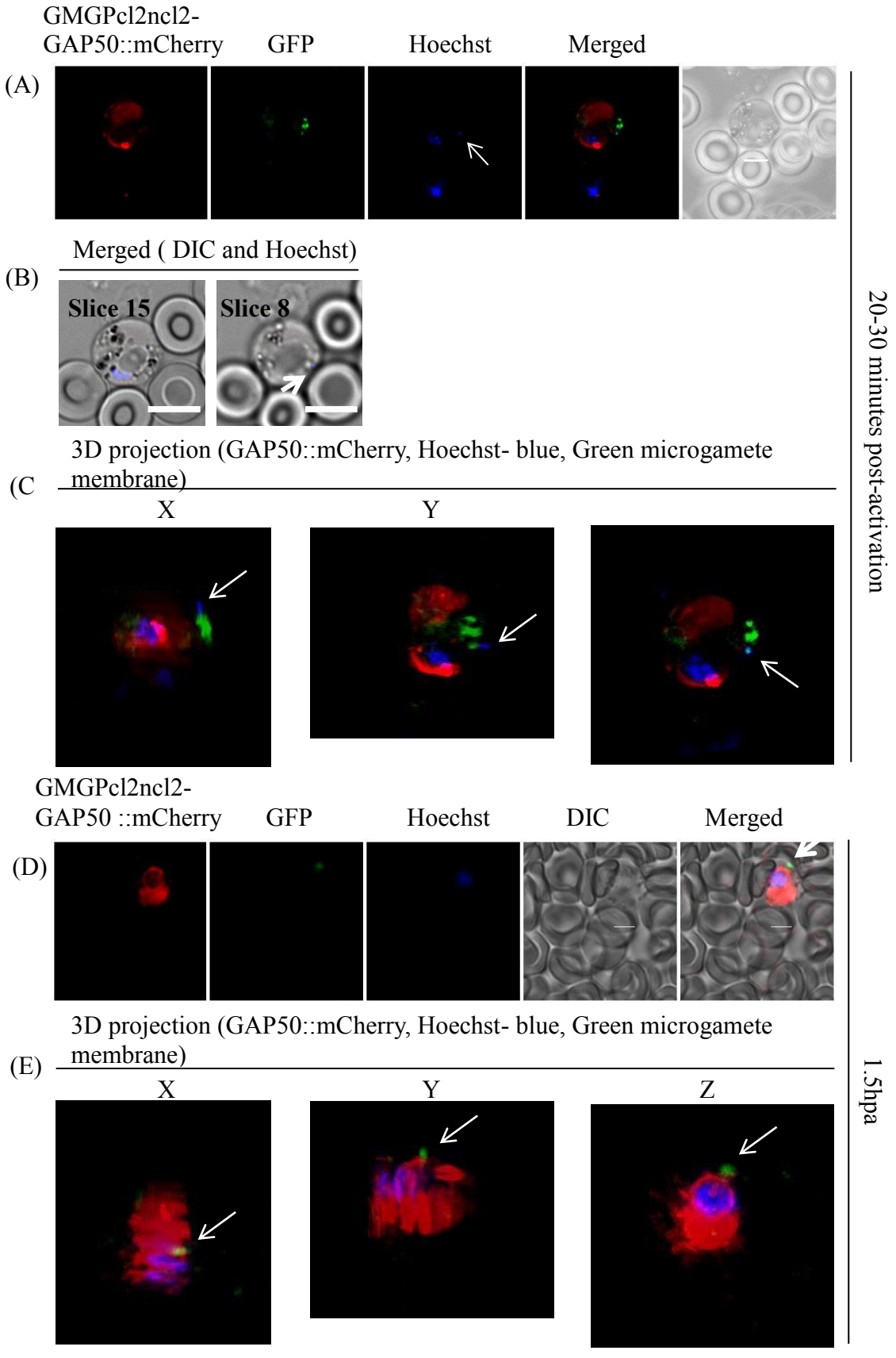
GMGPcl2ncl2-GAP50::mCherry
GFP
Hoechst
Merged
(A)
Merged (DIC and Hoechst)
(B)
Slice 15
Slice 8
3D projection (GAP50::mCherry, Hoechst- blue, Green microgamete membrane)
(C
X
Y
20-30 minutes post-activation
GMGPcl2ncl2-GAP50 ::mCherry
GFP
Hoechst
DIC
Merged
(D)
3D projection (GAP50::mCherry, Hoechst- blue, Green microgamete membrane)
(E)
X
Y
Z
1.5hpa

(F) GAP50::mCherry, Blue-Hoechst, Green membrane of male gamete (GMGPcl2ncl2-*gap50::mcherry* parasites)

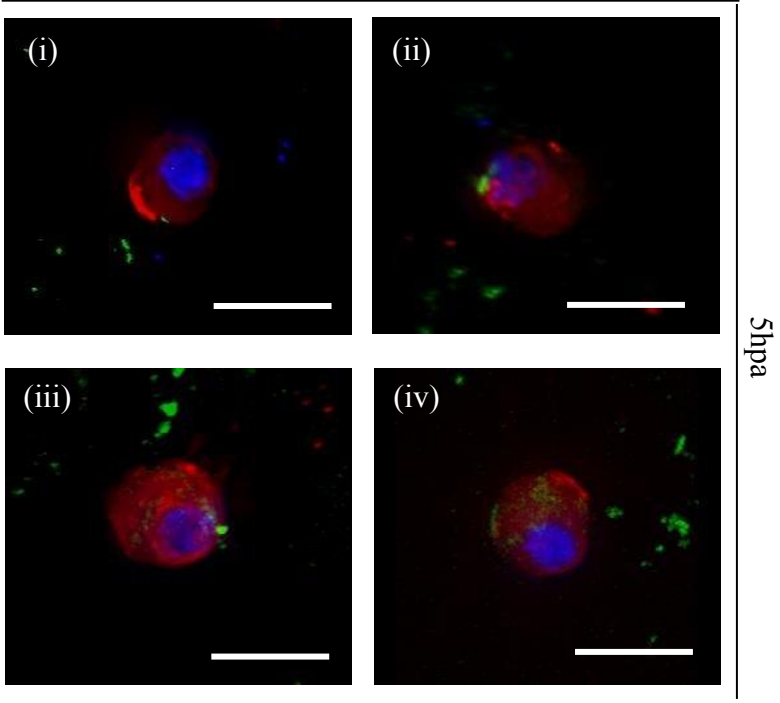

(G GAP50::mCherry, Blue-Hoechst, Green membrane of male gamete (GMGPcl2ncl2-*gap50::mcherry*)

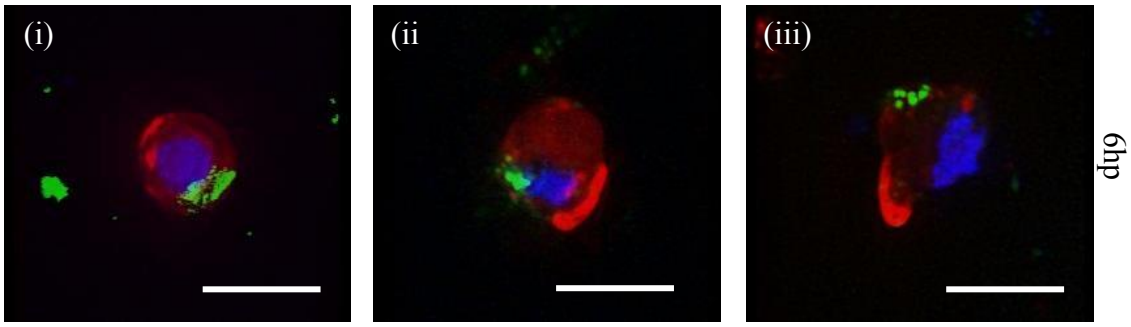

(H GAP50::mCherry, Blue-Hoechst, Green membrane of male gamete

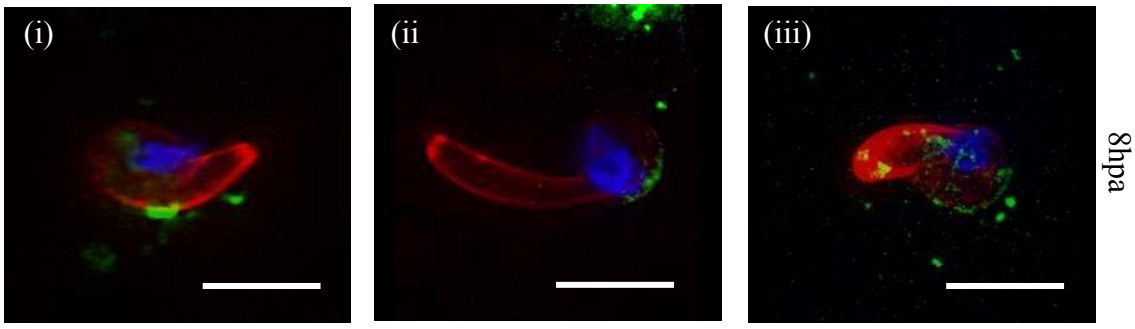

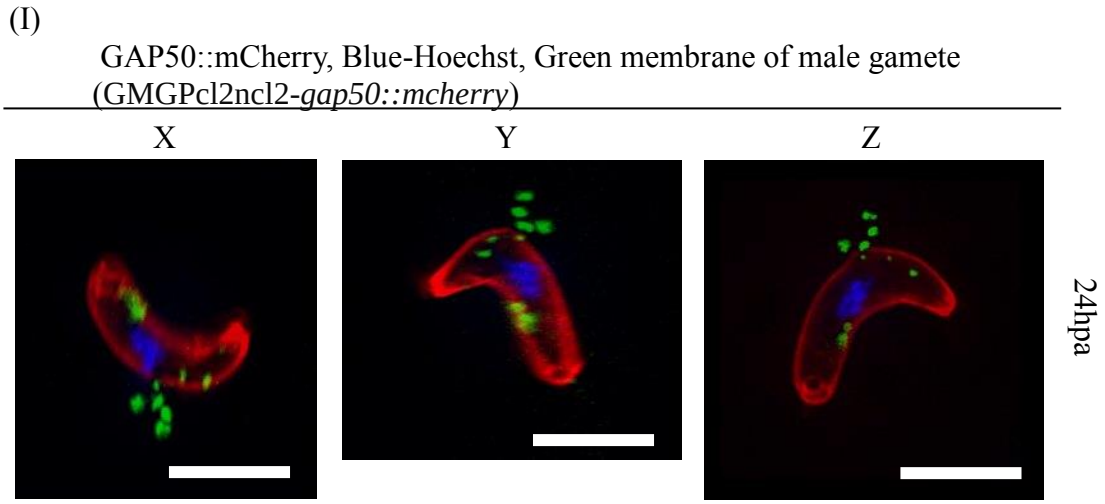

Figure 4.4.2 Point of male gamete fusion with respect to point of emergence of apical bud.

(A) Quick projection images showing a green microgamete attached (see white arrow) to red female gamete and (B) merged DIC and Hoechst (Deltavision deconvoluted single slice) images showing nucleus of male gamete attached to the surface female gamete. Slice 15 showing female nucleus and slice 8 showing male nucleus (see white arrow). (C) Deltavision deconvoluted 3D projection across X,Y and Z axis of a green male gamete attached to red female gamete shown in A. White arrows show nucleus of male gamete. (D) 1.5h zygote showing a green point over the surface of red female gamete and (E) Deltavision deconvoluted 3D projection of the 1.5h zygote across X,Y and Z axis. White arrows show green dots. (F) Zygote showing either a green point (i, ii and iii) or the green patch (iv) over the surface 5h zygote. (G) 6h retorts showing either a green point (ii) or the green patch/ multiple points (i and iii) over the surface. (H) 8h retorts showing either a green point (i) or the green patch (ii and iii) over the surface. (I) Deltavision deconvoluted 3D projections of ookinete across X,Y and Z axis showing green fluorescence over the red surface. Deconvoluted deltavision images of live parasites obtained from non-phenyhydrazine treated mice. Scale bar 3 μm for A and D, scale bar 5 μm for B, C, E to J.

4.5 Discussion, challenges and outlook of fusion project

Our results from Chapter 3 suggested that despite of knockdown of PbRab11A post-activation of gametocytes, the spherical cells that are presumed to be the resulting 24hpa forms still appeared to have a defined polarity. IMC markers and therefore the complete IMC is apically oriented with prominent apical bud, although clearly the banana shape morphology of the ookinete does not develop. Therefore, we concluded that Rab11A does not have a role in the establishment of zygote polarity. Hence, we would like to examine how polarity is established in *Plasmodium* zygote. One hypothesis is that the point of microgamete fusion cues for the point of emergence of apical bud in the *P. berghei* zygote. Consequently, we wanted to investigate if there is a correlation between the point of male gamete fusion and the emergence of focal point (apical bud) in the *P. berghei* zygote. Recently, it has been shown that polarity in *P. berghei* zygote is marked by ISP1 and that PPKL accumulated at the apical bud (Philip, Vaikkinen et al. 2012) of the *P. berghei* zygote is essential for the normal ookinete morphological development. Our current data show that GAP45 accumulates at the focal point at 4h zygote (Chapter 3- figure 3.5.1). It is also known that GAP50 localizes to the apical bud during ookinete development (K. Hughes- Waters group, unpublished data). Therefore, it is intriguing to monitor the fertilization process in several parasite lines generated, to enable analysis of polarity development with respect to the point of microgamete fusion, are as follows:

1) Membrane localized green male gametocytes::membrane localized red female gametocytes line (GMGPcl2ncl2-RFGP)
2) Membrane localised green male gametocytes and *ppkl::mcherry* (GMGPcl2ncl2-*ppkl::mcherry*)
3) Membrane localised green male gametocytes and *gap50::mcherry* (GMGPcl2ncl2-*gap50::mcherry*)
4) Membrane localized green male gametocytes and *isp1::mcherry* (GMGPcl2ncl2-*isp1::mcherry*)
5) Membrane localized green male gametocytes and *spindle pole body protein::mcherry* (GMGPcl2ncl2-*spbp::mcherry*)

These lines were all successfully generated and verified by PCR for correct plasmid integration. ISP1, SPBP were not visible via fluorescence microscopy, however, molecular diagnostics PCRs confirmed the correct plasmid integration at at-least at one of the ends (figure 5.3.1) – a finding that is often typical of single cross over integration events in this parasite. Lack of fluorescence could be because of the low expression levels of SPBP. Furthermore, a C-terminal tag on SPBP might be lethal to the parasite and so alternatively, N-terminal tagging might be useful. We attempted to express ISP1::mCherry under the control of endogenous *isp1* 5'UTR and P48/45 3'UTR, however, again we could not detect the expression of ISP1::mCherry. Therefore, replacing P48/45 3'UTR with those used by (Poulin, Patzewitz et al. 2013) might be beneficial to express ISP1::mCherry. Elimination of the episomes, parasite cloning and confirmation of plasmid integration at both the ends by Southern blotting, protein size confirmation by western blotting and perhaps even more sensitive microscopes are all needed to generate stable transgenic *P. berghei* parasites, to confirm the tag of respective proteins and to visualize mCherry tagged low expressing proteins. Cloning and microscopic analysis of GMGPcl2ncl2-RFGP parasite has to be completed although the data shown here are valid since the fluorescent signal allows identification of the relevant parasite forms.

Initial microscopy observation of the GMGPcl2ncl2-*ppkl::mcherry* parasites suggest localization of PPKL::mCherry at the apical bud of the ookinete and green fluorescence appeared cytoplasmic (figure 4.4.1 A). Initial microscopy experiments using GMGPcl2ncl2-*gap50::mcherry* have shown that the point of male gamete fusion is generally visible until first 5 to 6hpa and may be different from the point of emergence of apical bud (figure 4.4.2), however, more repeats are needed with other fluorescently tagged parasite lines to confirm the correlation of point of male gamete fusion with the point of emergence of apical bud. Also this hypothesis needs to be statistically significant. Analysis by diagnostic PCRs, parasite cloning and western blotting of GMGPcl2ncl2-*ppkl::mcherry* and diagnostic PCRs and western blotting of GMGPcl2ncl2-*gap50::mcherry* has to be done although again the fluorescent signals allow valid observations to be made. In GMGPcl2ncl2-*gap50::mcherry* parasites, it appears that green point on the surface of red females is visible, however, the auto fluorescence seen in WT parasites (as shown in Chapter 3-figure 3.2.2 C,) needs to be distinguished from the real GFP fluorescence of male gamete membrane by keeping WT parasite as a negative control. However, keeping WT ookinete cultures (obtained from non-phenylhydrazine treated mice) as a control will be time consuming due to the low amount of production of gametocytes (Chapter 2, Methods 2.1.2 f for

details about phenyl hydrazine treatment) and hence lengthening the time to locate WT parasites in a microscopic field therefore reducing the chances of getting images at a particular time point. Therefore, further repeats with more than one fluorescently tagged parasite lines mentioned above along with fast imaging techniques or purifying zygotes with MACS columns would be beneficial. Along with GMGPcl2ncl2-*gap50::mcherry*, GMGPcl2ncl2-*isp1::mcherry* parasite line would also be better to study the point of gamete fusion as ISP1 has been shown to present as a single dot on the surface of female gametocytes. However, GMGPcl2ncl2-RFGP would give more information about membrane fusion and would enable to study co-localization of green and red fluorescence of membranes. These lines will be used for further analysis of the fusion and integration events through more focussed microscopy analysis on live cells. To increase the chance of seeing the less abundant fluorescently tagged proteins that we failed to see on live cell imaging (such as SPBP) will be visualized in fixed cells with the use of an antibody raised against less abundant proteins/ raised against the fluorescent tag.

From the above experiments, it seems that the point of emergence of apical bud may be different from point of fusion of male gamete. The point of apical budding may be chosen randomly as discussed in Chapter 1: General Introduction under 1.6 or may be selected at a particular angle to the point of male gamete fusion/axis of polarity, however, signals from male gamete such as Centrin-1 (H. Patil, Waters group, unpublished data) and other possible unknown markers from male gamete may be vital for the development of zygote into the ookinete by conceivably triggering, at least some of, the signalling processes essential for zygote to ookinete development. Clearly, studying fertilization using fluorescently tagged cell lines during the zygote to ookinete transition should help to understand if the point of male gamete fusion correlates at all with the establishment/ development of zygote polarity or activation of signalling pathways needed for transition into the ookinete. More experimental repeats and robust experiments with the tools described in this chapter will certainly shed more light on the fundamental question of how polarity is established in the *P. berghei* zygotes.

Chapter 5: Future research directions

5.0 Future research directions

Current results allow us to predict that Rab11A is not involved in the establishment of zygote polarity, mitosis, activation of stored mRNAs nor extensive reactivation of transcription but in the establishment of the point of outgrowth of the retort form and conceivably in the delivery of plasma membrane to the growing apical outgrowth which is expected to be a coordinated process of Rab11A mediated membrane trafficking and cytoskeletal dynamics and is also essential for mosquito transmission.

Since, putting a cut off FPKM 10 in RNA-Seq data does not provide clear indication of up/down-regulation of transcripts, quantitative proteomic analysis of $_{p}$*clag::rab11a* parasites and therefore combining proteomic data with RNA-Seq would give more clear results.

The IMC and plasma membrane were shown to be separated by *C. septicum* α-toxin treatment in *T. gondii* (Wichroski, Melton et al. 2002, Gaskins, Gilk et al. 2004) and 20h spherical zygotes of *gap45* promoter swap have their IMC-microtubules detached from the plasma membrane (Sebastian, Brochet et al. 2012). This parasite line and *C. septicum* α-toxin treatment can be used to examine if Rab11A is exclusively associated with plasma membrane or IMC or both, by immunofluorescence microscopy including super-resolution microscopy, immunoelectron microscopy of fixed parasites with anti-Rab11A antibody along with either anti-IMC marker antibody (e.g. GAP45, GAP50) or with anti-Plasma membrane marker antibody (e.g. surface marker P25).

Additionally, detergent-based extraction of microtubules from plasma membrane and IMC (negative staining) has been studied in the *Plasmodium fallax* merozoite (Aikawa 1967) and *T. gondii* tachyzoite (Lemgruber, Kloetzel et al. 2009). Our attempts to perform negative staining and immunoelectron microscopy on *P. berghei* WT ookinetes were unsuccessful. Optimization of these protocols for *P. berghei* ookinetes will permit immunoelectron and immunofluorescence studies with anti-Rab11A antibody and demonstrate if PbRab11A interacts with microtubules. Recently, (Hehnly and Doxsey 2014) has shown that Rab11 vesicles are involved in the extension and the organization of microtubules. Also, we noticed apically-concentrated localization of Rab11A similar to SPBP . Therefore, it will be interesting to study whether or not Rab11A vesicles are associated with microtubules extension/organization or delivery of microtubule components and if Rab11A colocalizes with SPBP at apical complex of *P. berghei* zygotes.

PI4K and Rab11A are predicted to be involved in the membrane delivery in *P. falciparum* during cytokinesis (McNamara, Lee et al. 2013). Furthermore, I propose that Rab11A endosomes donate plasma membrane as well as regulate morphology probably through the interaction of microtubules and other unknown markers during the retort outgrowth of the *P. berghei* zygote (i.e. zygote to ookinete transition). It will be interesting to examine if Rab11A endosomes are involved in the transport of lipids and proteins to the growing plasma membrane in *P. berghei* zygotes. mRNA transport and localized translation appear to be important for a number of cellular events, including axis formation, and mRNA are transported as ribonucleo-protein particles [reviewed in (Donnelly, Fainzilber et al. 2010, Czaplinski 2014)]. Rab11 and Rab6 are predicted to be involved in the localization of *osk* mRNA in the *Drosophila* oocyte (Dollar, Struckhoff et al. 2002, Januschke, Nicolas et al. 2007). Similarly, whether or not Rab11A vesicles are involved in the transportation of (translationally stored) mRNAs to the growing apical bud of *P. berghei* zygotes can be studied by the combination of fluorescent in situ hybridization as well as immunofluorescence microscopy.

Anti-PbRab11A and anti-PbRab11B antibodies raised in this study will be useful to identify common interacting proteins of PbRab11A and PbRab11B and can be utilized to extract Rab11A endosomes allowing to perform the mass spectroscopic analysis for identification of Rab11A and Rab11B vesicle content. Further investigations to determine Rab11A interacting proteins in *Plasmodium* will expedite the understanding of Rab11A function.

Moreover, Rab11A tagged with fluorescent proteins such as iLOV or GFP to observe the flow of Rab11A containing vesicles in live zygotes and ookinetes with continuous live microscopy will help to understand whether or not Rab11A containing vesicles flow towards the apical complex.

However, we are also studying the hypothesis of point of male gamete fusion with respective to the point of emergence of the apical bud in *P. berghei* zygotes. To study this hypothesis, I have generated some fluorescent parasite lines. Some of these lines show the development of IMC in growing zygotes and feasibility of the strategy of ‘point of gamete fusion’, however, more detailed analysis and number of experimental repeats are required to conclude whether or not the point of gamete fusion cues directly or indirectly for the point of emergence of the apical bud.

It is also appealing to investigate if the surface area of young zygotes (first few hour post-activation) is any greater than the surface area of mature banana shape ookinetes. This will allow to understand whether and how much additional plasma membrane is synthesized during the zygoe –ookinete transition. Our GMGPcl2ncl2-RFGP parasite line may allow such

measurement of surface areas of young zygotes and ookinetes. Also, calculating the surface area of *$_p$clag::rab11a* young zygotes and spherical ookinetes will allow an investigation of the possibility that the plasma membrane delivery system is active or mis-regulated in absence of Rab11A.

Moreover, whether or not a male gamete donates any fertilization markers (such as CentrinI - H. Patil, unpublished data) to the female gamete, allowing zygote to coordinate cellular events, to establish and develop the polarity will be interesting.

Rab11B mediated transport has been proposed to be associated with biogenesis of IMC in *T. gondii* (Agop-Nersesian, Egarter et al. 2010). Correspondingly, it is exciting to examine the roles of Rab11B in *P. berghei* zygote development.

In summary, studying the above mechanisms will allow some of the fundamental questions about ookinete development to be answered, such as

- Does quantitative proteome analysis of *$_p$clag::rab11a* parasites provide more sensitive measure of cell morphological arrest?
- Does Rab11A interact with microtubules, its extension and organization in *P. berghei* zygotes?
- Is Rab11A associated with plasma membrane delivery? and does plasma membrane delivery take place in *P. berghei* zygotes?
- Does Rab11A colocalizes with SPBP in *P. berghei* apical complex?
- Is there mRNA transport and localized translation in *P. berghei* zygotes? and how these processes are regulated?
- Which are the common and particular interacting proteins of Rab11A and Rab11B?
- What is the content of Rab11A and Rab11B vesicles and their directionality?
- How polarity is established and developed in *P. berghei* zygotes? Does the point of gamete fusion cue for the point of emergence of apical bud?
- Is ookinete surface area greater than young zygote?
- Does a male gamete donate fertilization markers to a female gamete and assist in the establishment and development of polarity in *P. berghei* zygotes?
- Is Rab11B associated with IMC biogenesis in *P. berghei* zygotes?

Answering these fundamental questions may lead to develop novel anti-transmission blocking strategies, and these zygote developmental processes will also be correlated with the

developmental events of other infectious forms of *Plasmodium* such as sporozoites and merozoites.

6. References

Agop-Nersesian, C., S. Egarter, G. Langsley, B. J. Foth, D. J. Ferguson and M. Meissner (2010). "Biogenesis of the inner membrane complex is dependent on vesicular transport by the alveolate specific GTPase Rab11B." PLoS Pathog **6**(7): e1001029.

Agop-Nersesian, C., B. Naissant, F. Ben Rached, M. Rauch, A. Kretzschmar, S. Thiberge, R. Menard, D. J. Ferguson, M. Meissner and G. Langsley (2009). "Rab11A-controlled assembly of the inner membrane complex is required for completion of apicomplexan cytokinesis." PLoS Pathog **5**(1): e1000270.

Ai, E. and A. R. Skop (2009). "Endosomal recycling regulation during cytokinesis." Commun Integr Biol **2**(5): 444-447.

Aikawa, M. (1967). "Ultrastructure of the pellicular complex of Plasmodium fallax." J Cell Biol **35**(1): 103-113.

Aikawa, M., R. Carter, Y. Ito and M. M. Nijhout (1984). "New observations on gametogenesis, fertilization, and zygote transformation in Plasmodium gallinaceum." J Protozool **31**(3): 403-413.

Akogbeto, M. C., R. Djouaka and H. Noukpo (2005). "[Use of agricultural insecticides in Benin]." Bull Soc Pathol Exot **98**(5): 400-405.

Al-Khattaf, F. S., A. Z. Tremp and J. T. Dessens (2014). "Plasmodium alveolins possess distinct but structurally and functionally related multi-repeat domains." Parasitol Res.

Alano, P. and R. Carter (1990). "Sexual differentiation in malaria parasites." Annu Rev Microbiol **44**: 429-449.

Alexander, D. L., J. Mital, G. E. Ward, P. Bradley and J. C. Boothroyd (2005). "Identification of the moving junction complex of Toxoplasma gondii: a collaboration between distinct secretory organelles." PLoS Pathog **1**(2): e17.

Allary, M., J. Schrevel and I. Florent (2002). "Properties, stage-dependent expression and localization of Plasmodium falciparum M1 family zinc-aminopeptidase." Parasitology **125**(Pt 1): 1-10.

Aly, A. S. and K. Matuschewski (2005). "A malarial cysteine protease is necessary for Plasmodium sporozoite egress from oocysts." J Exp Med **202**(2): 225-230.

Aly, A. S., A. M. Vaughan and S. H. Kappe (2009). "Malaria parasite development in the mosquito and infection of the mammalian host." Annu Rev Microbiol **63**: 195-221.

Amino, R., S. Thiberge, B. Martin, S. Celli, S. Shorte, F. Frischknecht and R. Ménard (2006). "Quantitative imaging of Plasmodium transmission from mosquito to mammal." Nat Med **12**(2): 220-224.

An, X. and N. Mohandas (2008). "Disorders of red cell membrane." Br J Haematol **141**(3): 367-375.

Anamika, N. Srinivasan and A. Krupa (2005). "A genomic perspective of protein kinases in Plasmodium falciparum." Proteins **58**(1): 180-189.

Andenmatten, N., S. Egarter, A. J. Jackson, N. Jullien, J. P. Herman and M. Meissner (2013). "Conditional genome engineering in Toxoplasma gondii uncovers alternative invasion mechanisms." Nat Methods **10**(2): 125-127.

Anderson-White, B., J. R. Beck, C. T. Chen, M. Meissner, P. J. Bradley and M. J. Gubbels (2012). "Cytoskeleton assembly in Toxoplasma gondii cell division." Int Rev Cell Mol Biol **298**: 1-31.

Angrisano, F., Y. H. Tan, A. Sturm, G. I. McFadden and J. Baum (2012). "Malaria parasite colonisation of the mosquito midgut--placing the Plasmodium ookinete centre stage." Int J Parasitol **42**(6): 519-527.

Anifandis, G., C. Messini, K. Dafopoulos, S. Sotiriou and I. Messinis (2014). "Molecular and cellular mechanisms of sperm-oocyte interactions opinions relative to in vitro fertilization (IVF)." Int J Mol Sci **15**(7): 12972-12997.

Antinori, S., L. Galimberti, L. Milazzo and M. Corbellino (2013). "Plasmodium knowlesi: the emerging zoonotic malaria parasite." Acta Trop **125**(2): 191-201.

Apodaca, G., L. A. Katz and K. E. Mostov (1994). "Receptor-mediated transcytosis of IgA in MDCK cells is via apical recycling endosomes." J Cell Biol **125**(1): 67-86.

Aregawi, M. W., A. S. Ali, A. W. Al-mafazy, F. Molteni, S. Katikiti, M. Warsame, R. J. Njau, R. Komatsu, E. Korenromp, M. Hosseini, D. Low-Beer, A. Bjorkman, U. D'Alessandro, M. Coosemans and M. Otten (2011). "Reductions in malaria and anaemia case and death burden at hospitals following scale-up of malaria control in Zanzibar, 1999-2008." Malar J **10**: 46.

Armstrong, C. M. and D. E. Goldberg (2007). "An FKBP destabilization domain modulates protein levels in Plasmodium falciparum." Nat Methods **4**(12): 1007-1009.

Arrighi, R. B. and H. Hurd (2002). "The role of Plasmodium berghei ookinete proteins in binding to basal lamina components and transformation into oocysts." Int J Parasitol **32**(1): 91-98.

Asale, A., Y. Getachew, W. Hailesilassie, N. Speybroeck, L. Duchateau and D. Yewhalaw (2014). "Evaluation of the efficacy of DDT indoor residual spraying and long-lasting insecticidal nets against insecticide resistant populations of Anopheles arabiensis Patton (Diptera: Culicidae) from Ethiopia using experimental huts." Parasit Vectors **7**: 131.

Ashley, E. A., J. Recht and N. J. White (2014). "Primaquine: the risks and the benefits." Malar J **13**: 418.

Attal, G. and G. Langsley (1996). "A Plasmodium falciparum homologue of a rab specific GDP dissociation inhibitor." Mol Biochem Parasitol **79**(1): 91-95.

Aurrecoechea, C., J. Brestelli, B. P. Brunk, J. Dommer, S. Fischer, B. Gajria, X. Gao, A. Gingle, G. Grant, O. S. Harb, M. Heiges, F. Innamorato, J. Iodice, J. C. Kissinger, E. Kraemer, W. Li, J. A. Miller, V. Nayak, C. Pennington, D. F. Pinney, D. S. Roos, C. Ross, C. J. Stoeckert, C. Treatman and

H. Wang (2009). "PlasmoDB: a functional genomic database for malaria parasites." Nucleic Acids Res **37**(Database issue): D539-543.

Baer, K., C. Klotz, S. H. Kappe, T. Schnieder and U. Frevert (2007). "Release of hepatic Plasmodium yoelii merozoites into the pulmonary microvasculature." PLoS Pathog **3**(11): e171.

Baker, D. A. (2010). "Malaria gametocytogenesis." Mol Biochem Parasitol **172**(2): 57-65.

Bannister, L. H., J. M. Hopkins, R. E. Fowler, S. Krishna and G. H. Mitchell (2000). "Ultrastructure of rhoptry development in Plasmodium falciparum erythrocytic schizonts." Parasitology **121 (Pt 3)**: 273-287.

Barale, J. C., T. Blisnick, H. Fujioka, P. M. Alzari, M. Aikawa, C. Braun-Breton and G. Langsley (1999). "Plasmodium falciparum subtilisin-like protease 2, a merozoite candidate for the merozoite surface protein 1-42 maturase." Proc Natl Acad Sci U S A **96**(11): 6445-6450.

Barry, A. E. and A. Arnott (2014). "Strategies for designing and monitoring malaria vaccines targeting diverse antigens." Front Immunol **5**: 359.

Baton, L. A. and L. C. Ranford-Cartwright (2005). "Spreading the seeds of million-murdering death: metamorphoses of malaria in the mosquito." Trends Parasitol **21**(12): 573-580.

Baum, J., T. W. Gilberger, F. Frischknecht and M. Meissner (2008). "Host-cell invasion by malaria parasites: insights from Plasmodium and Toxoplasma." Trends Parasitol **24**(12): 557-563.

Baum, J., A. T. Papenfuss, G. R. Mair, C. J. Janse, D. Vlachou, A. P. Waters, A. F. Cowman, B. S. Crabb and T. F. de Koning-Ward (2009). "Molecular genetics and comparative genomics reveal RNAi is not functional in malaria parasites." Nucleic Acids Res **37**(11): 3788-3798.

Baum, J., D. Richard, J. Healer, M. Rug, Z. Krnajski, T. W. Gilberger, J. L. Green, A. A. Holder and A. F. Cowman (2006). "A conserved molecular motor drives cell invasion and gliding motility across malaria life cycle stages and other apicomplexan parasites." J Biol Chem **281**(8): 5197-5208.

Behnia, R. and S. Munro (2005). "Organelle identity and the signposts for membrane traffic." Nature **438**(7068): 597-604.

Beier, J. C. (1998). "Malaria parasite development in mosquitoes." Annu Rev Entomol **43**: 519-543.

Beier, J. C., J. R. Davis, J. A. Vaughan, B. H. Noden and M. S. Beier (1991). "Quantitation of Plasmodium falciparum sporozoites transmitted in vitro by experimentally infected Anopheles gambiae and Anopheles stephensi." Am J Trop Med Hyg **44**(5): 564-570.

Bergman, L. W., K. Kaiser, H. Fujioka, I. Coppens, T. M. Daly, S. Fox, K. Matuschewski, V. Nussenzweig and S. H. Kappe (2003). "Myosin A tail domain interacting protein (MTIP) localizes to the inner membrane complex of Plasmodium sporozoites." J Cell Sci **116**(Pt 1): 39-49.

Bianchi, E., B. Doe, D. Goulding and G. J. Wright (2014). "Juno is the egg Izumo receptor and is essential for mammalian fertilization." Nature **508**(7497): 483-487.

Billker, O., S. Dechamps, R. Tewari, G. Wenig, B. Franke-Fayard and V. Brinkmann (2004). "Calcium and a calcium-dependent protein kinase regulate gamete formation and mosquito transmission in a malaria parasite." Cell **117**(4): 503-514.

Billker, O., V. Lindo, M. Panico, A. E. Etienne, T. Paxton, A. Dell, M. Rogers, R. E. Sinden and H. R. Morris (1998). "Identification of xanthurenic acid as the putative inducer of malaria development in the mosquito." Nature **392**(6673): 289-292.

Billker, O., M. K. Shaw, G. Margos and R. E. Sinden (1997). "The roles of temperature, pH and mosquito factors as triggers of male and female gametogenesis of Plasmodium berghei in vitro." Parasitology **115 (Pt 1)**: 1-7.

Blackman, M. J. and L. H. Bannister (2001). "Apical organelles of Apicomplexa: biology and isolation by subcellular fractionation." Mol Biochem Parasitol **117**(1): 11-25.

Blackman, M. J., H. Fujioka, W. H. Stafford, M. Sajid, B. Clough, S. L. Fleck, M. Aikawa, M. Grainger and F. Hackett (1998). "A subtilisin-like protein in secretory organelles of Plasmodium falciparum merozoites." J Biol Chem **273**(36): 23398-23409.

Blagborough, A. M. and R. E. Sinden (2009). "Plasmodium berghei HAP2 induces strong malaria transmission-blocking immunity in vivo and in vitro." Vaccine **27**(38): 5187-5194.

Bojang, K. A. (2006). "RTS,S/AS02A for malaria." Expert Rev Vaccines **5**(5): 611-615.

Boothroyd, J. C. and J. F. Dubremetz (2008). "Kiss and spit: the dual roles of Toxoplasma rhoptries." Nat Rev Microbiol **6**(1): 79-88.

Bosch, J., M. H. Paige, A. B. Vaidya, L. W. Bergman and W. G. Hol (2012). "Crystal structure of GAP50, the anchor of the invasion machinery in the inner membrane complex of Plasmodium falciparum." J Struct Biol **178**(1): 61-73.

Bousema, J. T., C. J. Drakeley, J. Kihonda, J. C. Hendriks, N. I. Akim, W. Roeffen and R. W. Sauerwein (2007). "A longitudinal study of immune responses to Plasmodium falciparum sexual stage antigens in Tanzanian adults." Parasite Immunol **29**(6): 309-317.

Bowman, S., D. Lawson, D. Basham, D. Brown, T. Chillingworth, C. M. Churcher, A. Craig, R. M. Davies, K. Devlin, T. Feltwell, S. Gentles, R. Gwilliam, N. Hamlin, D. Harris, S. Holroyd, T. Hornsby, P. Horrocks, K. Jagels, B. Jassal, S. Kyes, J. McLean, S. Moule, K. Mungall, L. Murphy, K. Oliver, M. A. Quail, M. A. Rajandream, S. Rutter, J. Skelton, R. Squares, S. Squares, J. E. Sulston, S. Whitehead, J. R. Woodward, C. Newbold and B. G. Barrell (1999). "The complete nucleotide sequence of chromosome 3 of Plasmodium falciparum." Nature **400**(6744): 532-538.

Boyle, M. J., D. W. Wilson and J. G. Beeson (2013). "New approaches to studying Plasmodium falciparum merozoite invasion and insights into invasion biology." Int J Parasitol **43**(1): 1-10.

Brabin, B. J. (1983). "An analysis of malaria in pregnancy in Africa." Bull World Health Organ **61**(6): 1005-1016.

Bradley, P. J., C. Ward, S. J. Cheng, D. L. Alexander, S. Coller, G. H. Coombs, J. D. Dunn, D. J. Ferguson, S. J. Sanderson, J. M. Wastling and J. C. Boothroyd (2005). "Proteomic analysis of rhoptry

organelles reveals many novel constituents for host-parasite interactions in Toxoplasma gondii." J Biol Chem **280**(40): 34245-34258.

Braks, J. A., B. Franke-Fayard, H. Kroeze, C. J. Janse and A. P. Waters (2006). "Development and application of a positive-negative selectable marker system for use in reverse genetics in Plasmodium." Nucleic Acids Res **34**(5): e39.

Brancucci, N. M., N. L. Bertschi, L. Zhu, I. Niederwieser, W. H. Chin, R. Wampfler, C. Freymond, M. Rottmann, I. Felger, Z. Bozdech and T. S. Voss (2014). "Heterochromatin protein 1 secures survival and transmission of malaria parasites." Cell Host Microbe **16**(2): 165-176.

Brecht, S., H. Erdhart, M. Soete and D. Soldati (1999). "Genome engineering of Toxoplasma gondii using the site-specific recombinase Cre." Gene **234**(2): 239-247.

Brochet, M., M. O. Collins, T. K. Smith, E. Thompson, S. Sebastian, K. Volkmann, F. Schwach, L. Chappell, A. R. Gomes, M. Berriman, J. C. Rayner, D. A. Baker, J. Choudhary and O. Billker (2014). "Phosphoinositide metabolism links cGMP-dependent protein kinase G to essential Ca^{2+} signals at key decision points in the life cycle of malaria parasites." PLoS Biol **12**(3): e1001806.

Bull, P. C., B. S. Lowe, M. Kortok and K. Marsh (1999). "Antibody recognition of Plasmodium falciparum erythrocyte surface antigens in Kenya: evidence for rare and prevalent variants." Infect Immun **67**(2): 733-739.

Bullen, H. E., C. J. Tonkin, R. A. O'Donnell, W. H. Tham, A. T. Papenfuss, S. Gould, A. F. Cowman, B. S. Crabb and P. R. Gilson (2009). "A novel family of Apicomplexan glideosome-associated proteins with an inner membrane-anchoring role." J Biol Chem **284**(37): 25353-25363.

Burke, J. E., A. J. Inglis, O. Perisic, G. R. Masson, S. H. McLaughlin, F. Rutaganira, K. M. Shokat and R. L. Williams (2014). "Structures of PI4KIIIβ complexes show simultaneous recruitment of Rab11 and its effectors." Science **344**(6187): 1035-1038.

Bushell, E. S., A. Ecker, T. Schlegelmilch, D. Goulding, G. Dougan, R. E. Sinden, G. K. Christophides, F. C. Kafatos and D. Vlachou (2009). "Paternal effect of the nuclear formin-like protein MISFIT on Plasmodium development in the mosquito vector." PLoS Pathog **5**(8): e1000539.

Calderaro, A., G. Piccolo, C. Gorrini, S. Rossi, S. Montecchini, M. L. Dell Anna, F. De Conto, M. C. Medici, C. Chezzi and M. C. Arcangeletti (2013). "Accurate identification of the six human Plasmodium spp. causing imported malaria, including Plasmodium ovale wallikeri and Plasmodium knowlesi." Malar J **12**(1): 321.

Carter, V., S. Shimizu, M. Arai and J. T. Dessens (2008). "PbSR is synthesized in macrogametocytes and involved in formation of the malaria crystalloids." Mol Microbiol **68**(6): 1560-1569.

Carvalho, T. A., M. G. Queiroz, G. L. Cardoso, I. G. Diniz, A. N. Silva, A. Y. Pinto and J. F. Guerreiro (2012). "Plasmodium vivax infection in Anajás, State of Pará: no differential resistance profile among Duffy-negative and Duffy-positive individuals." Malar J **11**: 430.

Cavalier-Smith, T. (1993). "Kingdom protozoa and its 18 phyla." Microbiol Rev **57**(4): 953-994.

Chakrabarti, D., T. Azam, C. DelVecchio, L. Qiu, Y. I. Park and C. M. Allen (1998). "Protein prenyl transferase activities of Plasmodium falciparum." Mol Biochem Parasitol **94**(2): 175-184.

Chakrabarti, D., T. Da Silva, J. Barger, S. Paquette, H. Patel, S. Patterson and C. M. Allen (2002). "Protein farnesyltransferase and protein prenylation in Plasmodium falciparum." J Biol Chem **277**(44): 42066-42073.

Chant, J. (1994). "Cell polarity in yeast." Trends Genet **10**(9): 328-333.

Chapman, S., C. Faulkner, E. Kaiserli, C. Garcia-Mata, E. I. Savenkov, A. G. Roberts, K. J. Oparka and J. M. Christie (2008). "The photoreversible fluorescent protein iLOV outperforms GFP as a reporter of plant virus infection." Proc Natl Acad Sci U S A **105**(50): 20038-20043.

Chattopadhyay, D., G. Langsley, M. Carson, R. Recacha, L. DeLucas and C. Smith (2000). "Structure of the nucleotide-binding domain of Plasmodium falciparum rab6 in the GDP-bound form." Acta Crystallogr D Biol Crystallogr **56**(Pt 8): 937-944.

Chattopadhyay, D., C. D. Smith, J. Barchue and G. Langsley (2000). "Plasmodium falciparum rab6 GTPase: expression, purification, crystallization and preliminary crystallographic studies." Acta Crystallogr D Biol Crystallogr **56**(Pt 8): 1017-1019.

Chaturvedi, S., H. Qi, D. Coleman, A. Rodriguez, P. I. Hanson, B. Striepen, D. S. Roos and K. A. Joiner (1999). "Constitutive calcium-independent release of Toxoplasma gondii dense granules occurs through the NSF/SNAP/SNARE/Rab machinery." J Biol Chem **274**(4): 2424-2431.

Chen, H., C. C. Kuo, H. Kang, A. S. Howell, T. R. Zyla, M. Jin and D. J. Lew (2012). "Cdc42p regulation of the yeast formin Bni1p mediated by the effector Gic2p." Mol Biol Cell **23**(19): 3814-3826.

Cherfils, J. and M. Zeghouf (2013). "Regulation of small GTPases by GEFs, GAPs, and GDIs." Physiol Rev **93**(1): 269-309.

Christie, J. M., K. Hitomi, A. S. Arvai, K. A. Hartfield, M. Mettlen, A. J. Pratt, J. A. Tainer and E. D. Getzoff (2012). "Structural tuning of the fluorescent protein iLOV for improved photostability." J Biol Chem **287**(26): 22295-22304.

Chutna, O., S. Goncalves, A. Villar-Pique, P. Guerreiro, Z. Marijanovic, T. Mendes, J. Ramalho, E. Emmanouilidou, S. Ventura, J. Klucken, D. C. Barral, F. Giorgini, K. Vekrellis and T. F. Outeiro (2014). "The small GTPase Rab11 co-localizes with alpha-synuclein in intracellular inclusions and modulates its aggregation, secretion and toxicity." Hum Mol Genet.

Cohen, J., S. Benns, J. Vekemans and A. Leach (2010). "[The malaria vaccine candidate RTS,S/AS is in phase III clinical trials]." Ann Pharm Fr **68**(6): 370-379.

COHEN, S., I. A. McGREGOR and S. CARRINGTON (1961). "Gamma-globulin and acquired immunity to human malaria." Nature **192**: 733-737.

Coleman, B. I., K. M. Skillman, R. H. Jiang, L. M. Childs, L. M. Altenhofen, M. Ganter, Y. Leung, I. Goldowitz, B. F. Kafsack, M. Marti, M. Llinás, C. O. Buckee and M. T. Duraisingh (2014). "A

Plasmodium falciparum histone deacetylase regulates antigenic variation and gametocyte conversion." Cell Host Microbe **16**(2): 177-186.

Cooke, B. M., N. Mohandas and R. L. Coppel (2004). "Malaria and the red blood cell membrane." Semin Hematol **41**(2): 173-188.

Coppens, I., D. J. Sullivan and S. T. Prigge (2010). "An update on the rapid advances in malaria parasite cell biology." Trends Parasitol **26**(6): 305-310.

Counihan, N. A., M. Kalanon, R. L. Coppel and T. F. de Koning-Ward (2013). "Plasmodium rhoptry proteins: why order is important." Trends Parasitol **29**(5): 228-236.

Cowman, A. F. and B. S. Crabb (2006). "Invasion of red blood cells by malaria parasites." Cell **124**(4): 755-766.

Czaplinski, K. (2014). "Understanding mRNA trafficking: are we there yet?" Semin Cell Dev Biol **32**: 63-70.

D'Adamo, P., M. Masetti, V. Bianchi, L. Morè, M. L. Mignogna, M. Giannandrea and S. Gatti (2014). "RAB GTPases and RAB-interacting proteins and their role in the control of cognitive functions." Neurosci Biobehav Rev.

de Castro, F. A., G. E. Ward, R. Jambou, G. Attal, V. Mayau, G. Jaureguiberry, C. Braun-Breton, D. Chakrabarti and G. Langsley (1996). "Identification of a family of Rab G-proteins in Plasmodium falciparum and a detailed characterisation of pfrab6." Mol Biochem Parasitol **80**(1): 77-88.

de Koning-Ward, T. F., P. R. Gilson, J. A. Boddey, M. Rug, B. J. Smith, A. T. Papenfuss, P. R. Sanders, R. J. Lundie, A. G. Maier, A. F. Cowman and B. S. Crabb (2009). "A newly discovered protein export machine in malaria parasites." Nature **459**(7249): 945-949.

de Koning-Ward, T. F., A. Olivieri, L. Bertuccini, A. Hood, F. Silvestrini, K. Charvalias, P. Berzosa Díaz, G. Camarda, T. F. McElwain, T. Papenfuss, J. Healer, L. Baldassarri, B. S. Crabb, P. Alano and L. C. Ranford-Cartwright (2008). "The role of osmiophilic bodies and Pfg377 expression in female gametocyte emergence and mosquito infectivity in the human malaria parasite Plasmodium falciparum." Mol Microbiol **67**(2): 278-290.

Deligianni, E., R. N. Morgan, L. Bertuccini, T. W. Kooij, A. Laforge, C. Nahar, N. Poulakakis, H. Schüler, C. Louis, K. Matuschewski and I. Siden-Kiamos (2011). "Critical role for a stage-specific actin in male exflagellation of the malaria parasite." Cell Microbiol **13**(11): 1714-1730.

Deligianni, E., R. N. Morgan, L. Bertuccini, C. C. Wirth, N. C. Silmon de Monerri, L. Spanos, M. J. Blackman, C. Louis, G. Pradel and I. Siden-Kiamos (2013). "A perforin-like protein mediates disruption of the erythrocyte membrane during egress of Plasmodium berghei male gametocytes." Cell Microbiol **15**(8): 1438-1455.

Dembélé, L., J. F. Franetich, A. Lorthiois, A. Gego, A. M. Zeeman, C. H. Kocken, R. Le Grand, N. Dereuddre-Bosquet, G. J. van Gemert, R. Sauerwein, J. C. Vaillant, L. Hannoun, M. J. Fuchter, T. T. Diagana, N. A. Malmquist, A. Scherf, G. Snounou and D. Mazier (2014). "Persistence and activation of malaria hypnozoites in long-term primary hepatocyte cultures." Nat Med **20**(3): 307-312.

Deng, C. Y., W. L. Lei, X. H. Xu, X. C. Ju, Y. Liu and Z. G. Luo (2014). "JIP1 mediates anterograde transport of Rab10 cargos during neuronal polarization." J Neurosci **34**(5): 1710-1723.

Dessens, J. T., A. L. Beetsma, G. Dimopoulos, K. Wengelnik, A. Crisanti, F. C. Kafatos and R. E. Sinden (1999). "CTRP is essential for mosquito infection by malaria ookinetes." EMBO J **18**(22): 6221-6227.

Dessens, J. T., J. Mendoza, C. Claudianos, J. M. Vinetz, E. Khater, S. Hassard, G. R. Ranawaka and R. E. Sinden (2001). "Knockout of the rodent malaria parasite chitinase pbCHT1 reduces infectivity to mosquitoes." Infect Immun **69**(6): 4041-4047.

Dessens, J. T., I. Sidén-Kiamos, J. Mendoza, V. Mahairaki, E. Khater, D. Vlachou, X. J. Xu, F. C. Kafatos, C. Louis, G. Dimopoulos and R. E. Sinden (2003). "SOAP, a novel malaria ookinete protein involved in mosquito midgut invasion and oocyst development." Mol Microbiol **49**(2): 319-329.

Dhekne, H. S., N. H. Hsiao, P. Roelofs, M. Kumari, C. L. Slim, E. H. Rings and S. C. van Ijzendoorn (2014). "Myosin Vb and Rab11a regulate phosphorylation of ezrin in enterocytes." J Cell Sci **127**(Pt 5): 1007-1017.

Dijksterhuis, J. and D. Molenaar (2013). "Vesicle trafficking via the Spitzenkörper during hyphal tip growth in Rhizoctonia solani." Antonie Van Leeuwenhoek **103**(4): 921-931.

Dobrowolski, J. M. and L. D. Sibley (1996). "Toxoplasma invasion of mammalian cells is powered by the actin cytoskeleton of the parasite." Cell **84**(6): 933-939.

Doerig, C., J. Endicott and D. Chakrabarti (2002). "Cyclin-dependent kinase homologues of Plasmodium falciparum." Int J Parasitol **32**(13): 1575-1585.

Doherty, J. F., M. Pinder, N. Tornieporth, C. Carton, L. Vigneron, P. Milligan, W. R. Ballou, C. A. Holland, K. E. Kester, G. Voss, P. Momin, B. M. Greenwood, K. P. McAdam and J. Cohen (1999). "A phase I safety and immunogenicity trial with the candidate malaria vaccine RTS,S/SBAS2 in semi-immune adults in The Gambia." Am J Trop Med Hyg **61**(6): 865-868.

Dollar, G., E. Struckhoff, J. Michaud and R. S. Cohen (2002). "Rab11 polarization of the Drosophila oocyte: a novel link between membrane trafficking, microtubule organization, and oskar mRNA localization and translation." Development **129**(2): 517-526.

Donnelly, C. J., M. Fainzilber and J. L. Twiss (2010). "Subcellular communication through RNA transport and localized protein synthesis." Traffic **11**(12): 1498-1505.

Doolan, D. L., C. Dobaño and J. K. Baird (2009). "Acquired immunity to malaria." Clin Microbiol Rev **22**(1): 13-36, Table of Contents.

Doritchamou, J., G. Bertin, A. Moussiliou, P. Bigey, F. Viwami, S. Ezinmegnon, N. Fievet, A. Massougbodji, P. Deloron and N. Tuikue Ndam (2012). "First-trimester Plasmodium falciparum infections display a typical "placental" phenotype." J Infect Dis **206**(12): 1911-1919.

Drinkwater, N., R. S. Bamert, K. Kannan Sivaraman, A. Paiardini and S. McGowan (2015). "X-ray crystal structures of an orally available aminopeptidase inhibitor, Tosedostat, bound to anti-malarial drug targets PfA-M1 and PfA-M17." Proteins.

Eastman, R. T. and D. A. Fidock (2009). "Artemisinin-based combination therapies: a vital tool in efforts to eliminate malaria." Nat Rev Microbiol **7**(12): 864-874.

Ecker, A., E. S. Bushell, R. Tewari and R. E. Sinden (2008). "Reverse genetics screen identifies six proteins important for malaria development in the mosquito." Mol Microbiol **70**(1): 209-220.

Ecker, A., S. B. Pinto, K. W. Baker, F. C. Kafatos and R. E. Sinden (2007). "Plasmodium berghei: plasmodium perforin-like protein 5 is required for mosquito midgut invasion in Anopheles stephensi." Exp Parasitol **116**(4): 504-508.

Eichner, M., H. H. Diebner, L. Molineaux, W. E. Collins, G. M. Jeffery and K. Dietz (2001). "Genesis, sequestration and survival of Plasmodium falciparum gametocytes: parameter estimates from fitting a model to malariatherapy data." Trans R Soc Trop Med Hyg **95**(5): 497-501.

Eksi, S., B. Czesny, G. J. van Gemert, R. W. Sauerwein, W. Eling and K. C. Williamson (2006). "Malaria transmission-blocking antigen, Pfs230, mediates human red blood cell binding to exflagellating male parasites and oocyst production." Mol Microbiol **61**(4): 991-998.

Elliott, D. A., M. T. McIntosh, H. D. Hosgood, S. Chen, G. Zhang, P. Baevova and K. A. Joiner (2008). "Four distinct pathways of hemoglobin uptake in the malaria parasite Plasmodium falciparum." Proc Natl Acad Sci U S A **105**(7): 2463-2468.

Esseltine, J. L., F. M. Ribeiro and S. S. Ferguson (2012). "Rab8 modulates metabotropic glutamate receptor subtype 1 intracellular trafficking and signaling in a protein kinase C-dependent manner." J Neurosci **32**(47): 16933-16942a.

Etxebeste, O., E. Herrero-García, L. Araújo-Bazán, A. B. Rodríguez-Urra, A. Garzia, U. Ugalde and E. A. Espeso (2009). "The bZIP-type transcription factor FlbB regulates distinct morphogenetic stages of colony formation in Aspergillus nidulans." Mol Microbiol **73**(5): 775-789.

Evangelista, M., S. Zigmond and C. Boone (2003). "Formins: signaling effectors for assembly and polarization of actin filaments." J Cell Sci **116**(Pt 13): 2603-2611.

Ezougou, C. N., F. Ben-Rached, D. K. Moss, J. W. Lin, S. Black, E. Knuepfer, J. L. Green, S. M. Khan, A. Mukhopadhyay, C. J. Janse, I. Coppens, H. Yera, A. A. Holder and G. Langsley (2014). "Plasmodium falciparum Rab5B is an N-terminally myristoylated Rab GTPase that is targeted to the parasite's plasma and food vacuole membranes." PLoS One **9**(2): e87695.

Feachem, R. G., A. A. Phillips, J. Hwang, C. Cotter, B. Wielgosz, B. M. Greenwood, O. Sabot, M. H. Rodriguez, R. R. Abeyasinghe, T. A. Ghebreyesus and R. W. Snow (2010). "Shrinking the malaria map: progress and prospects." Lancet **376**(9752): 1566-1578.

Feng, G., J. A. Simpson, E. Chaluluka, M. E. Molyneux and S. J. Rogerson (2010). "Decreasing burden of malaria in pregnancy in Malawian women and its relationship to use of intermittent preventive therapy or bed nets." PLoS One **5**(8): e12012.

Ferguson, D. J., N. Sahoo, R. A. Pinches, J. M. Bumstead, F. M. Tomley and M. J. Gubbels (2008). "MORN1 has a conserved role in asexual and sexual development across the apicomplexa." Eukaryot Cell **7**(4): 698-711.

Finlay, B. B. (2005). "Bacterial virulence strategies that utilize Rho GTPases." Curr Top Microbiol Immunol **291**: 1-10.

Fitri, L. E., N. E. Jahja, I. R. Huwae, M. B. Nara and N. Berens-Riha (2014). "Congenital malaria in newborns selected for low birth-weight, anemia, and other possible symptoms in Maumere, Indonesia." Korean J Parasitol **52**(6): 639-644.

Florent, I., Z. Derhy, M. Allary, M. Monsigny, R. Mayer and J. Schrével (1998). "A Plasmodium falciparum aminopeptidase gene belonging to the M1 family of zinc-metallopeptidases is expressed in erythrocytic stages." Mol Biochem Parasitol **97**(1-2): 149-160.

Florent, I., E. Mouray, F. Dali Ali, H. Drobecq, S. Girault, J. Schrével, C. Sergheraert, P. Grellier and I. Florenta (2000). "Cloning of Plasmodium falciparum protein disulfide isomerase homologue by affinity purification using the antiplasmodial inhibitor 1,4-bis[3-[N-(cyclohexyl methyl)amino]propyl]piperazine." FEBS Lett **484**(3): 246-252.

Fowler, J. E., Z. Vejlupkova, B. W. Goodner, G. Lu and R. S. Quatrano (2004). "Localization to the rhizoid tip implicates a Fucus distichus Rho family GTPase in a conserved cell polarity pathway." Planta **219**(5): 856-866.

Francia, M. E. and B. Striepen (2014). "Cell division in apicomplexan parasites." Nat Rev Microbiol.

Franke-Fayard, B., H. Trueman, J. Ramesar, J. Mendoza, M. van der Keur, R. van der Linden, R. E. Sinden, A. P. Waters and C. J. Janse (2004). "A Plasmodium berghei reference line that constitutively expresses GFP at a high level throughout the complete life cycle." Mol Biochem Parasitol **137**(1): 23-33.

Frénal, K., V. Polonais, J. B. Marq, R. Stratmann, J. Limenitakis and D. Soldati-Favre (2010). "Functional dissection of the apicomplexan glideosome molecular architecture." Cell Host Microbe **8**(4): 343-357.

Fries, H. C., M. B. Lamers, J. van Deursen, T. Ponnudurai and J. H. Meuwissen (1990). "Biosynthesis of the 25-kDa protein in the macrogametes/zygotes of Plasmodium falciparum." Exp Parasitol **71**(2): 229-235.

Garcia, G. E., R. A. Wirtz, J. R. Barr, A. Woolfitt and R. Rosenberg (1998). "Xanthurenic acid induces gametogenesis in Plasmodium, the malaria parasite." J Biol Chem **273**(20): 12003-12005.

Gardiner, D. L., D. C. Holt, E. A. Thomas, D. J. Kemp and K. R. Trenholme (2000). "Inhibition of Plasmodium falciparum clag9 gene function by antisense RNA." Mol Biochem Parasitol **110**(1): 33-41.

Gardner, M. J., N. Hall, E. Fung, O. White, M. Berriman, R. W. Hyman, J. M. Carlton, A. Pain, K. E. Nelson, S. Bowman, I. T. Paulsen, K. James, J. A. Eisen, K. Rutherford, S. L. Salzberg, A. Craig, S. Kyes, M. S. Chan, V. Nene, S. J. Shallom, B. Suh, J. Peterson, S. Angiuoli, M. Pertea, J. Allen, J. Selengut, D. Haft, M. W. Mather, A. B. Vaidya, D. M. Martin, A. H. Fairlamb, M. J. Fraunholz, D. S. Roos, S. A. Ralph, G. I. McFadden, L. M. Cummings, G. M. Subramanian, C. Mungall, J. C. Venter, D. J. Carucci, S. L. Hoffman, C. Newbold, R. W. Davis, C. M. Fraser and B. Barrell (2002).

"Genome sequence of the human malaria parasite Plasmodium falciparum." Nature **419**(6906): 498-511.

Gaskins, E., S. Gilk, N. DeVore, T. Mann, G. Ward and C. Beckers (2004). "Identification of the membrane receptor of a class XIV myosin in Toxoplasma gondii." J Cell Biol **165**(3): 383-393.

Gentile, J. E., S. S. Rund and G. R. Madey (2015). "Modelling sterile insect technique to control the population of Anopheles gambiae." Malar J **14**(1): 92.

Gerald, N., B. Mahajan and S. Kumar (2011). "Mitosis in the human malaria parasite Plasmodium falciparum." Eukaryot Cell **10**(4): 474-482.

Ghorbal, M., M. Gorman, C. R. Macpherson, R. M. Martins, A. Scherf and J. J. Lopez-Rubio (2014). "Genome editing in the human malaria parasite Plasmodium falciparum using the CRISPR-Cas9 system." Nat Biotechnol **32**(8): 819-821.

Ghosh, A., M. J. Edwards and M. Jacobs-Lorena (2000). "The journey of the malaria parasite in the mosquito: hopes for the new century." Parasitol Today **16**(5): 196-201.

Ghosh, A. K., I. Coppens, H. Gårdsvoll, M. Ploug and M. Jacobs-Lorena (2011). "Plasmodium ookinetes coopt mammalian plasminogen to invade the mosquito midgut." Proc Natl Acad Sci U S A **108**(41): 17153-17158.

Gilson, P. R. and B. S. Crabb (2009). "Morphology and kinetics of the three distinct phases of red blood cell invasion by Plasmodium falciparum merozoites." Int J Parasitol **39**(1): 91-96.

Gnazzo, M. M. and A. R. Skop (2014). "Spindlegate: the biological consequences of disrupting traffic." Dev Cell **28**(5): 480-482.

Goldberg, D. E. (2005). "Hemoglobin degradation." Curr Top Microbiol Immunol **295**: 275-291.

Goldfless, S. J., J. C. Wagner and J. C. Niles (2014). "Versatile control of Plasmodium falciparum gene expression with an inducible protein-RNA interaction." Nat Commun **5**: 5329.

Goodson, H. V., C. Valetti and T. E. Kreis (1997). "Motors and membrane traffic." Curr Opin Cell Biol **9**(1): 18-28.

Gould, S. B., W. H. Tham, A. F. Cowman, G. I. McFadden and R. F. Waller (2008). "Alveolins, a new family of cortical proteins that define the protist infrakingdom Alveolata." Mol Biol Evol **25**(6): 1219-1230.

Grosshans, B. L., D. Ortiz and P. Novick (2006). "Rabs and their effectors: achieving specificity in membrane traffic." Proc Natl Acad Sci U S A **103**(32): 11821-11827.

Grove, S. N. and C. E. Bracker (1970). "Protoplasmic organization of hyphal tips among fungi: vesicles and Spitzenkorper." J Bacteriol **104**(2): 989-1009.

Grueninger, H. and K. Hamed (2013). "Transitioning from malaria control to elimination: the vital role of ACTs." Trends Parasitol **29**(2): 60-64.

Gubbels, M. J., S. Vaishnava, N. Boot, J. F. Dubremetz and B. Striepen (2006). "A MORN-repeat protein is a dynamic component of the Toxoplasma gondii cell division apparatus." J Cell Sci **119**(Pt 11): 2236-2245.

Guerreiro, A., E. Deligianni, J. M. Santos, P. A. Silva, C. Louis, A. Pain, C. J. Janse, B. Franke-Fayard, C. K. Carret, I. Siden-Kiamos and G. R. Mair (2014). "Genome-wide RIP-Chip analysis of translational repressor-bound mRNAs in the Plasmodium gametocyte." Genome Biol **15**(11): 493.

Gupta, S. K. (2014). "Role of zona pellucida glycoproteins during fertilization in humans." J Reprod Immunol.

Gutman, J., D. Mwandama, R. E. Wiegand, D. Ali, D. P. Mathanga and J. Skarbinski (2013). "Effectiveness of intermittent preventive treatment with sulfadoxine-pyrimethamine during pregnancy on maternal and birth outcomes in Machinga district, Malawi." J Infect Dis **208**(6): 907-916.

Guttery, D. S., A. A. Holder and R. Tewari (2012). "Sexual development in Plasmodium: lessons from functional analyses." PLoS Pathog **8**(1): e1002404.

Guttery, D. S., B. Poulin, D. J. Ferguson, B. Szöőr, B. Wickstead, P. L. Carroll, C. Ramakrishnan, D. Brady, E. M. Patzewitz, U. Straschil, L. Solyakov, J. L. Green, R. E. Sinden, A. B. Tobin, A. A. Holder and R. Tewari (2012). "A unique protein phosphatase with kelch-like domains (PPKL) in Plasmodium modulates ookinete differentiation, motility and invasion." PLoS Pathog **8**(9): e1002948.

Guttery, D. S., B. Poulin, A. Ramaprasad, R. J. Wall, D. J. Ferguson, D. Brady, E. M. Patzewitz, S. Whipple, U. Straschil, M. H. Wright, A. M. Mohamed, A. Radhakrishnan, S. T. Arold, E. W. Tate, A. A. Holder, B. Wickstead, A. Pain and R. Tewari (2014). "Genome-wide functional analysis of Plasmodium protein phosphatases reveals key regulators of parasite development and differentiation." Cell Host Microbe **16**(1): 128-140.

Guyatt, H. L. and R. W. Snow (2001). "The epidemiology and burden of Plasmodium falciparum-related anemia among pregnant women in sub-Saharan Africa." Am J Trop Med Hyg **64**(1-2 Suppl): 36-44.

Haldar, K., N. L. Hiller, C. van Ooij and S. Bhattacharjee (2005). "Plasmodium parasite proteins and the infected erythrocyte." Trends Parasitol **21**(9): 402-403.

Hall, N., M. Karras, J. D. Raine, J. M. Carlton, T. W. Kooij, M. Berriman, L. Florens, C. S. Janssen, A. Pain, G. K. Christophides, K. James, K. Rutherford, B. Harris, D. Harris, C. Churcher, M. A. Quail, D. Ormond, J. Doggett, H. E. Trueman, J. Mendoza, S. L. Bidwell, M. A. Rajandream, D. J. Carucci, J. R. Yates, F. C. Kafatos, C. J. Janse, B. Barrell, C. M. Turner, A. P. Waters and R. E. Sinden (2005). "A comprehensive survey of the Plasmodium life cycle by genomic, transcriptomic, and proteomic analyses." Science **307**(5706): 82-86.

Hall, N., A. Pain, M. Berriman, C. Churcher, B. Harris, D. Harris, K. Mungall, S. Bowman, R. Atkin, S. Baker, A. Barron, K. Brooks, C. O. Buckee, C. Burrows, I. Cherevach, C. Chillingworth, T. Chillingworth, Z. Christodoulou, L. Clark, R. Clark, C. Corton, A. Cronin, R. Davies, P. Davis, P. Dear, F. Dearden, J. Doggett, T. Feltwell, A. Goble, I. Goodhead, R. Gwilliam, N. Hamlin, Z. Hance, D. Harper, H. Hauser, T. Hornsby, S. Holroyd, P. Horrocks, S. Humphray, K. Jagels, K. D. James, D.

Johnson, A. Kerhornou, A. Knights, B. Konfortov, S. Kyes, N. Larke, D. Lawson, N. Lennard, A. Line, M. Maddison, J. McLean, P. Mooney, S. Moule, L. Murphy, K. Oliver, D. Ormond, C. Price, M. A. Quail, E. Rabbinowitsch, M. A. Rajandream, S. Rutter, K. M. Rutherford, M. Sanders, M. Simmonds, K. Seeger, S. Sharp, R. Smith, R. Squares, S. Squares, K. Stevens, K. Taylor, A. Tivey, L. Unwin, S. Whitehead, J. Woodward, J. E. Sulston, A. Craig, C. Newbold and B. G. Barrell (2002). "Sequence of Plasmodium falciparum chromosomes 1, 3-9 and 13." Nature **419**(6906): 527-531.

Han, Y. S., J. Thompson, F. C. Kafatos and C. Barillas-Mury (2000). "Molecular interactions between Anopheles stephensi midgut cells and Plasmodium berghei: the time bomb theory of ookinete invasion of mosquitoes." EMBO J **19**(22): 6030-6040.

Harding, C. R. and M. Meissner (2014). "The inner membrane complex through development of Toxoplasma gondii and Plasmodium." Cell Microbiol **16**(5): 632-641.

Harinasuta, T., P. Suntharasamai and C. Viravan (1965). "Chloroquine-resistant falciparum malaria in Thailand." Lancet **2**(7414): 657-660.

Harrington, W. E., T. K. Mutabingwa, E. Kabyemela, M. Fried and P. E. Duffy (2011). "Intermittent treatment to prevent pregnancy malaria does not confer benefit in an area of widespread drug resistance." Clin Infect Dis **53**(3): 224-230.

Harris, P. K., S. Yeoh, A. R. Dluzewski, R. A. O'Donnell, C. Withers-Martinez, F. Hackett, L. H. Bannister, G. H. Mitchell and M. J. Blackman (2005). "Molecular identification of a malaria merozoite surface sheddase." PLoS Pathog **1**(3): 241-251.

Hawking, F., M. E. Wilson and K. Gammage (1971). "Evidence for cyclic development and short-lived maturity in the gametocytes of Plasmodium falciparum." Trans R Soc Trop Med Hyg **65**(5): 549-559.

Hehnly, H. and S. Doxsey (2014). "Rab11 endosomes contribute to mitotic spindle organization and orientation." Dev Cell **28**(5): 497-507.

Heiss, K., H. Nie, S. Kumar, T. M. Daly, L. W. Bergman and K. Matuschewski (2008). "Functional characterization of a redundant Plasmodium TRAP family invasin, TRAP-like protein, by aldolase binding and a genetic complementation test." Eukaryot Cell **7**(6): 1062-1070.

Herm-Gotz, A., C. Agop-Nersesian, S. Munter, J. S. Grimley, T. J. Wandless, F. Frischknecht and M. Meissner (2007). "Rapid control of protein level in the apicomplexan Toxoplasma gondii." Nat Methods **4**(12): 1003-1005.

Herm-Götz, A., S. Weiss, R. Stratmann, S. Fujita-Becker, C. Ruff, E. Meyhöfer, T. Soldati, D. J. Manstein, M. A. Geeves and D. Soldati (2002). "Toxoplasma gondii myosin A and its light chain: a fast, single-headed, plus-end-directed motor." EMBO J **21**(9): 2149-2158.

Herrera, S., A. Gómez, O. Vera, J. Vergara, A. Valderrama-Aguirre, A. Maestre, F. Méndez, R. Wang, C. E. Chitnis, S. S. Yazdani and M. Arévalo-Herrera (2005). "Antibody response to Plasmodium vivax antigens in Fy-negative individuals from the Colombian Pacific coast." Am J Trop Med Hyg **73**(5 Suppl): 44-49.

Hill, A. V. (2011). "Vaccines against malaria." Philos Trans R Soc Lond B Biol Sci **366**(1579): 2806-2814.

Hill, J. and P. Kazembe (2006). "Reaching the Abuja target for intermittent preventive treatment of malaria in pregnancy in African women: a review of progress and operational challenges." Trop Med Int Health **11**(4): 409-418.

Hirai, M., M. Arai, S. Kawai and H. Matsuoka (2006). "PbGCbeta is essential for Plasmodium ookinete motility to invade midgut cell and for successful completion of parasite life cycle in mosquitoes." J Biochem **140**(5): 747-757.

Hirst, J., G. H. Borner, R. Antrobus, A. A. Peden, N. A. Hodson, D. A. Sahlender and M. S. Robinson (2012). "Distinct and overlapping roles for AP-1 and GGAs revealed by the "knocksideways" system." Curr Biol **22**(18): 1711-1716.

Hoffman, S. L., L. M. Goh, T. C. Luke, I. Schneider, T. P. Le, D. L. Doolan, J. Sacci, P. de la Vega, M. Dowler, C. Paul, D. M. Gordon, J. A. Stoute, L. W. Church, M. Sedegah, D. G. Heppner, W. R. Ballou and T. L. Richie (2002). "Protection of humans against malaria by immunization with radiation-attenuated Plasmodium falciparum sporozoites." J Infect Dis **185**(8): 1155-1164.

Hollingdale, M. R., J. L. Leef, M. McCullough and R. L. Beaudoin (1981). "In vitro cultivation of the exoerythrocytic stage of Plasmodium berghei from sporozoites." Science **213**(4511): 1021-1022.

Horton, A. C. and M. D. Ehlers (2003). "Neuronal polarity and trafficking." Neuron **40**(2): 277-295.

Howard, R. J. (1981). "Ultrastructural analysis of hyphal tip cell growth in fungi: Spitzenkörper, cytoskeleton and endomembranes after freeze-substitution." J Cell Sci **48**: 89-103.

Howe, R., M. Kelly, J. Jimah, D. Hodge and A. R. Odom (2013). "Isoprenoid biosynthesis inhibition disrupts Rab5 localization and food vacuolar integrity in Plasmodium falciparum." Eukaryot Cell **12**(2): 215-223.

Howell, A. S. and D. J. Lew (2012). "Morphogenesis and the cell cycle." Genetics **190**(1): 51-77.

Hoyer, S., S. Nguon, S. Kim, N. Habib, N. Khim, S. Sum, E. M. Christophel, S. Bjorge, A. Thomson, S. Kheng, N. Chea, S. Yok, S. Top, S. Ros, U. Sophal, M. M. Thompson, S. Mellor, F. Ariey, B. Witkowski, C. Yeang, S. Yeung, S. Duong, R. D. Newman and D. Menard (2012). "Focused Screening and Treatment (FSAT): a PCR-based strategy to detect malaria parasite carriers and contain drug resistant P. falciparum, Pailin, Cambodia." PLoS One **7**(10): e45797.

Hu, K., J. Johnson, L. Florens, M. Fraunholz, S. Suravajjala, C. DiLullo, J. Yates, D. S. Roos and J. M. Murray (2006). "Cytoskeletal components of an invasion machine--the apical complex of Toxoplasma gondii." PLoS Pathog **2**(2): e13.

Hu, K., T. Mann, B. Striepen, C. J. Beckers, D. S. Roos and J. M. Murray (2002). "Daughter cell assembly in the protozoan parasite Toxoplasma gondii." Mol Biol Cell **13**(2): 593-606.

Hu, K., D. S. Roos and J. M. Murray (2002). "A novel polymer of tubulin forms the conoid of Toxoplasma gondii." J Cell Biol **156**(6): 1039-1050.

Hulden, L. (2011). "Activation of the hypnozoite: a part of Plasmodium vivax life cycle and survival." Malar J **10**: 90.

Hviid, L. and A. T. Jensen (2015). "PfEMP1 - A Parasite Protein Family of Key Importance in Plasmodium falciparum Malaria Immunity and Pathogenesis." Adv Parasitol **88**: 51-84.

Ishino, T., Y. Chinzei and M. Yuda (2005). "A Plasmodium sporozoite protein with a membrane attack complex domain is required for breaching the liver sinusoidal cell layer prior to hepatocyte infection." Cell Microbiol **7**(2): 199-208.

Ishino, T., Y. Orito, Y. Chinzei and M. Yuda (2006). "A calcium-dependent protein kinase regulates Plasmodium ookinete access to the midgut epithelial cell." Mol Microbiol **59**(4): 1175-1184.

Jambou, R., A. Zahraoui, B. Olofsson, A. Tavitian and G. Jaureguiberry (1996). "Small GTP-binding proteins in Plasmodium falciparum." Biol Cell **88**(3): 113-121.

Janse, C. J., T. Ponnudurai, A. H. Lensen, J. H. Meuwissen, J. Ramesar, M. Van der Ploeg and J. P. Overdulve (1988). "DNA synthesis in gametocytes of Plasmodium falciparum." Parasitology **96 (Pt 1)**: 1-7.

Janse, C. J., P. F. van der Klooster, H. J. van der Kaay, M. van der Ploeg and J. P. Overdulve (1986). "DNA synthesis in Plasmodium berghei during asexual and sexual development." Mol Biochem Parasitol **20**(2): 173-182.

Januschke, J., E. Nicolas, J. Compagnon, E. Formstecher, B. Goud and A. Guichet (2007). "Rab6 and the secretory pathway affect oocyte polarity in Drosophila." Development **134**(19): 3419-3425.

Jenkins, N., J. R. Saam and S. E. Mango (2006). "CYK-4/GAP provides a localized cue to initiate anteroposterior polarity upon fertilization." Science **313**(5791): 1298-1301.

Jewett, T. J. and L. D. Sibley (2003). "Aldolase forms a bridge between cell surface adhesins and the actin cytoskeleton in apicomplexan parasites." Mol Cell **11**(4): 885-894.

Jing, J. and R. Prekeris (2009). "Polarized endocytic transport: The roles of Rab11 and Rab11-FIPs in regulating cell polarity." Histology and Histopathology **24**(9): 1171-1180.

Johnson, D. I. (1999). "Cdc42: An essential Rho-type GTPase controlling eukaryotic cell polarity." Microbiol Mol Biol Rev **63**(1): 54-105.

Johnson, D. I. and J. R. Pringle (1990). "Molecular characterization of CDC42, a Saccharomyces cerevisiae gene involved in the development of cell polarity." J Cell Biol **111**(1): 143-152.

Johnston, W. L. and J. W. Dennis (2012). "The eggshell in the C. elegans oocyte-to-embryo transition." Genesis **50**(4): 333-349.

Jones, M. L., E. L. Kitson and J. C. Rayner (2006). "Plasmodium falciparum erythrocyte invasion: a conserved myosin associated complex." Mol Biochem Parasitol **147**(1): 74-84.

Jones, S., L. Grignard, I. Nebie, J. Chilongola, D. Dodoo, R. Sauerwein, M. Theisen, W. Roeffen, S. K. Singh, R. K. Singh, S. Singh, E. Kyei-Baafour, K. Tetteh, C. Drakeley and T. Bousema (2015).

"Naturally acquired antibody responses to recombinant Pfs230 and Pfs48/45 transmission blocking vaccine candidates." J Infect.

Kadota, K., T. Ishino, T. Matsuyama, Y. Chinzei and M. Yuda (2004). "Essential role of membrane-attack protein in malarial transmission to mosquito host." Proc Natl Acad Sci U S A **101**(46): 16310-16315.

Kafsack, B. F., N. Rovira-Graells, T. G. Clark, C. Bancells, V. M. Crowley, S. G. Campino, A. E. Williams, L. G. Drought, D. P. Kwiatkowski, D. A. Baker, A. Cortés and M. Llinás (2014). "A transcriptional switch underlies commitment to sexual development in malaria parasites." Nature **507**(7491): 248-252.

Kang, P. J., L. Béven, S. Hariharan and H. O. Park (2010). "The Rsr1/Bud1 GTPase interacts with itself and the Cdc42 GTPase during bud-site selection and polarity establishment in budding yeast." Mol Biol Cell **21**(17): 3007-3016.

Kappe, S. H., K. Kaiser and K. Matuschewski (2003). "The Plasmodium sporozoite journey: a rite of passage." Trends Parasitol **19**(3): 135-143.

Kariu, T., T. Ishino, K. Yano, Y. Chinzei and M. Yuda (2006). "CelTOS, a novel malarial protein that mediates transmission to mosquito and vertebrate hosts." Mol Microbiol **59**(5): 1369-1379.

Kats, L. M., B. M. Cooke, R. L. Coppel and C. G. Black (2008). "Protein trafficking to apical organelles of malaria parasites - building an invasion machine." Traffic **9**(2): 176-186.

Keder, A. and A. Carmena (2013). "Cytoplasmic protein motility and polarized sorting during asymmetric cell division." Wiley Interdiscip Rev Dev Biol **2**(6): 797-808.

Kelly, E. E., C. P. Horgan and M. W. McCaffrey (2012). "Rab11 proteins in health and disease." Biochem Soc Trans **40**(6): 1360-1367.

Kenthirapalan, S., A. P. Waters, K. Matuschewski and T. W. Kooij (2012). "Flow cytometry-assisted rapid isolation of recombinant Plasmodium berghei parasites exemplified by functional analysis of aquaglyceroporin." Int J Parasitol **42**(13-14): 1185-1192.

Kenthirapalan, S., A. P. Waters, K. Matuschewski and T. W. Kooij (2014). "Copper-transporting ATPase is important for malaria parasite fertility." Mol Microbiol **91**(2): 315-325.

Khan, S. M., B. Franke-Fayard, G. R. Mair, E. Lasonder, C. J. Janse, M. Mann and A. P. Waters (2005). "Proteome analysis of separated male and female gametocytes reveals novel sex-specific Plasmodium biology." Cell **121**(5): 675-687.

Khater, E. I., R. E. Sinden and J. T. Dessens (2004). "A malaria membrane skeletal protein is essential for normal morphogenesis, motility, and infectivity of sporozoites." J Cell Biol **167**(3): 425-432.

Khosravi-Far, R., R. J. Lutz, A. D. Cox, L. Conroy, J. R. Bourne, M. Sinensky, W. E. Balch, J. E. Buss and C. J. Der (1991). "Isoprenoid modification of rab proteins terminating in CC or CXC motifs." Proc Natl Acad Sci U S A **88**(14): 6264-6268.

Kim, D., G. Pertea, C. Trapnell, H. Pimentel, R. Kelley and S. L. Salzberg (2013). "TopHat2: accurate alignment of transcriptomes in the presence of insertions, deletions and gene fusions." Genome Biol **14**(4): R36.

Klinovska, K., N. Sebkova and K. Dvorakova-Hortova (2014). "Sperm-egg fusion: a molecular enigma of mammalian reproduction." Int J Mol Sci **15**(6): 10652-10668.

Klöpper, T. H., N. Kienle, D. Fasshauer and S. Munro (2012). "Untangling the evolution of Rab G proteins: implications of a comprehensive genomic analysis." BMC Biol **10**: 71.

Kobayashi, H., K. Etoh, N. Ohbayashi and M. Fukuda (2014). "Rab35 promotes the recruitment of Rab8, Rab13 and Rab36 to recycling endosomes through MICAL-L1 during neurite outgrowth." Biol Open **3**(9): 803-814.

Kono, M., S. Herrmann, N. B. Loughran, A. Cabrera, K. Engelberg, C. Lehmann, D. Sinha, B. Prinz, U. Ruch, V. Heussler, T. Spielmann, J. Parkinson and T. W. Gilberger (2012). "Evolution and architecture of the inner membrane complex in asexual and sexual stages of the malaria parasite." Mol Biol Evol **29**(9): 2113-2132.

Koyama, F. C., R. Y. Ribeiro, J. L. Garcia, M. F. Azevedo, D. Chakrabarti and C. R. Garcia (2012). "Ubiquitin proteasome system and the atypical kinase PfPK7 are involved in melatonin signaling in Plasmodium falciparum." J Pineal Res **53**(2): 147-153.

Kozminski, K. G., L. Beven, E. Angerman, A. H. Tong, C. Boone and H. O. Park (2003). "Interaction between a Ras and a Rho GTPase couples selection of a growth site to the development of cell polarity in yeast." Mol Biol Cell **14**(12): 4958-4970.

Krafsur, E. S., C. J. Whitten and J. E. Novy (1987). "Screwworm eradication in North and Central America." Parasitol Today **3**(5): 131-137.

Krai, P., S. Dalal and M. Klemba (2014). "Evidence for a Golgi-to-endosome protein sorting pathway in Plasmodium falciparum." PLoS One **9**(2): e89771.

Kreidenweiss, A., A. V. Hopkins and B. Mordmüller (2013). "2A and the auxin-based degron system facilitate control of protein levels in Plasmodium falciparum." PLoS One **8**(11): e78661.

Kremer, K., D. Kamin, E. Rittweger, J. Wilkes, H. Flammer, S. Mahler, J. Heng, C. J. Tonkin, G. Langsley, S. W. Hell, V. B. Carruthers, D. J. Ferguson and M. Meissner (2013). "An overexpression screen of Toxoplasma gondii Rab-GTPases reveals distinct transport routes to the micronemes." PLoS Pathog **9**(3): e1003213.

Krotoski, W. A. (1989). "The hypnozoite and malarial relapse." Prog Clin Parasitol **1**: 1-19.

Kumar, N. and R. Carter (1985). "Biosynthesis of two stage-specific membrane proteins during transformation of Plasmodium gallinaceum zygotes into ookinetes." Mol Biochem Parasitol **14**(2): 127-139.

Kuwahata, M., R. Wijesinghe, M. F. Ho, A. Pelecanos, A. Bobogare, L. Landry, H. Bugora, A. Vallely and J. McCarthy (2010). "Population screening for glucose-6-phosphate dehydrogenase

deficiencies in Isabel Province, Solomon Islands, using a modified enzyme assay on filter paper dried bloodspots." Malar J **9**: 223.

Lacroix, C., D. Giovannini, A. Combe, D. Y. Bargieri, S. Späth, D. Panchal, L. Tawk, S. Thiberge, T. G. Carvalho, J. C. Barale, P. Bhanot and R. Ménard (2011). "FLP/FRT-mediated conditional mutagenesis in pre-erythrocytic stages of Plasmodium berghei." Nat Protoc **6**(9): 1412-1428.

Lal, K., M. J. Delves, E. Bromley, J. M. Wastling, F. M. Tomley and R. E. Sinden (2009). "Plasmodium male development gene-1 (mdv-1) is important for female sexual development and identifies a polarised plasma membrane during zygote development." Int J Parasitol **39**(7): 755-761.

Lal, K., J. H. Prieto, E. Bromley, S. J. Sanderson, J. R. Yates, J. M. Wastling, F. M. Tomley and R. E. Sinden (2009). "Characterisation of Plasmodium invasive organelles; an ookinete microneme proteome." Proteomics **9**(5): 1142-1151.

Langer, R. C. and J. M. Vinetz (2001). "Plasmodium ookinete-secreted chitinase and parasite penetration of the mosquito peritrophic matrix." Trends Parasitol **17**(6): 269-272.

Langmead, B. and S. L. Salzberg (2012). "Fast gapped-read alignment with Bowtie 2." Nat Methods **9**(4): 357-359.

Langsley, G. and D. Chakrabarti (1996). "Plasmodium falciparum: the small GTPase rab11." Exp Parasitol **83**(2): 250-251.

Langsley, G., V. van Noort, C. Carret, M. Meissner, E. P. de Villiers, R. Bishop and A. Pain (2008). "Comparative genomics of the Rab protein family in Apicomplexan parasites." Microbes Infect **10**(5): 462-470.

Lanzer, M., H. Wickert, G. Krohne, L. Vincensini and C. Braun Breton (2006). "Maurer's clefts: a novel multi-functional organelle in the cytoplasm of Plasmodium falciparum-infected erythrocytes." Int J Parasitol **36**(1): 23-36.

Lapierre, L. A., K. M. Avant, C. M. Caldwell, A. Oztan, G. Apodaca, B. C. Knowles, J. T. Roland, N. A. Ducharme and J. R. Goldenring (2012). "Phosphorylation of Rab11-FIP2 regulates polarity in MDCK cells." Mol Biol Cell **23**(12): 2302-2318.

Lasonder, E., Y. Ishihama, J. S. Andersen, A. M. Vermunt, A. Pain, R. W. Sauerwein, W. M. Eling, N. Hall, A. P. Waters, H. G. Stunnenberg and M. Mann (2002). "Analysis of the Plasmodium falciparum proteome by high-accuracy mass spectrometry." Nature **419**(6906): 537-542.

Lasonder, E., C. J. Janse, G. J. van Gemert, G. R. Mair, A. M. Vermunt, B. G. Douradinha, V. van Noort, M. A. Huynen, A. J. Luty, H. Kroeze, S. M. Khan, R. W. Sauerwein, A. P. Waters, M. Mann and H. G. Stunnenberg (2008). "Proteomic profiling of Plasmodium sporozoite maturation identifies new proteins essential for parasite development and infectivity." PLoS Pathog **4**(10): e1000195.

Laurentino, E. C., S. Taylor, G. R. Mair, E. Lasonder, R. Bartfai, H. G. Stunnenberg, H. Kroeze, J. Ramesar, B. Franke-Fayard, S. M. Khan, C. J. Janse and A. P. Waters (2011). "Experimentally controlled downregulation of the histone chaperone FACT in Plasmodium berghei reveals that it is critical to male gamete fertility." Cell Microbiol **13**(12): 1956-1974.

Lawpoolsri, S., E. Y. Klein, P. Singhasivanon, S. Yimsamran, N. Thanyavanich, W. Maneeboonyang, L. L. Hungerford, J. H. Maguire and D. L. Smith (2009). "Optimally timing primaquine treatment to reduce Plasmodium falciparum transmission in low endemicity Thai-Myanmar border populations." Malar J **8**: 159.

Leiden_Malaria_Research_Group. "P. berghei - Model of malaria." from https://www.lumc.nl/org/parasitologie/research/malaria/berghei-model/.

Lemgruber, L., J. A. Kloetzel, W. Souza and R. C. Vommaro (2009). "Toxoplasma gondii: further studies on the subpellicular network." Mem Inst Oswaldo Cruz **104**(5): 706-709.

Li, J. L., D. A. Baker and L. S. Cox (2000). "Sexual stage-specific expression of a third calcium-dependent protein kinase from Plasmodium falciparum." Biochim Biophys Acta **1491**(1-3): 341-349.

Liu, Y., R. Tewari, J. Ning, A. M. Blagborough, S. Garbom, J. Pei, N. V. Grishin, R. E. Steele, R. E. Sinden, W. J. Snell and O. Billker (2008). "The conserved plant sterility gene HAP2 functions after attachment of fusogenic membranes in Chlamydomonas and Plasmodium gametes." Genes Dev **22**(8): 1051-1068.

Lock, J. G. and J. L. Stow (2005). "Rab11 in recycling endosomes regulates the sorting and basolateral transport of E-cadherin." Mol Biol Cell **16**(4): 1744-1755.

Loirand, G. and P. Pacaud (2010). "The role of rho protein signaling in hypertension." Nature Reviews Cardiology **7**(11): 637-647.

Luo, J., L. K. McGinnis and W. H. Kinsey (2009). "Fyn kinase activity is required for normal organization and functional polarity of the mouse oocyte cortex." Mol Reprod Dev **76**(9): 819-831.

Maestre, A., C. Muskus, V. Duque, O. Agudelo, P. Liu, A. Takagi, F. B. Ntumngia, J. H. Adams, K. L. Sim, S. L. Hoffman, G. Corradin, I. D. Velez and R. Wang (2010). "Acquired antibody responses against Plasmodium vivax infection vary with host genotype for duffy antigen receptor for chemokines (DARC)." PLoS One **5**(7): e11437.

Mahairaki, V., T. Voyatzi, I. Sidén-Kiamos and C. Louis (2005). "The Anopheles gambiae gamma1 laminin directly binds the Plasmodium berghei circumsporozoite- and TRAP-related protein (CTRP)." Mol Biochem Parasitol **140**(1): 119-121.

Mahajan, B., R. Noiva, A. Yadava, H. Zheng, V. Majam, K. V. Mohan, J. K. Moch, J. D. Haynes, H. Nakhasi and S. Kumar (2006). "Protein disulfide isomerase assisted protein folding in malaria parasites." Int J Parasitol **36**(9): 1037-1048.

Mahajan, B., A. Selvapandiyan, N. J. Gerald, V. Majam, H. Zheng, T. Wickramarachchi, J. Tiwari, H. Fujioka, J. K. Moch, N. Kumar, L. Aravind, H. L. Nakhasi and S. Kumar (2008). "Centrins, cell cycle regulation proteins in human malaria parasite Plasmodium falciparum." J Biol Chem **283**(46): 31871-31883.

Mahajan, R. C., U. Farooq, M. L. Dubey and N. Malla (2005). "Genetic polymorphism in Plasmodium falciparum vaccine candidate antigens." Indian J Pathol Microbiol **48**(4): 429-438.

Maier, A. G., J. A. Braks, A. P. Waters and A. F. Cowman (2006). "Negative selection using yeast cytosine deaminase/uracil phosphoribosyl transferase in Plasmodium falciparum for targeted gene deletion by double crossover recombination." Mol Biochem Parasitol **150**(1): 118-121.

Mair, G. R., J. A. Braks, L. S. Garver, J. C. Wiegant, N. Hall, R. W. Dirks, S. M. Khan, G. Dimopoulos, C. J. Janse and A. P. Waters (2006). "Regulation of sexual development of Plasmodium by translational repression." Science **313**(5787): 667-669.

Mair, G. R., E. Lasonder, L. S. Garver, B. M. Franke-Fayard, C. K. Carret, J. C. Wiegant, R. W. Dirks, G. Dimopoulos, C. J. Janse and A. P. Waters (2010). "Universal features of post-transcriptional gene regulation are critical for Plasmodium zygote development." PLoS Pathog **6**(2): e1000767.

malERA_Consultative_Group_on_Drugs (2011). "A research agenda for malaria eradication: drugs." PLoS Med **8**(1): e1000402.

Mann, T. and C. Beckers (2001). "Characterization of the subpellicular network, a filamentous membrane skeletal component in the parasite Toxoplasma gondii." Mol Biochem Parasitol **115**(2): 257-268.

Markus, M. B. (2011). "The hypnozoite concept, with particular reference to malaria." Parasitol Res **108**(1): 247-252.

Markus, M. B. (2011). "Malaria: origin of the term "hypnozoite"." J Hist Biol **44**(4): 781-786.

Marsh, K. and R. J. Howard (1986). "Antigens induced on erythrocytes by P. falciparum: expression of diverse and conserved determinants." Science **231**(4734): 150-153.

Marsh, K. and S. Kinyanjui (2006). "Immune effector mechanisms in malaria." Parasite Immunol **28**(1-2): 51-60.

Martin-Deleon, P. A. (2011). "Germ-cell hyaluronidases: their roles in sperm function." Int J Androl **34**(5 Pt 2): e306-318.

Martin, M. (2011). "Cutadapt removes adapter sequences from high-throughput sequencing reads." EMBL.net Journal Bioinformatics in action **17**.

Martínez, P. A., N. Yandar, L. P. Lesmes, M. Forero, O. Pérez-Leal, M. E. Patarroyo and J. M. Lozano (2009). "Passive transfer of Plasmodium falciparum MSP-2 pseudopeptide-induced antibodies efficiently controlled parasitemia in Plasmodium berghei-infected mice." Peptides **30**(2): 330-342.

Matter, K. and I. Mellman (1994). "Mechanisms of cell polarity: sorting and transport in epithelial cells." Curr Opin Cell Biol **6**(4): 545-554.

Matuschewski, K., A. C. Nunes, V. Nussenzweig and R. Ménard (2002). "Plasmodium sporozoite invasion into insect and mammalian cells is directed by the same dual binding system." EMBO J **21**(7): 1597-1606.

Matz, J. M. and T. W. Kooij (2015). "Towards genome-wide experimental genetics in the in vivo malaria model parasite Plasmodium berghei." Pathog Glob Health **109**(2): 46-60.

Mazier, D., R. L. Beaudoin, S. Mellouk, P. Druilhe, B. Texier, J. Trosper, F. Miltgen, I. Landau, C. Paul and O. Brandicourt (1985). "Complete development of hepatic stages of Plasmodium falciparum in vitro." Science **227**(4685): 440-442.

Mbu, R. E., W. A. Takang, H. J. Fouedjio, F. Y. Fouelifack, F. N. Tumasang and R. Tonye (2014). "Clinical malaria among pregnant women on combined insecticide treated nets (ITNs) and intermittent preventive treatment (IPTp) with sulphadoxine-pyrimethamine in Yaounde, Cameroon." BMC Womens Health **14**: 68.

McGoldrick, C. A., C. Gruver and G. S. May (1995). "myoA of Aspergillus nidulans encodes an essential myosin I required for secretion and polarized growth." J Cell Biol **128**(4): 577-587.

MCGREGOR, I. A. (1964). "THE PASSIVE TRANSFER OF HUMAN MALARIAL IMMUNITY." Am J Trop Med Hyg **13**: SUPPL 237-239.

McNamara, C. W., M. C. Lee, C. S. Lim, S. H. Lim, J. Roland, A. Nagle, O. Simon, B. K. Yeung, A. K. Chatterjee, S. L. McCormack, M. J. Manary, A. M. Zeeman, K. J. Dechering, T. R. Kumar, P. P. Henrich, K. Gagaring, M. Ibanez, N. Kato, K. L. Kuhen, C. Fischli, M. Rottmann, D. M. Plouffe, B. Bursulaya, S. Meister, L. Rameh, J. Trappe, D. Haasen, M. Timmerman, R. W. Sauerwein, R. Suwanarusk, B. Russell, L. Renia, F. Nosten, D. C. Tully, C. H. Kocken, R. J. Glynne, C. Bodenreider, D. A. Fidock, T. T. Diagana and E. A. Winzeler (2013). "Targeting Plasmodium PI(4)K to eliminate malaria." Nature **504**(7479): 248-253.

Meijering, E., O. Dzyubachyk and I. Smal (2012). "Methods for cell and particle tracking." Methods Enzymol **504**: 183-200.

Meissner, M., E. Krejany, P. R. Gilson, T. F. de Koning-Ward, D. Soldati and B. S. Crabb (2005). "Tetracycline analogue-regulated transgene expression in Plasmodium falciparum blood stages using Toxoplasma gondii transactivators." Proc Natl Acad Sci U S A **102**(8): 2980-2985.

Meissner, M., D. Schlüter and D. Soldati (2002). "Role of Toxoplasma gondii myosin A in powering parasite gliding and host cell invasion." Science **298**(5594): 837-840.

Ménard, D., C. Barnadas, C. Bouchier, C. Henry-Halldin, L. R. Gray, A. Ratsimbasoa, V. Thonier, J. F. Carod, O. Domarle, Y. Colin, O. Bertrand, J. Picot, C. L. King, B. T. Grimberg, O. Mercereau-Puijalon and P. A. Zimmerman (2010). "Plasmodium vivax clinical malaria is commonly observed in Duffy-negative Malagasy people." Proc Natl Acad Sci U S A **107**(13): 5967-5971.

Ménard, R., A. A. Sultan, C. Cortes, R. Altszuler, M. R. van Dijk, C. J. Janse, A. P. Waters, R. S. Nussenzweig and V. Nussenzweig (1997). "Circumsporozoite protein is required for development of malaria sporozoites in mosquitoes." Nature **385**(6614): 336-340.

Ménard, R., J. Tavares, I. Cockburn, M. Markus, F. Zavala and R. Amino (2013). "Looking under the skin: the first steps in malarial infection and immunity." Nat Rev Microbiol **11**(10): 701-712.

Mendes, C., F. Dias, J. Figueiredo, V. G. Mora, J. Cano, B. de Sousa, V. E. do Rosário, A. Benito, P. Berzosa and A. P. Arez (2011). "Duffy negative antigen is no longer a barrier to Plasmodium vivax--

molecular evidences from the African West Coast (Angola and Equatorial Guinea)." PLoS Negl Trop Dis **5**(6): e1192.

Menéndez, C., A. Bardají, B. Sigauque, S. Sanz, J. J. Aponte, S. Mabunda and P. L. Alonso (2010). "Malaria prevention with IPTp during pregnancy reduces neonatal mortality." PLoS One **5**(2): e9438.

Mercier, C., K. D. Adjogble, W. Däubener and M. F. Delauw (2005). "Dense granules: are they key organelles to help understand the parasitophorous vacuole of all apicomplexa parasites?" Int J Parasitol **35**(8): 829-849.

Merckx, A., K. Le Roch, M. P. Nivez, D. Dorin, P. Alano, G. J. Gutierrez, A. R. Nebreda, D. Goldring, C. Whittle, S. Patterson, D. Chakrabarti and C. Doerig (2003). "Identification and initial characterization of three novel cyclin-related proteins of the human malaria parasite Plasmodium falciparum." J Biol Chem **278**(41): 39839-39850.

Mikolajczak, S. A. and S. H. Kappe (2006). "A clash to conquer: the malaria parasite liver infection." Mol Microbiol **62**(6): 1499-1506.

Mikolajczak, S. A., H. Silva-Rivera, X. Peng, A. S. Tarun, N. Camargo, V. Jacobs-Lorena, T. M. Daly, L. W. Bergman, P. de la Vega, J. Williams, A. S. Aly and S. H. Kappe (2008). "Distinct malaria parasite sporozoites reveal transcriptional changes that cause differential tissue infection competence in the mosquito vector and mammalian host." Mol Cell Biol **28**(20): 6196-6207.

Ming, M., J. VanWye, C. J. Janse, A. P. Waters and K. Haldar (1999). "Gene organization of rab6, a marker for the novel Golgi of Plasmodium." Mol Biochem Parasitol **100**(2): 217-222.

Miura, K., E. Takashima, B. Deng, G. Tullo, A. Diouf, S. E. Moretz, D. Nikolaeva, M. Diakite, R. M. Fairhurst, M. P. Fay, C. A. Long and T. Tsuboi (2013). "Functional comparison of Plasmodium falciparum transmission-blocking vaccine candidates by the standard membrane-feeding assay." Infect Immun **81**(12): 4377-4382.

Miyata, T., T. Harakuni, H. Sugawa, J. Sattabongkot, A. Kato, M. Tachibana, M. Torii, T. Tsuboi and T. Arakawa (2011). "Adenovirus-vectored Plasmodium vivax ookinete surface protein, Pvs25, as a potential transmission-blocking vaccine." Vaccine **29**(15): 2720-2726.

Molina-Cruz, A., L. S. Garver, A. Alabaster, L. Bangiolo, A. Haile, J. Winikor, C. Ortega, B. C. van Schaijk, R. W. Sauerwein, E. Taylor-Salmon and C. Barillas-Mury (2013). "The human malaria parasite Pfs47 gene mediates evasion of the mosquito immune system." Science **340**(6135): 984-987.

Mondragon, R. and E. Frixione (1996). "Ca(2+)-dependence of conoid extrusion in Toxoplasma gondii tachyzoites." J Eukaryot Microbiol **43**(2): 120-127.

Moon, R. W., C. J. Taylor, C. Bex, R. Schepers, D. Goulding, C. J. Janse, A. P. Waters, D. A. Baker and O. Billker (2009). "A cyclic GMP signalling module that regulates gliding motility in a malaria parasite." PLoS Pathog **5**(9): e1000599.

Mori, T., H. Kuroiwa, T. Higashiyama and T. Kuroiwa (2006). "GENERATIVE CELL SPECIFIC 1 is essential for angiosperm fertilization." Nat Cell Biol **8**(1): 64-71.

Morrissette, N. S. and L. D. Sibley (2002). "Cytoskeleton of apicomplexan parasites." Microbiol Mol Biol Rev **66**(1): 21-38; table of contents.

Moxon, C. A., G. E. Grau and A. G. Craig (2011). "Malaria: modification of the red blood cell and consequences in the human host." Br J Haematol **154**(6): 670-679.

Mubyazi, G., P. Bloch, M. Kamugisha, A. Kitua and J. Ijumba (2005). "Intermittent preventive treatment of malaria during pregnancy: a qualitative study of knowledge, attitudes and practices of district health managers, antenatal care staff and pregnant women in Korogwe District, North-Eastern Tanzania." Malar J **4**: 31.

Muthuswamy, S. K. and B. Xue (2012). "Cell polarity as a regulator of cancer cell behavior plasticity." Annu Rev Cell Dev Biol **28**: 599-625.

N'Guessan, R., V. Corbel, M. Akogbéto and M. Rowland (2007). "Reduced efficacy of insecticide-treated nets and indoor residual spraying for malaria control in pyrethroid resistance area, Benin." Emerg Infect Dis **13**(2): 199-206.

Nacer, A., A. Underhill and H. Hurd (2008). "The microneme proteins CTRP and SOAP are not essential for Plasmodium berghei ookinete to oocyst transformation in vitro in a cell free system." Malar J **7**: 82.

Nelson, W. J. (2003). "Adaptation of core mechanisms to generate cell polarity." Nature **422**(6933): 766-774.

Nelson, W. J. and C. Yeaman (2001). "Protein trafficking in the exocytic pathway of polarized epithelial cells." Trends Cell Biol **11**(12): 483-486.

Newey, S. E., V. Velamoor, E. E. Govek and L. Van Aelst (2005). "Rho GTPases, dendritic structure, and mental retardation." Journal of Neurobiology **64**(1): 58-74.

Ngassa Mbenda, H. G. and A. Das (2014). "Molecular evidence of Plasmodium vivax mono and mixed malaria parasite infections in Duffy-negative native Cameroonians." PLoS One **9**(8): e103262.

Nielsen, M. A., T. Staalsoe, J. A. Kurtzhals, B. Q. Goka, D. Dodoo, M. Alifrangis, T. G. Theander, B. D. Akanmori and L. Hviid (2002). "Plasmodium falciparum variant surface antigen expression varies between isolates causing severe and nonsevere malaria and is modified by acquired immunity." J Immunol **168**(7): 3444-3450.

Nijhout, M. M. and R. Carter (1978). "Gamete development in malaria parasites: bicarbonate-dependent stimulation by pH in vitro." Parasitology **76**(1): 39-53.

Nishimura, K., T. Fukagawa, H. Takisawa, T. Kakimoto and M. Kanemaki (2009). "An auxin-based degron system for the rapid depletion of proteins in nonplant cells." Nat Methods **6**(12): 917-922.

Nkya, T., R. Poupardin, F. Laporte, I. Akhouayri, F. Mosha, S. Magesa, W. Kisinza and J. P. David (2014). "Impact of agriculture on the selection of insecticide resistance in the malaria vector Anopheles gambiae : a multigenerational study in controlled conditions." Parasit Vectors **7**(1): 480.

Okamoto, T. (2010). "Gamete fusion site on the egg cell and autonomous establishment of cell polarity in the zygote." Plant Signal Behav **5**(11): 1464-1467.

Oliva, C. F., M. J. Vreysen, S. Dupé, R. S. Lees, J. R. Gilles, L. C. Gouagna and R. Chhem (2014). "Current status and future challenges for controlling malaria with the sterile insect technique: technical and social perspectives." Acta Trop **132 Suppl**: S130-139.

Opitz, C. and D. Soldati (2002). "'The glideosome': a dynamic complex powering gliding motion and host cell invasion by Toxoplasma gondii." Mol Microbiol **45**(3): 597-604.

Orias, E. (2014). "Membrane fusion: HAP2 protein on a short leash." Curr Biol **24**(18): R831-833.

Orr, R. Y., N. Philip and A. P. Waters (2012). "Improved negative selection protocol for Plasmodium berghei in the rodent malarial model." Malar J **11**: 103.

Otto, T. D., U. Böhme, A. P. Jackson, M. Hunt, B. Franke-Fayard, W. A. Hoeijmakers, A. A. Religa, L. Robertson, M. Sanders, S. A. Ogun, D. Cunningham, A. Erhart, O. Billker, S. M. Khan, H. G. Stunnenberg, J. Langhorne, A. A. Holder, A. P. Waters, C. I. Newbold, A. Pain, M. Berriman and C. J. Janse (2014). "A comprehensive evaluation of rodent malaria parasite genomes and gene expression." BMC Biol **12**(1): 86.

Pagola, S., P. W. Stephens, D. S. Bohle, A. D. Kosar and S. K. Madsen (2000). "The structure of malaria pigment beta-haematin." Nature **404**(6775): 307-310.

Park, H. O. and E. Bi (2007). "Central roles of small GTPases in the development of cell polarity in yeast and beyond." Microbiol Mol Biol Rev **71**(1): 48-96.

Park, H. O., P. J. Kang and A. W. Rachfal (2002). "Localization of the Rsr1/Bud1 GTPase involved in selection of a proper growth site in yeast." J Biol Chem **277**(30): 26721-26724.

Pasvol, G. (2010). "Protective hemoglobinopathies and Plasmodium falciparum transmission." Nat Genet **42**(4): 284-285.

Paton, M. G., G. C. Barker, H. Matsuoka, J. Ramesar, C. J. Janse, A. P. Waters and R. E. Sinden (1993). "Structure and expression of a post-transcriptionally regulated malaria gene encoding a surface protein from the sexual stages of Plasmodium berghei." Mol Biochem Parasitol **59**(2): 263-275.

Patzewitz, E. M., D. S. Guttery, B. Poulin, C. Ramakrishnan, D. J. Ferguson, R. J. Wall, D. Brady, A. A. Holder, B. Szöőr and R. Tewari (2013). "An ancient protein phosphatase, SHLP1, is critical to microneme development in Plasmodium ookinetes and parasite transmission." Cell Rep **3**(3): 622-629.

Pereira-Leal, J. B., A. N. Hume and M. C. Seabra (2001). "Prenylation of Rab GTPases: molecular mechanisms and involvement in genetic disease." FEBS Lett **498**(2-3): 197-200.

Philip, N., H. J. Vaikkinen, L. Tetley and A. P. Waters (2012). "A unique Kelch domain phosphatase in Plasmodium regulates ookinete morphology, motility and invasion." PLoS One **7**(9): e44617.

Pino, P., S. Sebastian, E. A. Kim, E. Bush, M. Brochet, K. Volkmann, E. Kozlowski, M. Llinás, O. Billker and D. Soldati-Favre (2012). "A tetracycline-repressible transactivator system to study essential genes in malaria parasites." Cell Host Microbe **12**(6): 824-834.

Ponzi, M., I. Sidén-Kiamos, L. Bertuccini, C. Currà, H. Kroeze, G. Camarda, T. Pace, B. Franke-Fayard, E. C. Laurentino, C. Louis, A. P. Waters, C. J. Janse and P. Alano (2009). "Egress of Plasmodium berghei gametes from their host erythrocyte is mediated by the MDV-1/PEG3 protein." Cell Microbiol **11**(8): 1272-1288.

Port, J. R., C. Nguetse, S. Adukpo and T. P. Velavan (2014). "A reliable and rapid method for molecular detection of malarial parasites using microwave irradiation and loop mediated isothermal amplification." Malar J **13**(1): 454.

Poulin, B., E. M. Patzewitz, D. Brady, O. Silvie, M. H. Wright, D. J. Ferguson, R. J. Wall, S. Whipple, D. S. Guttery, E. W. Tate, B. Wickstead, A. A. Holder and R. Tewari (2013). "Unique apicomplexan IMC sub-compartment proteins are early markers for apical polarity in the malaria parasite." Biol Open **2**(11): 1160-1170.

Prajapati, S. K. and O. P. Singh (2013). "Remodeling of human red cells infected with Plasmodium falciparum and the impact of PHIST proteins." Blood Cells Mol Dis **51**(3): 195-202.

Prekeris, R., J. Klumperman and R. H. Scheller (2000). "A Rab11/Rip11 protein complex regulates apical membrane trafficking via recycling endosomes." Mol Cell **6**(6): 1437-1448.

Proellocks, N. I., R. L. Coppel and K. L. Waller (2010). "Dissecting the apicomplexan rhoptry neck proteins." Trends Parasitol **26**(6): 297-304.

Prommana, P., C. Uthaipibull, C. Wongsombat, S. Kamchonwongpaisan, Y. Yuthavong, E. Knuepfer, A. A. Holder and P. J. Shaw (2013). "Inducible knockdown of Plasmodium gene expression using the glmS ribozyme." PLoS One **8**(8): e73783.

Putaporntip, C., T. Hongsrimuang, S. Seethamchai, T. Kobasa, K. Limkittikul, L. Cui and S. Jongwutiwes (2009). "Differential prevalence of Plasmodium infections and cryptic Plasmodium knowlesi malaria in humans in Thailand." J Infect Dis **199**(8): 1143-1150.

Quevillon, E., T. Spielmann, K. Brahimi, D. Chattopadhyay, E. Yeramian and G. Langsley (2003). "The Plasmodium falciparum family of Rab GTPases." Gene **306**: 13-25.

Raabe, A. C., O. Billker, H. J. Vial and K. Wengelnik (2009). "Quantitative assessment of DNA replication to monitor microgametogenesis in Plasmodium berghei." Mol Biochem Parasitol **168**(2): 172-176.

Rached, F. B., C. Ndjembo-Ezougou, S. Chandran, H. Talabani, H. Yera, V. Dandavate, P. Bourdoncle, M. Meissner, U. Tatu and G. Langsley (2012). "Construction of a Plasmodium falciparum Rab-interactome identifies CK1 and PKA as Rab-effector kinases in malaria parasites." Biol Cell **104**(1): 34-47.

Raibaud, A., K. Brahimi, C. W. Roth, P. T. Brey and D. M. Faust (2006). "Differential gene expression in the ookinete stage of the malaria parasite Plasmodium berghei." Mol Biochem Parasitol **150**(1): 107-113.

Raibaud, A., P. Lupetti, R. E. Paul, D. Mercati, P. T. Brey, R. E. Sinden, J. E. Heuser and R. Dallai (2001). "Cryofracture electron microscopy of the ookinete pellicle of Plasmodium gallinaceum reveals the existence of novel pores in the alveolar membranes." J Struct Biol **135**(1): 47-57.

Ramakrishnan, C., J. T. Dessens, R. Armson, S. B. Pinto, A. M. Talman, A. M. Blagborough and R. E. Sinden (2011). "Vital functions of the malarial ookinete protein, CTRP, reside in the A domains." Int J Parasitol **41**(10): 1029-1039.

Ramphul, U. N., L. S. Garver, A. Molina-Cruz, G. E. Canepa and C. Barillas-Mury (2015). "Plasmodium falciparum evades mosquito immunity by disrupting JNK-mediated apoptosis of invaded midgut cells." Proc Natl Acad Sci U S A **112**(5): 1273-1280.

Read, M., T. Sherwin, S. P. Holloway, K. Gull and J. E. Hyde (1993). "Microtubular organization visualized by immunofluorescence microscopy during erythrocytic schizogony in Plasmodium falciparum and investigation of post-translational modifications of parasite tubulin." Parasitology **106 (Pt 3)**: 223-232.

Reininger, L., O. Billker, R. Tewari, A. Mukhopadhyay, C. Fennell, D. Dorin-Semblat, C. Doerig, D. Goldring, L. Harmse, L. Ranford-Cartwright and J. Packer (2005). "A NIMA-related protein kinase is essential for completion of the sexual cycle of malaria parasites." J Biol Chem **280**(36): 31957-31964.

Reininger, L., R. Tewari, C. Fennell, Z. Holland, D. Goldring, L. Ranford-Cartwright, O. Billker and C. Doerig (2009). "An essential role for the Plasmodium Nek-2 Nima-related protein kinase in the sexual development of malaria parasites." J Biol Chem **284**(31): 20858-20868.

Reininger, L., J. M. Wilkes, H. Bourgade, D. Miranda-Saavedra and C. Doerig (2011). "An essential Aurora-related kinase transiently associates with spindle pole bodies during Plasmodium falciparum erythrocytic schizogony." Mol Microbiol **79**(1): 205-221.

Reuther, G. W. and C. J. Der (2000). "The Ras branch of small GTPases: Ras family members don't fall far from the tree." Curr Opin Cell Biol **12**(2): 157-165.

Reynaga-Pena, C. G. and S. Bartnicki-Garcia (1997). "Apical branching in a temperature sensitive mutant of Aspergillus niger." Fungal Genet Biol **22**(3): 153-167.

Richard, D., L. M. Kats, C. Langer, C. G. Black, K. Mitri, J. A. Boddey, A. F. Cowman and R. L. Coppel (2009). "Identification of rhoptry trafficking determinants and evidence for a novel sorting mechanism in the malaria parasite Plasmodium falciparum." PLoS Pathog **5**(3): e1000328.

Richards, J. S. and J. G. Beeson (2009). "The future for blood-stage vaccines against malaria." Immunol Cell Biol **87**(5): 377-390.

Ridzuan, M. A., R. W. Moon, E. Knuepfer, S. Black, A. A. Holder and J. L. Green (2012). "Subcellular location, phosphorylation and assembly into the motor complex of GAP45 during Plasmodium falciparum schizont development." PLoS One **7**(3): e33845.

Riglar, D. T., D. Richard, D. W. Wilson, M. J. Boyle, C. Dekiwadia, L. Turnbull, F. Angrisano, D. S. Marapana, K. L. Rogers, C. B. Whitchurch, J. G. Beeson, A. F. Cowman, S. A. Ralph and J. Baum (2011). "Super-resolution dissection of coordinated events during malaria parasite invasion of the human erythrocyte." Cell Host Microbe **9**(1): 9-20.

Riquelme, M., E. L. Bredeweg, O. Callejas-Negrete, R. W. Roberson, S. Ludwig, A. Beltrán-Aguilar, S. Seiler, P. Novick and M. Freitag (2014). "The Neurospora crassa exocyst complex tethers Spitzenkörper vesicles to the apical plasma membrane during polarized growth." Mol Biol Cell **25**(8): 1312-1326.

Riquelme, M., R. W. Roberson, D. P. McDaniel and S. Bartnicki-Garcia (2002). "The effects of ropy-1 mutation on cytoplasmic organization and intracellular motility in mature hyphae of Neurospora crassa." Fungal Genet Biol **37**(2): 171-179.

Riquelme, M. and E. Sánchez-León (2014). "The Spitzenkörper: a choreographer of fungal growth and morphogenesis." Curr Opin Microbiol **20**: 27-33.

Robinson, M. S., D. A. Sahlender and S. D. Foster (2010). "Rapid inactivation of proteins by rapamycin-induced rerouting to mitochondria." Dev Cell **18**(2): 324-331.

Rodríguez, M. e. C., J. Martínez-Barnetche, A. Alvarado-Delgado, C. Batista, R. S. Argotte-Ramos, S. Hernández-Martínez, L. González Cerón, J. A. Torres, G. Margos and M. H. Rodríguez (2007). "The surface protein Pvs25 of Plasmodium vivax ookinetes interacts with calreticulin on the midgut apical surface of the malaria vector Anopheles albimanus." Mol Biochem Parasitol **153**(2): 167-177.

Roeffen, W., B. Mulder, K. Teelen, M. Bolmer, W. Eling, G. A. Targett, P. J. Beckers and R. Sauerwein (1996). "Association between anti-Pfs48/45 reactivity and P. falciparum transmission-blocking activity in sera from Cameroon." Parasite Immunol **18**(2): 103-109.

Roestenberg, M., M. McCall, J. Hopman, J. Wiersma, A. J. Luty, G. J. van Gemert, M. van de Vegte-Bolmer, B. van Schaijk, K. Teelen, T. Arens, L. Spaarman, Q. de Mast, W. Roeffen, G. Snounou, L. Rénia, A. van der Ven, C. C. Hermsen and R. Sauerwein (2009). "Protection against a malaria challenge by sporozoite inoculation." N Engl J Med **361**(5): 468-477.

Russell, D. G. and R. G. Burns (1984). "The polar ring of coccidian sporozoites: a unique microtubule-organizing centre." J Cell Sci **65**: 193-207.

Ryan, J. R., J. A. Stoute, J. Amon, R. F. Dunton, R. Mtalib, J. Koros, B. Owour, S. Luckhart, R. A. Wirtz, J. W. Barnwell and R. Rosenberg (2006). "Evidence for transmission of Plasmodium vivax among a duffy antigen negative population in Western Kenya." Am J Trop Med Hyg **75**(4): 575-581.

Sack, B. K., J. L. Miller, A. M. Vaughan, A. Douglass, A. Kaushansky, S. Mikolajczak, A. Coppi, G. Gonzalez-Aseguinolaza, M. Tsuji, F. Zavala, P. Sinnis and S. H. Kappe (2014). "Model for in vivo assessment of humoral protection against malaria sporozoite challenge by passive transfer of monoclonal antibodies and immune serum." Infect Immun **82**(2): 808-817.

Saeed, S., V. Carter, A. Z. Tremp and J. T. Dessens (2010). "Plasmodium berghei crystalloids contain multiple LCCL proteins." Mol Biochem Parasitol **170**(1): 49-53.

Sahi, S., S. Rai, M. Chaudhary and V. Nain (2014). "Modeling of human M1 aminopeptidases for in silico screening of potential Plasmodium falciparum alanine aminopeptidase (PfA-M1) specific inhibitors." Bioinformation **10**(8): 518-525.

Sam-Yellowe, T. Y., L. Florens, T. Wang, J. D. Raine, D. J. Carucci, R. Sinden and J. R. Yates (2004). "Proteome analysis of rhoptry-enriched fractions isolated from Plasmodium merozoites." J Proteome Res **3**(5): 995-1001.

Sandhinand, U., K. Pinswasdi and J. M. Neely (1965). "CHLOROQUINE-RESISTANT STRAIN OF PLASMODIUM FALCIPARUM FROM KHAO MAI KHAEO, THAILAND." Am J Trop Med Hyg **14**: 354-357.

Santos, J. M., M. Lebrun, W. Daher, D. Soldati and J. F. Dubremetz (2009). "Apicomplexan cytoskeleton and motors: key regulators in morphogenesis, cell division, transport and motility." Int J Parasitol **39**(2): 153-162.

Sardet, C., A. Paix, F. Prodon, P. Dru and J. Chenevert (2007). "From oocyte to 16-cell stage: cytoplasmic and cortical reorganizations that pattern the ascidian embryo." Dev Dyn **236**(7): 1716-1731.

Sardet, C., F. Prodon, G. Pruliere and J. Chenevert (2004). "[Polarization of eggs and embryos: some common principles]." Med Sci (Paris) **20**(4): 414-423.

Sato, K. I. (2014). "Transmembrane Signal Transduction in Oocyte Maturation and Fertilization: Focusing on Xenopus laevis as a Model Animal." Int J Mol Sci **16**(1): 114-134.

Saxena, A. K., K. Singh, H. P. Su, M. M. Klein, A. W. Stowers, A. J. Saul, C. A. Long and D. N. Garboczi (2006). "The essential mosquito-stage P25 and P28 proteins from Plasmodium form tile-like triangular prisms." Nat Struct Mol Biol **13**(1): 90-91.

Sebastian, S., M. Brochet, M. O. Collins, F. Schwach, M. L. Jones, D. Goulding, J. C. Rayner, J. S. Choudhary and O. Billker (2012). "A Plasmodium calcium-dependent protein kinase controls zygote development and transmission by translationally activating repressed mRNAs." Cell Host Microbe **12**(1): 9-19.

Seiler, S., F. E. Nargang, G. Steinberg and M. Schliwa (1997). "Kinesin is essential for cell morphogenesis and polarized secretion in Neurospora crassa." Embo j **16**(11): 3025-3034.

Shahabuddin, M. (2002). "Do Plasmodium ookinetes invade a specific cell type in the mosquito midgut?" Trends Parasitol **18**(4): 157-161.

Shahabuddin, M. and D. C. Kaslow (1994). "Plasmodium: parasite chitinase and its role in malaria transmission." Exp Parasitol **79**(1): 85-88.

Shahabuddin, M. and P. F. Pimenta (1998). "Plasmodium gallinaceum preferentially invades vesicular ATPase-expressing cells in Aedes aegypti midgut." Proc Natl Acad Sci U S A **95**(7): 3385-3389.

Sharma, B., R. D. Ambedkar and A. K. Saxena (2009). "A very large C-loop in EGF domain IV is characteristic of the P28 family of ookinete surface proteins." J Mol Model **15**(3): 309-321.

Shen, B., K. M. Brown, T. D. Lee and L. D. Sibley (2014). "Efficient gene disruption in diverse strains of Toxoplasma gondii using CRISPR/CAS9." MBio **5**(3): e01114-01114.

Shimizu, H., I. Nagamori, N. Yabuta and H. Nojima (2009). "GAK, a regulator of clathrin-mediated membrane traffic, also controls centrosome integrity and chromosome congression." J Cell Sci **122**(Pt 17): 3145-3152.

Siden-Kiamos, I., A. Ecker, S. Nybäck, C. Louis, R. E. Sinden and O. Billker (2006). "Plasmodium berghei calcium-dependent protein kinase 3 is required for ookinete gliding motility and mosquito midgut invasion." Mol Microbiol **60**(6): 1355-1363.

Siden-Kiamos, I., M. Ganter, A. Kunze, M. Hliscs, M. Steinbüchel, J. Mendoza, R. E. Sinden, C. Louis and K. Matuschewski (2011). "Stage-specific depletion of myosin A supports an essential role in motility of malarial ookinetes." Cell Microbiol **13**(12): 1996-2006.

Sietsma, J. H., A. Beth Din, V. Ziv, K. A. Sjollema and O. Yarden (1996). "The localization of chitin synthase in membranous vesicles (chitosomes) in Neurospora crassa." Microbiology **142 (Pt 7)**: 1591-1596.

Silverman-Gavrila, L. B. and R. R. Lew (2001). "Regulation of the tip-high [Ca2+] gradient in growing hyphae of the fungus Neurospora crassa." Eur J Cell Biol **80**(6): 379-390.

Silvestrini, F., Z. Bozdech, A. Lanfrancotti, E. Di Giulio, E. Bultrini, L. Picci, J. L. Derisi, E. Pizzi and P. Alano (2005). "Genome-wide identification of genes upregulated at the onset of gametocytogenesis in Plasmodium falciparum." Mol Biochem Parasitol **143**(1): 100-110.

Sinden, R. E. (1984). "The biology of Plasmodium in the mosquito." Experientia **40**(12): 1330-1343.

Sinden, R. E. (2009). "Malaria, sexual development and transmission: retrospect and prospect." Parasitology **136**(12): 1427-1434.

Sinden, R. E. and P. F. Billingsley (2001). "Plasmodium invasion of mosquito cells: hawk or dove?" Trends Parasitol **17**(5): 209-212.

Sinden, R. E., E. U. Canning and B. Spain (1976). "Gametogenesis and fertilization in Plasmodium yoelii nigeriensis: a transmission electron microscope study." Proc R Soc Lond B Biol Sci **193**(1110): 55-76.

Sinden, R. E., R. H. Hartley and L. Winger (1985). "The development of Plasmodium ookinetes in vitro: an ultrastructural study including a description of meiotic division." Parasitology **91 (Pt 2)**: 227-244.

Sinha, A., K. R. Hughes, K. K. Modrzynska, T. D. Otto, C. Pfander, N. J. Dickens, A. A. Religa, E. Bushell, A. L. Graham, R. Cameron, B. F. Kafsack, A. E. Williams, M. Llinás, M. Berriman, O. Billker and A. P. Waters (2014). "A cascade of DNA-binding proteins for sexual commitment and development in Plasmodium." Nature **507**(7491): 253-257.

Sloat, B. F., A. Adams and J. R. Pringle (1981). "Roles of the CDC24 gene product in cellular morphogenesis during the Saccharomyces cerevisiae cell cycle." J Cell Biol **89**(3): 395-405.

Smithuis, F., M. K. Kyaw, O. Phe, T. Win, P. P. Aung, A. P. Oo, A. L. Naing, M. Y. Nyo, N. Z. Myint, M. Imwong, E. Ashley, S. J. Lee and N. J. White (2010). "Effectiveness of five artemisinin

combination regimens with or without primaquine in uncomplicated falciparum malaria: an open-label randomised trial." Lancet Infect Dis **10**(10): 673-681.

Sologub, L., A. Kuehn, S. Kern, J. Przyborski, R. Schillig and G. Pradel (2011). "Malaria proteases mediate inside-out egress of gametocytes from red blood cells following parasite transmission to the mosquito." Cell Microbiol **13**(6): 897-912.

Spielmann, T., G. N. Montagna, L. Hecht and K. Matuschewski (2012). "Molecular make-up of the Plasmodium parasitophorous vacuolar membrane." Int J Med Microbiol **302**(4-5): 179-186.

Staines, H. M., T. Powell, S. L. Thomas and J. C. Ellory (2004). "Plasmodium falciparum-induced channels." Int J Parasitol **34**(6): 665-673.

Stanisic, D. I., A. E. Barry and M. F. Good (2013). "Escaping the immune system: How the malaria parasite makes vaccine development a challenge." Trends Parasitol **29**(12): 612-622.

Stoute, J. A., K. E. Kester, U. Krzych, B. T. Wellde, T. Hall, K. White, G. Glenn, C. F. Ockenhouse, N. Garcon, R. Schwenk, D. E. Lanar, P. Sun, P. Momin, R. A. Wirtz, C. Golenda, M. Slaoui, G. Wortmann, C. Holland, M. Dowler, J. Cohen and W. R. Ballou (1998). "Long-term efficacy and immune responses following immunization with the RTS,S malaria vaccine." J Infect Dis **178**(4): 1139-1144.

Straimer, J., M. C. Lee, A. H. Lee, B. Zeitler, A. E. Williams, J. R. Pearl, L. Zhang, E. J. Rebar, P. D. Gregory, M. Llinás, F. D. Urnov and D. A. Fidock (2012). "Site-specific genome editing in Plasmodium falciparum using engineered zinc-finger nucleases." Nat Methods **9**(10): 993-998.

Striepen, B. (2007). Switching parasite proteins on and off. Nat Methods. United States. **4:** 999-1000.

Sultan, A. A., V. Thathy, T. F. de Koning-Ward and V. Nussenzweig (2001). "Complementation of Plasmodium berghei TRAP knockout parasites using human dihydrofolate reductase gene as a selectable marker." Mol Biochem Parasitol **113**(1): 151-156.

Swysen, C., J. Vekemans, M. Bruls, S. Oyakhirome, C. Drakeley, P. Kremsner, B. Greenwood, O. Ofori-Anyinam, B. Okech, T. Villafana, T. Carter, B. Savarese, A. Duse, A. Reijman, C. Ingram, J. Frean, B. Ogutu and C. T. P. Committee (2011). "Development of standardized laboratory methods and quality processes for a phase III study of the RTS, S/AS01 candidate malaria vaccine." Malar J **10**: 223.

Ta, T. H., S. Hisam, M. Lanza, A. I. Jiram, N. Ismail and J. M. Rubio (2014). "First case of a naturally acquired human infection with Plasmodium cynomolgi." Malar J **13**: 68.

Taheri-Talesh, N., Y. Xiong and B. R. Oakley (2012). "The functions of myosin II and myosin V homologs in tip growth and septation in Aspergillus nidulans." PLoS One **7**(2): e31218.

Takahashi, S., K. Kubo, S. Waguri, A. Yabashi, H. W. Shin, Y. Katoh and K. Nakayama (2012). "Rab11 regulates exocytosis of recycling vesicles at the plasma membrane." J Cell Sci.

Takeshita, N., A. Ohta and H. Horiuchi (2005). "CsmA, a class V chitin synthase with a myosin motor-like domain, is localized through direct interaction with the actin cytoskeleton in Aspergillus nidulans." Mol Biol Cell **16**(4): 1961-1970.

Talman, A. M., O. Domarle, F. E. McKenzie, F. Ariey and V. Robert (2004). "Gametocytogenesis: the puberty of Plasmodium falciparum." Malar J **3**: 24.

Talman, A. M., C. Lacroix, S. R. Marques, A. M. Blagborough, R. Carzaniga, R. Ménard and R. E. Sinden (2011). "PbGEST mediates malaria transmission to both mosquito and vertebrate host." Mol Microbiol **82**(2): 462-474.

Tangpukdee, N., C. Duangdee, P. Wilairatana and S. Krudsood (2009). "Malaria diagnosis: a brief review." Korean J Parasitol **47**(2): 93-102.

Taylor, C. J., L. McRobert and D. A. Baker (2008). "Disruption of a Plasmodium falciparum cyclic nucleotide phosphodiesterase gene causes aberrant gametogenesis." Mol Microbiol **69**(1): 110-118.

Teirlinck, A. C., M. B. McCall, M. Roestenberg, A. Scholzen, R. Woestenenk, Q. de Mast, A. J. van der Ven, C. C. Hermsen, A. J. Luty and R. W. Sauerwein (2011). "Longevity and composition of cellular immune responses following experimental Plasmodium falciparum malaria infection in humans." PLoS Pathog **7**(12): e1002389.

Templeton, T. J., D. C. Kaslow and D. A. Fidock (2000). "Developmental arrest of the human malaria parasite Plasmodium falciparum within the mosquito midgut via CTRP gene disruption." Mol Microbiol **36**(1): 1-9.

Tepass, U. (2012). "The apical polarity protein network in Drosophila epithelial cells: regulation of polarity, junctions, morphogenesis, cell growth, and survival." Annu Rev Cell Dev Biol **28**: 655-685.

Tewari, R., D. Dorin, R. Moon, C. Doerig and O. Billker (2005). "An atypical mitogen-activated protein kinase controls cytokinesis and flagellar motility during male gamete formation in a malaria parasite." Mol Microbiol **58**(5): 1253-1263.

Tewari, R., U. Straschil, A. Bateman, U. Böhme, I. Cherevach, P. Gong, A. Pain and O. Billker (2010). "The systematic functional analysis of Plasmodium protein kinases identifies essential regulators of mosquito transmission." Cell Host Microbe **8**(4): 377-387.

Thathy, V., H. Fujioka, S. Gantt, R. Nussenzweig, V. Nussenzweig and R. Ménard (2002). "Levels of circumsporozoite protein in the Plasmodium oocyst determine sporozoite morphology." EMBO J **21**(7): 1586-1596.

Thompson, J., D. Fernandez-Reyes, L. Sharling, S. G. Moore, W. M. Eling, S. A. Kyes, C. I. Newbold, F. C. Kafatos, C. J. Janse and A. P. Waters (2007). "Plasmodium cysteine repeat modular proteins 1-4: complex proteins with roles throughout the malaria parasite life cycle." Cell Microbiol **9**(6): 1466-1480.

Thongdee, P., W. Chaijaroenkul, J. Kuesap and K. Na-Bangchang (2014). "Nested-PCR and a new ELISA-based NovaLisa test kit for malaria diagnosis in an endemic area of Thailand." Korean J Parasitol **52**(4): 377-381.

Tidyman, W. E. and K. A. Rauen (2009). "The RASopathies: developmental syndromes of Ras/MAPK pathway dysregulation." Current Opinion in Genetics & Development **19**(3): 230-236.

Tomas, A. M., G. Margos, G. Dimopoulos, L. H. van Lin, T. F. de Koning-Ward, R. Sinha, P. Lupetti, A. L. Beetsma, M. C. Rodriguez, M. Karras, A. Hager, J. Mendoza, G. A. Butcher, F. Kafatos, C. J. Janse, A. P. Waters and R. E. Sinden (2001). "P25 and P28 proteins of the malaria ookinete surface have multiple and partially redundant functions." EMBO J **20**(15): 3975-3983.

Torralba, S., I. B. Heath and F. P. Ottensmeyer (2001). "Ca(2+) shuttling in vesicles during tip growth in Neurospora crassa." Fungal Genet Biol **33**(3): 181-193.

Touray, M. G., A. Warburg, A. Laughinghouse, A. U. Krettli and L. H. Miller (1992). "Developmentally regulated infectivity of malaria sporozoites for mosquito salivary glands and the vertebrate host." J Exp Med **175**(6): 1607-1612.

Tran, J. Q., J. C. de Leon, C. Li, M. H. Huynh, W. Beatty and N. S. Morrissette (2010). "RNG1 is a late marker of the apical polar ring in Toxoplasma gondii." Cytoskeleton (Hoboken) **67**(9): 586-598.

Trapnell, C., D. G. Hendrickson, M. Sauvageau, L. Goff, J. L. Rinn and L. Pachter (2013). "Differential analysis of gene regulation at transcript resolution with RNA-seq." Nat Biotechnol **31**(1): 46-53.

Tremp, A. Z., F. S. Al-Khattaf and J. T. Dessens (2014). "Distinct temporal recruitment of Plasmodium alveolins to the subpellicular network." Parasitol Res **113**(11): 4177-4188.

Tremp, A. Z., V. Carter, S. Saeed and J. T. Dessens (2013). "Morphogenesis of Plasmodium zoites is uncoupled from tensile strength." Mol Microbiol **89**(3): 552-564.

Tremp, A. Z. and J. T. Dessens (2011). "Malaria IMC1 membrane skeleton proteins operate autonomously and participate in motility independently of cell shape." J Biol Chem **286**(7): 5383-5391.

Tremp, A. Z., E. I. Khater and J. T. Dessens (2008). "IMC1b is a putative membrane skeleton protein involved in cell shape, mechanical strength, motility, and infectivity of malaria ookinetes." J Biol Chem **283**(41): 27604-27611.

Trottein, F., T. Triglia and A. F. Cowman (1995). "Molecular cloning of a gene from Plasmodium falciparum that codes for a protein sharing motifs found in adhesive molecules from mammals and plasmodia." Mol Biochem Parasitol **74**(2): 129-141.

Tsai, Y. L., R. E. Hayward, R. C. Langer, D. A. Fidock and J. M. Vinetz (2001). "Disruption of Plasmodium falciparum chitinase markedly impairs parasite invasion of mosquito midgut." Infect Immun **69**(6): 4048-4054.

Tufet-Bayona, M., C. J. Janse, S. M. Khan, A. P. Waters, R. E. Sinden and B. Franke-Fayard (2009). "Localisation and timing of expression of putative Plasmodium berghei rhoptry proteins in merozoites and sporozoites." Mol Biochem Parasitol **166**(1): 22-31.

Ullrich, O., S. Reinsch, S. Urbe, M. Zerial and R. G. Parton (1996). "Rab11 regulates recycling through the pericentriolar recycling endosome." J Cell Biol **135**(4): 913-924.

Umeh, R., S. Oguche, T. Oguonu, S. Pitmang, E. Shu, J. T. Onyia, C. A. Daniyam, D. Shwe, A. Ahmad, E. Jongert, G. Catteau, M. Lievens, O. Ofori-Anyinam and A. Leach (2014).

"Immunogenicity and safety of the candidate RTS,S/AS01 vaccine in young Nigerian children: A randomized, double-blind, lot-to-lot consistency trial." Vaccine **32**(48): 6556-6562.

Vaishnava, S., D. P. Morrison, R. Y. Gaji, J. M. Murray, R. Entzeroth, D. K. Howe and B. Striepen (2005). "Plastid segregation and cell division in the apicomplexan parasite Sarcocystis neurona." J Cell Sci **118**(Pt 15): 3397-3407.

van Dijk, M. R., C. J. Janse, J. Thompson, A. P. Waters, J. A. Braks, H. J. Dodemont, H. G. Stunnenberg, G. J. van Gemert, R. W. Sauerwein and W. Eling (2001). "A central role for P48/45 in malaria parasite male gamete fertility." Cell **104**(1): 153-164.

van Dijk, M. R., B. C. van Schaijk, S. M. Khan, M. W. van Dooren, J. Ramesar, S. Kaczanowski, G. J. van Gemert, H. Kroeze, H. G. Stunnenberg, W. M. Eling, R. W. Sauerwein, A. P. Waters and C. J. Janse (2010). "Three members of the 6-cys protein family of Plasmodium play a role in gamete fertility." PLoS Pathog **6**(4): e1000853.

van Schaijk, B. C., M. R. van Dijk, M. van de Vegte-Bolmer, G. J. van Gemert, M. W. van Dooren, S. Eksi, W. F. Roeffen, C. J. Janse, A. P. Waters and R. W. Sauerwein (2006). "Pfs47, paralog of the male fertility factor Pfs48/45, is a female specific surface protein in Plasmodium falciparum." Mol Biochem Parasitol **149**(2): 216-222.

Van Wye, J., N. Ghori, P. Webster, R. R. Mitschler, H. G. Elmendorf and K. Haldar (1996). "Identification and localization of rab6, separation of rab6 from ERD2 and implications for an 'unstacked' Golgi, in Plasmodium falciparum." Mol Biochem Parasitol **83**(1): 107-120.

Vanderberg, J. P. and U. Frevert (2004). "Intravital microscopy demonstrating antibody-mediated immobilisation of Plasmodium berghei sporozoites injected into skin by mosquitoes." Int J Parasitol **34**(9): 991-996.

Vaughan, A. M., A. S. Aly and S. H. Kappe (2008). "Malaria parasite pre-erythrocytic stage infection: gliding and hiding." Cell Host Microbe **4**(3): 209-218.

Verdín, J., S. Bartnicki-Garcia and M. Riquelme (2009). "Functional stratification of the Spitzenkörper of Neurospora crassa." Mol Microbiol **74**(5): 1044-1053.

Vigil, D., J. Cherfils, K. L. Rossman and C. J. Der (2010). "Ras superfamily GEFs and GAPs: validated and tractable targets for cancer therapy?" Nature Reviews Cancer **10**(12): 842-857.

Villarroel-Campos, D., L. Gastaldi, C. Conde, A. Caceres and C. Gonzalez-Billault (2014). "Rab-mediated trafficking role in neurite formation." J Neurochem **129**(2): 240-248.

Virag, A. and S. D. Harris (2006). "The Spitzenkorper: a molecular perspective." Mycol Res **110**(Pt 1): 4-13.

Vlachou, D., G. Lycett, I. Sidén-Kiamos, C. Blass, R. E. Sinden and C. Louis (2001). "Anopheles gambiae laminin interacts with the P25 surface protein of Plasmodium berghei ookinetes." Mol Biochem Parasitol **112**(2): 229-237.

Vlachou, D., T. Zimmermann, R. Cantera, C. J. Janse, A. P. Waters and F. C. Kafatos (2004). "Real-time, in vivo analysis of malaria ookinete locomotion and mosquito midgut invasion." Cell Microbiol **6**(7): 671-685.

Volkmann, K., C. Pfander, C. Burstroem, M. Ahras, D. Goulding, J. C. Rayner, F. Frischknecht, O. Billker and M. Brochet (2012). "The alveolin IMC1h is required for normal ookinete and sporozoite motility behaviour and host colonisation in Plasmodium berghei." PLoS One **7**(7): e41409.

von Seidlein, L. and B. M. Greenwood (2003). "Mass administrations of antimalarial drugs." Trends Parasitol **19**(10): 452-460.

Wagner, J. C., R. J. Platt, S. J. Goldfless, F. Zhang and J. C. Niles (2014). "Efficient CRISPR-Cas9-mediated genome editing in Plasmodium falciparum." Nat Methods **11**(9): 915-918.

Wampfler, R., F. Mwingira, S. Javati, L. Robinson, I. Betuela, P. Siba, H. P. Beck, I. Mueller and I. Felger (2013). "Strategies for detection of Plasmodium species gametocytes." PLoS One **8**(9): e76316.

Wass, M. N., R. Stanway, A. M. Blagborough, K. Lal, J. H. Prieto, D. Raine, M. J. Sternberg, A. M. Talman, F. Tomley, J. Yates and R. E. Sinden (2012). "Proteomic analysis of Plasmodium in the mosquito: progress and pitfalls." Parasitology **139**(9): 1131-1145.

Weber, I., D. Assmann, E. Thines and G. Steinberg (2006). "Polar localizing class V myosin chitin synthases are essential during early plant infection in the plant pathogenic fungus Ustilago maydis." Plant Cell **18**(1): 225-242.

Weiss, G. E., P. R. Gilson, T. Taechalertpaisarn, W. H. Tham, N. W. de Jong, K. L. Harvey, F. J. Fowkes, P. N. Barlow, J. C. Rayner, G. J. Wright, A. F. Cowman and B. S. Crabb (2015). "Revealing the sequence and resulting cellular morphology of receptor-ligand interactions during Plasmodium falciparum invasion of erythrocytes." PLoS Pathog **11**(2): e1004670.

Welz, T., J. Wellbourne-Wood and E. Kerkhoff (2014). "Orchestration of cell surface proteins by Rab11." Trends Cell Biol.

Wichroski, M. J., J. A. Melton, C. G. Donahue, R. K. Tweten and G. E. Ward (2002). "Clostridium septicum alpha-toxin is active against the parasitic protozoan Toxoplasma gondii and targets members of the SAG family of glycosylphosphatidylinositol-anchored surface proteins." Infect Immun **70**(8): 4353-4361.

Wickert, H. and G. Krohne (2007). "The complex morphology of Maurer's clefts: from discovery to three-dimensional reconstructions." Trends Parasitol **23**(10): 502-509.

Wirth, C. C., S. Glushakova, M. Scheuermayer, U. Repnik, S. Garg, D. Schaack, M. M. Kachman, T. Weißbach, J. Zimmerberg, T. Dandekar, G. Griffiths, C. E. Chitnis, S. Singh, R. Fischer and G. Pradel (2014). "Perforin-like protein PPLP2 permeabilizes the red blood cell membrane during egress of Plasmodium falciparum gametocytes." Cell Microbiol **16**(5): 709-733.

Woldearegai, T. G., P. G. Kremsner, J. F. Kun and B. Mordmüller (2013). "Plasmodium vivax malaria in Duffy-negative individuals from Ethiopia." Trans R Soc Trop Med Hyg **107**(5): 328-331.

Wongsrichanalai, C., A. L. Pickard, W. H. Wernsdorfer and S. R. Meshnick (2002). "Epidemiology of drug-resistant malaria." Lancet Infect Dis **2**(4): 209-218.

World_Malaria_Report (2014). World Malaria Report 2014

Wu, C. F., N. S. Savage and D. J. Lew (2013). "Interaction between bud-site selection and polarity-establishment machineries in budding yeast." Philos Trans R Soc Lond B Biol Sci **368**(1629): 20130006.

Wu, Y., R. D. Ellis, D. Shaffer, E. Fontes, E. M. Malkin, S. Mahanty, M. P. Fay, D. Narum, K. Rausch, A. P. Miles, J. Aebig, A. Orcutt, O. Muratova, G. Song, L. Lambert, D. Zhu, K. Miura, C. Long, A. Saul, L. H. Miller and A. P. Durbin (2008). "Phase 1 trial of malaria transmission blocking vaccine candidates Pfs25 and Pvs25 formulated with montanide ISA 51." PLoS One **3**(7): e2636.

Yadouleton, A. W., A. Asidi, R. F. Djouaka, J. Braïma, C. D. Agossou and M. C. Akogbeto (2009). "Development of vegetable farming: a cause of the emergence of insecticide resistance in populations of Anopheles gambiae in urban areas of Benin." Malar J **8**: 103.

Yadouleton, A. W., G. Padonou, A. Asidi, N. Moiroux, S. Bio-Banganna, V. Corbel, R. N'guessan, D. Gbenou, I. Yacoubou, K. Gazard and M. C. Akogbeto (2010). "Insecticide resistance status in Anopheles gambiae in southern Benin." Malar J **9**: 83.

Yamashita, R. A. and G. S. May (1998). "Constitutive activation of endocytosis by mutation of myoA, the myosin I gene of Aspergillus nidulans." J Biol Chem **273**(23): 14644-14648.

Yamashita, R. A., N. Osherov and G. S. May (2000). "Localization of wild type and mutant class I myosin proteins in Aspergillus nidulans using GFP-fusion proteins." Cell Motil Cytoskeleton **45**(2): 163-172.

Yeoman, J. A., E. Hanssen, A. G. Maier, N. Klonis, B. Maco, J. Baum, L. Turnbull, C. B. Whitchurch, M. W. Dixon and L. Tilley (2011). "Tracking Glideosome-associated protein 50 reveals the development and organization of the inner membrane complex of Plasmodium falciparum." Eukaryot Cell **10**(4): 556-564.

Young, J. A., Q. L. Fivelman, P. L. Blair, P. de la Vega, K. G. Le Roch, Y. Zhou, D. J. Carucci, D. A. Baker and E. A. Winzeler (2005). "The Plasmodium falciparum sexual development transcriptome: a microarray analysis using ontology-based pattern identification." Mol Biochem Parasitol **143**(1): 67-79.

Yuda, M., S. Iwanaga, S. Shigenobu, G. R. Mair, C. J. Janse, A. P. Waters, T. Kato and I. Kaneko (2009). "Identification of a transcription factor in the mosquito-invasive stage of malaria parasites." Mol Microbiol **71**(6): 1402-1414.

Yuda, M., H. Sakaida and Y. Chinzei (1999). "Targeted disruption of the plasmodium berghei CTRP gene reveals its essential role in malaria infection of the vector mosquito." J Exp Med **190**(11): 1711-1716.

Yuda, M., K. Yano, T. Tsuboi, M. Torii and Y. Chinzei (2001). "von Willebrand Factor A domain-related protein, a novel microneme protein of the malaria ookinete highly conserved throughout Plasmodium parasites." Mol Biochem Parasitol **116**(1): 65-72.

Zhang, C., B. Xiao, Y. Jiang, Y. Zhao, Z. Li, H. Gao, Y. Ling, J. Wei, S. Li, M. Lu, X. Z. Su, H. Cui and J. Yuan (2014). "Efficient editing of malaria parasite genome using the CRISPR/Cas9 system." MBio **5**(4): e01414-01414.

Zieler, H. and J. A. Dvorak (2000). "Invasion in vitro of mosquito midgut cells by the malaria parasite proceeds by a conserved mechanism and results in death of the invaded midgut cells." Proc Natl Acad Sci U S A **97**(21): 11516-11521.

Zimmerman, P. A., M. U. Ferreira, R. E. Howes and O. Mercereau-Puijalon (2013). "Red blood cell polymorphism and susceptibility to Plasmodium vivax." Adv Parasitol **81**: 27-76.

7. Appendix

7.1 Appendix A

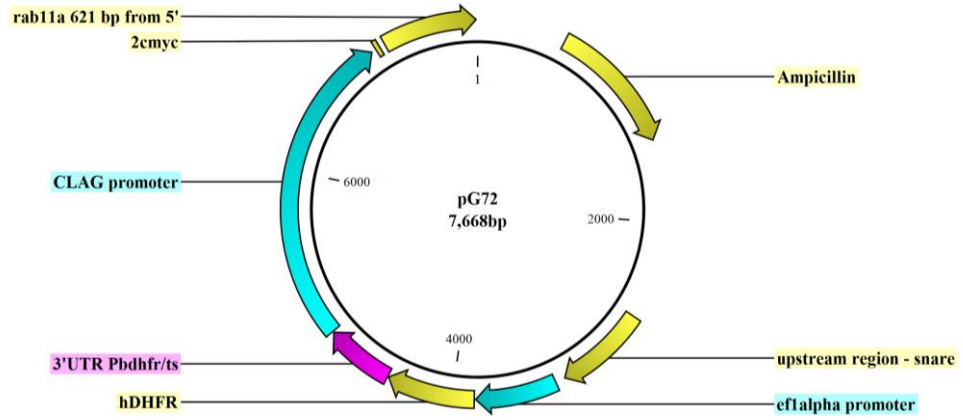

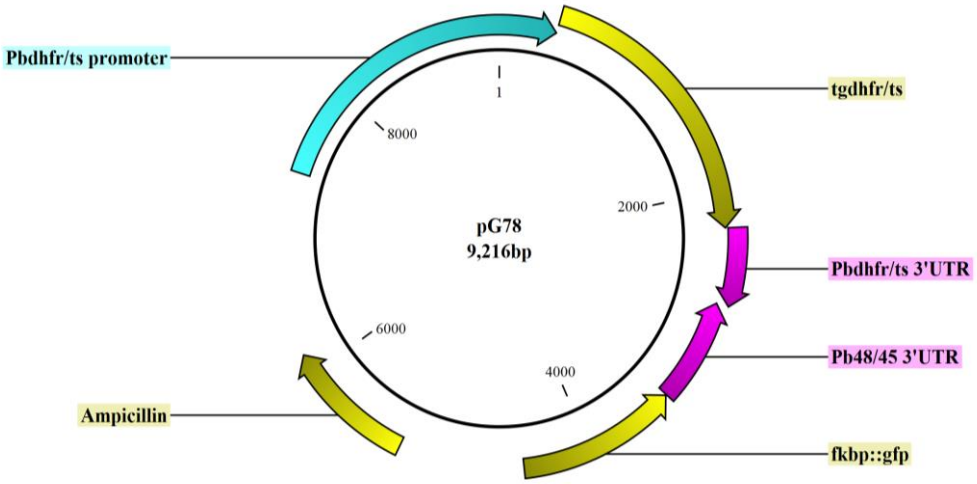

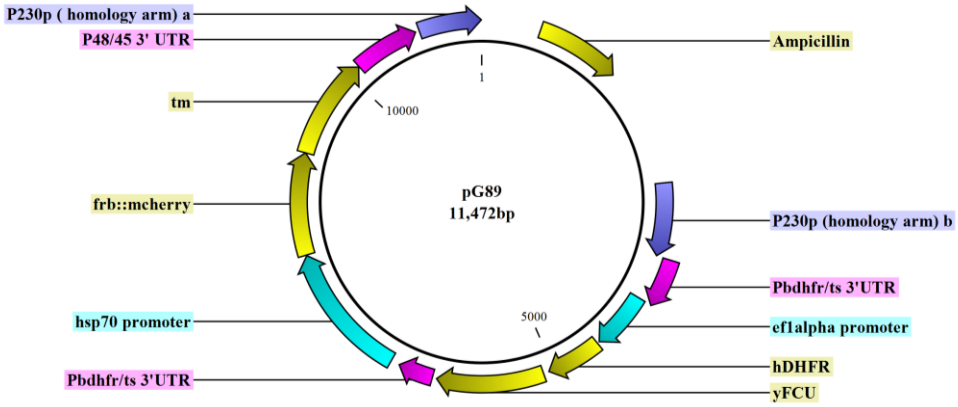

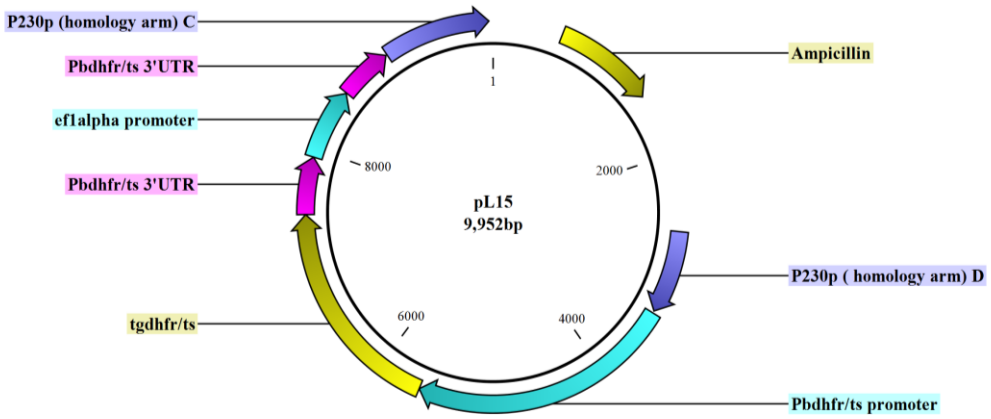
P230p (homology arm) C
Pbdhfr/ts 3'UTR
ef1alpha promoter
Pbdhfr/ts 3'UTR
tgdhfr/ts
Ampicillin
P230p (homology arm) D
Pbdhfr/ts promoter
1
2000
4000
6000
8000
pL15
9,952bp

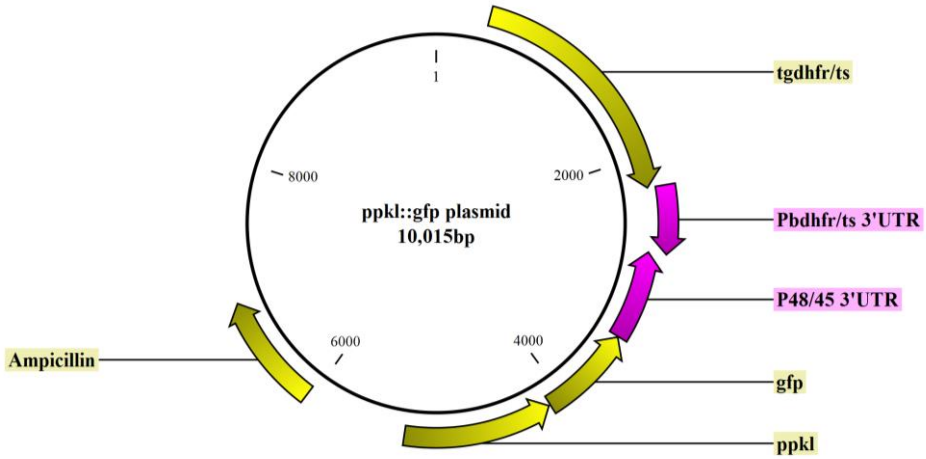
tgdhfr/ts
Pbdhfr/ts 3'UTR
P48/45 3'UTR
gfp
ppkl
Ampicillin
1
2000
4000
6000
8000
ppkl::gfp plasmid
10,015bp

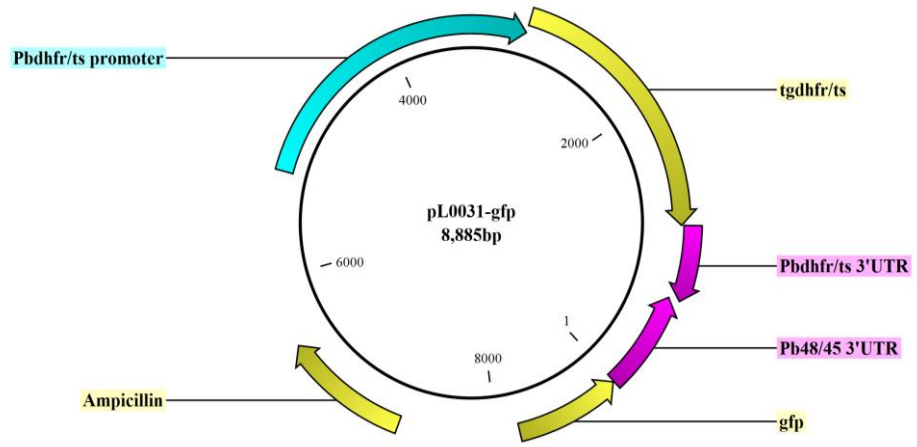
Pbdhfr/ts promoter
tgdhfr/ts
Pbdhfr/ts 3'UTR
Pb48/45 3'UTR
gfp
Ampicillin
1
2000
4000
6000
8000
pL0031-gfp
8,885bp

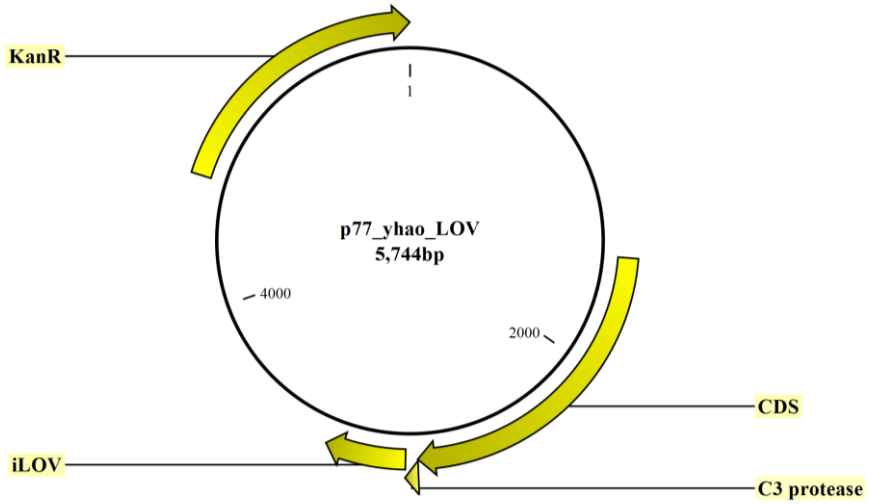

Figure 1 Basic vectors (CLC maps) used to generate plasmids mentioned in this study.

Number	Primer sequence	*Restriction Site*
GU0013	TGCTCTAGAATGAATTTTAAATACAGTTTTATT	
GU0014	TGCTCTAGATTACATTACTATCACGTAAATAAC	
GU1504	GTAGGTACCATATTTAAACAGATTAAGTACCGAAGATAAT	*KpnI*
GU1505	AGACTCGAGTTTTTATCATTTGGATAATTAATTCTTATATTTATTC	*XhoI*
GU1507	AAGCTCGAGATGGCTATGAGTAAAGGAGAAGA	*XhoI*
GU1508	GATGGTACCAATACCCCAATACGAATATTTGTAACA	*KpnI*
GU1509	CTAGGTACCCCCGGGTTCTATTAATAAAAAATATAAATATATGTATGTGTTAA	*XmaI+KpnI*
GU1515	GATGTCGACCCCTTTGTATAGTTCATCCATGCCATG	*SalI*
GU1587	GATGGTACCATTTTTATAAATGAAGCAATACCACATTTTTA	*KpnI*
GU1588	GTGCCCGGGATGGTGAGCAAGGGCGAG	*XmaI*
GU1589	CCTCCCGGGCGCATATCGAAATGATGCTATCA	*XmaI*
GU1620	TGACAAGCTTTTGGTATAAACCTAACTTCTCCAGG	*HindIII*
GU1621	GGATCCGCGGCCCTTTCTTATAATTACCTAAGGGC	*SacII*
GU1622	GGCGGTACCCTATTCCATTCACGTAAATGTTAGCA	*KpnI*
GU1623	CGCTGATATCCTCGAGTTTTATATCGTTTTATTTTATTAATATTTTTAATTTACAAAT	*EcoRV/XhoI*
GU1624	CGCTGATATCCTCGAGCAATTACCATACAATACTTATATATACACAC	*EcoRV/XhoI*
GU1766	CGGGATCAGCAAAAATTGATGAAAG	
GU1767	GTAGCGAATTCTACGCCTATAG	
GU1933	GATGGATCCATGGCTATGGTGAGCAAGGGCGAG	*BamHI*
GU1934	TGTCATATGTTACTTGTACAGCTCGTCCATG	*NdeI*
GU1935	CTTGAGCAGACTTCTCTATGATTAAACC	
GU1936	CATGAACGAAAATTTATATGAACAGCTACC	
GU1948	GCATGTAATTCATGTAAATGTTCCTGTGG	
GU1949	CATTCACATTTGCATTCTTGAGGGC	

GU1950	GGTTGTGGATGTAGGGGAGCTG	
GU1951	GCATCATTGGCGCCTTTAACTTTATGG	
GU1952	GCCTGATATGGACAGTAGAACCTTTG	
GU1953	CTAAGATTAACTCCTCTTATGTTACATTCAGAACG	
GU2002	AGTGGATCCCCTCCTTTCATATTCTTTGATAAAAAAGAGGAT	*BamHI*
GU2003	GTAGTTGGAGATAAACCTATTTATTCGATATCAGGTTTATCCAGGGGTA	*EcoRV*
GU2004	TACCCCTGGATAAACCTGATATCGAATAAATAGGTTTATCTCCAACTAC	*EcoRV*
GU2005	TTAGCGGCCGCTTGTGGATGGAGTAAAAGGATTAA	*NotI*
GU2016	GACACATTTTACTTATAGAAGAAGGC	
GU2017	GGAATTGATATGGCTGTAAAGGA	
GU2020	AGTCCCGGGTTTGTATAGTTCATCCATGCCATG	*XmaI/SmaI*
GU2023	GGAGCTAGCTATTTAATACCTTTTTGTGTTATGTATAAATATAAC	*NheI*
GU2035	GAATTAAGCTGGGCTGCAGG	
GU2036	GAATTACCTGAAAAGTCACATCC	
GU2037	AAGTTTTGGTTTTAGATGCCCAG	
GU2038	CCCCACATTTAACTGATTTTCAC	
GU2039	ATGCAGCTGGCACGACAG	
GU2041	GCCCTCGCCCTCGATC	
GU2042	AAGGCTAGCATGGCTATGAGTAAAGGAGAAGA	*NheI*
GU2096	GGCCAGCATTGGGTCTAATA	
GU2097	GCCTTTCTCCTCCTGGAC	
GU2098	CGCTGTGTCCCAGAACATG	
GU2138	CTACTCGAGTTCTATTAATAAAAAATATAAATATATGTATGTGTTAA	*XhoI*
GU2139	GATCTCGAGATGGCTATGGTGAGCAAGGG	*XhoI*
GU2140	TGTGTCGACTTACTTGTACAGCTCGTCCATG	*SalI*
GU2143	CATCATCATTATTATCTTCGGTACTTAA	
GU2144	GGTACTGCATCTATATTTATAAAAAAAAATGA	

GU2171	TGTGTCGACCTTGTACAGCTCGTCCATGC	*SalI*
GU2366	AAGGGTACCCAGATAACAATAATAATATTGATTCTGTTTTATTTC	*KpnI*
GU2367	AAGGCTAGCTATTTAATACCTTTTTGTGTTATGTATAAATATAACTA	*NheI*
GU2368	AGATCCGCGGATAATACGGTATTCATATAATAAATATACAAAATATATAG	*SacII*
GU2369	TGACAAGCTTTCAAGAAGGAAAACATGTTGGTATAAAC	*HindIII*
GU2370	AAGGCTAGCATGGCTATGAGTAAAGGAGAAGAAC	*NheI*
GU2373	GCCCCGCGGATTAACCGAAGTTTGGATAAATCATATGTAT	*SacII*
GU2374	ATTGGATCCAATGTTAAACATTCTGCTGTTGTTCATAC	*BamHI*
GU2386	AGTGGATCC TTTCATATTCTTTGATAAAAAAGAGGAT	*BamHI*
GU2387	ATAAAATATTTAAATAATGTATTTCCTATAAATAAATTTACAGA	
GU2388	GTTCATTTTGGAGCAGTTATATCAATGT	
GU2389	TTTTTTATTTATTTATAAGCAAATATATATTTTTATATATTTATACAC	
GU2390	ATCAATATTAATATTTTTTCTTTGTAAAATTGAATAGTGA	
GU2391	TGATTTTGCATTACTTGTTCGAAAAATTTCT	
GU2392	CGACACGGAAATGTTGAATACTCAT	
GU2393	TTGAAATAGGGATAATAAATATTCATTATAATCAG	
GU2394	ATGACGATTGTAAATTTAAAAAGCAAGATTAAT	
GU2395	TCATTATTAAGTTTATCATTATTTTTAATAAGATCGT	
GU2396	ATTTTTTTGAAATGAAAAAGTATTATTTGAACAATTATAT	
GU2402	GCCCCCGGGTTATTTGTATAGTTCATCCATGCCAT	*XmaI*
GU2435	CATGATATCTTTGTATAGTTCATCCATGCCATGT	*EcoRV*
GU2453	ATGCCCATGTTCTGGGACAC	
GU2454	CCAAGATTAGATCGATATGTAAAATTTTCAAAT	
GU2455	AGCATGCACATATAAATACATTAAACACC	
GU2456	CTTTTAACTCGATTCTATTAACAAGGGTA	
GU2457	TACCCTTGTTAATAGAATCGAGTTAAAAG	
GU2459	GCTATGGTCATATTACCATTTTTGGTAT	

GU2460	GACCTGCAGGCATGCAAG	
GU2461	ATGAATATTTCTAAAACATTGTTTAGCGTATTTT	
GU2462	CAAATCGGAGTATATGTCTATGAATGAA	
GU2463	CGAATAGTTGCGATATTGATATAAGTC	
GU2490	GTGTGCAGTTTTTGTTTTAAATTAAATAAATAAAC	
GU2491	GCGGCTAGCATGATCGGTACCATTGAGAAGAATTT	*KpnI*
GU2492	CGCGATATCTACGTGGTCAGAACCATCCAG	*EcoRV*
GU2666	CCTAGTTATATTTATACATAACACAAAAAGG	
GU2667	GCTGCAGTATTTCATCGGCGT	
GU2857	TTACCCGGGATGTCAATGAAAGAGGATTATTACGATTA	*XmaI*
GU2858	TTCGCGGCCGCTCAACAGCATTTTGTTTTTGTTTTTTTTTCAT	*NotI*
GU2862	ATAGGTACCGTTCAAGTTAAATGTCCAAAAATTATAAAAAG	*KpnI*
GU2863	GTCGAATTCATATTTTCTATATTTTCGGTTGTTTGTTCATT	*EcoRI*
GU2864	TAGGCGGCCGCATGGGGAATATTGTATCCTGTTGTT	*NotI*
GU2865	CCAGGATCCTTAATTTTTTTTATAATCTCTCATAATATAAATAAATAAGTTTTT	*BamHI*
GU2866	CTATTTTGAGTTTTTCTTAATATATAGAGAATAAAAAATGATATCTTTATGTTTGGTGAAATATAAATATTTTTATACAA	*EcoRV*
GU2867	TTGTATAAAAATATTTATATTTCACCAAACATAAAGATATCATTTTTTATTCTCTATATATTAAGAAAAACTCAAAATAG	*EcoRV*
GU2868	GGATACAGCAGGCCAAGAAAG	
GU2869	TTAGTTATATCATAAACTAGCAATGCCC	
GU2915	GATGTTTTTTATATATTATAGTTAAAAACTATCACG	
GU2919	ATCGGATCCTATTTTGAATAGTTTATTCTTTTATTAATAAATTTATATTCACACAAA	*BamHI*
GU2920	TCAGGATCCAGCAGTTAAGCAATGCTTTTTTATAAATTCATAAAA	*BamHI*
GU2923	TCAGATATCATCATGATGAGTAAAGGAGAAGAACTTTTCAC	*EcoRV*
GU2924	GAAATTATTAGTGATGAAAAAGAAATATATGAATT	
GU2925	GATTTTATTTTTTGTCACAAGATTTTGCTG	
GU2926	TATTTGGTGATGGAATGGCAAAATC	

GU2927	GCACTTGCTTTGTTTTACTCAAAAAG
GU2928	ACGACCAGACACACCGGT
GU2929	TGTAAACTTAAGCATAAAGAGCTCG
GU2989	CAAATTAGAGAAGAAATTAAGTAAATAAATGTATA
GU2990	AATATATATTAGTCAAAGAATGTTGAGATAAAG
GU2991	AGTTGGTGAATGAAATAAGATCATGG
GU2992	ATTAGGTTTGTTTAAAAATGCATGAAGCTA
GU2993	GTTGAATCTCTTGCCGACTGAT
GU2994	TATTTTATTTCCACAATATTTATTTATTATTTATTGTTGA
GU2995	TGATACCGCGAGACCCAC
GU2996	CGGCCGCATGGGGAATAT

Table 2 Total primers used for PCR amplifications, generation of plasmids and diagnostic PCRs.

Gene ID	Description	Log2(fold change) at gametocytes stage	Log2(fold change) at ookinete stage
		(WT-GFP v $_{p}$*clag::rab11a*)	**(WT-GFP v $_{p}$*clag::rab11a*)**
PBANKA_051500	25 kDa ookinete surface antigen precursor (P25)	-	-
PBANKA_051490	28 kDa ookinete surface protein (P28)	-	-
PBANKA_145930	actin I	-	-
PBANKA_050510	ADP-ribosylation factor, putative (ARF1)	-	-
PBANKA_041770	alpha tubulin 1	-	-
PBANKA_052270	alpha tubulin 2	-	-
PBANKA_121770	ATP-dependent RNA Helicase (DOZI)	-	-
PBANKA_080050	chitinase (CHT1)	-*	-
PBANKA_041290	circumsporozoite- and TRAP-related protein (CTRP)	-1.26508	-
PBANKA_110990	conserved Plasmodium protein, unknown function	-	-
PBANKA_136440	conserved Plasmodium protein, unknown function	-1.53257	-
PBANKA_093210	DHHC-type zinc finger protein, putative	-	-
PBANKA_121430	enolase, putative (ENO)	-	-

PBANKA_133890	glideosome associated protein with multiple membrane spans 1, putative (GAPM1)	-	-
PBANKA_052390	glideosome associated protein with multiple membrane spans 2, putative (GAPM2)	-	-
PBANKA_103540	glideosome associated protein with multiple membrane spans 3, putative (GAPM3)	-1.61416	-
PBANKA_111530	glideosome-associated protein 40, putative (GAP40)	-	-
PBANKA_143760	glideosome-associated protein 45, putative	-	-
PBANKA_122330	GTPase, Rab18, putative	-	-
PBANKA_040260	inner membrane complex protein 1a (IMC1a)	-1.55766	-[+]
PBANKA_090710	inner membrane complex protein 1b (IMC1b)	-	-
PBANKA_143660	inner membrane complex protein 1h (IMC1h)	-	-
PBANKA_120940	inner membrane complex protein, putative	-	-
PBANKA_123730	inner membrane complex protein, putative	-	-
PBANKA_132430	inner membrane complex protein, putative	-	-
PBANKA_135850	inner membrane complex protein, putative	-*	-
PBANKA_040270	membrane skeletal protein, putative	-	-
PBANKA_120200	membrane skeletal protein, putative	-	-

PBANKA_124060	membrane skeletal protein, putative	-	-
PBANKA_135570	myosin A (MyoA)	-	-
PBANKA_145950	myosin light chain 1, putative,myosin A tail domain interacting protein MTIP, putative (MTIP)	-1.70637	-
PBANKA_132950	protein phosphatase containing kelch-like domains (PPKL)	-	-
PBANKA_141890	Rab GTPase 11a (Rab11a)	-3.40816	-
PBANKA_135410	Rab GTPase 11b	-1.26062	-
PBANKA_111350	Rab1a, putative	-	-
PBANKA_111230	Rab1b, putative	-	-
PBANKA_030800	Rab5a, GTPase, putative	-	-
PBANKA_140910	Rab5b, GTPase, putative	-	-
PBANKA_020650	Rab5c, GTPase, putative	-	-
PBANKA_090410	Rab6	-	-
PBANKA_081900	secreted acid phosphatase, putative,glideosome-associated protein 50, putative (GAP50)	-	-
PBANKA_144580	small GTPase Rab2, putative	-	-
PBANKA_130130	trailer hitch homolog, putative (CITH)	-	-

PBANKA_092730	zinc finger, DHHC-type, putative	-	-
PBANKA_040820	calcium-dependent protein kinse 3 (CDPK3)	-1.02298	-0.29378

Table 2 Selected 45 transcripts containing surface markers, secretory proteins, IMC and glideosome associated proteins and Rabs.

Only one out of these 45 transcripts is deregulated in $_{p}$*clag::rab11a* ookinete stage as compared to the transcriptome of WT-GFP ookinete.

Only eight out of these 45 transcripts are deregulated in $_{p}$*clag::rab11a* gametocyte stage as compared to the transcriptome of WT-GFP gametocytes.

* Not detected in gametocyte stage ($_{p}$*clag::rab11a* as well as WT-GFP)

+ Not detected in ookinete stage ($_{p}$*clag::rab11a* as well as WT-GFP)

7.2 Appendix B

Please check the CD provided with this thesis.

Contents of CD

1. Table 1 to 6 RNA-Seq data in MS Excel
2. A PDF version of this thesis.